THE PHOTOLYSIS OF SOME ALKYL-SUBSTITUTED STANNANES

A Thesis

by

Albert E. Platt, A.R.I.C.

Submitted to the University of Keele in partial fulfilment of the requirements for the degree of Doctor of Philosophy.

University of Keele
February 1969

ACKNOWLEDGMENTS

In presenting this thesis I would like to thank the following:

Professor H.D. Springall for providing the laboratory facilities for this research project.

The Ministry of Aviation (now the Ministry of Technology) for providing a maintenance grant 1966-69 and a grant for apparatus 1966-69.

Dr. R.B. Cundall for his supervision in the absence of Dr. P. Borrell, December 1967 - June 1968.

The following members of the group for numerous discussions: Dr. P. Cashmore, Dr. J. Sedlar, Dr. A. Cervenka, R. Gutteridge, J.D. Holmes and in particular G. Millward for his assistance in building the mass-spectrometer and construction of the computer program.

Mrs P.M. Bebb who typed this thesis.

In particular, I am indebted to Dr. Peter Borrell for his helpful criticism and encouragement throughout this project.

All the work reported in this thesis was carried out by the author, under the supervision of Dr. P. Borrell.

ABSTRACT

Studies have been made on the photolytic decomposition of tetramethyl, ethyl trimethyl and n-propyl trimethyl stannane. A number of expected decomposition products, for example ethane from $Sn(CH_3)_4$, were found in each case and the effects of time, added gases, reactant pressure and temperature on the product yields was studied. The yields of the products increased linearly with time up to about 15 minutes and thereafter the rate of production decreased due to solid formation on the cell window. Addition of inert gases caused a decrease in product yield to a constant value over a short range of pressure. Further increase in inert gas pressure had little effect and consequently the existence of two excited intermediate states was proposed. Addition of radical scavengers, oxygen and nitric oxide, decreased the yields further and some products were completely eliminated. From the effects of inert gases and radical scavengers it was possible to calculate the fraction of each product formed by molecular elimination and the fraction of free radical origin. Increasing the parent stannane pressure increased the product yields linearly to varying extents, the increases being ascribed to radical abstraction reactions.

The results of the above experiments aided the elucidation of the primary reaction schemes which have been proposed for tetramethyl and ethyl trimethyl stannane. The quantum yields of the primary reactions were estimated after calculation of the radical quantum yields at zero pressure.

Tetramethyl Stannane:

$$Sn(CH_3)_4 + h\nu \rightarrow Sn(CH_3)_4^{*} \rightarrow 3CH_3 + SnCH_3 \quad \phi = 0.35$$
$$\downarrow \quad \phi = 0.70$$
$$Sn(CH_3)_4^{**}$$

In addition there are two molecular elimination reactions, having small quantum yields 0.01, from which equal amounts of methane and ethane arise.

Ethyl Trimethyl Stannane:

$$C_2H_5Sn(CH_3)_3 + h\nu \rightarrow C_2H_5Sn(CH_3)_3^{*} \rightarrow C_2H_5 + 2CH_3 + SnCH_3 \quad \phi = 0.12$$
$$\downarrow \quad \phi = 0.88$$
$$C_2H_5Sn(CH_3)_3^{**}$$

Similarly three more primary reactions are postulated giving rise to molecular elimination products methane, ethane and ethylene.

Increasing the number of carbon atoms in the alkyl groups leads to an increase in molecular elimination particularly of olefins. In the case of n-propyl trimethyl stannane ethylene and propylene are largely of molecular origin.

The decrease in quantum yields with pressure of added gas is thought to be due to collisional deactivation of the second excited

state intermediate which may be a triplet or a vibrationally excited state. This second state may be arrived at by a self-quenching or energy transfer process.

The effect of temperature on the rates of formation of methane and ethane from tetramethyl stannane led to the postulation of a hydrogen abstraction reaction, with a derived rate constant equal to $5 \times 10^9 e^{\frac{-10,020}{RT}}$, and a methyl group abstraction reaction, with a derived rate constant equal to $3 \times 10^7 e^{\frac{-5,950}{RT}}$. The effect of temperature on the rates of formation of the products from ethyl trimethyl stannane led to the general conclusion that hydrogen abstraction ~~is favoured~~ and also a more stoichiometric distribution of products according to the methyl to ethyl content in ethyl trimethyl stannane ~~is~~ favoured.

Estimates have been made of the decomposition life-times of the second excited state for each of the three alkyl substituted stannanes.

C O N T E N T S

1. INTRODUCTION

1.1 Preliminary Remarks

The chemical reactions that are dependent on the absorption of visible and ultraviolet light are the subject of Photochemistry and until the 1940's, despite the obvious importance of photochemical reactions in photosynthesis and related phenomena, it received only limited attention. Prior to this period only systematic studies, dealing with detailed analysis of a number of gas-phase reactions, were undertaken.

Advancement of the analytical techniques, for example gas chromatography and mass spectroscopy, and reliability of the sources of visible and ultraviolet light over the past two to three decades has aided the photochemist to elucidate, with considerably more precision, the kinetics of the reactions involved. Under suitable conditions photochemistry may provide a short route to the synthesis of systems which are essentially unavailable by alternative synthetic methods. This aspect, coupled with the development of spectroscopic techniques for the direct study of transient intermediates has increased the flexibility and interest in photochemistry.

The idea that reactions involving free atoms may be of importance in chemical mechanisms came from Photochemistry and once the

significance of the Einstein Law of Photochemical Equivalence was recognised it became apparent that chain mechanisms must be responsible for the very large yields of reactions such as the photosynthesis of hydrogen chloride. The suggestion that organic chain reactions involving free radicals may occur in a similar way was made by H.S. Taylor[1] in 1925. In subsequent years such free radical mechanisms for photochemical reactions became increasingly prevalent. It was first shown by F. Paneth and W. Hafeditz[2] that free radicals, formed in the thermal decomposition of lead tetramethyl, could be detected by the now well-known "mirror technique". This work proved conclusively that methyl and ethyl radicals were capable of existence for an appreciable fraction of a second at room temperature and low pressures.

Metal alkyls have in the past been used photochemically for the purpose of studying the reactions of free radicals in the gas, liquid and solid phases. In the gas phase, this has been confined to alkyl derivatives of zinc, cadmium, mercury and lead. The liquid phase photochemistry has included more elaborate compounds, for example metal carbonyls and some of their derivatives and "Sandwich" compounds.

The Ministry of Aviation (now the Ministry of Technology) expressed considerable interest in the photochemistry of gaseous metal compounds connected with the deposition of metal films from the gas phase for use in the preparation of printed circuits. This research project was thus financed to study the photochemistry of gaseous compounds which may be useful in giving films of conducting or semi-conducting material.

The alkyl derivatives of tin were chosen as the compounds to study, their vapour pressures being high enough to facilitate handling in the gas phase and also SnO_2 would form a very good semi-conductor layer if a tin film was oxidised. Alkyl stannane photolysis would also be an extension on what has already been covered.

The introduction to this thesis includes the absorption spectra of some metal alkyls and the energy diagrams which conform to the observed spectra, a section on excited states, although little is known of the excited states involved in metal alkyls; photosensitisation which can be of considerable importance under certain conditions; radical reactions and their rate constants which are of primary importance in the photolysis of metal alkyls, pyrolysis and radiolysis which can be indicative as to the possibility of certain types of reactions taking place, mass spectroscopy as a possible analytical tool and also involves similar reactions; photolysis of metal alkyls already studied and the thermodynamics of metal alkyls and their possible reactions and the stability of metal alkyl radicals. The final section is a summary of the information gathered from the previous sections.

1.2 Absorption Spectra

The absorption spectra of metal alkyls were the subject of two reports, the first by Asundi, Bhasker Rao and Samuel[3] and the second in sections by Thompson and Linnett.[4-7] Those obtained by the former authors are shown in Figure 1.1, but they were unable to give the same definition and number of diffuse bands as the latter authors. The systems of bands obtained by Linnett and Thompson for certain compounds are shown in Figure 1.2 and interpreted satisfactorily by means of the energy diagrams shown in Figures 1.3 to 1.5. In all cases the band systems were overlapped by a continuous absorption which in general had well defined cut off limits. The band systems and continua agreed with that obtained by Terenin and Prelishajeva[8] and Duncan and Murray[9] in the case of zinc dimethyl which had no band system. The assumed ground state frequencies fall into line with the Raman frequencies.

The spectrum obtained for tetramethyl stannane was described by Linnett and Thompson as a continuum with a long wavelength limit of 2200Å. The short wavelength limit of their spectrometer appeared to be 2000Å and so the spectra of tetramethyl, tetrapropyl and tetrabutyl stannane were obtained at Laboratoire de Haute Pression, C.N.R.S., Bellvue, by the courtesty of Professor J. Romand, to short wavelength limits of 1500 Å and these are shown in Figure 1.6. The extinction coefficients at specific wavelengths are shown in Table 1.1 and are plotted in Figure 1.7.

TABLE 1.1

Wavelength	Molar extinction coefficient x 10^{-3} in litres/mole/cm.		
	$Sn(CH_3)_4$	$Sn(C_3H_7)_4$	$Sn(C_4H_9)_4$
2200 A	0.548	0.1657	
2150	0.7021	0.8189	
2100	1.743	1.000	
2050	3.684	2.440	
2000	7.766	4.734	3.033
1950	9.438	6.142	1.903
1900	11.45	9.032	1.903
1850	12.74	9.032	7.078
1800	10.84	7.720	9.651
1750	7.288	7.312	5.799
1700	5.711	5.893	5.026
1650	7.463	6.267	3.450
1600	13.86	9.832	3.822
1550	19.87	14.20	0.3866
1500	22.06	18.03	

Figure 1.1

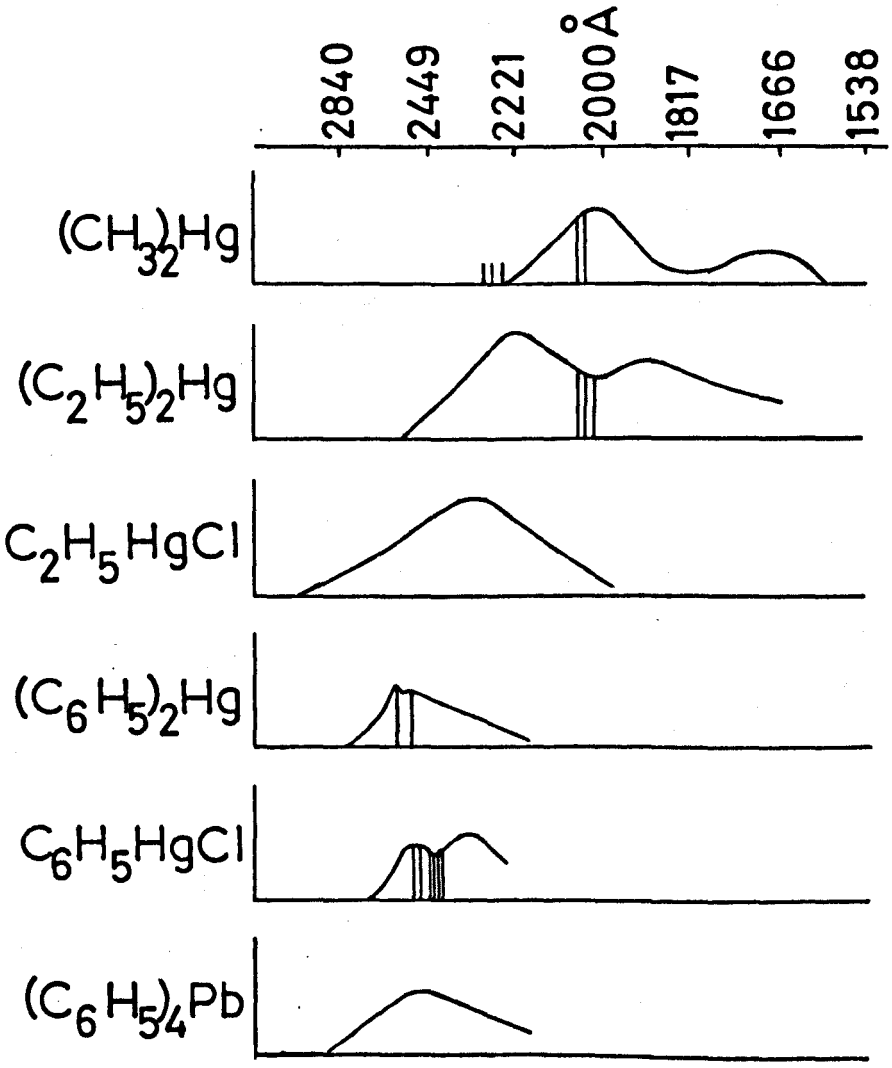
2840
2449
2221
2000Å
1817
1666
1538
$(CH_3)_2Hg$
$(C_2H_5)_2Hg$
C_2H_5HgCl
$(C_6H_5)_2Hg$
C_6H_5HgCl
$(C_6H_5)_4Pb$

Figure 1.2

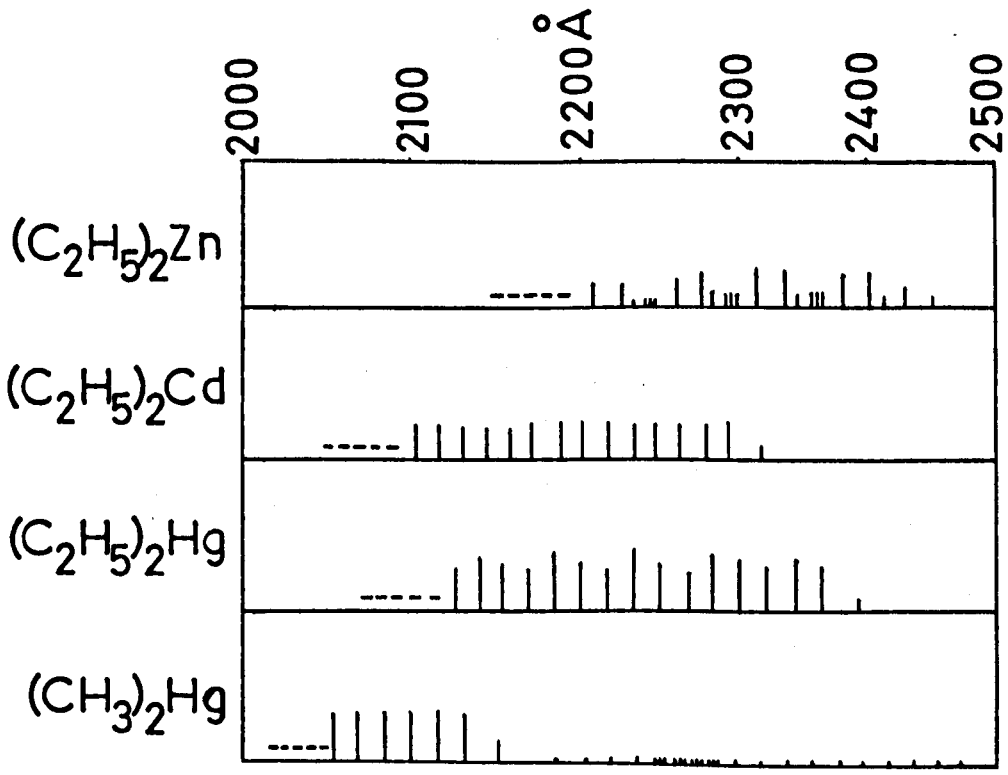
2000
2100
2200 Å
2300
2400
2500
$(C_2H_5)_2Zn$
$(C_2H_5)_2Cd$
$(C_2H_5)_2Hg$
$(CH_3)_2Hg$

Figure 1.3

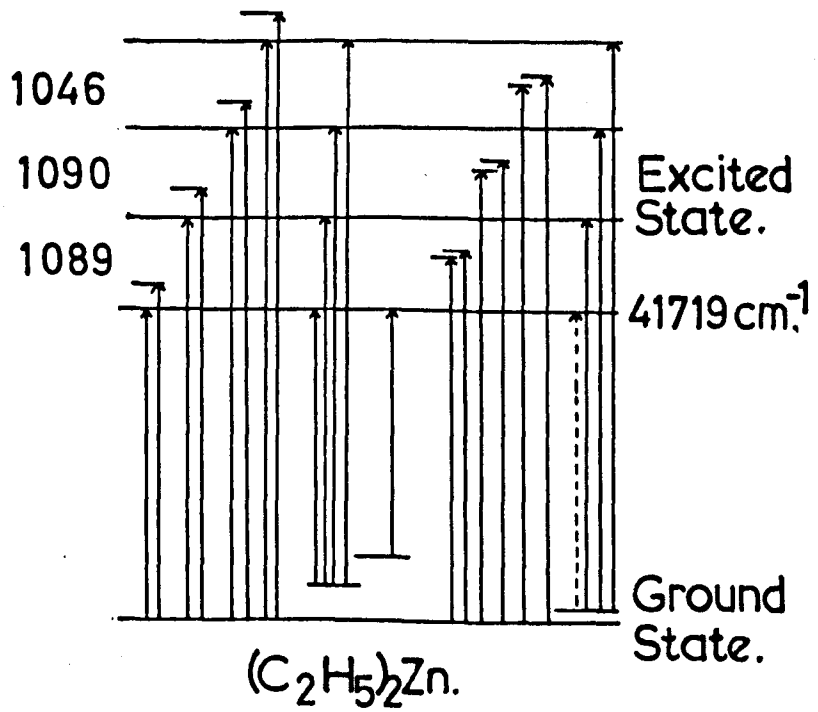
1046
1090
1089
Excited State.
41719 cm.-1
Ground State.
(C2H5)2Zn.

Figure 1.4

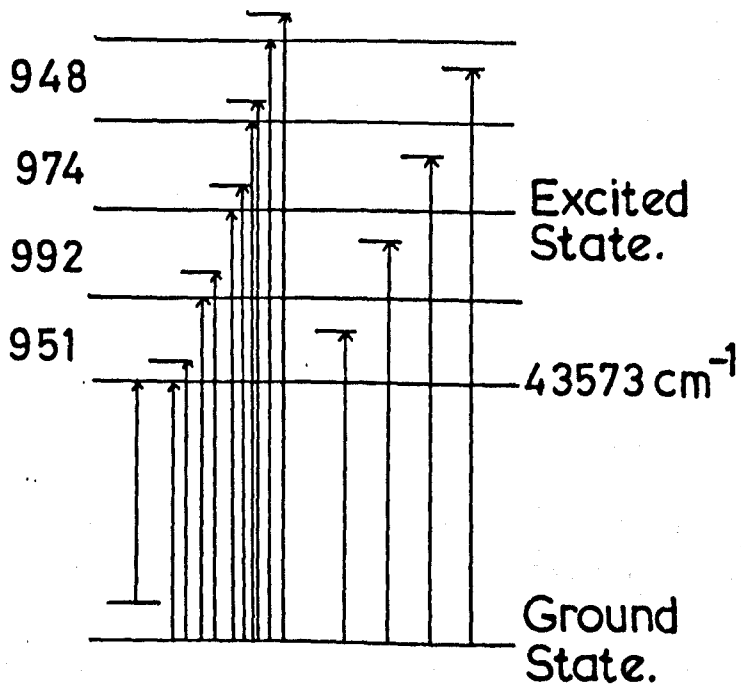

$(C_2H_5)_2Cd$

Figure 1.5

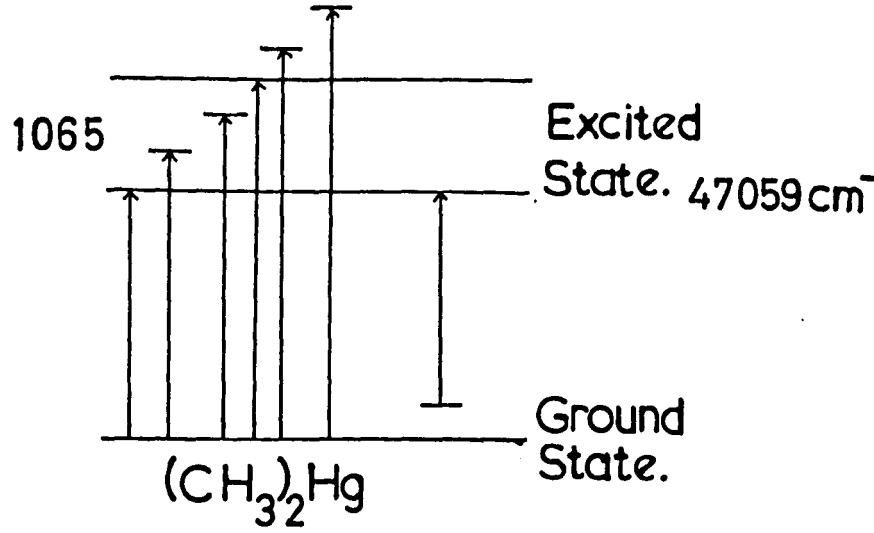
1065
Excited
State. 47059 cm-1
Ground
State.
(CH3)2Hg

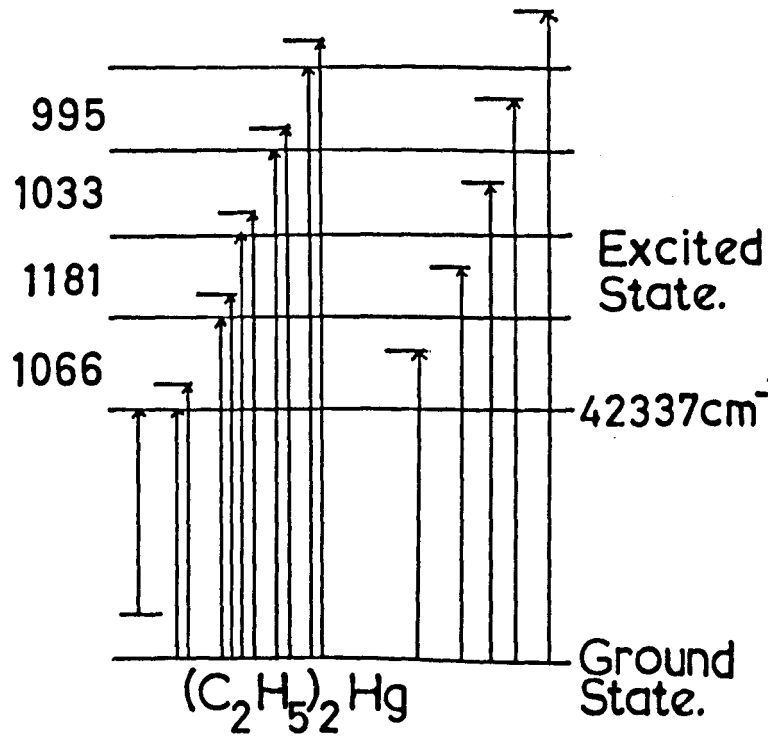
995
1033
1181
1066
Excited
State.
42337cm-1
Ground
State.
(C2H5)2Hg

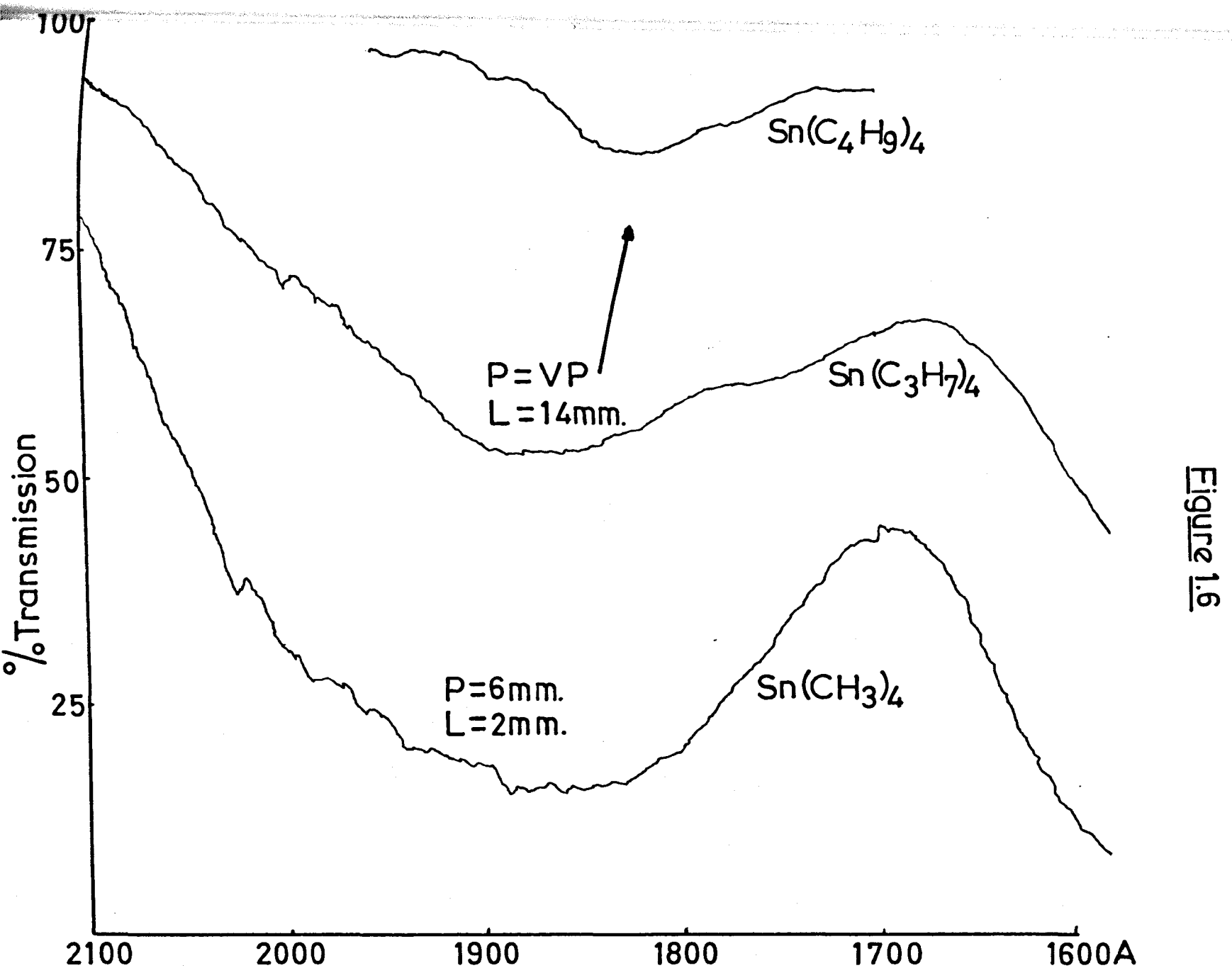
100
75
50
25
% Transmission
$Sn(C_4H_9)_4$
P = VP
L = 14mm.
$Sn(C_3H_7)_4$
P = 6mm.
L = 2mm.
$Sn(CH_3)_4$
2100
2000
1900
1800
1700
1600A

Figure 16

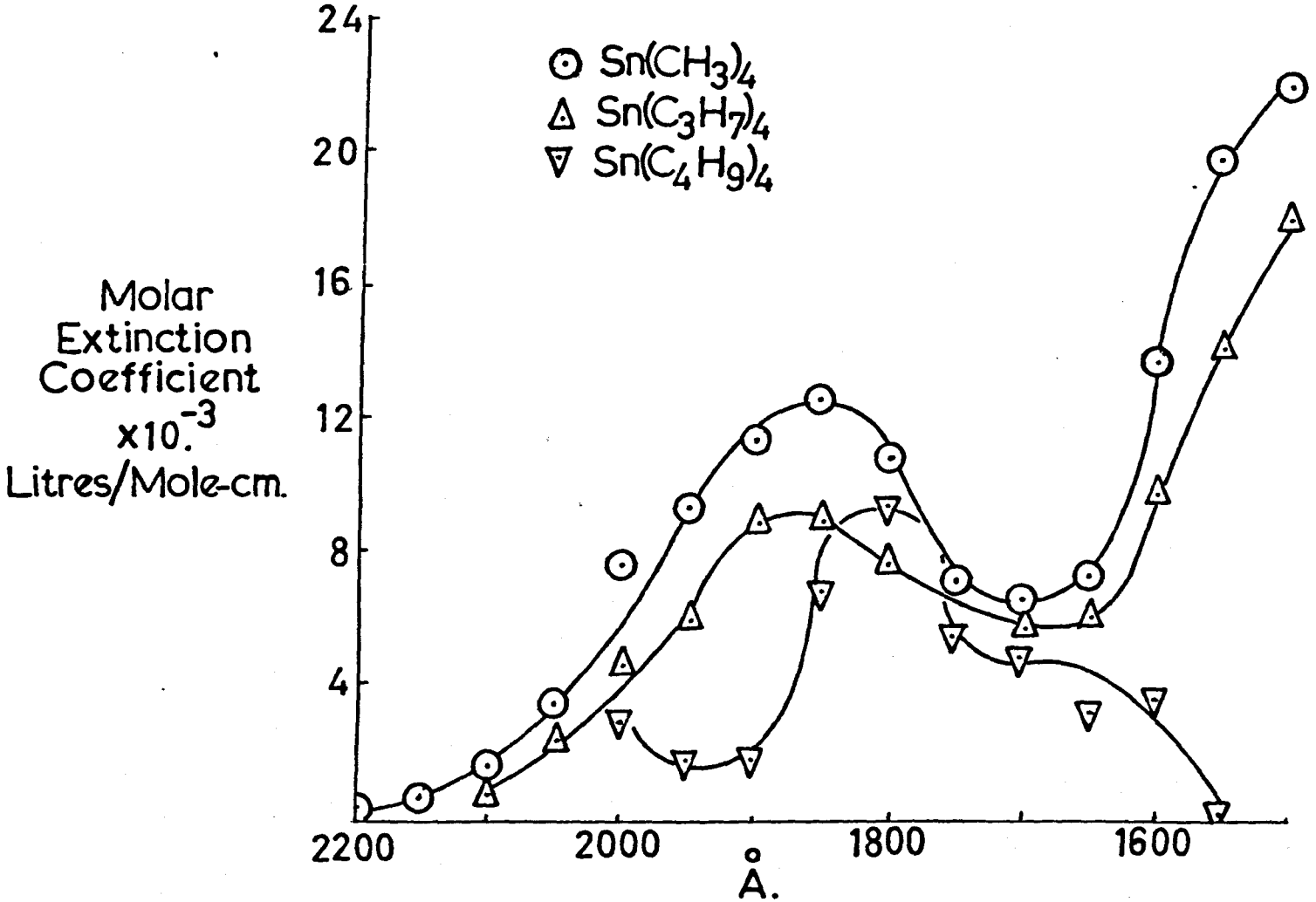
Molar Extinction Coefficient x10.-3 Litres/Mole-cm.
24
20
16
12
8
4
Sn(CH3)4
Sn(C3H7)4
Sn(C4H9)4
2200
2000
1800
1600
Å.

Figure 1.7

Thompson and Linnett came to the conclusion that the electronic excitation occurred in the metal-carbon linkages. This was after considering that the electronic excitation energy did not vary uniformly, mercury compounds being anomalous. The anomalous nature of the vibration frequencies of mercury alkyls has been referred to by Thompson and Linnett[5] and Popala Pai.[10]

The ultraviolet spectra of compounds of Group IV elements were studied by Petuchoff, Miranoff and Pekorigin.[11] The influence of substituents $-XR_3$ on $CH_2=CH-(CH_2)_n-XR_3$ was looked at where R is an alkyl radical and X is either Si, Ge or Sn. There exists a relationship between the bathochromic effect of the molecule and the * position of the absorption maxima of the molecule XR_4. The longer the wavelength of maximum absorption the greater the bathochromic shift and $\lambda_{max.}$ is dependent on the difference between the energy of the ground state and the excited state. This means that the effect is connected not only with the ground state of the substituent but also its excited state.

Since the effect is quite considerable these states must be determined by the valency electrons which form the σ-bonds and not the d-orbitals; the energy differences of which are so small and would not cause significant changes in the spectra. This agrees fully with the conclusions of Linnett and Thompson and it may be assumed that the $\lambda_{max.}$ i.e. 1850Å for $Sn(Me)_4$ is due to electronic excitation of the σ-bond.

1.3 Excited States

By international agreement the symbol for the upper state is written first and that for the lower state last regardless of whether the process is absorption or emission.[12] In enumerative notation singlet states are labelled S_0, S_1, S_2 etc, in order of increasing energy with So being the ground state and triplets[13] are labelled T_1, T_2, T_3 etc. Mulliken[14,15] employs different capital letters to represent the states, N (normal) being the ground state and V, Q, R for example representing excited states. One can also describe electronic transitions in terms of the initial and final orbitals occupied by the single electron involved in the transition;[16] a relatively simple system but less precise than say symmetry notation.

Once an excited singlet S_1 state has been produced by the electronic transition from a ground state the energy gained from the exciting light may be lost by the following processes,[16] as illustrated with an adapted Jablonski diagram, Figure 1.8:-

1. Dissociation of a vibronic state to yield photochemical products.
2. Collisional deactivation of a vibronic state.
3. Fluorescence: radiative conversion to the ground state.
4. Internal conversion: non-radiative conversion to the ground state, internal conversion from higher excited states to the lowest singlet state takes place very fast, 10^{-13} - 10^{-14} secs.

Figure 1.8

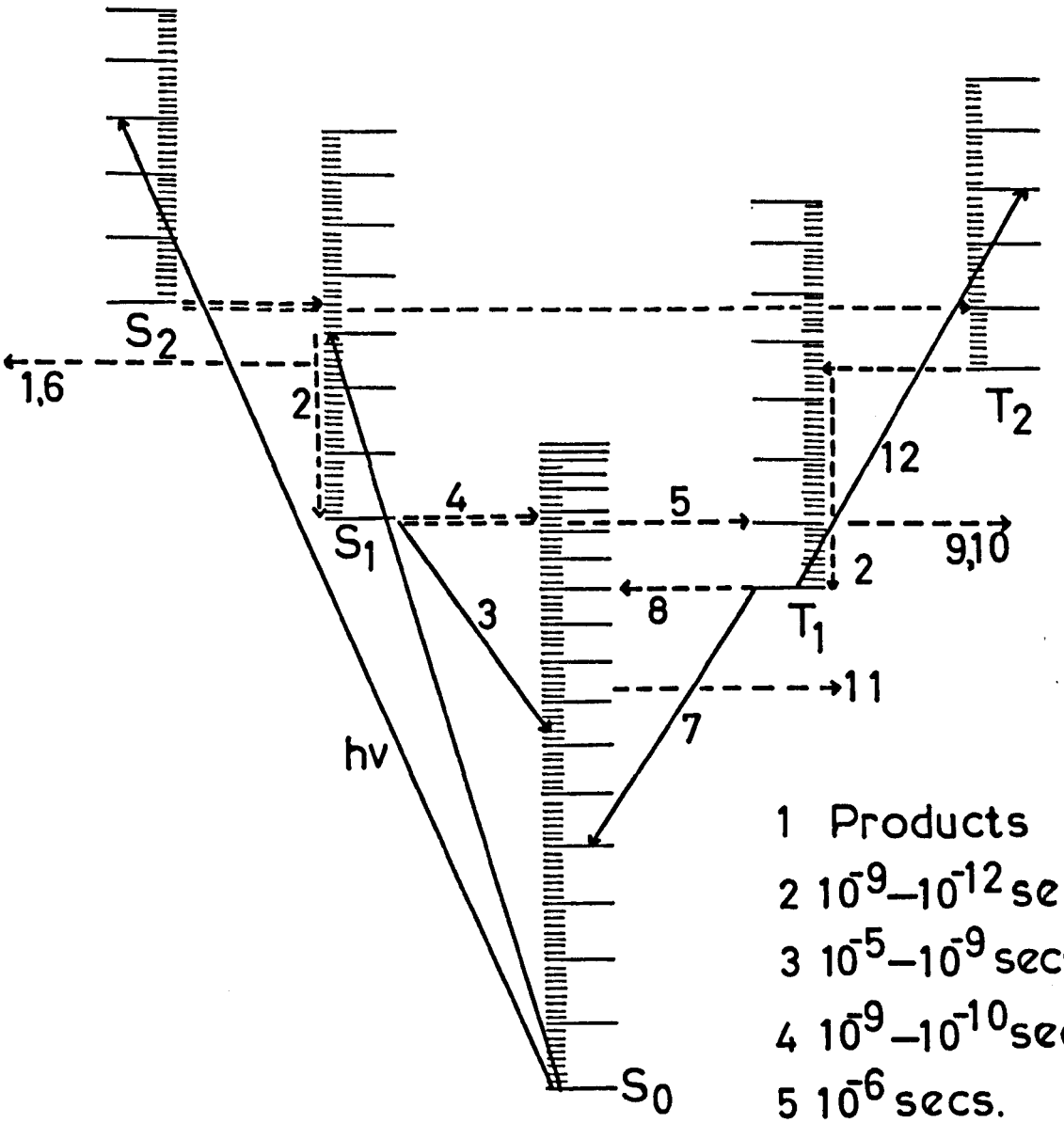

1 Products

2 10^{-9}–10^{-12} secs.

3 10^{-5}–10^{-9} secs.

4 10^{-9}–10^{-10} secs.

5 10^{-6} secs.

6 Products

7 10^{-5}–10^{-3} secs.

8 as 5

9 Products

10 Transfer

11 Products

5. Intersystem crossing: non-radiative transition to a vibrationally excited triplet state which is then vibronically deactivated.

6. Energy transfer non-radiatively to a neighbouring molecule.

The triplet state produced in (5) may lose its energy by:-

7. Phosphorescence: radiative intercombination with the ground state.

8. Internal conversion: non-radiative intercombination with the ground state.

9. Photochemical dissociation from the ground state.

10. Triplet-Triplet energy transfer: non-radiative transfer of electronic energy to a neighbouring molecule.

The ground state molecule produced by internal conversions (4) and (8), may be highly vibrationally excited and may lose its energy by:-

11. Dissociation of the vibrationally excited ground state to yield photochemical products.

There is another possible mode of action of a triplet state and that is, 12. Absorption of more light resulting in triplet-triplet absorption bands.

If an excited molecule is not deactivated or does not decompose, it will return to the ground state after a certain length of time with emission of radiation (3). If $A_{n.m.}$ is the average number of transition per molecule per second between the upper state (n) and lower state (m), the mean life of state n is defined as:

$$= \frac{1}{A_{n.m.}} \qquad 1.I$$

$A_{n.m.}$ is the Einstein transition probability of spontaneous emission, and governs the intensity of emission from the upper state. Hence each excited state has a mean life - τ, and if a molecule is to undergo reaction in the excited state the rate constant for the reaction must be shorter than the mean lifetime. The mean lifetime is also inversely proportional to the absorption strength of the excited state. The Beer-Lambert Law[17] states that the integrated fraction of light absorbed by an assembly of molecules is proportional to the number of absorbing systems in the light path, viz.

$$\log \frac{I_o}{I} = \varepsilon.c.l. \qquad \text{1.II}$$

where I_o and I are the incident and transmitted intensities respectively, l the path length in cms. and c the concentration in moles per litre, ε is the molar extinction coefficient in litres per mole per cm. The mean lifetime and ε are related by:-

$$\int_{V_1}^{V_2} \varepsilon dV = \frac{\lambda o^2}{8\pi} \frac{No}{\tau} \qquad \text{1.III}$$

where λo is the wavelength of the maximum of absorption band, No is Avogadro's Number and V_1 and V_2, the limits of the absorption band, are in units of frequency. The value of $\int_{V_1}^{V_2} \varepsilon dV$ may be taken as ε_{max}.

times the peak width at half peak height. In the near U.V. this can be approximated to

$$\tau = \frac{10^{-4}}{\epsilon_{max.}} \qquad \text{(reference 18)} \qquad \text{1.IV}$$

Thus for the transition in tetramethyl stannane where $\epsilon_{max.}$ is of the order of 12,000 litres/mole/cm, τ is of the order of 8×10^{-9} secs.

1.4 Photosensitisation

In order that a photochemical reaction may occur it is necessary in the first place that the magnitude of the quantum of the incident light be large enough and secondly that the light be absorbed. In many cases compounds have dissociation energies corresponding to wavelengths in a convenient region of the spectrum but are themselves transparent in that region. If a molecule, that can absorb the necessary wavelength and transfer the energy to the transparent compound, is added it is possible to produce what is termed a photosensitised dissociation or reaction. It can be seen that under certain conditions, for example irradiation of a compound with a low pressure mercury vapour lamp which has a maximum output at 2537Å which is also absorbed by mercury atoms, exclusion of certain atoms or molecules must be absolute otherwise the reaction produced may be sensitised. (See Table 1.2 for Hg.)[19]

The mercury-sensitised decomposition of mercury dimethyl at low pressure was studied by Kabarle.[20] It was shown to proceed by the reaction

$$Hg^{*} + Hg(CH_3)_2 \rightarrow (Hg + HgCH_3 + CH_3) \rightarrow Hg + Hg + 2CH_3 \qquad 1.1$$

and the rate constant for methyl radical combination equal to $k = 8 \times 10^{-11}$ molecules^{-1}cc.sec.$^{-1}$ was determined. In experiments with a 1:1 mixture of ordinary and deuterated mercury dimethyl the recombination product CD_3HgCH_3 could not be detected.

TABLE 1.2

	Hg
PRINCIPAL QUANTUM NUMBER, n:	6
Singlet - Singlet	
$n\,(^1P_1) \rightarrow n\,(^1So) + h\nu$	
wavelength; Å	1849
Energy k-cals/Einstein	154.6
Radiative lifetime seconds	1.3×10^{-9}
Triplet - Singlet	
$n\,(^3P_1) \rightarrow n\,(^1So) + h\nu$	
wavelength; Å	2537
Energy k-cals/Einstein	112.7
Radiative lifetime seconds	1.1×10^{-7}

1.5 Radical Reactions

As far as the photolysis of metal alkyls are concerned radical reactions are of extreme importance. Besides the normal combination and disproportionation reactions that radicals can take part in, the only other type of reaction that may be relevant is referred to as fragmentation. The most common example of this type is known as β-fragmentation, in which the pair of electrons beta to the odd electron splits up and a radical is ejected:

$$-\overset{\overset{R}{|}}{\underset{\bullet\bullet}{C}}-\overset{\bullet}{C}- \quad \rightarrow \quad R^{\bullet} + >C = C< \qquad 1.2$$

This reaction is the reverse of addition to a double bond and generally gives rise to a more stable radical.

In Table 1.3 are listed the rate constants of relevant radical reactions. Further up-to-date values that are important are ratios of disproportionation to combination. These are given in Table 1.3a.

TABLE 1.3

REACTION	TEMP.	PRESS.	k is in litre/mole/sec. log k	REFERENCE
$CH_3 + CH_3 \rightarrow C_2H_6$	135°C	30 mm	10.52	48
"	165°C		10.57	81
"	161°C	9 mmHe	10.13	82
"	344°C	$2\text{-}25\times10^{-3}$ mm	9.92	82
"	814°C	$Hg(CH_3)_2$	9.62	82
"	125,135°C		10.38	83
"	165,175°C		10.30	83
"	134°C	230 mm	10.36	84
$CH_3 + C_2H_5 \rightarrow CH_4 + C_2H_4$	25-175°C	40-80 mm	9.2	85
"	110-200°C		9.3	86
$CH_3 + C_2H_5 \rightarrow C_3H_8$	25-175°C	40-80 mm	10.6	85
"	100°C		10.62	87
$C_2H_5 + C_2H_5 \rightarrow C_4H_{10}$	150°C	0-80 mm	10.2	47
"	50°C	46 mm	10.18	88
"	100°C	36 mm	10.3	89
"	150°C	8 mm	10.62	89
$C_2H_5 + C_2H_5 \rightarrow C_2H_6 + C_2H_4$	150°C	0-80 mm	9.8	88
"	50°C	46 mm	9.3	88
"	100°C	36 mm	9.5	88
"	150°C	8 mm	9.7	88
"	50°C	15-80 mm	9.4	90
"	100°C	15-80 mm	9.5	90
"	150°C	15-80 mm	9.8	90
$CH_3 + C_3H_7$				

TABLE 1.3a[93]

$$R + R' \xrightarrow{kd} RH + \text{olefin} \qquad 1.3$$

$$R + R' \xrightarrow{kc} R\text{-}R' \qquad 1.4$$

R	R'	kd/kc	Temperature
CH_3	C_2H_5	0.036	298°K
C_2H_5	C_2H_5	0.135	298°K
CH_3	$n\text{-}C_3H_7$	0.058	298°K
$n\text{-}C_3H_7$	$n\text{-}C_3H_7$	0.154	298°K

1.6 Pyrolysis

Pyrolysis can in certain cases be quite helpful in indicating the types of reactions that can take place in the photochemistry although no direct linkage can be made. The classical work of Paneth and Hafedtz[2] which demonstrated the presence of free radicals in the thermal decomposition of lead tetramethyl and the wide applicability of free radical mechanism to the kinetics of vapour phase thermal decomposition of both metal alkyl and organic compounds led to attempts being made to account for the kinetics of so-called quasi unimolecular reactions in terms of atomic and free radical mechanisms.[22]

In view of these facts and investigations carried out by Yeddanapolli and Schubert[23] on $Al(CH_3)_3$ and Taylor and Cunningham[24] on $Hg(CH_3)_2$ it is surprising to find that the thermal decomposition of tetramethyl stannane was reported by Waring and Horton,[25] 1945, to be of first order dependence in $Sn(CH_3)_4$ concentration involving not a free radical mechanism but essentially a molecular rearrangement as shown below:

$$Sn(CH_3)_4 \rightarrow \begin{cases} Sn + 2C_2H_4 + 2H_2 & 1.5 \\ Sn + C_2H_4 + 2CH_4 & 1.6 \\ Sn + C + 3CH_4 & 1.7 \end{cases}$$

Although the possibility of rupture on the Sn-C bond to give free radicals was recognised it was, however, accorded only a negligible

probability.

The experimental results of Waring and Horton were re-examined by Sathyamurphy, Swaminathan and Yeddanapolli[26] and were shown to fit in better with a three halves order on tetramethyl stannane concentration and a free radical mechanism rather than a first order dependence and a molecular rearrangement. The proposed free radical mechanism may be represented by the following sequence of reactions:

$$Sn(CH_3)_4 \rightarrow Sn(CH_3)_3 + CH_3 \qquad 1.8$$

$Sn(CH_3)_3$ may further break down to give more methyl radicals and ultimately tin. The CH_3 radicals react with metal alkyl according to the equation

$$Sn(CH_3)_4 + CH_3 \rightarrow CH_4 + Sn(CH_3)_3\dot{C}H_2 \qquad 1.9$$

The latter may, by analogy with other complex radicals, tend to lose a CH_3 and revert to a stable molecule thus

$$Sn(CH_3)_3\dot{C}H_2 \rightarrow CH_3 + (CH_3)_2Sn = CH_2 \qquad 1.10$$

The chain ending process is the recombination of the methyl radicals.

The small percentages of ethylene and hydrogen were accounted

for partly by dissociation of ethane and partly by the breakdown of the metal alkyl molecules according to the equations suggested by Waring and Horton.

The pyrolysis of lead tetramethyl was studied by Pratt and Parnell[27] but the most recent investigation is by Hoare, Ting-Man Li and Walsh[28] in a static system in the presence and absence of toluene. The major products were found to be methane and ethane and in the absence of toluene, propane and a smaller amount of ethylene were minor products. Under the conditions used, the tetramethyl lead pyrolysis was homogeneous and non-chain. Included in the reaction steps were

$$CH_3^{\bullet} + Pb(CH_3)_4 \xrightarrow{k_{11}} CH_4 + (CH_3)_3Pb\dot{C}H_2 \qquad 1.11$$

$$CH_3 + C_6H_5CH_3 \xrightarrow{k_{12}} CH_4 + C_6H_5\dot{C}H_2 \qquad 1.12$$

$$CH_3 + CH_3 \xrightarrow{k_{13}} C_2H_6 \qquad 1.13$$

Values were obtained for $k_{11}/k_{13}^{\frac{1}{2}}$ over the temperature range 140 - 371°C and $E_{11} - \frac{1}{2}E_{13}$ was found to be 14.1 ± 0.9 k-cals. per mole. The value of $E_{12} - \frac{1}{2}E_{13}$ was 12.6 ± 0.5 k-cals. per mole.

1.7 Radiolysis

Here again as in pyrolysis further information may be gained as to the types of reactions that can be possible in photolysis of stannanes. In the radiolysis of liquid tetramethyl stannane[29] the most important products are ethyl trimethyl stannane, hexamethyl distannane and bis-(trimethyl stanyl) methylene. These compounds may refer to the formation of $(CH_3)_3\dot{S}nCH_2$ radicals originating from the sequence

$$Sn(CH_3)_4 \rightarrow CH_3 + Sn(CH_3)_3 \qquad 1.14$$

$$CH_3 + Sn(CH_3)_4 \rightarrow CH_4 + (CH_3)_3\dot{S}nCH_2 \qquad 1.15$$

This is further established by the identification of methane and ethane.

Irradiation of dimethyl diethyl stannane caused the formation of numerous products. Ethyl trimethyl stannane, methyl triethyl and small quantities of tetramethyl stannane were detected. The gas chromatograms showed other compounds which were not identified but were tentatively assumed to be tetra alkyl stannanes with one higher alkyl group in the molecule e.g. propyl or butyl. The greater number of combinations leads to a greater number of compounds with Sn-Sn bonds.

Also tetraethyl stannane behaves in a similar way as shown below

$$Sn(C_2H_5)_4 \rightarrow {}^{\bullet}Sn(C_2H_5)_3 + C_2H_5 \qquad 1.16$$

$$2\ Sn(C_2H_5)_3 \rightarrow (C_2H_5)_3Sn\text{-}Sn(C_2H_5)_3 \qquad 1.17$$

$$C_2H_5 + Sn(C_2H_5)_4 \rightarrow C_2H_6 + {}^{\bullet}C_2H_4Sn(C_2H_5)_3 \qquad 1.18$$

$$\dot{C}_2H_4Sn(C_2H_5)_3 \rightarrow {}^{\bullet}Sn(C_2H_5)_3 + C_2H_4 \qquad 1.19$$

On prolonged irradiation all examined samples became yellow suggesting the formation of tin organic compounds with a number of Sn-Sn bonds per molecule. The colour was stable until the samples were opened to the atmosphere. Addition of oxygen as a radical scavenger strongly depresses the product formation, but new unidentified compounds appeared in the gas chromatogram.

The radiolysis of liquid mercury di-n-hexyl[30] gave mercury, hexane, hexene and dodecane as the principle products indicating that only mercury-carbon bond cleavage takes place. The ratio of disproportionatio to combination of n-hexyl radicals in this environment was 0.73. A study of the effect of varying the dose-rate on the system indicated that the chain reaction

$$C_6H_{13}^{\bullet} + Hg(C_6H_{13})_2 \rightarrow C_6H_{14} + C_6H_{12} + Hg + C_6H_{13}^{\bullet} \qquad 1.20$$

takes place. The rate constant for this reaction was estimated as 38 litres per moles per sec. being low due to a low pre-exponential factor.

1.8 Mass Spectroscopy

It is thought possible that mass spectroscopy may be a useful tool in indicating the types of compounds that are formed in the proposed photolysis. The behaviour of tetramethyl stannane[72] corresponds qualitatively to that of tetramethyl germane and tetramethyl lead. The main fragment ions, in order of abundance, are $Sn(CH_3)_3^+$, $SnCH_3^+$, $Sn(CH_3)_2^+$, Sn^+, CH_3^+, Sn^+ and $SnCH_2^+$. The relative proportions in Table 1.4 were obtained from reference 74.

TABLE 1.4

ION	SnR_4^+	SnR_3^+	SnR_2^+	SnR^+	SnH^+	Sn^+	R^+
RELATIVE PROPORTION	0.6	100	21	27	6	12	2

($R = CH_3$)

The mass spectroscopy of tin compounds is complicated by the fact that tin has several isotopes which are stable.

TABLE 1.5

ATOMIC WEIGHT	ABUNDANCE
112	1.0 %
116	14.3 %
117	7.6 %
118	24.0 %
119	8.6 %
120	32.9 %
122	4.9 %
124	5.9 %

This of course may lead to difficulties in finding products from mass spectra since in normal circumstances a large proportion of product must be present in order to be observed in the mass spectra.

With higher alkyl substituents[73,74] ligand loss by elimination of an unsaturated hydrocarbon with hydrogen rearrangement gives rise to many of the intense peaks in their spectra. This process is a minor one in the fragmentation of the molecular ion but is a major one in the fragmentation of (M-R) ions.

$$SnR_3^+ \rightarrow SnR_2H^+ \rightarrow SnRH_2^+ \qquad 1.21$$

The elimination of neutral ligand pairs by reaction

$$Sn(Me)_3^+ \rightarrow SnMe^+ \qquad 1.22$$

has been observed.

In contrast to the corresponding lead alkyls the spectra of tin alkyls show a low abundance of ions from which part of a ligand is lost, however the reaction

$$:SnR^+ \rightarrow :SnCH_3^+ \qquad 1.23$$

was observed in the cases of $Sn(C_3H_7)_4$ and $Sn(C_4H_9)_4$.

1.9 Photolysis

1.9a Gas Phase

This section is split up into three parts covering the gas phase photolysis of metal hydrides, metal carbonyls and metal alkyls. The former two groups are small but of sufficient interest in that it is possible that metal hydrogen bonds may be formed in elimination of C_2H_4 from the $Sn-C_2H_5$ group of ethyl trimethyl stannane, also metal carbonyls have metal carbon bonds and their breakdown may be similar to metal alkyls.

1.9a.1 Metal Hydrides

The first report of any photolysis of metal hydrides appeared in 1910 by A. Smits and A.H.W. Aren[31] who reported the photodecomposition of Stibine. Cheesman and Emeleus[32] in studying the absorption spectra of arsine and also Stibine recorded that from AsH_3 hydrogen was formed together with a brown black deposit which they presumed to be arsenic. Long exposures of SbH_3 were impossible at room temperature owing to its rapid surface decomposition.

Both the sensitised and unsensitised decomposition of germane were studied by Romeyn and Noyes[33] and they lead largely to the reaction

$$GeH_4 \rightarrow Ge + 2H_2 \qquad 1.24$$

The removal of one hydrogen atom from Germane appeared to be followed by a series of stepwise eliminations too rapid however to be decisive in determining the rate.

The mercury photosensitised decomposition of gaseous arsine[34] corresponds to the stoichiometric equation

$$AsH_3 \rightarrow As + {}^3/_2H_2 \qquad 1.25$$

The rate of decomposition was directly proportional to the intensity and was independent of arsine pressure.

The sensitised decomposition of monosilane[35] gave hydrogen and a solid product of a polymeric nature, the composition of $SiH_x (x < 0.9)$ suggests a mixture of silicon and polymer. The mercury sensitised decomposition of monosilane has recently been studied by Niki and Mains[36] and gave quantum yields of 1.8 for hydrogen and 0.6 for disilane. Polymeric silicon hydride was deposited on the walls. The failure of a large concentration of ethylene to reduce the yield or isotopic distribution of hydrogen from the decomposition of a SiH_4-SiD_4 indicates that the reaction between atomic hydrogen and monosilane is very rapid.

1.9a.2 Metal Carbonyls

Spectral measurements reported by Garratt and Thompson[37] led to the suggestion of the following mechanism for the photochemical decomposition of nickel carbonyl:

$$Ni(CO)_4 + h\nu \rightarrow Ni(CO)_3 + CO \qquad 1.26$$

$$Ni(CO)_3 \rightarrow Ni + 3CO \qquad 1.27$$

This was substantiated by Garratt and Thompson[38] when they measured the rate of photochemical decomposition of $Ni(CO)_4$ using light of varying wavelengths in the gas phase and in the solvents CCl_4, C_6H_{14} and cyclohexane. In the gas phase a thermal recombination balances the photochemical decomposition so that no change was observed. In the solvents the quantum efficiency increased somewhat with frequency from a threshold value corresponding to the limit of continuous absorption in the spectrum. Taken as a whole the results complied with the mechanism above plus

$$Ni(CO)_3 + CO \rightarrow Ni(CO)_4 \qquad 1.28$$

In 1961 Callear[39] studied the photodecomposition of $Ni(CO)_4$ by flash photolysis and showed that at low conversion the rate of reaction depended on the square of the flash energy. This was

interpreted by the mechanism

$$Ni(CO)_4 + h\nu \rightarrow Ni(CO)_3 + CO \qquad 1.26$$

$$Ni(CO)_3 + h\nu \rightarrow Ni(CO)_2 + CO \qquad 1.29$$

$$2Ni(CO)_2 \rightarrow \text{solid products} \qquad 1.30$$

The decomposition was strongly inhibited by carbon monoxide which recombined with $Ni(CO)_2$ and $Ni(CO)_3$ and required a third body. At high pressures, the mean collision efficiencies of the reactions

$$Ni(CO)_3 + CO \xrightarrow{M} Ni(CO)_4 \qquad 1.31$$

$$Ni(CO)_2 + CO \xrightarrow{M} Ni(CO)_3 \qquad 1.32$$

were about 3×10^{-3}, the mean lifetime of chemically activated $Ni(CO)_4$ was 7×10^{-9} secs.

1.9a.3 Metal Alkyls

Terenin and co-workers[8,41,42] investigated the photolysis of mercury dimethyl and showed by the Paneth technique[2] that free radicals were formed in the photolysis, the maximum yield of radicals occurring at about 2100Å wavelength of incident light. In the photolysis of lead tetramethyl Leighton and Mortensen[43] similarly detected methyl radicals.

A more detailed investigation of the photolysis of mercury dimethyl was made by Linnett and Thompson[6] who used radiation of 2537Å wavelength and found that ethane was almost the sole product at room temperature. On this basis they suggested that the primary step in the decomposition was

$$Hg(CH_3)_2 \xrightarrow{h\nu} Hg + C_2H_6 \qquad 1.33$$

In a later paper[7] they investigated the effect of temperature and presence of nitric oxide on the reaction. The results showed that the quantum yields increased at higher temperatures, above the value of unity obtained at room temperature. The results in the presence of nitric oxide were complex but favoured the idea of a free radical mechanism.

$Hg(CH_3)_2 + h\nu$	→	$HgCH_3 + CH_3$	1.34
$HgCH_3$	→	$Hg + CH_3$	1.35
$Hg(CH_3)_2 + HgCH_3$	→	$Hg + C_2H_6 + HgCH_3$	1.36
$CH_3 + Hg(CH_3)_2$	→	$HgCH_3 + C_2H_6$	1.37
$CH_3 + Hg(CH_3)_2$	→	$Hg + CH_3 + C_2H_6$	1.38
$2CH_3$	→	C_2H_6	1.39
$CH_3 + HgCH_3$	→	$Hg + C_2H_6$	1.40
$2\ HgCH_3$	→	$2\ Hg + C_2H_6$	1.41

This mechanism explains the results provided it is assumed that the activation energies of reactions 1.34, 1.35, 1.36 are high. They will thus have no effect at room temperature and the quantum yield of unity would be due to the sequence 1.34, 1.35, 1.36 or 1.34, 1.39, 1.40, 1.41. At higher temperatures the occurrence of reactions 1.36, 1.37 and 1.38 will give the whole reaction chain characteristics and cause the quantum yield to rise. Linnett and Thompson estimated an activation energy of 10.7 k. cals. per mole for the chain carrying step. This corresponds probably to that of reaction 1.37 as 1.38.

Since Leighton and Mortensen found higher quantum yields for the photolysis of lead tetramethyl than were found in their case, Linnett and Thompson suggested that the activation energy of the reaction of methyl radicals with lead tetramethyl was lower than 10 k.cals per mole.

Cunningham and Taylor[24] investigated the photolysis of mercury dimethyl in more detail and with special emphasis on the effect of hydrogen on the reaction. In the presence of hydrogen the rate increased several fold, and the formation of methane was greatly increased. They interpreted this as being due to

$$CH_3 + H_2 \rightarrow CH_4 + H^\bullet \qquad 1.42$$

$$H^\bullet + Hg(CH_3)_2 \rightarrow CH_4 + Hg + CH_3 \qquad 1.43$$

On the basis of this mechanism a steady state treatment of the results yielded a value of 8.1 k-cals. per mole (see also ref. 44) for the activation energy of reaction 1.42 if it is assumed that E = 0 for the recombination of two methyl radicals.

They suggested that ethane arose entirely from recombination in the absence of hydrogen, but the increase in quantum yield with rise in temperature indicated perhaps

$$CH_3 + Hg(CH_3)_2 \rightarrow C_2H_6 + Hg + CH_3 \qquad 1.38$$

The photolysis of mercury diethyl and zinc diethyl was investigated by Moore and Taylor.[45] The products at low temperature were ethylene and ethane in roughly equal quantities and hydrogen and butene also in equal quantities, together with considerable quantities of butane. At higher temperatures ethane increased relative to ethylene

and hydrogen was no longer a product. Moore and Taylor accounted for the increased quantum yields at higher temperatures by a chain mechanism similar to that for mercury dimethyl viz.

$$C_2H_5 + M(C_2H_5)_2 \rightarrow C_4H_{10} + C_2H_5 + M \qquad 1.44$$

$$\rightarrow C_2H_4 + C_2H_6 + C_2H_5 + M \qquad 1.45$$

The rates of formation of methane and ethane during irradiation of mercury dimethyl as functions of intensity, pressure and temperature were studied by Gomer and Noyes.[46] At temperatures below 250°C methane was thought to be formed by reaction

$$CH_3 + Hg(CH_3)_2 \rightarrow CH_4 + CH_3HgCH_2 \qquad 1.46$$

(This was also suggested by Moore and Taylor to explain methane formation in the absence of hydrogen). Ethane was formed by at least two processes, one of which was the combination of methyl radicals and the other was the reaction of methyl radicals with mercury dimethyl which proceeded through an unstable intermediate addition complex.

In 1951 Ivin and Steacie[47] investigated the disproportionation and combination of ethyl radicals. They photolysed mercury diethyl vapour in a static system over a pressure range 0 - 80 mm. and a temperature range 75 - 200°C. Rotating sector techniques enabled a complete determination of the velocity constants of the combination and

disproportionation of ethyl radicals and the following reaction:

$$C_2H_5 + Hg(C_2H_5)_2 \rightarrow C_2H_4 + C_2H_6 + Hg + C_2H_5 \quad 1.47$$

The rotating sector technique was applied to a determination of the rate constants of methyl radical combination in the photo-decomposition of acetone and mercury dimethyl by Gomer and Kistiakowsky.[48] The resulting value of the rate constant was $2.1 \times 10^9 T^{\frac{1}{2}}$ litres/mole/sec. with an activation energy of E = 0 ± 700 cals. regardless of the radical source. The determination of the rate constant made possible the calculation of the rate constants for several reactions:

		k.(litre/mole/sec.)
$CH_3 + CH_3 \rightarrow$	C_2H_6	$2.1 \times 10^9 T^{\frac{1}{2}}$
$CH_3 + (CH_3)_2CO \rightarrow$	$CH_4 + ...$	$1.8 \times 10^7 T^{\frac{1}{2}} e^{\frac{-9500}{RT}}$
$CH_3 + Hg(CH_3)_2 \rightarrow$	$CH_4 + ...$	$4.1 \times 10^6 T^{\frac{1}{2}} e^{\frac{9000}{RT}}$
$CH_3 + (CH_2)_2CO \rightarrow$	$CH_4 + ...$	$1.4 \times 10^6 T^{\frac{1}{2}} e^{\frac{-9000}{RT}}$
$CH_3 + C_4H_{10} \rightarrow$	$CH_4 + ...$	$3.6 \times 10^6 T^{\frac{1}{2}} e^{\frac{-8200}{RT}}$

(Refer also to Dorfman and Gomer[49]).

Values obtained for activation energies agreed quite well with those of Trotman-Dickenson and Steacie.[50]

The photochemical decomposition of the trialkyl gallium compounds $Ga(Me)_3$, $Ga(Et)_3$, $Ga(isopropyl)_3$, and $Ga(isobutyl)_3$ was reported in 1951 by

Plust.[51] Anderson and Taylor[52] reported the photochemical decomposition of dimethyl cadmium.

Miller and Steacie[53] investigated the rate at room temperature of recombination of methyl radicals by photolysing $Hg(CH_3)_2$ in the presence of nitric oxide and compared the rates of the reactions

$$CH_3 + CH_3 \xrightarrow{k_{39}} C_2H_6 \qquad 1.39$$

$$CH_3 + NO \xrightarrow{k_{48}} CH_3NO \qquad 1.48$$

It was calculated that $k_{39}^{\frac{1}{2}}/k_{48}$ is approximately equal to 3×10^{-5} (moles sec./cc.)$^{\frac{1}{2}}$. If Forsyth's[54] value for k_{48} is acceptable the ratio leads to a collision yield of methyl radical combination 4.4×10^{-5}.

The reactions of methyl radicals formed in the photolysis of acetone and deutero-acetone in the presence of a large number of compounds[55,56] were studied over the temperature range 25 - 340°C. The activation energies found for hydrogen abstraction were obtained.

Rebbert and Steacie[57] studied the photolysis of dimethyl mercury over the temperature range 125 - 250°C. Their results indicated that methane was formed only by an abstraction reaction and ethane only by recombination at least under the conditions used in the experiments. The main steps in the reaction were postulated as being

$Hg(CH_3)_2 + h\nu$	→	$Hg + 2CH_3$	1.49
$CH_3 + Hg(CH_3)_2$	→	$CH_4 + CH_2HgCH_3$	1.46
$CH_3 + CH_3$	→	C_2H_6	1.39
$CH_3 + CH_2HgCH_3$	→	$C_2H_5HgCH_3$	1.50
$2CH_2HgCH_3$	→	$(CH_3HgCH_2)_2$	1.51

The reaction

CH_2HgCH_3	→	$CH_2 + Hg + CH_3$	1.52

was excluded since such a reaction would lead to chains and would increase the amount of $Hg(CH_3)_2$ decomposed as the temperature was increased and this was not the case. Moreover Polanyi[58] postulated that the CH_2HgCH_3 radical is stable even at temperatures over 500°C. The reaction

$CH_3 + Hg(CH_3)_2$	→	$C_2H_6 + Hg + CH_3$	1.38

was also excluded because this would lead to chain reactions. From the results a value of 10.8 k.cals per mole for $E_{46} - \frac{1}{2}E_{39}$ was obtained. The results were in good agreement with those of Gomer and Noyes[46] and Gomer and Kistiakowsky.[48] The slight increase in ethane yield was accounted for by the increased light absorption with temperature. The last two reactions of the mechanism were included to remove the CH_3HgCH_2 radical

formed in methane production. No attempt was made to isolate these products, the only supporting evidence being the increase in absorption with temperature. Reaction 1.38 was also excluded by Ingold and Lossing[82] who followed the production of radicals in the reaction by means of a mass spectrometer.

Bradley, Melville and Robb[59] studied the disproportionation and recombination of ethyl radicals over a range of pressures and various conditions to separate the various mechanisms which occur. They showed that in addition to the normal two body reaction, a three body reaction is important at high pressures, whilst at low pressures wall reactions become prominent.

The photolytic decomposition of lead tetramethyl was studied in the vapour phase by Clouston and Cook[60] using flash photolysis. During the photolysis an absorption system in the region of 3000Å was observed with a lifetime not exceeding 400 μsec. The experimental conditions were such that a transition due to the free methyl radical or a lead polymeric radical seemed most likely to be for the band system. It is now known that the methyl radical absorbs at much shorter wavelengths.

Rebbert and Ausloos[61] studied the gas phase photolysis of CD_3COCD_3 in the presence of CH_3HgCH_3 from 100 - 180°C. From isotopic distributions of the methane and ethane fractions evidence was obtained for the occurrence of the reaction

$$CD_3 + Hg(CH_3)_2 \rightarrow CD_3HgCH_3 + CH_3 \quad E = 12.6 \text{ k.cals/mole} \quad 1.53$$

This reaction was also postulated to occur in the liquid and solid phase photolysis of CH_3HgCH_3 - CD_3HgCD_3 mixtures, it was concluded that cage recombination of methyl radicals does take place. Contrary to the conclusions reached by Derbyshire and Steacie[64] no evidence was obtained for hot radical effects in the liquid phase photolysis of dimethyl mercury.

The observed products from the flash photolysis of mercury diethyl at room temperature, carried out by Fischer and Main,[62] were butane, ethylene, ethane, propane and hydrogen in decreasing importance. Anticipated products from the ethyl mercury radical were not observed and good values for material balance were obtained. Because of the relatively high yield of ethylene it was necessary to invoke mechanisms involving hot ethyl radicals including unimolecular decomposition and disproportionation reactions, the latter resulted in the product ion of methyl radicals.

Mercury divinyl was photolysed in the gas phase at 50°C in a static system by Sherwood and Gunning.[63] The reaction products were 1,3 butadiene, ethylene and acetylene as well as traces of C_6-compounds. A mechanism was proposed which involved, as the primary reaction, the decomposition of the substrate molecule into two vinyl radicals and a mercury atom. The main reaction consuming substrate is

$$C_2H_3 + Hg(C_2H_3)_2 \rightarrow C_4H_6 + C_2H_3 + Hg \qquad 1.54$$

The chain-ending reactions are disproportionation and combination of vinyl radicals.

In general the metal alkyls that have been photolysed break down completely to metal and alkyl radicals and in the cases carried out in the last decade little evidence for chain mechanisms occurring was found except in the case of mercury divinyl. Hydrogen abstraction reactions occur but the products of the remaining radical is not solved. Evidence from isotopic experiments does not support the abstraction of alkyl groups although replacement of groups is suggested.

1.9b. Liquid Phase

The first kinetic study of the liquid phase photolysis of metal alkyls was carried out by Derbyshire and Steacie.[64] Photolysis of dimethyl mercury was carried out over the temperature range 25 to -80°C in n-hexane solution. The results indicated that methane was produced by an abstraction process involving the solvent and ethane produced by recombination of methyl radicals. They explained their results on the basis of hot radicals. In the initiating step

$$Hg(CH_3)_{2(liq)} \xrightarrow{h\nu} Hg + 2CH_3 \qquad 1.55$$

an excess of 60-k.cals per mole is available. Consequently the essential steps of the mechanism were presented as

$$Hg(CH_3)_2 + h\nu \rightarrow Hg + 2CH_3^* \qquad 1.56$$

$$CH_3^* + C_6H_{14} \rightarrow CH_3 + C_6H_{14} \qquad 1.57$$

$$CH_3^* + C_6H_{14} \rightarrow CH_4 + C_6H_{13} \qquad 1.58$$

$$CH_3 + CH_3 \rightarrow C_2H_6 \qquad 1.59$$

It was concluded that hot radicals were predominant at the low temperatures in the system used in spite of their relative unimportance at higher temperatures in the gas phase. Rebbert and Ausloos,[61] however,

found no evidence for hot radicals in the liquid or solid phase photolysis, it was concluded that cage recombination of methyl radicals does take place.

Other liquid phase reactions have been carried out by Razuvaev[65,66,67,68,69] et al. on organic compounds of mercury, tin, lead, chromium and indium, aluminium, phosphorus and lithium in which the metal compound was dissolved in a solvent, e.g. alkyl halide, which took part in the subsequent free radical reaction. For example,

$$Ar_2Hg + h\nu \rightarrow ArHg^{\bullet} + Ar^{\bullet} \qquad 1.60$$

$$ArHg^{\bullet} + CCl_4 \rightarrow ArHgCl + {}^{\bullet}CCl_3 \qquad 1.61$$

$$Ar^{\bullet} + CCl_4 \rightarrow ArCl + {}^{\bullet}CCl_3 \qquad 1.62$$

$$2CCl_3 \rightarrow C_2Cl_6 \qquad 1.63$$

or

$$Et_3Sn\text{-}SnEt_3 + 2Ph_3CCl \rightarrow 2Et_3SnCl + 2Ph_3C^{\bullet} \text{ etc.} \qquad 1.64$$

or

$$3(EPh)_2Cr^{o} + 4PhCH_2Cl \rightarrow 2(EtPh)_2CrCl + 2EtPh + 2(CH_2Ph)_2 \qquad 1.65$$

On irradiation by ultraviolet light as well as action of $AlCl_3$, tetraethyl stannane and hexaethyl distannane form dark red polymeric

organotin compounds. These decompose at 200°C evolving gases, tetraethyl stannane and tin, and were easily oxidised by air, and react with benzoyl peroxide and with CCl_4 in the presence of traces of air at normal temperatures i.e. take part in reactions characteristic of alkyl derivatives having Sn-Sn bonds.

Strohmeier et al.[70] have published a series of papers on the photochemistry of $M(CO)_6$ where M is Cr, Mo and W and of $C_5H_5Mn(CO)_3$ with a variety of nucleophiles. Their results show that at time zero the quantum yield of the photochemical primary step was equal to unity and was independent of the substrate, the reagent and the solvent. They proposed that the primary step involved a dissociation mechanism with the formation of a carbonyl of lower coordination number

$$M(CO)_6 \xrightarrow{h\nu} M(CO)_6^* \rightarrow M(CO)_5 + CO \qquad 1.66$$

1.10 Thermochemistry of Organometallic Compounds

By studying the thermochemistry of reactions that may take place it is possible to obtain information on the feasibility, from an energy point of view, of the reactions. To start with let us consider the basic reaction as forming the combination compounds and metal i.e.

$$MR_{2n}(g) \rightarrow M + nR\text{-}R(g) \ldots\ldots \qquad 1.67$$

In this reaction M, the metal atom, can either be in the solid or gaseous state and so two values will be obtained for the heat of reaction. The only thermochemical quantity that could be obtained for metal alkyls was their heats of formation[71] and those that are relevant are shown in Figure 1.9 plotted against their atomic numbers.

In Table 1.8 Columns (1) and (2) are the two values for each metal alkyls that can be obtained for the heat of reaction 1.67.

Figure 1.9

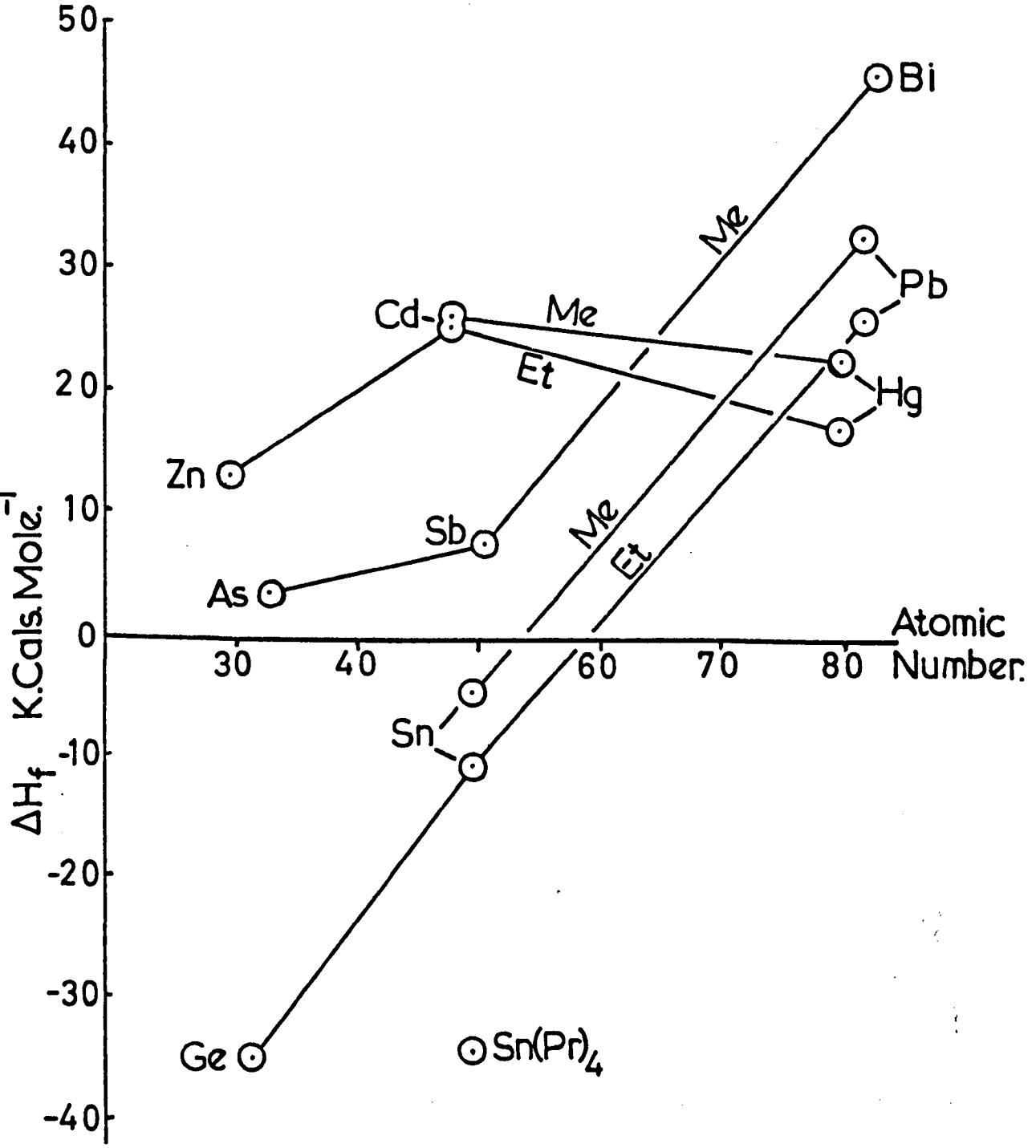
50
40
30
20
10
0
-10
-20
-30
-40
ΔHf K.Cals.Mole.-1
30
40
60
70
80
Atomic Number
Bi
Pb
Hg
Me
Et
Cd
Zn
Sb
As
Sn
Ge
Sn(Pr)4

TABLE 1.8 (Figure 1.10)

Compound	Heat of reaction 1.67 (k.cals. per mole) (1) Solid M	(2) Gaseous M	1.68 (3)
$Zn(CH_3)_2$	-33.34	- 2.14	+86.10
$Zn(C_2H_5)_2$	-43.15	-11.95	+69.60
$Cd(CH_3)_2$	-46.44	-19.69	+68.55
$Cd(C_2H_5)_2$	-55.65	-28.95	+52.65
$Hg(CH_3)_2$	-42.54	-27.89	+60.25
$Hg(C_2H_5)_2$	-47.35	-33.70	+48.85
$Hg(C_3H_7)_2$	-46.56	-31.91	-
$Hg(iso\text{-}C_3H_7)_2$	-51.79	-37.14	-
$Ge(C_2H_5)_4$	-25.7	+64.0	+227.6
$Ge(C_3H_7)_4$	-25.02	+75.15	+229.1
$Sn(CH_3)_4$	-35.87	+36.13	+212.6
$Sn(C_2H_5)_4$	-49.6	+22.4	+185.5
$Sn(C_3H_7)_4$	-45.32	+26.68	+190.6
$CH_2 = CHSn(CH_3)_3$	-36.36	+35.64	-
$Pb(CH_3)_4$	-73.07	-26.32	+150.2
$Pb(C_2H_5)_4$	-86.10	-39.35	+123.7
$Cr(C_6H_6)_2$	-14.06	+80.96	
$Cr(CO)_6$	+81.90	+176.90	
$Fe(CO)_5$	+40.92	+140.42	

Figure 1.10

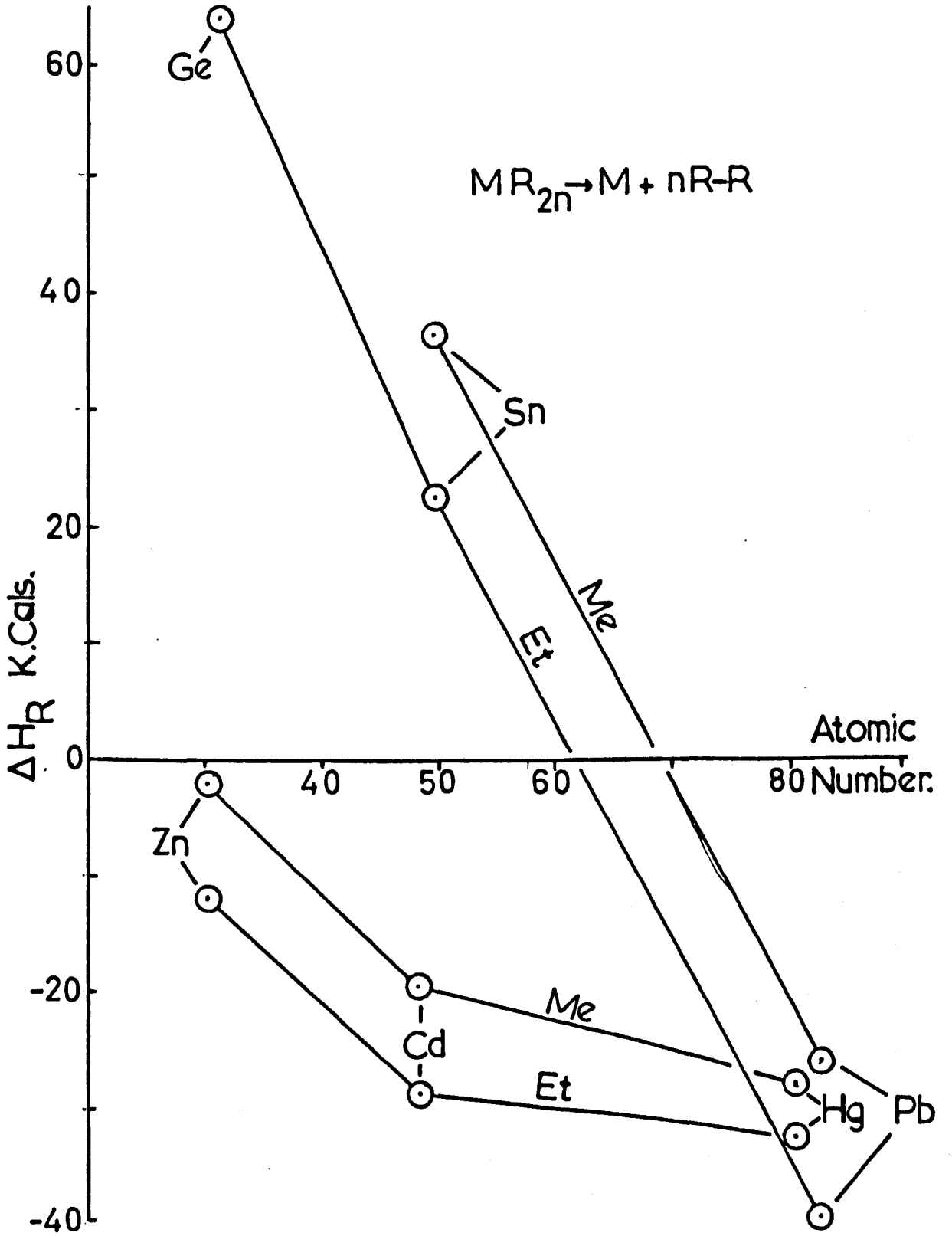
$MR_{2n} \rightarrow M + nR\text{-}R$
ΔH_R K.Cals.
60
40
20
0
-20
-40
40
50
60
80
Atomic Number.
Ge
Sn
Me
Et
Zn
Cd
Me
Et
Hg
Pb

It can be seen that the majority of reactions in which solid metal is formed are exothermic. Since single metal atoms in the gas phase must contain their heat of vapourisation it is the second column which is more realistic. This column shows that the compounds which have been decomposed to the metal, i.e. zinc, cadmium, mercury and lead, by ultraviolet radiation all give exothermic heats of reactions. The endothermic value of the Germanium and Tin compounds are however easily surmountable by the input of energy from ultraviolet light. This however does not mean that they can be decomposed since the values of the heat of reaction 1.67 gain energy by formation of products, i.e. more energy is required to completely separate the metal atom and the alkyl radicals.

A more precise approach would be to look at this primary decomposition, first of all as a complete step:

$$MR_n \rightarrow M + nR^{\bullet} \qquad 1.68$$

The values of the heats of this reaction plotted against the atomic number of the metal are shown in Figure 1.11. (See Table 1.8, Column 3).

These values give a more definite answer to the problem in hand and it can be seen that the Zn, Cd, Hg and Pb compounds have endothermic values all of which light of wavelength 2000 - 2800Å (main portion of medium pressure lamp) can overcome. However the Germanium and tin compounds seem excessively endothermic even to 1849Å radiation ≡ 156 k-cals. They would require light of wavelength 1240 - 1590Å to be completely decomposed.

However a reaction of the following nature cannot be excluded

Figure 1.11

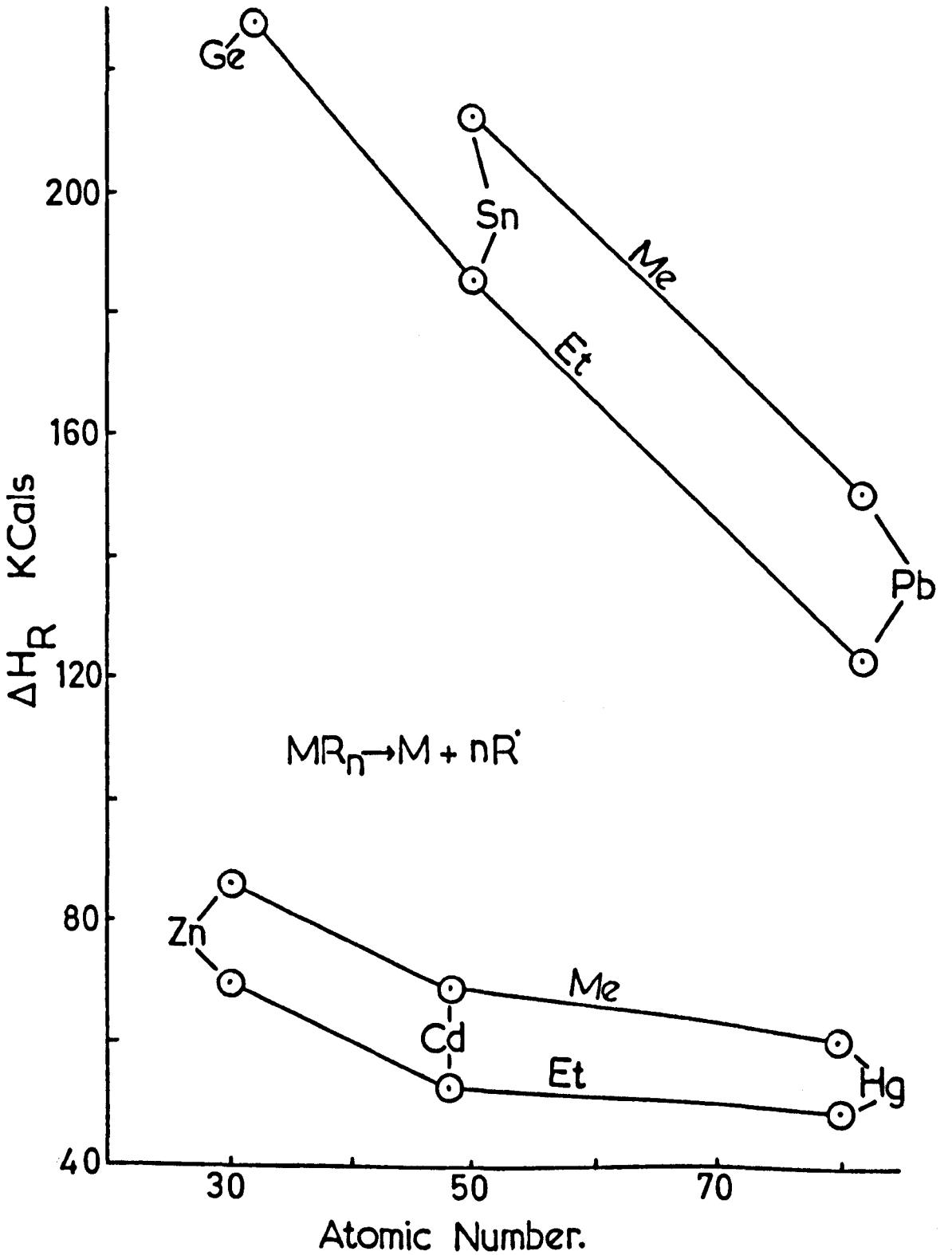
Ge
Sn
Pb
Me
Et
200
160
120
80
40
ΔH_R KCals
$MR_n \rightarrow M + nR^{\cdot}$
Zn
Cd
Hg
Me
Et
30
50
70
Atomic Number.

$$Sn(CH_3)_{4(g)} \rightarrow Sn_{(g)} + 2CH_3 + C_2H_6 \qquad 1.69$$

$$\Delta H = 124.1 \text{ kcals/mole}$$

There would be sufficient energy in light of wavelength 1849Å to give this process.

The work of Razuvaev[69] has shown that tetramethyl stannane can be decomposed by ultraviolet light eventually to metallic tin. The thermodynamics of the reaction

$$Sn(CH_3)_{4(liq)} \rightarrow Sn_{(solid)} + 2C_2H_{6(g)} \qquad 1.70$$

show it to be exothermic to the extent of 17.57 kcals/mole.

Similarly the formation of the polymer which presumably starts initially as the formation of the dimer i.e. hexamethyldistannane is also exothermic:

$$2Sn(CH_3)_4 \rightarrow (CH_3)_3SnSn(CH_3)_3 + C_2H_6 \qquad 1.71$$

$$\Delta H = - 18.64 \text{ kcals/mole}$$

When one further considers this reaction it becomes clear that breakdown of metal alkyls can be sequential, to some extent, as has been shown in the proposed mechanisms in Section 1.9a and also nickel

carbonyl decomposition shown by Callear.[39] It is possible to estimate the relative stability of the radicals $Sn(CH_3)_3$ and $Sn(CH_3)_3CH_2$ and to ensure some legitimacy in the calculations the same method was used to calculate the heats of formation of the analogous carbon compounds and found to be reasonable.

In obtaining the value of energy required to break the first methyl group from the rest of the molecule in $Sn(CH_3)_4$ the mean bond energy is of little use. The reaction of methyl radicals from diazomethane with $Sn(CH_3)_4$ was studied by Gowenlock[92] and his estimation of the bond energy of the first methyl-tin bond was 60 kcals. Using this value for the reaction

$$Sn(CH_3)_4 \rightarrow Sn(CH_3)_3 + CH_3 \qquad 1.72$$

the heat of formation of $Sn(CH_3)_3$ was found to be 21.4 kcals. Further breakdown of this radical cannot be followed sequentially. Complete breakdown

$$Sn(CH_3)_3 \rightarrow Sn_{(g)} + 3CH_3 \qquad 1.73$$

is endothermic to a value of 152 kcals/mole. There is the possibility that dimethyl stannyl radical may be stable or form a polymer i.e.

$$^{\bullet}Sn(CH_3)_3 \rightarrow :Sn(CH_3)_2 + CH_3 \qquad 1.74$$

Figure 1.12

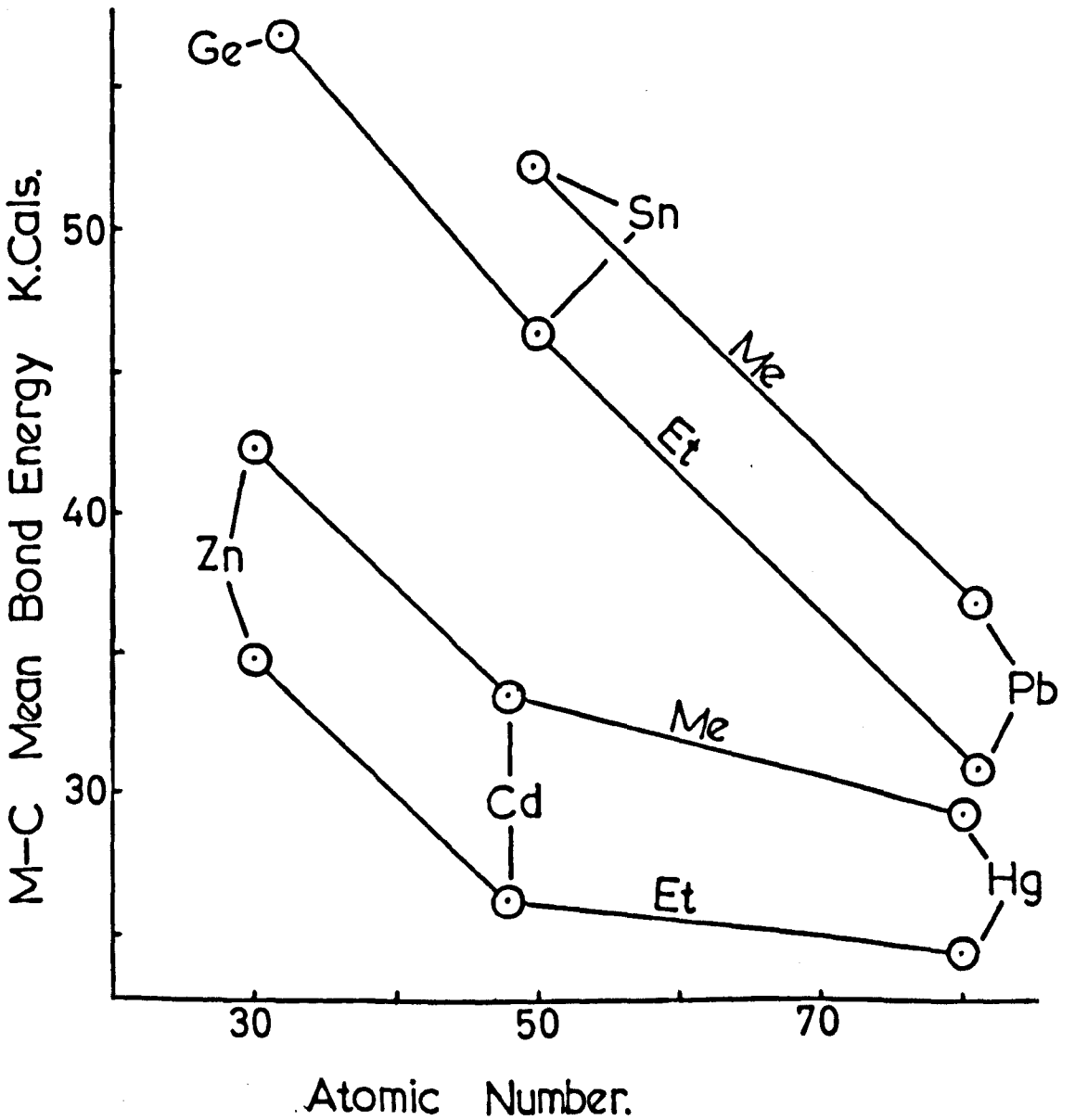
M–C Mean Bond Energy K.Cals.
50
40
30
Ge
Sn
Me
Et
Zn
Cd
Me
Et
Pb
Hg
30
50
70
Atomic Number.

The trimethyl stannyl methylene radical

$$Sn(CH_3)_4 \rightarrow H + (CH_3)_3\dot{S}nCH_2 \qquad 1.75$$

has a heat of formation of 42.3 kcals and requires more energy for complete breakdown than the trimethyl stannyl radical,

$$(CH_3)_3SnCH_2 \rightarrow Sn + CH_2 + 3CH_3 \qquad 1.76$$

221.7 kcals.

$$\text{or} \rightarrow Sn + C_2H_5 + 2CH_3 \qquad 1.77$$

123 kcals.

but partial breakdown cannot again be ruled out or rearrangement and elimination:

$$(CH_3)_3SnCH_2 \rightarrow (CH_3)_2Sn = CH_2 + CH_3 \qquad 1.78$$

Having obtained these values for the heats of formation of the stannyl radicals it is possible to look at the feasibility of abstraction reactions that can take place, e.g.

$$^{\bullet}CH_3 + Sn(CH_3)_4 \rightarrow C_2H_6 + {}^{\bullet}Sn(CH_3)_3 \qquad 1.79$$

exothermic -29 kcals.

$$^{\bullet}CH_3 + Sn(CH_3)_4 \rightarrow CH_4 + (CH_3)_3\dot{S}nCH_3 \qquad 1.80$$

exothermic -4.99 kcals.

The values of the heats of reactions show that both are possible though steric factors will play a large part in these reactions. Combination reactions can also be treated in the same way

$$^{\bullet}Sn(CH_3)_3 + {}^{\bullet}Sn(CH_3)_3 \rightarrow (CH_3)_3SnSn(CH_3)_3 \qquad 1.81$$

$$\Delta H = -50.4 \text{ kcals/mole}$$

Although this method of assessing the possibility of reactions and the stability of radicals does not give the rate at which these reactions take place the results may be of use in building up the mechanism.

1.11 Compilation of Available Information

The paper by Petuchoff[11] suggests that the broad absorption bond of tetramethyl stannane, with a maximum at 1850Å, is due to the electronic excitation of the metal-carbon bonds; Linnett and Thompson[4-7] agree with this. If this is so then irradiation of alkyl stannanes may lead to rupture of the metal-carbon bonds.

The excited state that is entered on absorption of light has not been predicted being presumably the singlet state. Whether inter-system crossing occurs to the triplet state or vibrationally excited ground state is unknown. In the series of experiments using the low pressure Hg-vapour lamp sensitisation can be ruled out as no reaction occurred when the acetic acid filter was in place. The reaction that occurred with the high pressure Hg-lamp may have been due to absorption in the 2200Å region.

From the photolysis of metal alkyls that have been carried out previously it is evident that radical reactions are of major concern and the rate constants listed in Section 1.5 may be useful in calculating rate constants of the radicals involved. It is, however, difficult to assess the significance of the work carried out prior to the middle 1950's, because of the enormous advance in analytical and spectroscopic techniques within the last decade. There is the possibility of molecular reactions occurring and those suggested in the pyrolysis by Waring and Horton[25] may be possible. The liquid phase radiolysis of tetra alkyl stannane by

Hoeppner[29] appears to suggest complete breakdown has not occurred but this may be due to cage effects restricting total elimination or insufficient energy for this requirement. The liquid phase photolysis by Razuvaev[69] seems to agree with the radiolysis, in polymer formation, but as photolysis is continued metal is deposited. This may be due to secondary photolysis occurring.

The thermodynamics, although limited, tends to suggest that complete dissociation even with radiation of light at 1849Å wavelength will not occur although the degree of sequential breakdown cannot be estimated. The reactions and stabilities of possible stannyl radicals appear to be favourable in relation to their existence. If the dissociation is indeed stepwise it is possible that the first methyl group on leaving may contain a large amount of energy making them hot radicals. However the large fragment remaining has quite a few degrees of freedom in which to dissipate the energy and thus the excess energy may not be as large as if the fraction remaining was monatomic.

2. EXPERIMENTAL

2.1 Introduction

Tetramethyl stannane or ethyl trimethyl stannane, at a known pressure, was introduced into the thermostatted reaction cell, in the first instance via a vacuum system part of which was a mercury diffusion pump and in the second instance via a mercury free vacuum system. The gas was irradiated for a known period of time using a high pressure mercury vapour lamp and a low pressure mercury lamp. In the latter case 1849 Å was the activating radiation emitted by the lamp and the amount of radiation reaching the cell was measured by chemical actinometry. After irradiation the reaction products were allowed sufficient time to thoroughly mix in the reaction cell before a gaseous sample was analysed by gas chromatography.

2.2 Materials

Tetramethyl stannane was obtained from K and K Laboratories, California (Kodak - British Distributors). This contained a small amount of lower boiling material which was removed by fraction distillation under nitrogen using a heated 2 ft. glass helix column and a variable take-off head.

Ethylene of research grade from Air Products and Chemicals Inc. was used in actinometry and did not require any purification.

Carbon dioxide was obtained from Air Products and Chemicals Inc. and was purified by a freeze-thaw technique and trap to trap sublimation.

Nitric oxide was obtained from Air Products and Chemicals Inc. and was purified but trap to trap distillation. Oxygen and oxygen free nitrogen were obtained from B.O.C. cylinders and required no purification. The nitrogen was dried over silica gel.

Octafluoro cyclobutane was received as a gift from Dr. R. Cundall, Chemistry Department, Nottingham University.

Materials for quantitative calibration were Matheson Research Grade Gases (methane, ethane, ethylene, propane).

Hexamethyl distannane was an Alfa Inorganics Inc. product.

2.3 Apparatus

The high vacuum apparatus is represented by Figure 2.1, also Plate 2.1.

In the first instance ultimate vacuum was realised by means of a mercury diffusion pump and this was backed by an Edwards Speedivac Rotary Oil pump (Type ES/35). The rotary pump was separated from the mercury pump by a trap cooled by liquid nitrogen, similarly the vacuum system was separated from the mercury pump. The combination of traps and pumps was capable of producing a vacuum better than 10^{-5} mm. Hg.

In the second instance an N.G.N. oil diffusion pump (Type O.P.W.125) was used in conjunction with the oil pump. The vacuum system again was separated from the diffusion pump and the diffusion pump from the rotary oil pump by traps cooled in liquid nitrogen. Ultimate vacuum of less than 10^{-5} mm. Hg. could be obtained in the Hg-free system.

Pure gases were introduced into the system via inlet A, liquified where possible in cooled traps and then thoroughly degassed before use or storage. Impure gases were purified by trap to trap distillation along the distillation train. The gases were stored in one litre bulbs which were fitted with freeze arms to assist recovery of the gases from the vacuum line.

Two reaction cells were used. Initially a cylinder quartz cell, two inches in length and two inches in diameter, was attached at point B via a B10 ground glass joint sealed with Edwards Picien wax. This was

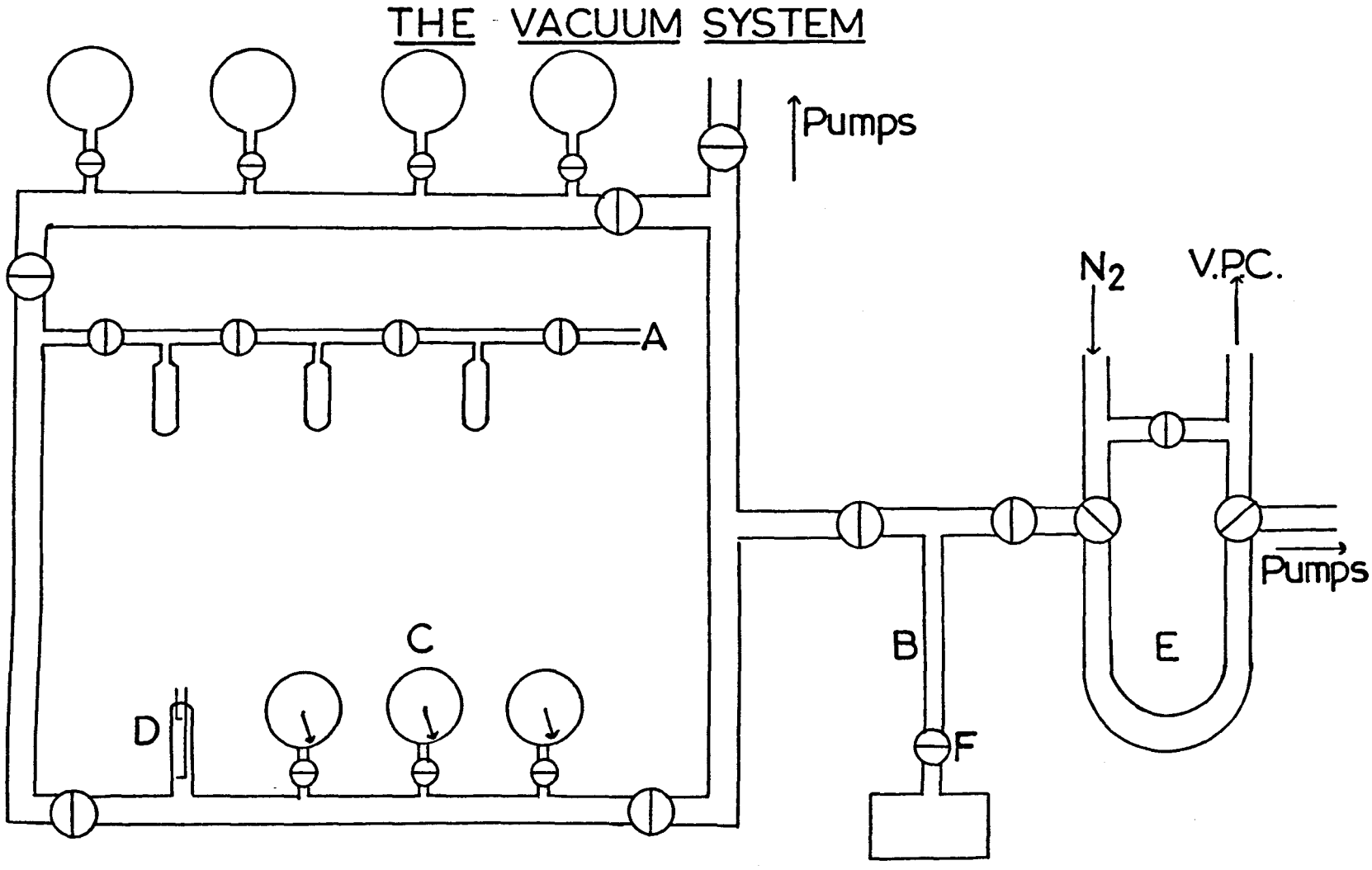

Figure 2.1

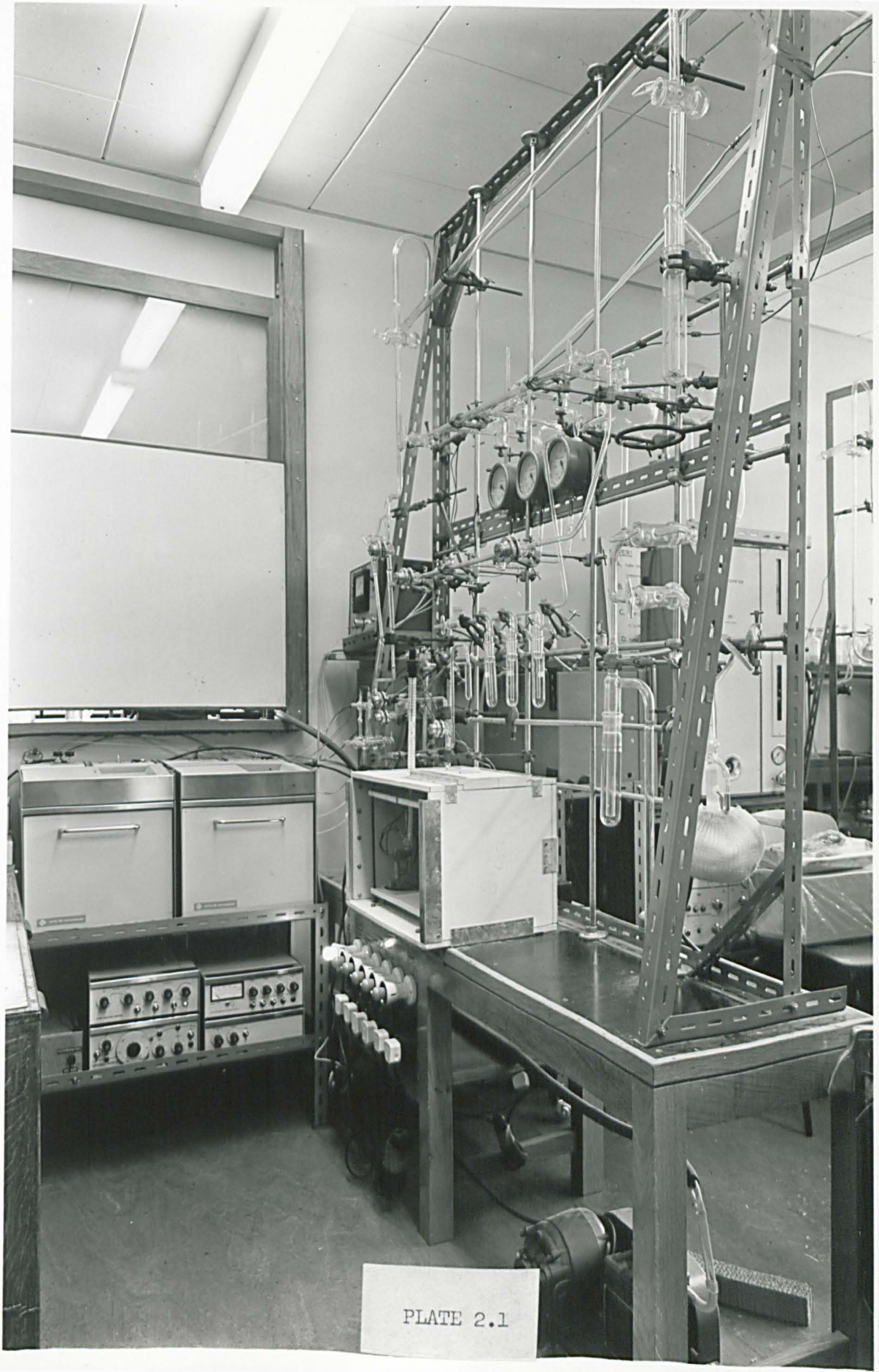

PLATE 2.1

however replaced by a cylindrical brass cell as shown in Figure 2.7.

Pressure measurements were made on Edwards Absolute Dial Gauges (Type C.G.3) at point C, calibrated 0 - 20 mm., 0 - 100 mm. and 0 - 760 mm. and also by means of an Autovac Pirani Gauge (Type 3294B), with a range 1-micron to 100 mm. Hg, attached to point D. It was necessary to check the calibration of the capsule gauges against a mercury manometer. The 0 - 20 mm. gauge was accurate, the 0 - 100 mm. gauge had a zero error of 1 mm., the 0 - 760 mm. gauge had a zero error of 13 mm. See Figures 2.2 to 2.5.

Gaseous samples were introduced into the gas phase chromatograph through a U-tube at point E. In the diagram, Figure 2.6, taps I and II were three-way glass stopcocks, while III was a straight-through stop-cock. A sample was taken for analysis by the following procedure:-

(a) Tap III remained open to allow unimpeded flow of carrier gas to the chromatograph.

(b) With tap I closed, tap II was opened to the pumping line so that the U-tube was evacuated. Tap II was then closed.

(c) Tap I was opened to the system containing the gas to be analysed. Sufficient time was allowed for pressure equilibration before tap I was closed.

(d) Tap I was briefly opened to the carrier stream and then closed. Carrier gas entered the U-tube and pushed the gas to be analysed into a slug against tap II.

(e) Before the gaseous slug had time to diffuse through the carrier gas taps I and II were simultaneously opened to the carrier gas

Figure 2.2

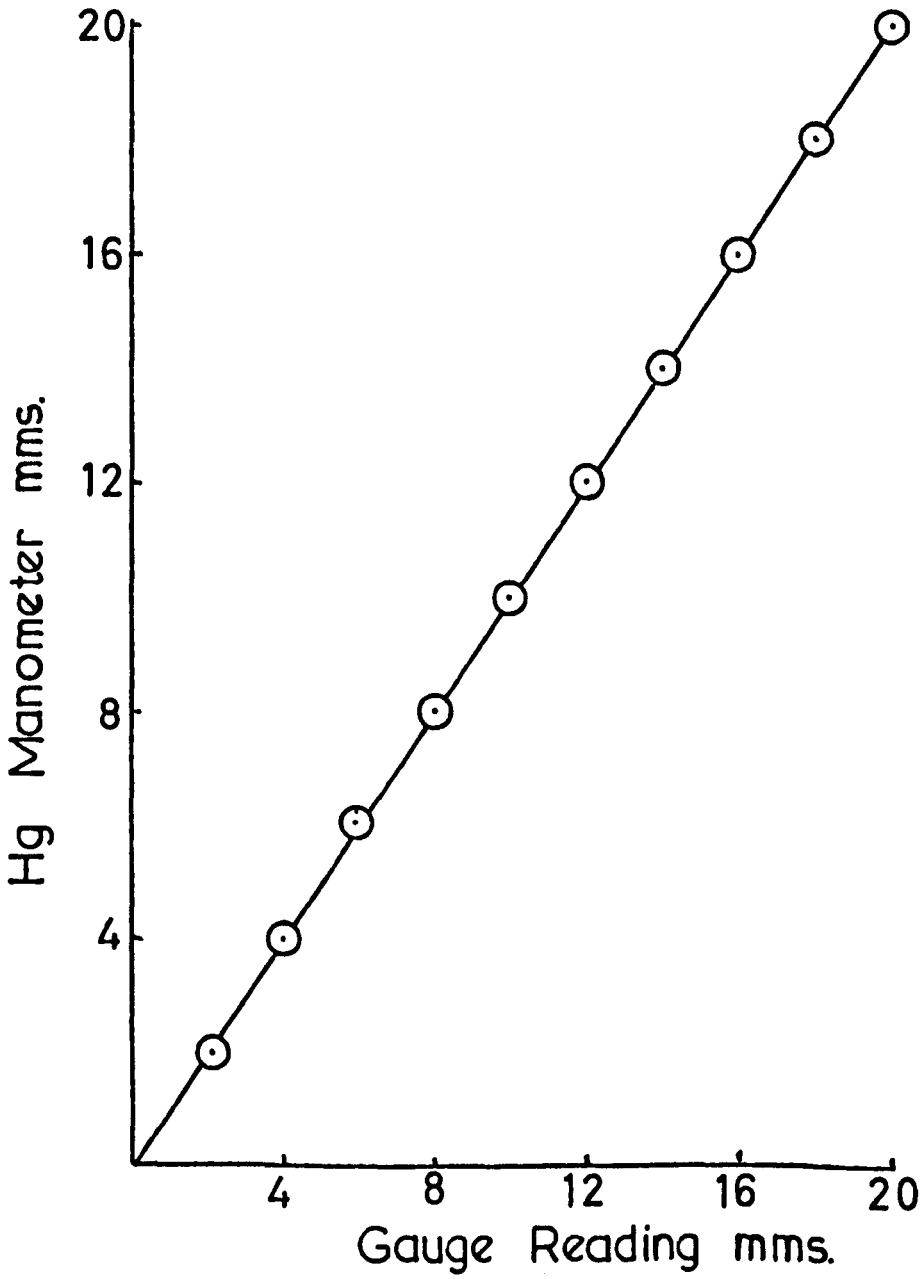

Figure 23

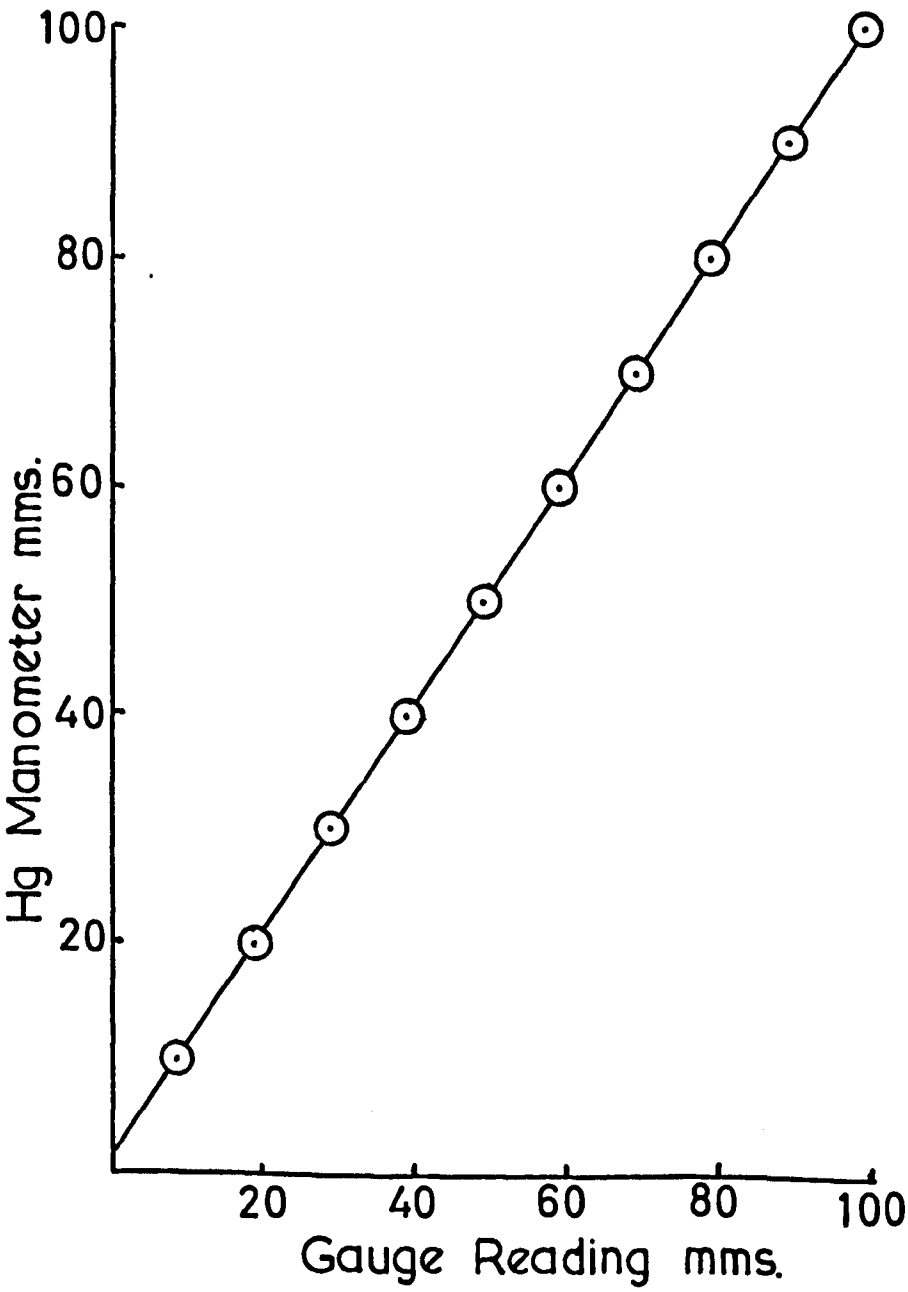
100
80
60
40
20
Hg Manometer mms.
20
40
60
80
100
Gauge Reading mms.

Figure 2.4

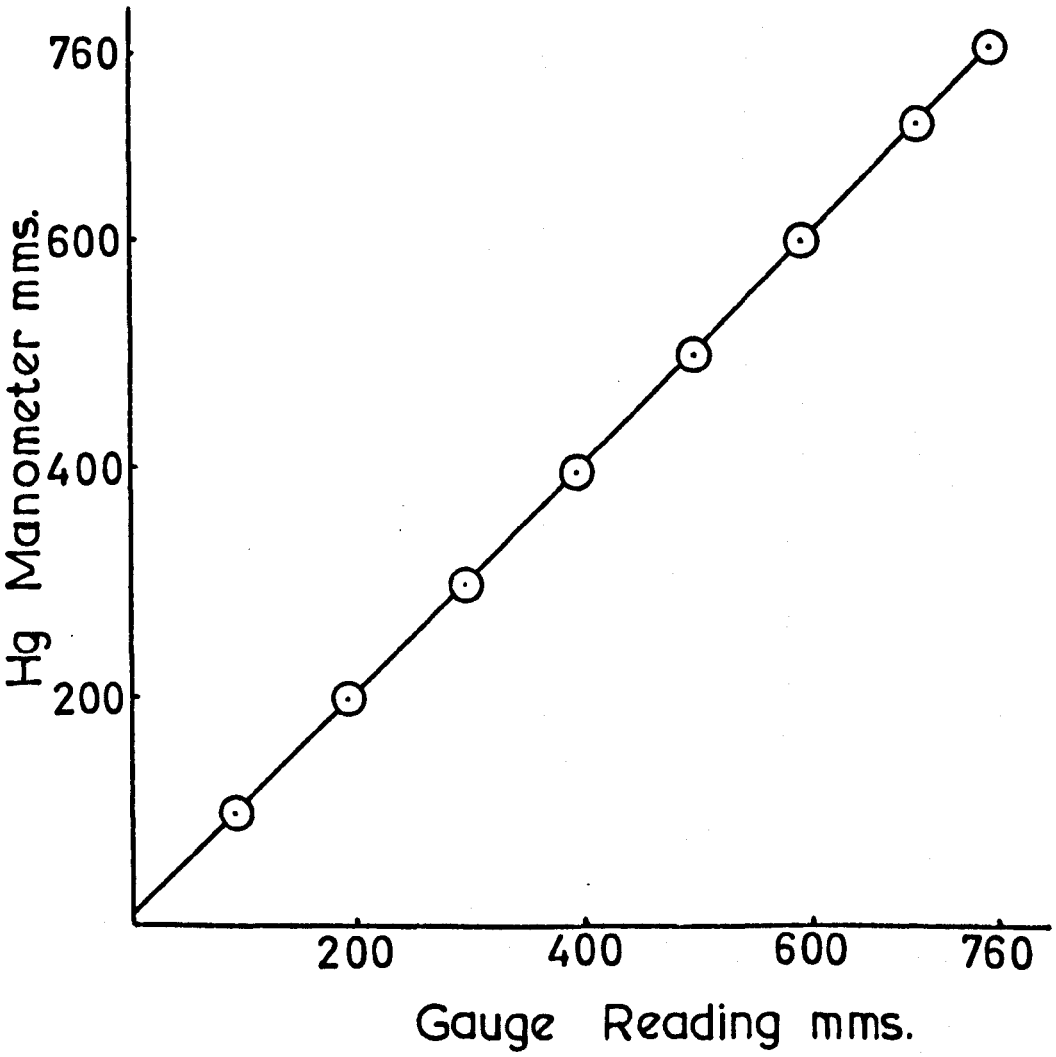
760
600
400
200
Hg Manometer mms.
200
400
600
760
Gauge Reading mms.

Figure 2.6

Gas Sampling Tube.

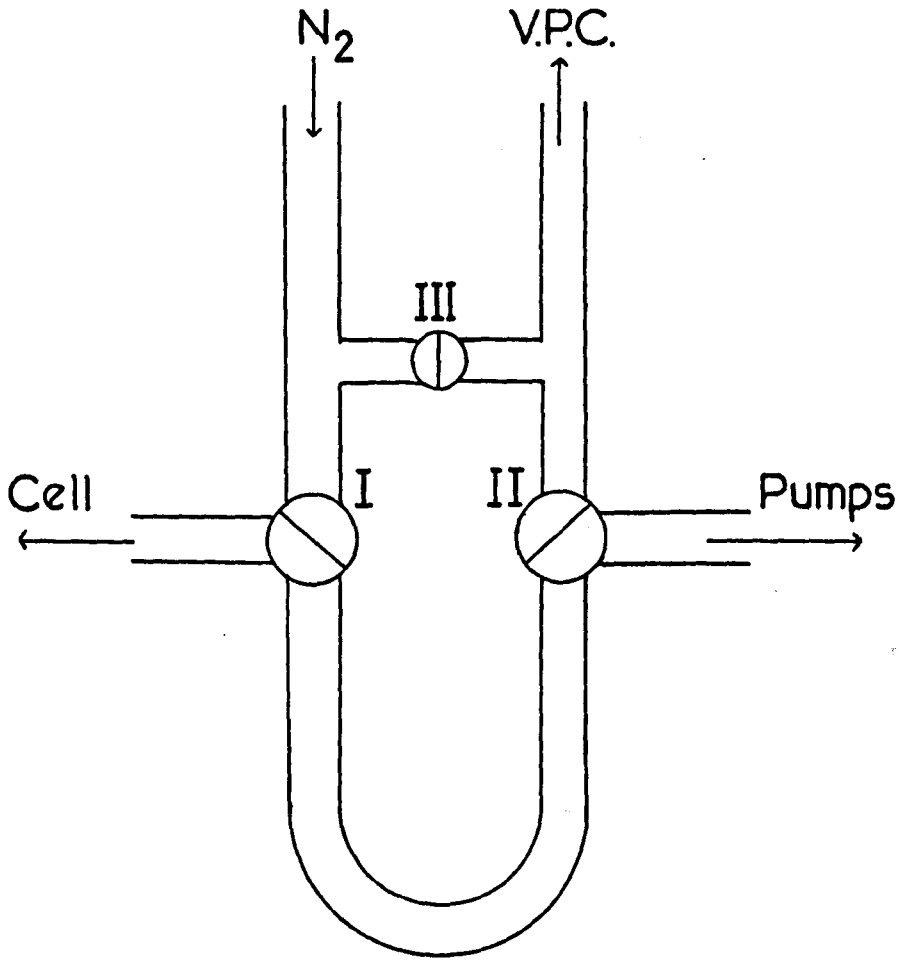

Volume of tube =6.01ml.

stream and tap III closed immediately afterwards. The sample was then carried into the gas chromatograph.

The volume of the U-tube was 6.013 mls. The total volume of gas before a sample was taken was 156.9 mls. Apart from the stopcocks I, II and III, which were lubricated with silicon grease, all stopcocks in contact with the reactant gases were greaseless Springham valves with fluorocarbon (Viton A) diaphragms. These did not absorb paraffin or olefin hydrocarbons. All other stopcocks in the system were lubricated with silicon grease.

The gas chromatograph unit consisted of a flame ionisation module and a katherometer module. (Type Pye 104 series, models 24 and 34). The recorder was a Vitatron (Type lin/log recorder UR100) model fitted with a disc integrator.

2.4 Reaction Cells

2.4.1 Vapour Phase

2.4.1a Cell

Originally the reaction cell was a quartz cylinder, two inches in length and two inches in diameter, with a side arm connecting it to the vacuum through a B10 joint at point B. The end windows were of quartz and were fused to the barrel. However, this arrangement proved unsatisfactory because during irradiation using the high pressure mercury vapour lamp a polymeric film was formed which could only be removed by aqua regia.

This difficulty was overcome by use of the metal cell illustrated in Figure 2.7. It consisted of a brass cylinder 80 mm. in length and 50 mm. in diameter with Spectrosil windows held on by O-rings and screwcaps. These provided for easy removal of the windows when they became coated with polymeric material and, when using the low pressure lamp, with metallic tin.

The side arm was attached to the cell via a glass to copper junction, the copper tubing being silver soldered into the wall of the cell. Connection to the vacuum line was direct, the B10 joint being unnecessary.

Spectrosil, a synthetic quartz produced by Thermal Syndicate Ltd., was used for the cell windows because of its transmission properties in the ultraviolet. A 10 mm. thick disc of spectrosil will transmit $\sim$90% of 1849 Å radiation incident upon it, Figure 2.8. The

Figure 2.7

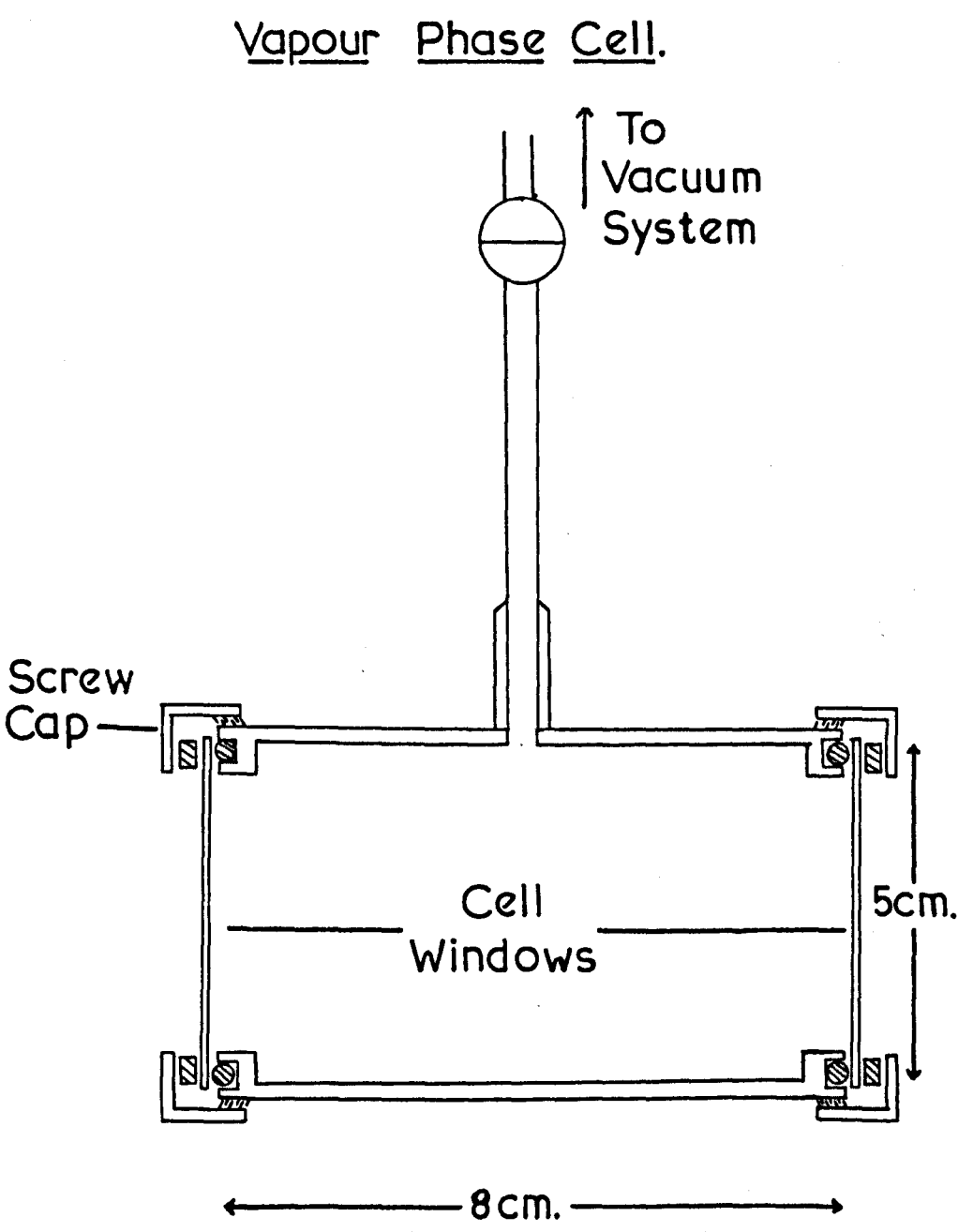
Vapour Phase Cell.
To Vacuum System
Screw Cap
Cell Windows
5cm.
8cm.

Figure 2.8

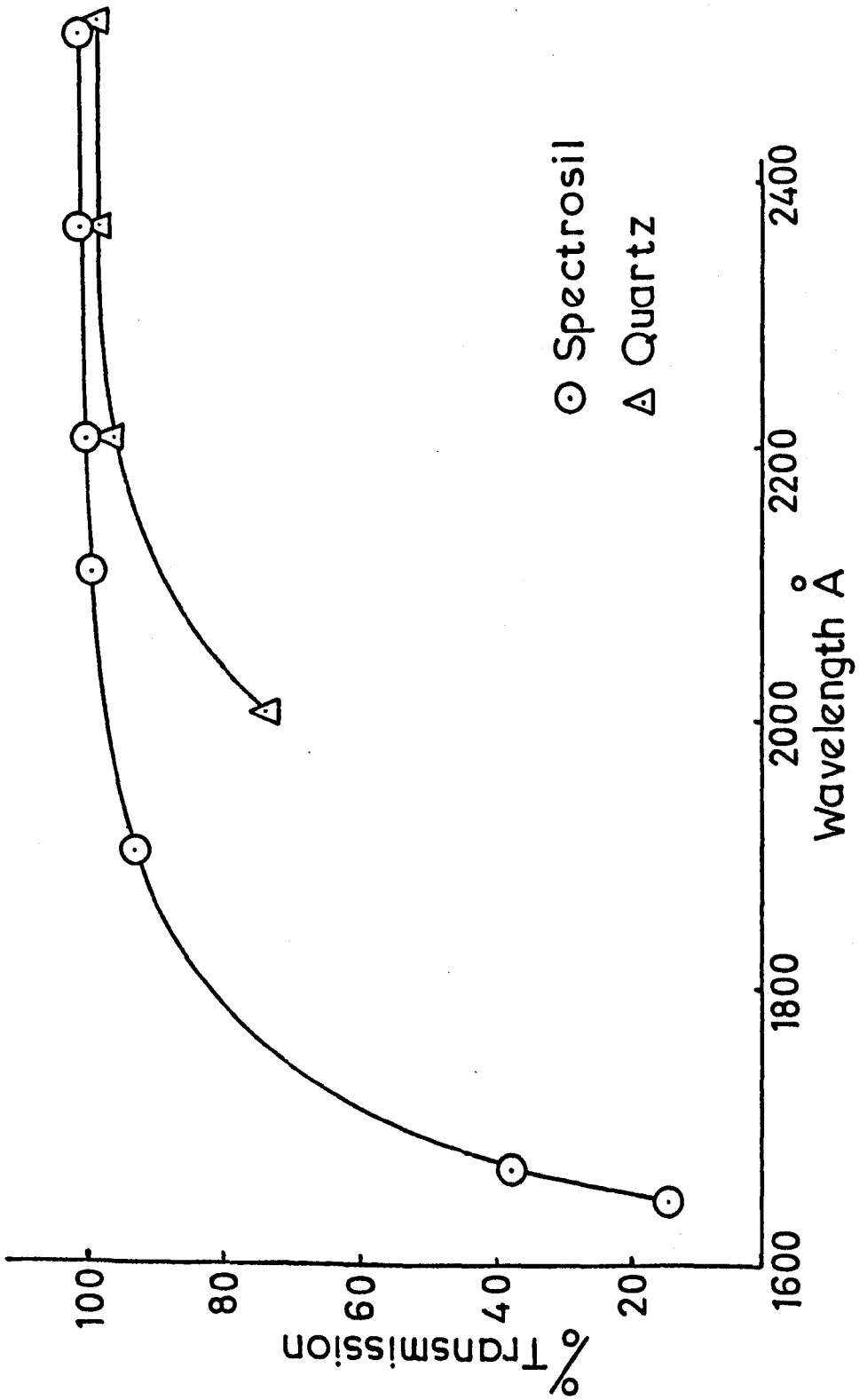
⊙ Spectrosil
△ Quartz
% Transmission
100
80
60
40
20
1600
1800
2000
2200
2400
Wavelength Å

total thickness of spectrosil traversed by the 1849 Å radiation before reaching the cell was < 5 mm.

2.4.1b Thermostat

The cell was enclosed in an air thermostat constructed of Sindanyo (compressed asbestos cement), Figure 2.9. The total volume of the thermostat was 24 litres and it was heated by a 1.5 kilowatt spiral heater and the gas was circulated by means of an electrically driven fan. The temperature was controlled by a mercury contact thermometer acting through a 'Sunvic' relay. Tests showed that at 150°C the temperature throughout the oven was constant to ± 1°C. The maximum temperature attainable in the thermostat oven was 200°C.

The thermostat was flushed continually with dry oxygen-free nitrogen as both oxygen and water vapour have absorption coefficients of 1.5 cm^{-1} at 1849 Å. The nitrogen was dried by passing the stream of gas over silica gel.

Figure 2.9

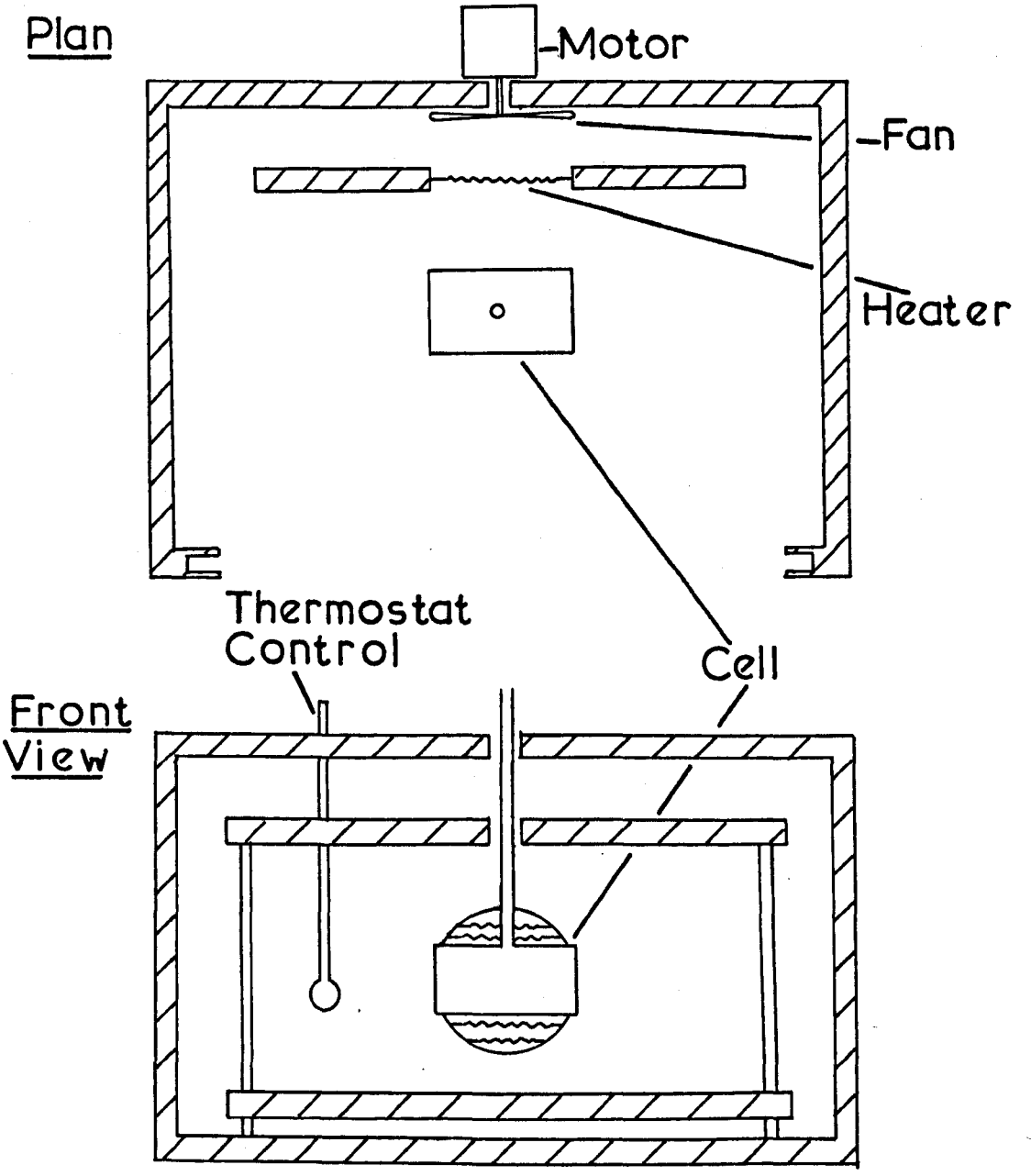

2.4.2 Liquid Phase

Reactions in the liquid phase were carried out in the apparatus shown in Figure 2.10. The apparatus was so designed as to give approximately 1.5 mm. of liquid around the lamp and it was stirred mechanically by a magnetic stirrer. The solutions were introduced into the reaction cell and nitrogen was bubbled through the sintered glass disc at the bottom of the cell to remove any oxygen in the solution. The volume of gas evolved was measured by means of a gas burette and the total gas analysis carried out at the end of the reaction.

Samples of the liquids were obtained at various times by means of the side arm and septun cap and a 10 µl syringe. The lamp used was a medium pressure mercury lamp (Hanovia 1-litre photochemical reactor).

Figure 2.10 215

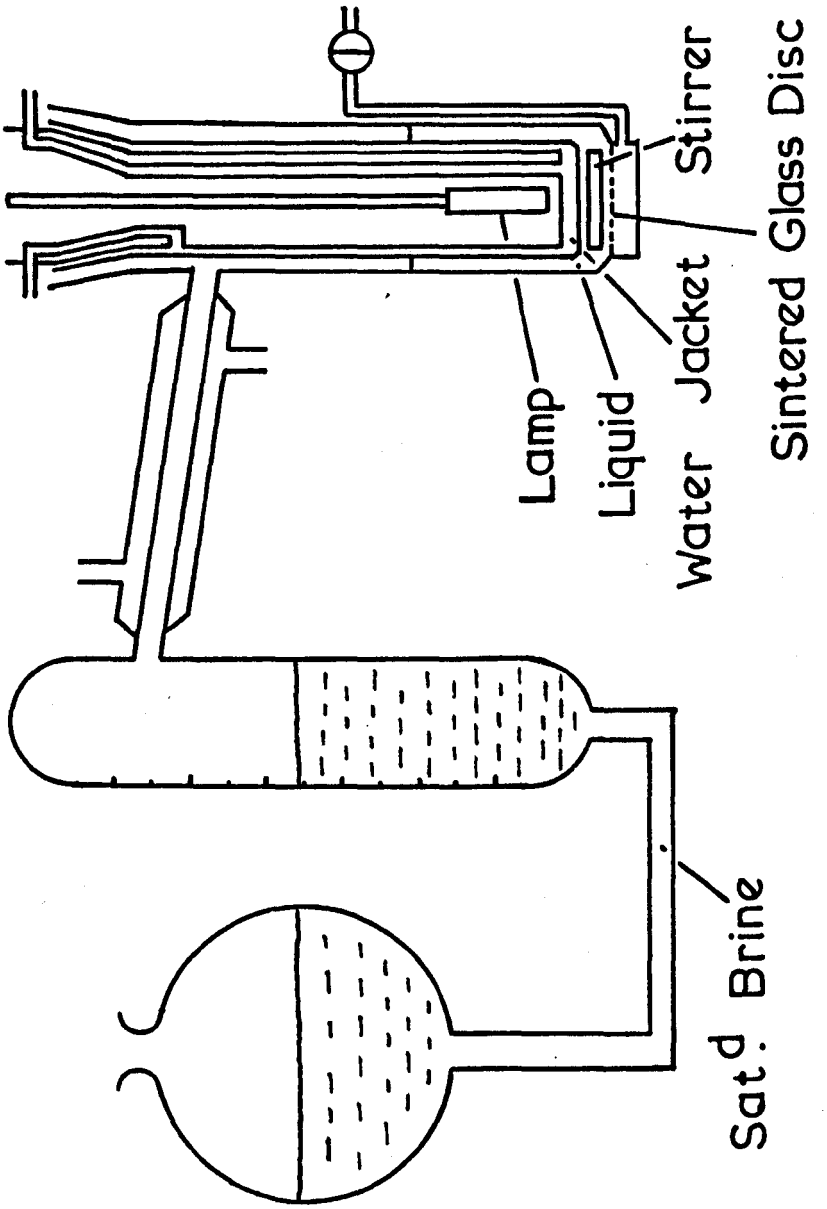

2.5 Light Sources

2.5.1 Ultraviolet

Preliminary experiments were carried out using a Wottan high pressure mercury vapour lamp (Type H.B.O 500 w.). No quantitative measurements of quantum yields were made using this lamp.

A 2 watt 12 inch spiral mercury vapour lamp (Hanovia Type 752/62) fitted with a spectrosil envelope was used in all the quantitative vapour phase experiments. Powered by a 1250 volt transformer it drew 10 mA at 340 v. The output of the lamp at 1849 Å as measured by ethylene and nitrous oxide actinometry was 6.46×10^{14} quanta per second which varied according to the geometry. The output of the lamp at 1849 Å did not fall noticeably over the total irradiation period. The output of a typical low pressure mercury vapour lamp in the ultraviolet is illustrated in Figure 2.11. The output of the two minor lines at 1942 and 2020 Å was found to be less than 10% of the 1849 Å line in a similar lamp.

The lamp was housed in a closed tube, Figure 2.12, constructed of Q.V.F. piping with an end window of spectrosil sealed on with araldite. The plane of the spiral was situated 8 cm. from the end window giving slight collimation. During an irradiation the lamp housing was flushed through with nitrogen.

The lamp housing for the high pressure mercury vapour lamp is shown in Figure 2.13. It consisted of a brass cylinder with a side arm

Figure 2.11

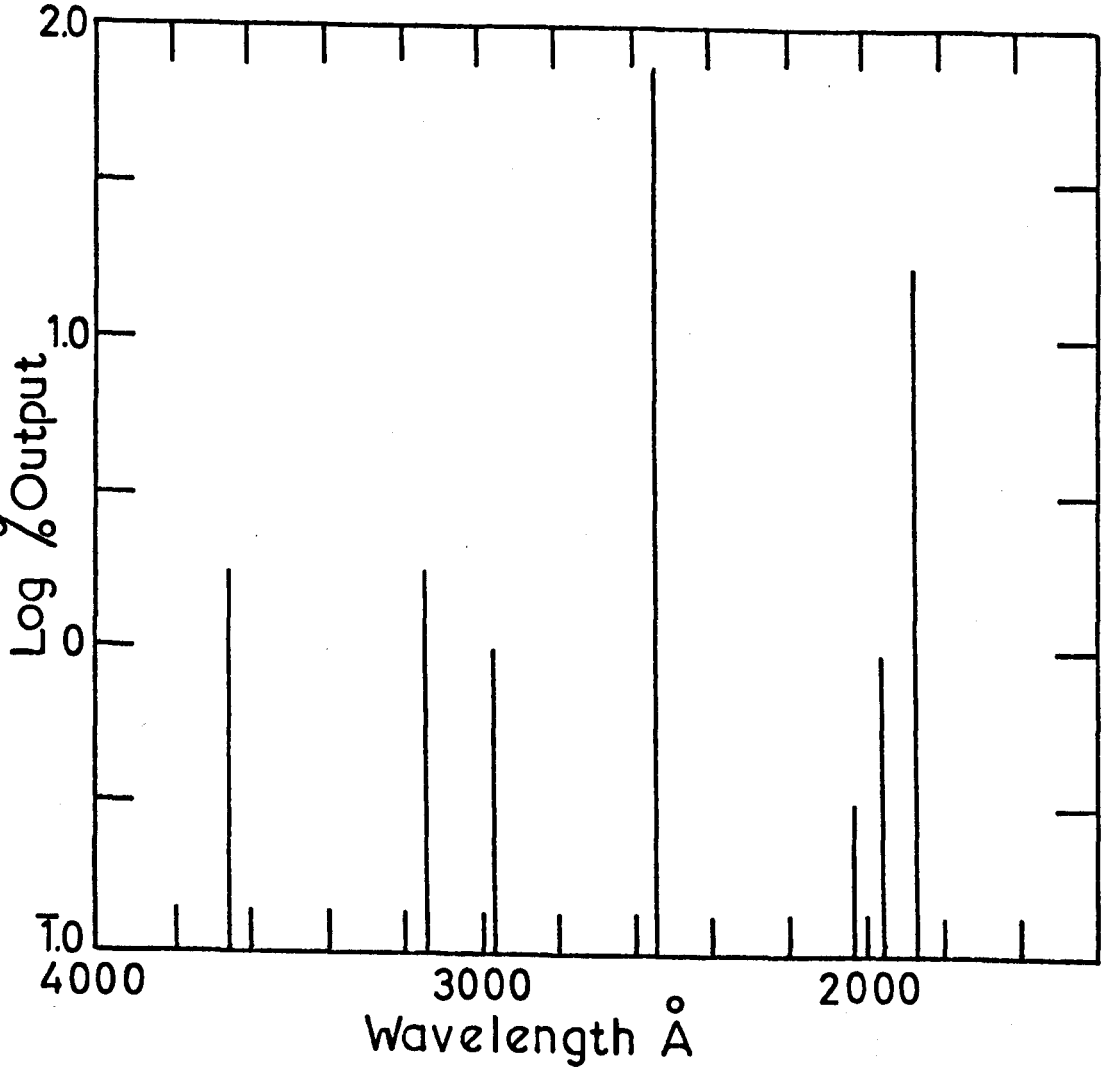

Figure 2.12

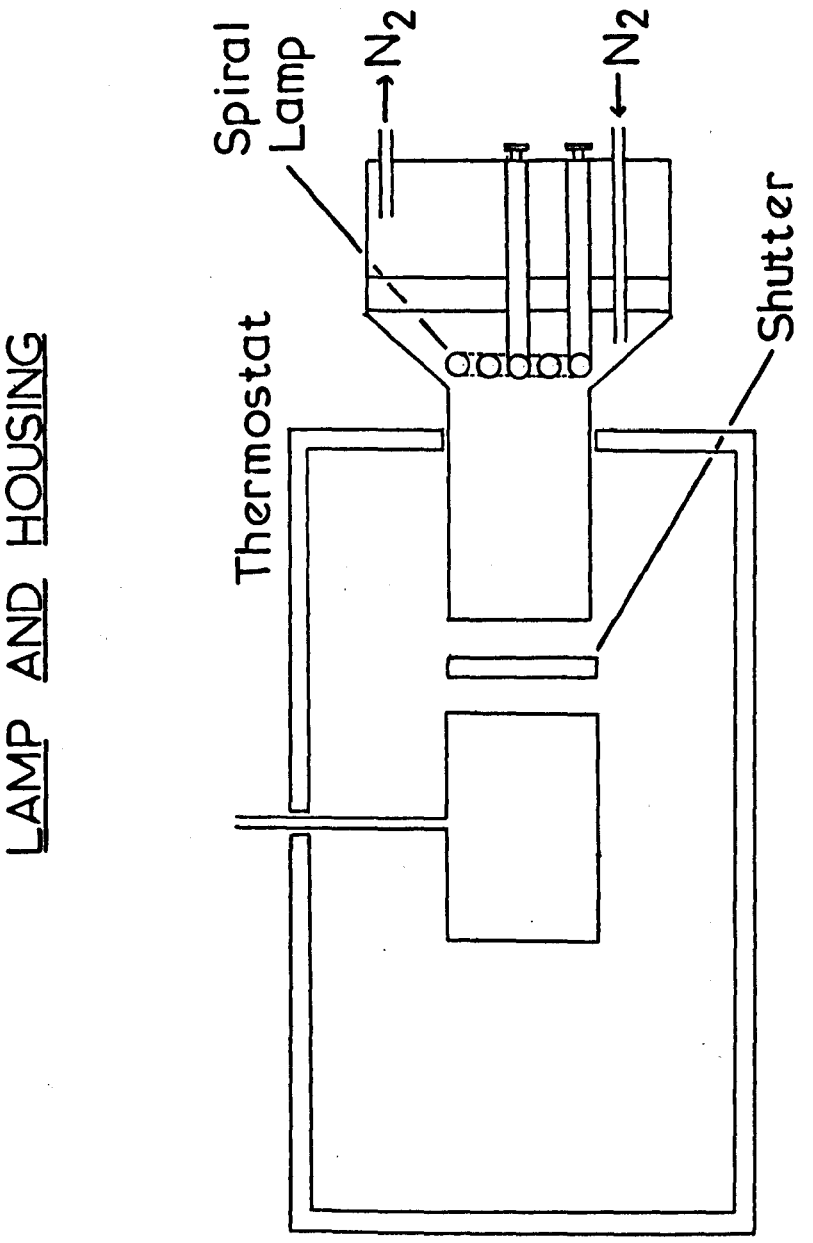

Figure 2.13

HIGH PRESSURE LAMP AND HOUSING.

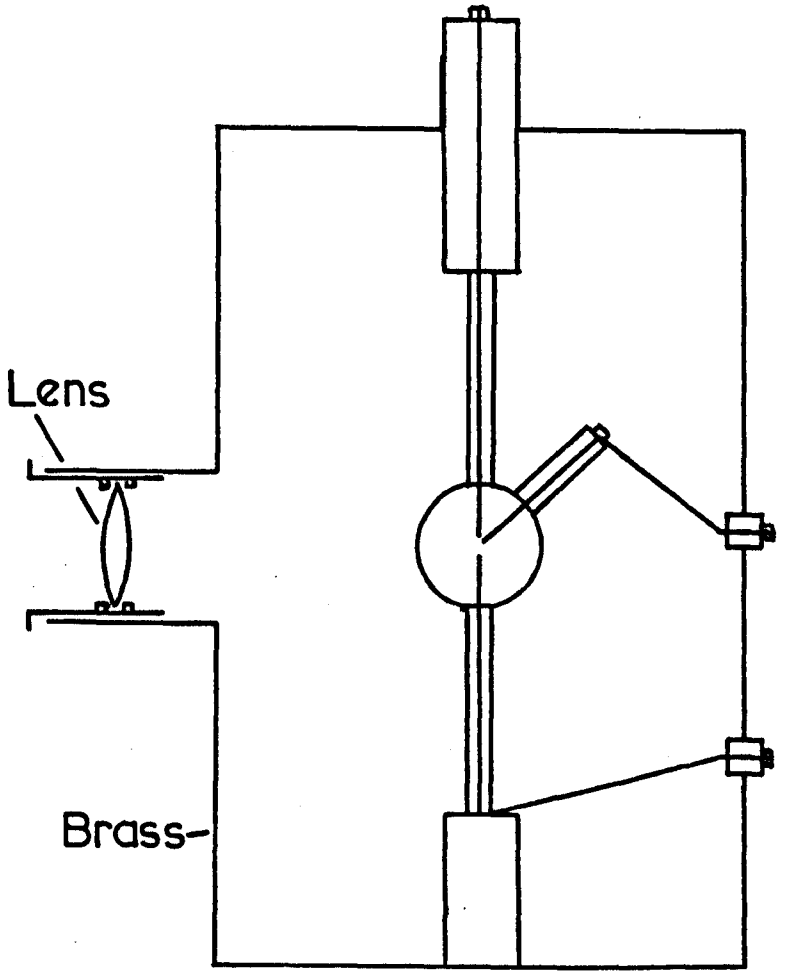

holding a quartz lens. The outside of the cylinder was sand blasted, to increase the surface area and thus heat dissipation. The inside was coated with Aquadag, a fine suspension of graphite in water, so that reflection of radiation did not occur inside the housing.

2.5.2 Optical System

Originally when using the high pressure mercury vapour lamp the radiation was collimated using a 2.25 inches diameter lens of focal length 2 inches made of spectrosil.

Using this lamp a minimum working temperature of the thermostat was 75°C was used due to the large amount of heat emitted by the lamp housing. The housing was situated outside the thermostat and a metal shutter, operated by a pull-cord, separated it from the cell.

In the case of the low pressure mercury vapour lamp the lamp housing was fixed so that the end window was 2 cm. from the cell, the thick walls of the brass screw cap of the cell acting to some extent as a collimator. Here again a metal shutter was used to isolate the cell.

Intensity stops were constructed of metal gauze of various gauges coated with black matt paint. The geometry was fixed by holding the stop in a short metal cylinder and the position of the stop between the lamp and the cell was fixed by lugs, on the foot of the stop, fitting into corresponding sockets on the foot of the thermostat.

The filter consisted of a 1 cm. 2% acetic acid solution the transmission properties of which are given in Figure 2.14.

The optical assembly of the liquid phase experiments consisted of a medium pressure lamp (Hanovia 1-litre photochemical reactor) cooled by water passing through a spectrosil envelope. Also nitrogen was passed between the lamp and the spectrosil envelope, see Figure 2.15. Due to

Figure 2.14

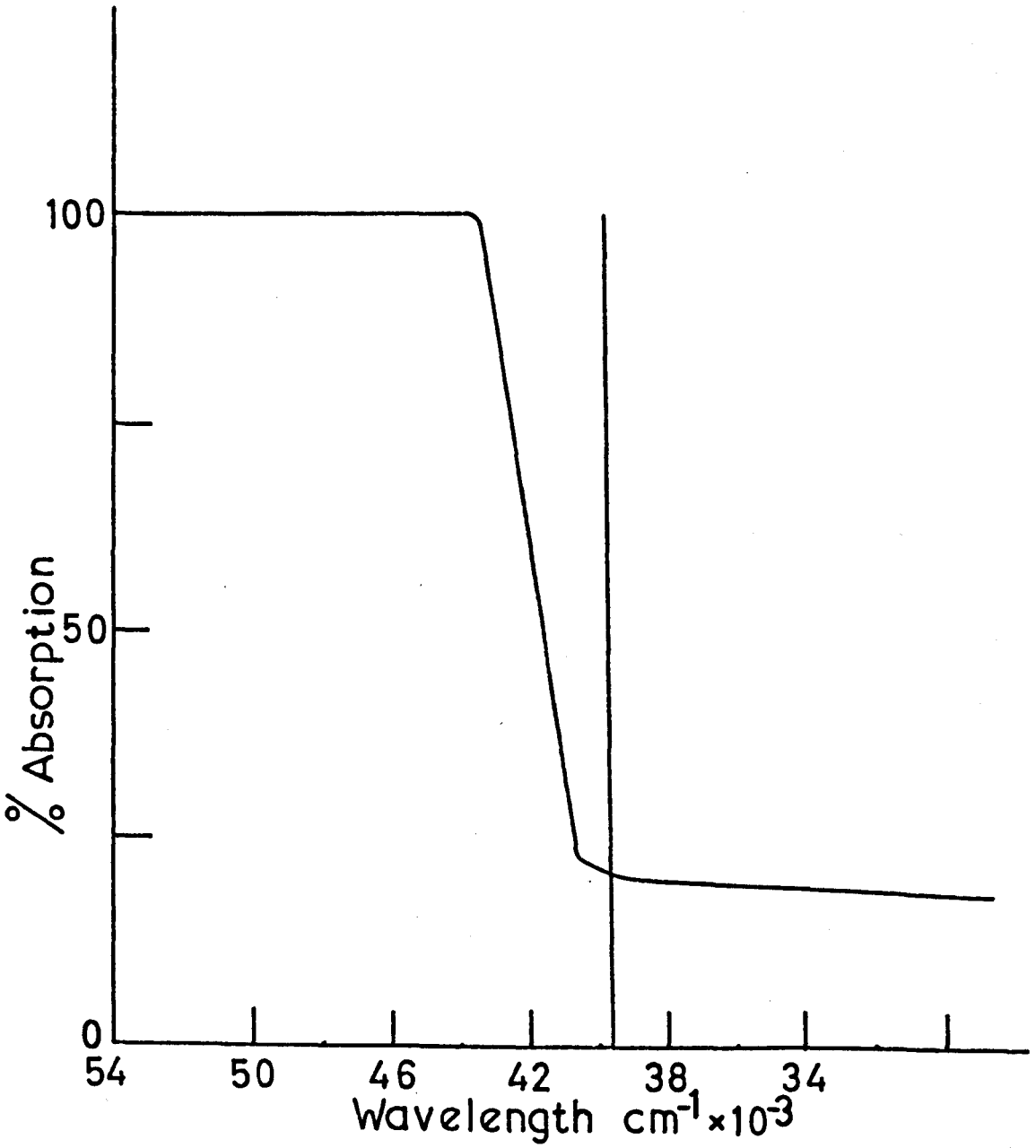

the water in between the lamp and the reaction liquid no temperature variation experiments could be carried out. Also no quantum yields could be obtained only relative rates of reactions.

2.6 Procedure

2.6.1 Vapour Phase

The reaction vessel was pumped under high vacuum for a period of half an hour prior to introducing a known pressure of the reactant gas into the cell. After admission of the gas, tap F (Figure 2.1) was closed and the gas given sufficient time to attain the cell temperature. The lamp was allowed a warm up period of ten minutes in the case of the low pressure lamp and fifteen minutes for the high pressure lamp before irradiation was commenced by removal of the shutter. Irradiation periods were in general of fifteen minutes and were terminated by switching off the lamp. During the warm up periods and irradiation periods both the lamp housing and thermostat were flushed through with dry nitrogen, a stream of nitrogen was also played on the space between the lamp and the cell.

On completion of irradiation the reaction products were allowed to stand for thirty minutes, before sampling into the gas chromatograph for analysis, to ensure that complete mixing of the gases occurred. When irradiation of a reactant gas was carried out in the presence of a non-condensable additive, i.e. N_2, argon, the gases were given half an hour before irradiation and half an hour after to enable thorough mixing to occur.

After each experiment the front window was removed and washed with chromic acid for several hours, secondly rinsed with distilled water

and then with acetone. The window was dried and the transmission at 1849 Å measured on the S.P. 700 spectrophotmeter. After insertion of a clean window the cell was pumped for several hours under high vacuum before another irradiation could take place.

2.6.2 Liquid Phase

Before the sample was introduced into the cell the whole was flushed out with nitrogen to remove any oxygen. 25 Mls. of the sample solution to be irradiated were placed into the cell and the quartz cooler attached with the lamp inside. Water was continually passed through the quartz jacket throughout each experiment. Nitrogen was then bubbled through the sintered glass disc to remove traces of oxygen from the solution. A condenser and gas burette were attached to the side arm and these were flushed out with nitrogen as well. After 2 - 3 hours the nitrogen flow was terminated and the magnetic stirrer switched on.

The lamp was then switched on and samples of the liquid were taken at various time intervals via the lower side arm through the septun cap. Samples of the gases were also taken at varying times and, like the liquid samples, were analysed by vapour phase chromatography. The total volume of gases evolved were measured by the gas burette at varying time intervals and so all the variables could be measured. However, no temperature experiments could be carried out due to the water jacket being in contact with the solution.

2.7 Polarography

Analysis of the metallic film produced in the experiments using the low pressure mercury vapour lamp was carried out using polarography. The instrument used was a manual polarograph of Southern Analytical Ltd. (Type A.1650). The quartz window on which the tin film had formed was washed with 12½ mls. of 4N hydrochloric acid and the washings collected in a 50 ml. graduated flask. The window was washed with distilled water and the washings added to the flask. Into the flask was then added a gelatine solution so that the concentration on 50 mls. would be 0.005 grms. per ml. KCl solution was added to give a solution 0.1 M in KCl when made up to 50 mls. The volume of the solution was then made up to the mark with distilled water and shaken vigorously to mix thoroughly. The flask was then placed in a thermostatted water bath to attain the temperature of 20°C.

10 Mls. of the solution were then placed in the polarograph cell and nitrogen bubbled through the solution to remove oxygen from the solution. After 20 minutes the nitrogen was stopped bubbling through the solution and played on to the surface so that no oxygen remained in the cell. The mercury drops were then allowed to fall and the voltage supply connected.

A typical polarogram obtained in standardising the instrument is shown in Figure 2.16. Standardisation was carried out by dissolving

Figure 2.16

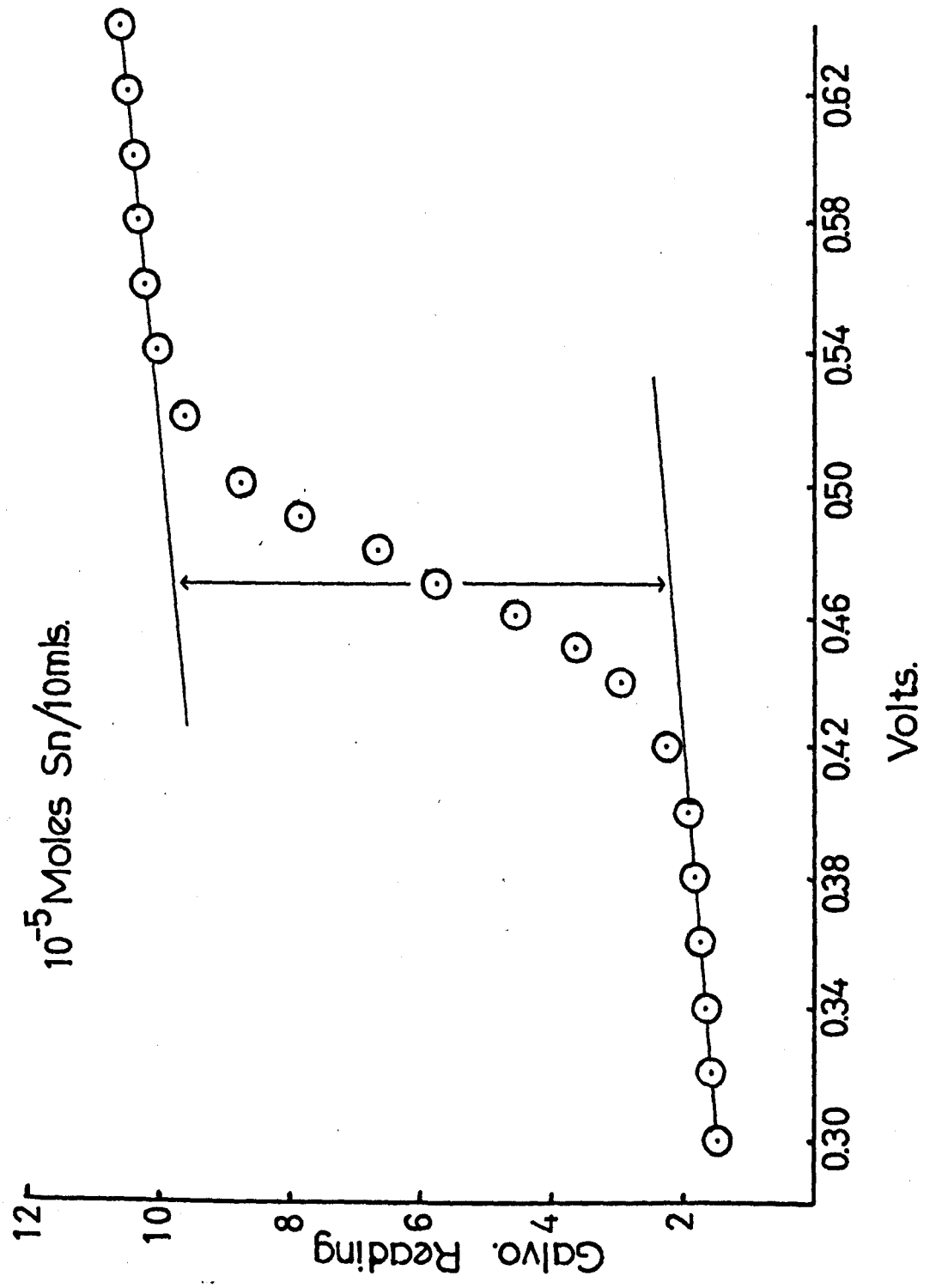
10^{-5} Moles Sn/10mls.
Galvo. Reading
12
10
8
9
7
2
0.30
0.34
0.38
0.42
0.46
0.50
0.54
0.58
0.62
Volts.

a known weight of Stannous chloride hydrate (Analar) in a solution normal to HCl, 0.1 M to KCl and containing 0.005 grms. gelatine per ml. The standard graph obtained is shown in Figure 2.17.

A second analysis was carried out by using a complete quartz cell in which the photolysis was carried out and also the solution made up so as to obtain all the metal deposited. It could be seen that the majority was however on the window, approximately 95%.

Figure 2.17

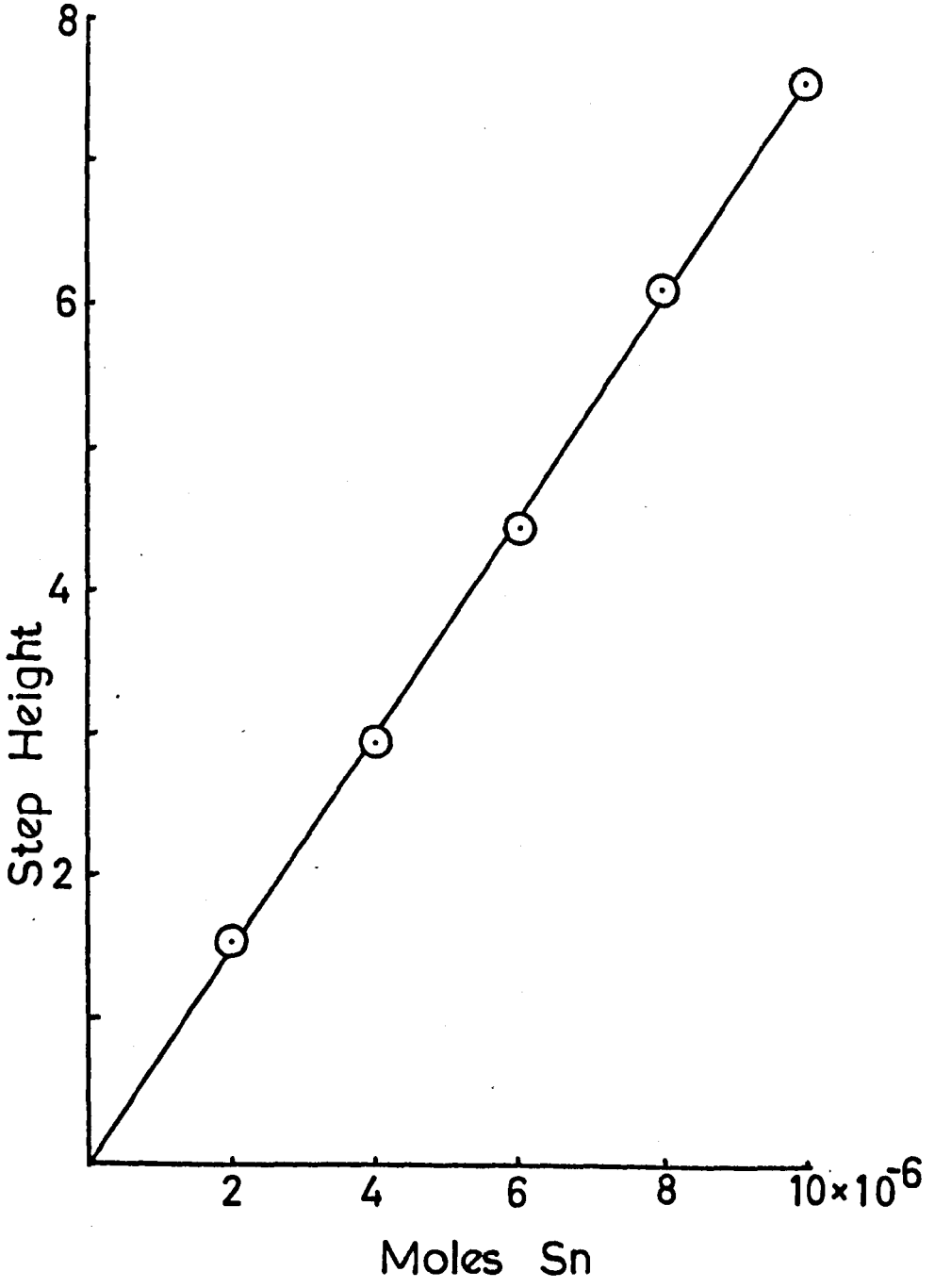

2.8 Mass Spectroscopy

During the period of preliminary investigations it was found necessary to obtain mass spectral data on the irradiated samples. Due to the prevailing parameters of adaptability, simplicity and economy an A.E.I. MS10 mass spectroscope was obtained in kit form and subsequently assembled (Plate 2.2).

The mass spectroscope consisted of three kits with certain accessories:

Kit A

Consisted of the analyses tube complete with ion source and collector with 0.02 inch slit, a set of heaters for baking the tube, and a stainless steel blank flange which was used to connect to the sampling system. Also an 1800 gauss permanent magnet and a control unit comprising of an electron beam control, autoscan accelerating voltage and main amplifier. Also an electrometer preamplifier with 10" o.h.m. input resistor of approximately 0.5 second response.

Kit B

Consisted of a diffusion pump with a stainless steel cold trap suitable for liquid nitrogen or solid CO_2, a tube/cold trap connector and heating band to bake out the connector, also a metrovac 033C water-cooled oil diffusion pump.

Kit C

Consisted of an G.D.R.1 rotary vacuum pump and backing line assembly.

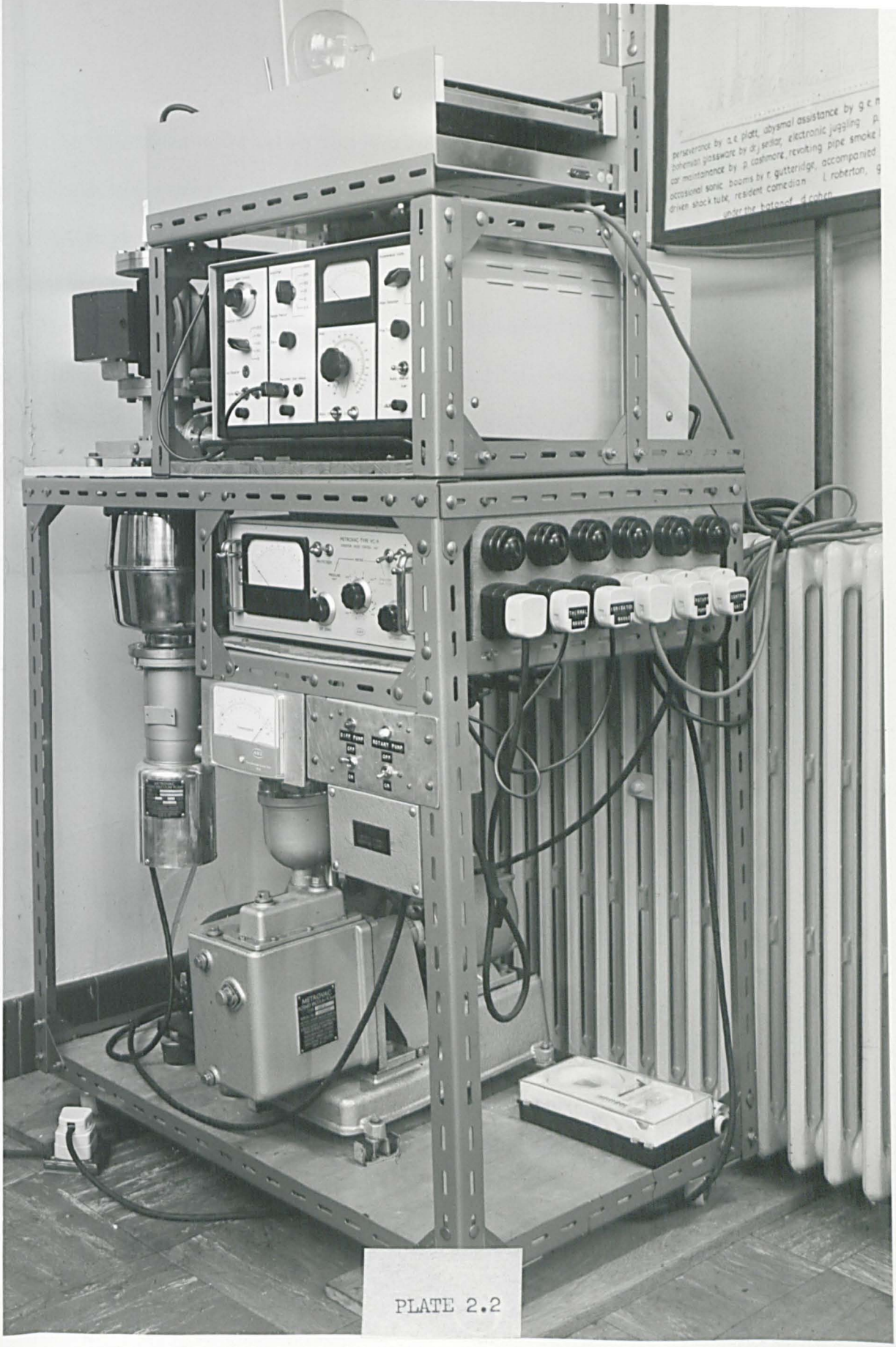

PLATE 2.2

The accessories to the three kits comprised of a Potentiometric recorder Unicam SP20, a bakeable insertion ion-gauge (Alpert type) and control unit VC9 and a thermocouple gauge VH8 and control unit VC12.

To the mass spectroscope when assembled was added a batch sampling system in between the two being a sintered metal diaphragm valve allowing only a pressure of 10^{-4} mm. to enter the mass-spectrometer head.

2.9 Computational Methods

In utilising the results of the temperature experiments in Section 3 to obtain activation energies and rate constants for the chain propagating reactions, it is necessary to calculate a considerable number of quantities.

If it is correct to say that methane is formed by two processes, a molecular reaction and an abstraction reaction, then the rate of methane formation (R_{Me}) can be expressed by the following equation:

$$R_{Me} = k_M[Sn(CH_3)_4^*] + k_H[CH_3][Sn(CH_3)_4] \qquad 2.I$$

where k_M is the rate constant for the molecular reaction and k_H that for the hydrogen abstraction reaction $Sn(CH_3)_4^*$ is the concentration of excited species and $Sn(CH_3)_4$ that for the tetramethyl stannane. By plotting R_{Me} against $[Sn(CH_3)_4]$, or the pressure of $Sn(CH_3)_4$, the intercept at the ordinate gives a value for $k_M[Sn(CH_3)_4^*]$ and the slope is $k_H[CH_3]$.

Similarly an equation can be built up for the rate of formation of ethane R_{Et}:

$$R_{Et} = k_M[Sn(CH_3)_4^*] + k_A[CH_3][Sn(CH_3)_4] + k_R[CH_3]^2 \qquad 2.II$$

By plotting R_{Et} against the pressure of $Sn(CH_3)_4$ the intercept of the ordinate gives $k_M[Sn(CH_3)_4^*] + k_R[CH_3]^2$ and the slope is equal to $k_A[CH_3]$. It can be seen that subtracting the intercept of the first plot from the second intercept a value of $k_R[CH_3]^2$ is obtained. Substituting a value for k_R [48] the methyl radical concentration is obtained. Values for k_H and k_A can then be obtained.

Hydrogen abstraction is related to radical combination by the equation

$$k_H = \frac{1}{RH} \cdot \frac{R'_{Me}}{R'^{\frac{1}{2}}_{Et}} \cdot k_R^{\frac{1}{2}} \qquad 2.III$$

where R'_{Me} is the rate of methane by hydrogen abstraction and R'_{Et} the rate of ethane formation by methyl radical combination. All the values in the equation and their variation of these values with temperature are known and so k_H can be calculated over the temperature range 25 - 150°C. The rate constant k_A can be calculated over the same range using equation 2.II.

All the calculations involved in obtaining the values of the rate constants were combined into a programme and the rate constants obtained were treated in a least squares method to give the activation energies and pre-exponential factors. The programme used is given below.

```
    1 FORMAT(116HCALCULATIONS OF RATE CONSTANTS & ACTIVATION ENERGIES FO
     1R TETRA METHYL STANNANE PHOTOLYSIS, WITH TEMPERATURE VARIATION)
    2 FORMAT(58HEQUATIONS & RESULTS BY A.E.PLATT
    3 FORMAT(28HADAPTED ON SEPTEMBER 18 1968/)
    4 FORMAT(15HVARIABLES USED,/)
    5 FORMAT(12X,17HMETHANE BY H ABS.,10X,19HETHANE BY RAD COMB.,10X,21H
     1ETHANE BY METHYL ABS.)
    6 FORMAT(11HNON RADICAL,8X,3HXNM,24X,3HXNE,29X,3HXNE,9X,21H=2.67*10*
     1*-9MOLES/MIN)
    8 FORMAT(10HRATE CONST,9X,3HXKM,24X,3HXKC,28X,3HXKCA)
    9 FORMAT(4HRATE,15X,3HRMA,25X,2HRC,29X,3HRCA)
    7 FORMAT(10HEXPT YIELD,10X,2HEM,25X,2HEE,30X,2HEE)
   10 FORMAT(11HACT.ENERGY,9X,2HEX,25X,2HEC,29X,3HECA)
      DIMENSION T(20),EM(20),EE(20),X(20),Y(20),XKM(20),XKC(20),XKCA(20)
     1,RMA(20),RCA(20),CY(20),DIF(20),RMAK(20),(20),ZIM(20)
      COMMON T,EM,EE,X,Y,XKM,XKC,XKCA,RMA,RC,RCA,CY,DIF,D,SLOPE,RMAK,C,E
     1X,FC,ECA,N,ZIM
      WRITE(2,1)
      WRITE(2,2)
      WRITE(2,3)
      WRITE(2,4)
      WRITE(2,5)
      WRITE(2,6)
      WRITE(2,7)
      WRITE(2,8)
      WRITE(2,9)
      WRITE(2,10)
      READ(7,11)N
   11FORMAT(I3)
      READ(7,12)XNM,XNE,RC,R
   12FORMAT(E10.3,E10.3,E11.4,F7.4)
      DO 14 I=1,N
      READ(7,13)T(I),EM(I),EE(I)
   13FORMAT(F7.2,E11.4,E11.4)
   14 CONTINUE
   15 FORMAT(37HOCALCULATIONS OF HYDROGEN ABSTRACTION)
      WRITE(2,15)
      DO 16 I=1,N
      RMA(I)=EM(I)-XNM
      RMAK(I)=RMA(I)/7.62
      XKC(I)=2.1*(10.0**9.0)*(SQRT(T(I)))
      C(I)=(5.0*T(I))/(760.0*22.4*298.0)
      XKM(I)=(RMAK(I)*(SQRT(XKC(I))))/(C(I)*(SQRT(RC)))
      X(I)=1./T(I)
   16 Y(I)=ALOG 10(XKM(I))
      CALL AQUIB
   17 FORMAT(4HTEMP,10X,15HRECIPROCAL TEMP,8X,2HKM,10X,9HLOG 10 KM,5X,21
     1 HCAL VALUE OF LOG10 KM,5X,20HDIF CALKM & INPUT KM)
      WRITE(2,17)
```

```
      DO 19 I=1,N
      WRITE(2,18)T(I),X(I),XKM(I),Y(I),CY(I),DIF(I)
   18 FORMAT(F6.1,10X,F8.6,7X,E14.7,6X,F7.4,14X,F7.4X,F7.4,17X,F8.4)
   19 CONTINUE
   20 FORMAT(39HOINTERCEPT=LOG PRE EXPONENTIAL FACTOR= ,F8.4)
      WRITE(2,20)D
      A=D
       EX=SLOPE*R*2.3026
   21 FORMAT(19HACTIVATION ENERGY= ,F10.3)
      WRITE(2,21)EX
      Z=EX
   22 FORMAT(38HOCALCULATIONS OF RADICAL RECOMBINATION)
      WRITE(2,22)
      DO 23 I=1,N
      XKC(I)=2.1*(10.0**9.0)*(SQRT(T(I)))
      X(I)=1./T(I)
      Y(I)=ALOG 10(XKC(I))
   23 CONTINUE
      CALL SQUIB
   24 FORMAT(4HTEMP,10X,15HRECIPROCAL TEMP,8X,2HKC,10X,9HLOG 10 KC,5X,21
     1HCALCULATED VALUE OF K,5X,20HDIF CALKM & INPUT KM)
      WRITE(2,24)
      DO 26 I=1,N
      WRITE(2,25)T(I),X(I),XKC(I),Y(I),CY(I),DIF(I)
   25 FORMAT(F6.1,10X,F8.6,7X,E14.7,6X,F7.4,14X,F7.4,17X,F8.4)
   26 CONTINUE
   27 FORMAT(39HOINTERCEPT=LOG PRE EXPONENTIAL FACTOR= ,F8.4)
      WRITE(2,27)D
      EC=SLOPE*R*2.3026
   28 FORMAT(19HACTIVATION ENERGY= ,F10.3)
      WRITE(2,28)EC
   45 FORMAT(46HOCALCULATIONS OF THE VALUE OF LOG10KM/SQRT(KC))
      WRITE(2,45)
   46 FORMAT(4HTEMP,10X,16HLOG10KM/SQRT(KC))
      WRITE(2,46)
      DO 32 I=1,N
   31 ZIM(I)=ALOG 10(A-(D/2))-((Z*EC)/(R*T(I)*2.3026))
   44 FORMAT(F6.1,11X,F13.6)
      WRITE(2,44)T(I),ZIM(I)
   32 CONTINUE
   33 FORMAT(35HOCALCULATIONS OF METHYL ABSTRACTION)
      WRITE(2,33)
      DO 34 I=1,N
      RCA(I)=EE(I)-RC-XNE
      XKC(I)=2.1*(10.0**9.0)*(SQRT(T(I)))
      XKCA(I)=(RCA(I)*(SQRT(XKC(I))))/(7.62*C(I)*(SQRT(RC)))
      X(I)=1.0/T(I)
      Y(I)=ALOG 10(XKCA(I))
```

```
34 CONTINUE
   CALL SQUIB
35 FORMAT(4HTEMP,10X,15HRECIPROCAL TEMP, 8X,3HKCA,10X,10HLOG 10 KCA,5X
  1,22HCAL VALUE OF LOG10 KCA,5X,22HDIF CALKCA & INPUT KCA)
   WRITE(2,35)
   DO 37 I=1,N
   WRITE(2,36)T(I),X(I),XKCA(I),Y(I),CY(I),DIF(I)
36 FORMAT(F6.1,10X,F8.6,7X,E14.7,6X,F7.4,14X,F7.4,17X,F8.4)
37 CONTINUE
38 FORMAT(39HOINTERCEPT=LOG PRE EXPONENTIAL FACTOR= ,F8.4)
   WRITE(2,38)D
   ECA=SLOPE*R*2.3026


39 FORMAT(19HACTIVATION ENERGY= ,F10.3)
   WRITE(2,39)ECA
   STOP
   END
```

```
   SUBROUTINE SQUIB
   DIMENSION T(20),EM(20),EE(20),Y(20),XKM(20),XKC(20),XKCA(20)
  1,RMA(20),RCA(20),CY(20),DIF(20),RMAK(20),C(20),ZIM(20)
   COMMON T,EM,EE,X,Y,XKM,XKC,XKCA,RMA,RC,RCA,CY,DIF,D,SLOPE,RMAK,C,E
  1X,EC,ECA,N,ZIM
   SUMX=0
   SUMY=0
   SUMXY=0
   SUMXX=0
   DO 40 I=1,N
   SUMX=SUMX+X(I)
   SUMY=SUMY+Y(I)
   SUMXY=SUMXY+X(I)*Y(I)
40 SUMXX=SUMXX+X(I)*X(I)
   G=N
   DENOM=(G*SUMXX)-(SUMX**2)
   SLOPE=(G*SUMXY-SUMX*SUMY)/DENOM
   D=(SUMY/G)-(SLOPE*SUMX/G)
   DO 41 I=1,N
   CY(I)=(SLOPE*X(I))+D
   DIF(I)=CY(I)-Y(I)
41 CONTINUE
   RETURN
   END
```

Where the following are the variables used:

XMM: Rate of formation of methane by molecular elimination in moles/min.

EM: Yield of methane in moles/min.

XKM: Rate constant for hydrogen abstraction reaction.

EX: Activation energy for hydrogen abstraction reaction.

XKC: Rate constant for methyl radical combination in litres/moles/sec.

RC: Rate of ethane formation by radical combination.

EC: Activation energy for methyl radical combination.

XMM:
XME: Rate of formation of ethane by molecular elimination.

EE: Yield of ethane in moles/min.

XKCA: Rate constant for methyl group abstraction.

CCA: Rate of formation of ethane by methyl group abstraction.

ECA: Activation energy of methyl group abstraction.

2.10 Actinometry

The output of the lamp at 1849 Å was measured using ethylene as a chemical actinometer. The quantum yield for the formation of acetylene (1.0) and hydrogen (0.8 ± 0.1) were originally given to us by Dr. H. Rommel[75] and subsequently published by Beckey, Groth, Okabe and Rommel.[76] The values were determined using nitrous oxide as an actinometer.[77,78,79] Due to the importance of the figure for the ϕH_2 from ethylene it was decided to remeasure this using nitrous oxide as an actinometer.

Several steady state experiments were carried out with nitrous oxide and ethylene in order to determine the yields of nitrogen and hydrogen respectively. In each case 100 mm. of gas was irradiated and after allowing sufficient time (1 hr.) for the products to mix, they were analysed by gas chromatography using a 6 ft. column packed with a molecular sieve (5A) using hydrogen as a carrier gas in the detection of N_2 and nitrogen as a carrier gas in the detection of hydrogen. The detector used was a Pye (Series 104) katharometer. The results of these experiments have been reported in reference 80 along with experiments conducted on another apparatus and using a different low pressure lamp. Figures 2.18 - 19 give the standard calibrations for H_2 and N_2 using the katharometer and molecular sieve column.

TABLE 2.1

Nitrous Oxide	Yield N_2
100 mm.	27.71×10^{-7} moles
100 mm.	27.75×10^{-7} moles

Ethylene	Yield H_2
100 mm.	11.77×10^{-7} moles
100 mm.	11.77×10^{-7} moles

Quantum yield of H_2 from ethylene

$$\phi_{H_2} = \frac{\text{yield } N_2 \times \phi N_2}{\text{yield } H_2} \qquad 2.IV$$

$$= 0.61 \pm 0.01$$

2.11 Analysis

Qualitative and quantitative measurements were performed on a Pye Series "104" Gas Chromatograph fitted with both a katharometer and a hydrogen ionisation detector.

Qualitative analyses were made on a variety of columns listed in Table 2.2. The inert support material where necessary was 60 - 80 mesh celite.

TABLE 2.2

	Column Stationary Phase	Length (ft.)	Temperature	Carrier Gas
1.	10% Apiezon-L	9 ft.	65 - 145°C	N_2
2.	10% Polyethylene Glycol Adipate	9 ft.	60 - 140°C	N_2
3.	Silver Nitrate on Ethylene Glycol	6 ft.	35°, 40°C	N_2
4.	Molecular Sieves MS5A	6 ft.	30°C	N_2, H_2
5.	Polyethylene Glycol on Chromasorb W.	a) 9 ft. b) 15 ft.	120°C 120°C (Preparative)	N_2 N_2
6.	Poropak Q (80 - 100 mesh)	9 ft.	50°C	N_2

Quantitative analyses were conducted on columns (1) and (6). Calibration was made by using mixture of authentic sample with nitrogen. Table 2.3 shows the relationship between the peak height, recorder on a Vitatron lin/log, recorder with a 0 - 10 mV range, and the molar quantities of the pure compounds. Figures 2.20 - 27 give the calibration plots.

TABLE 2.3

Compound	Figure	Column	Column Temp.	N_2 Pressure	1 cm = Moles
Methane	2.20	Poropak	50°	20	54.126×10^{-12}
Ethane	2.21	Poropak	50°	20	133.36×10^{-12}
Me_3SnH	2.22	Ap - L	100°	20	-
Me_3SnEt	2.23	Ap - L	100°	20	-
$Me_3SnSnMe_3$	2.24	Ap - L	100°	20	84.21×10^{-12}
Ethylene	2.25	Poropak	50°	20	97.14×10^{-12}
Propane	2.26	Poropak	50°	20	56.33×10^{-11}
Butane	2.27	Ap - L	65°	20	18.37×10^{-12}

The relationship cms - moles in this table involves the factor necessary to change volume of U-tube to total sample volume.

Figure 2.18

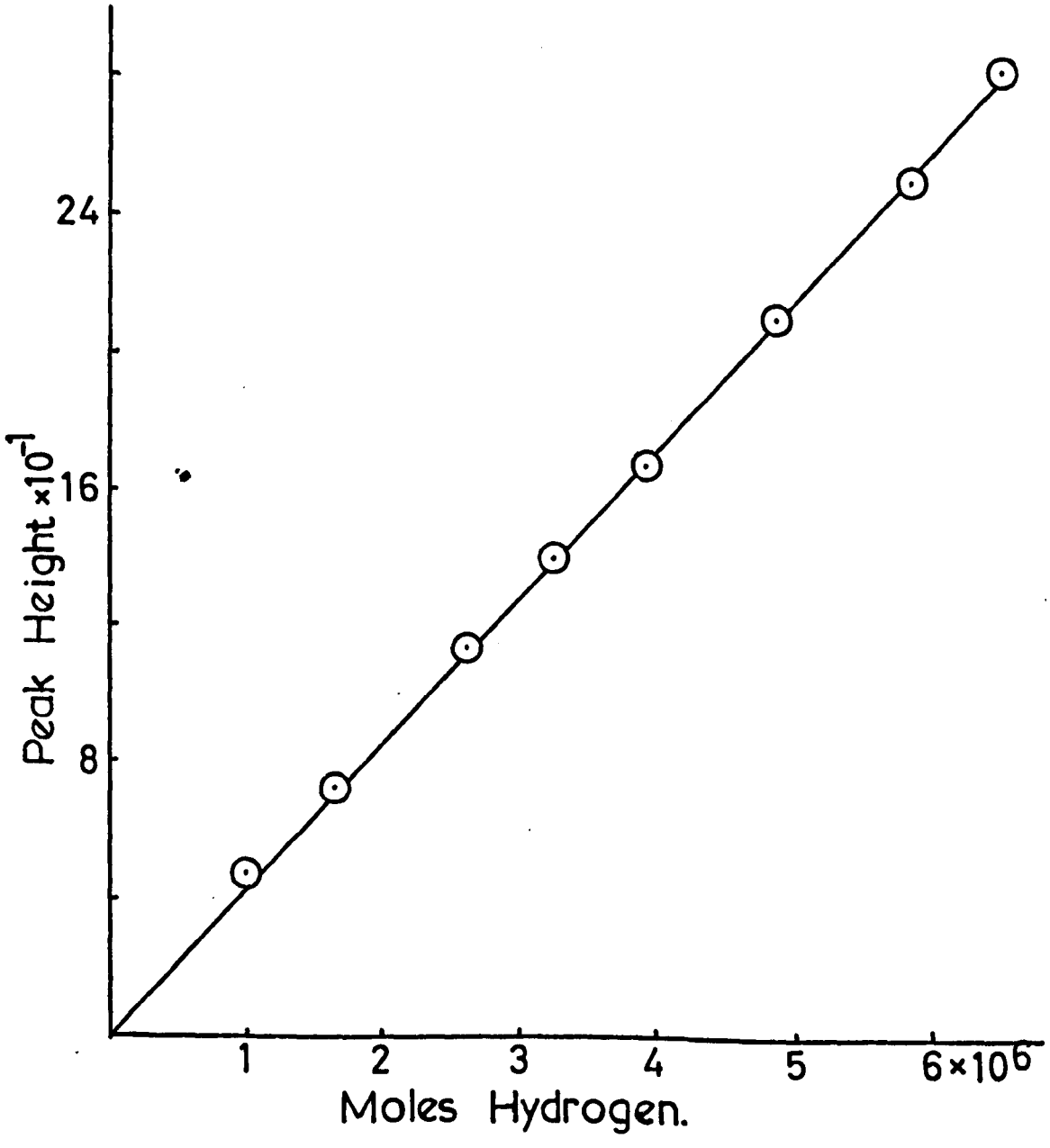

Figure 2.19

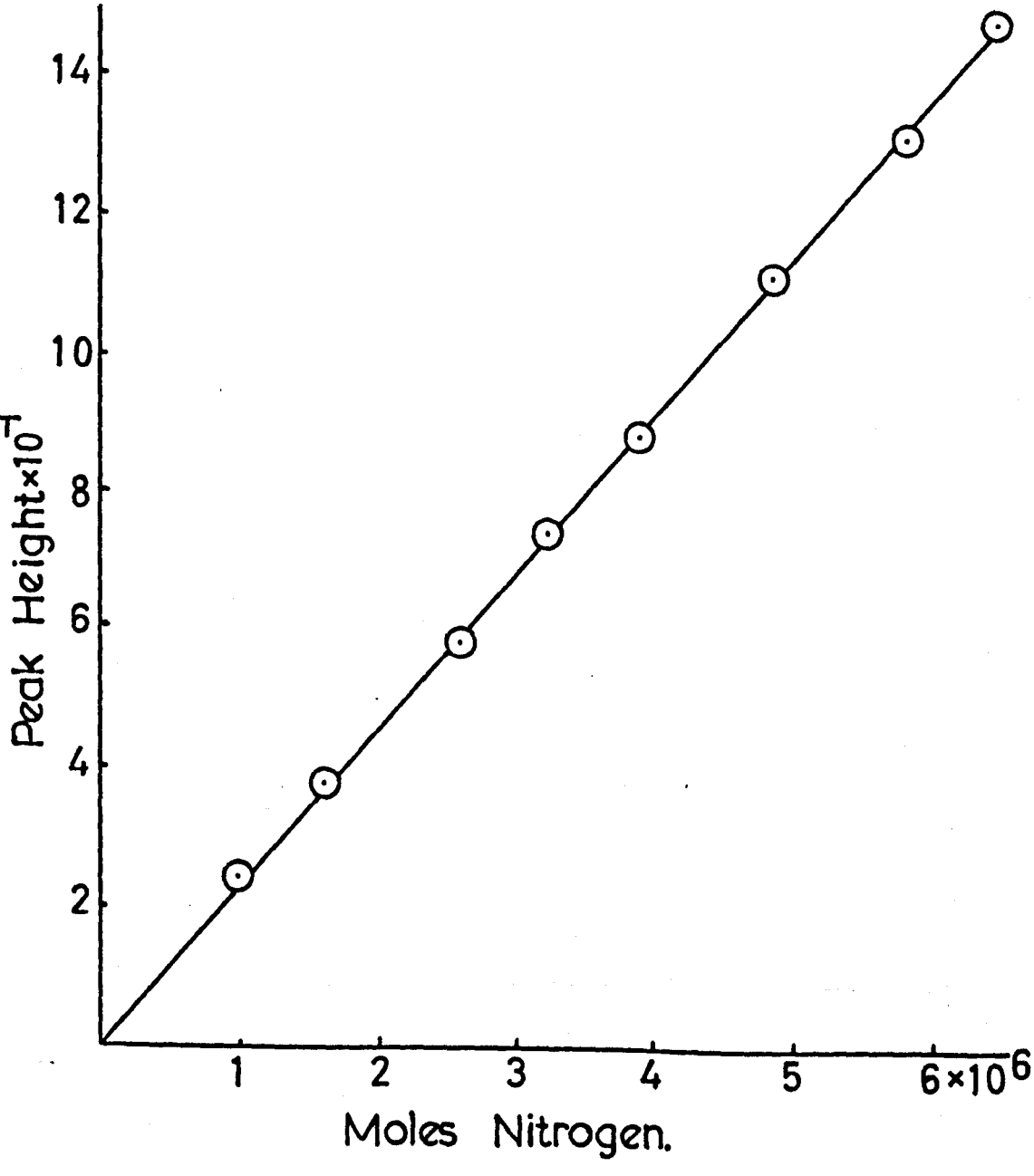

Figure 2.20

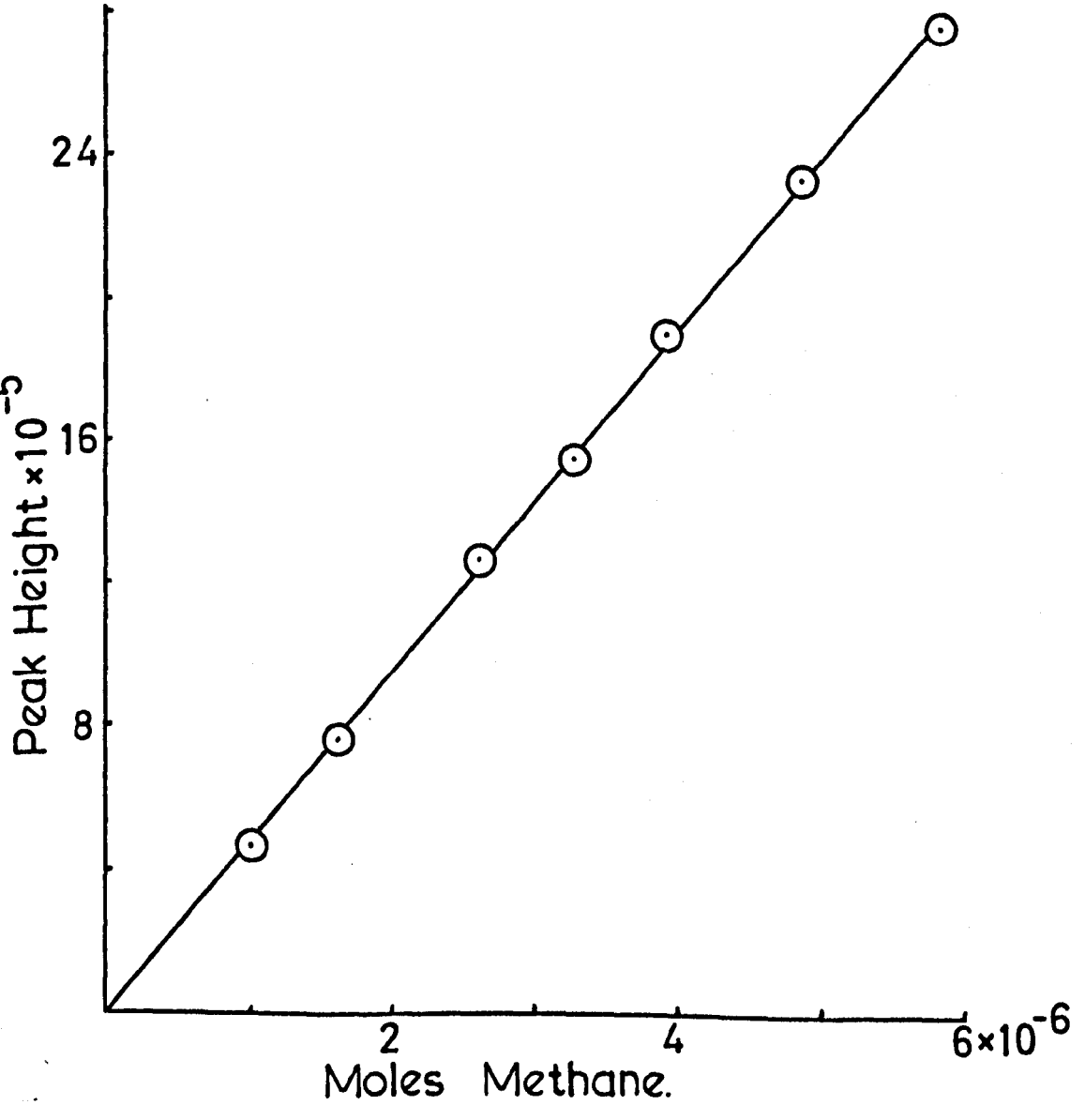

Figure 2.21

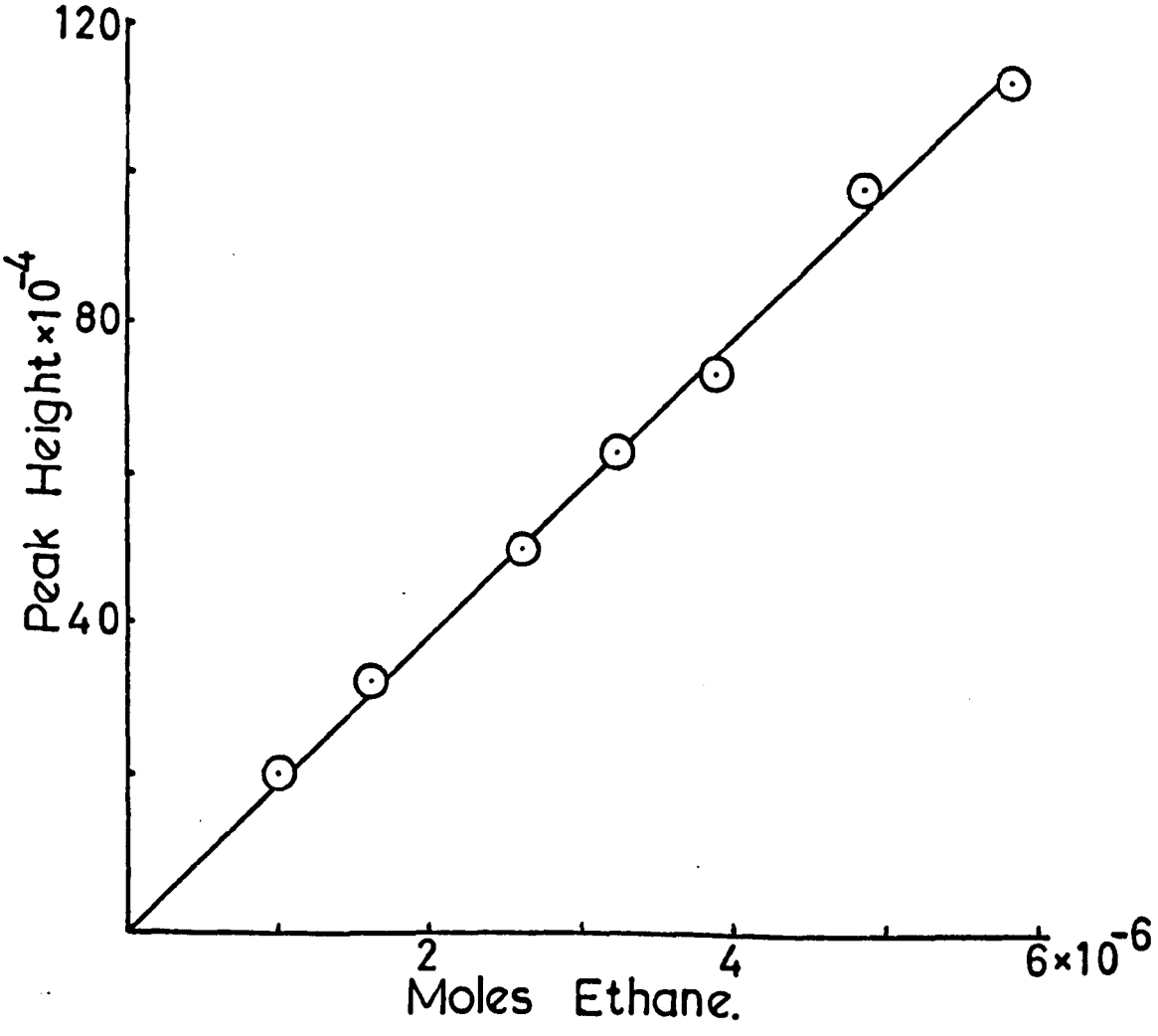

Figure 2.23

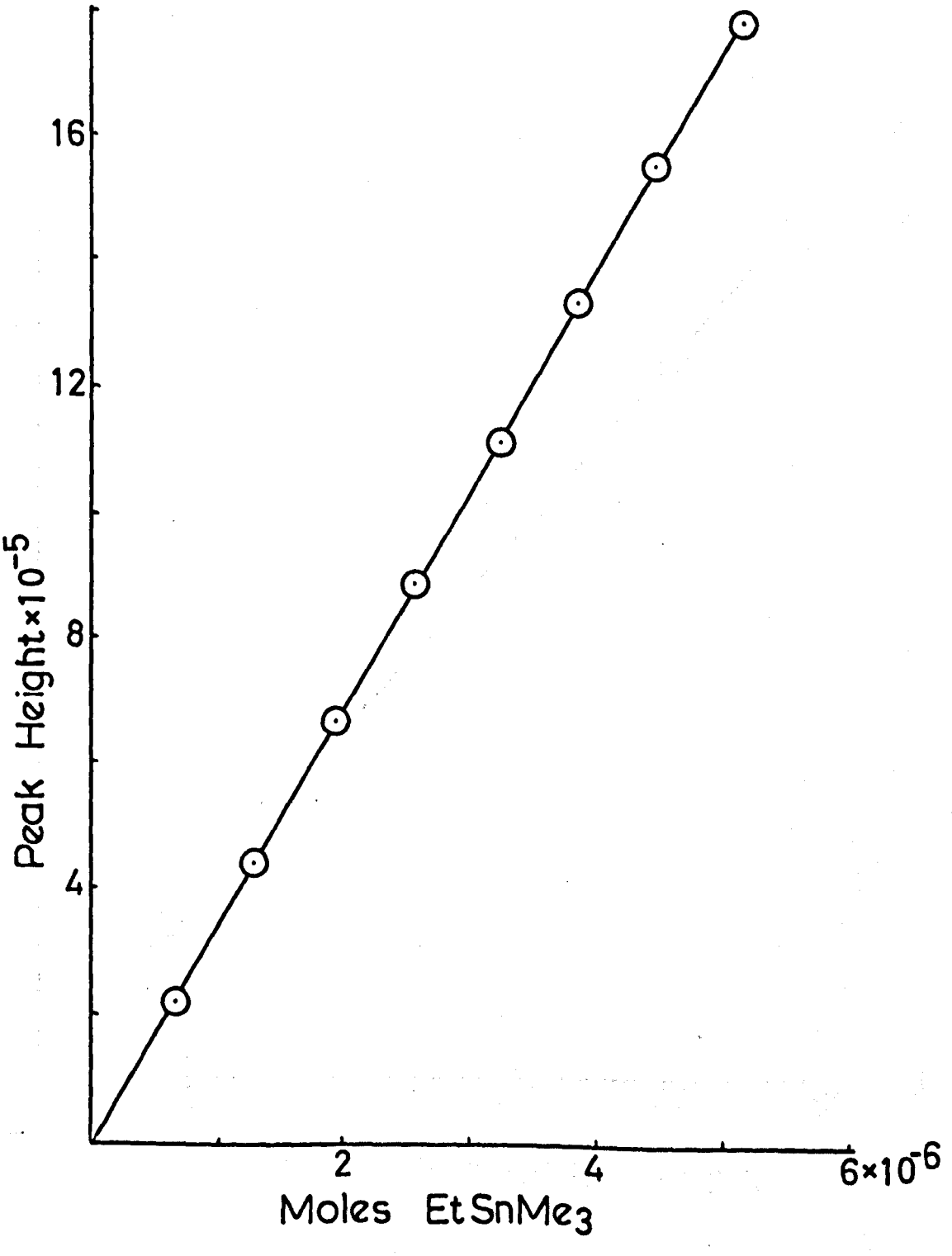

Figure 2.24

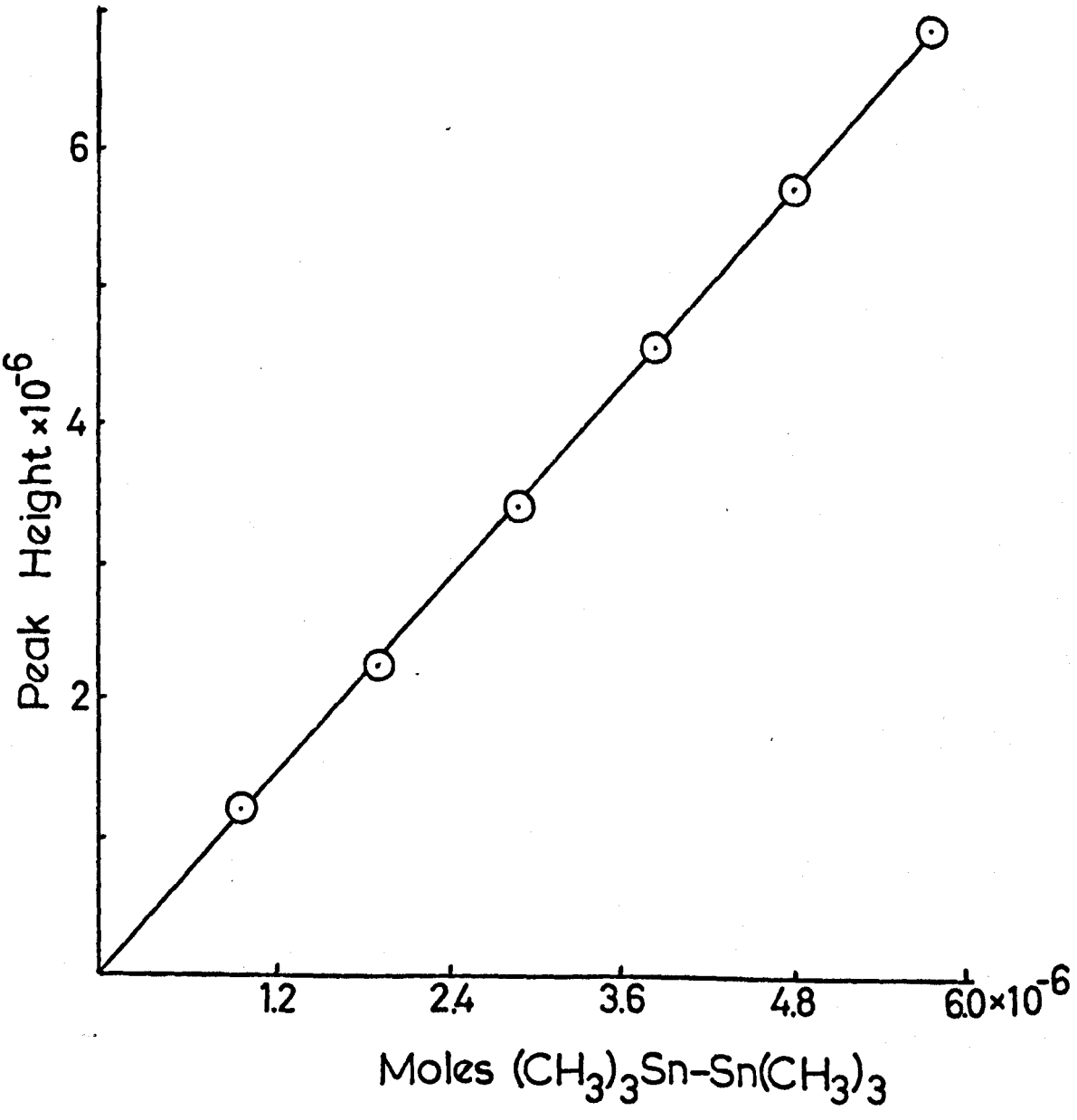

Figure 2.25

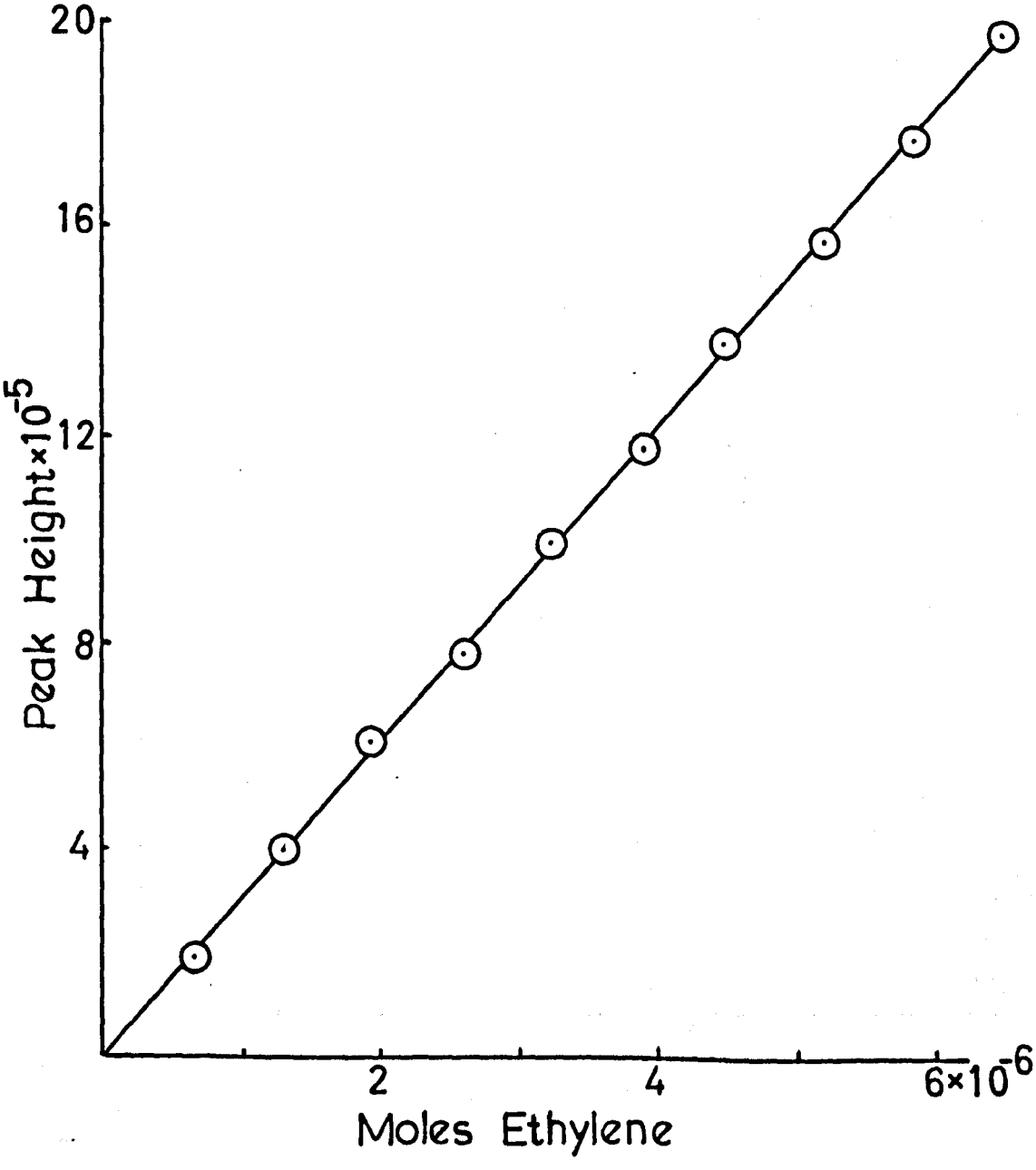

Figure 2.26

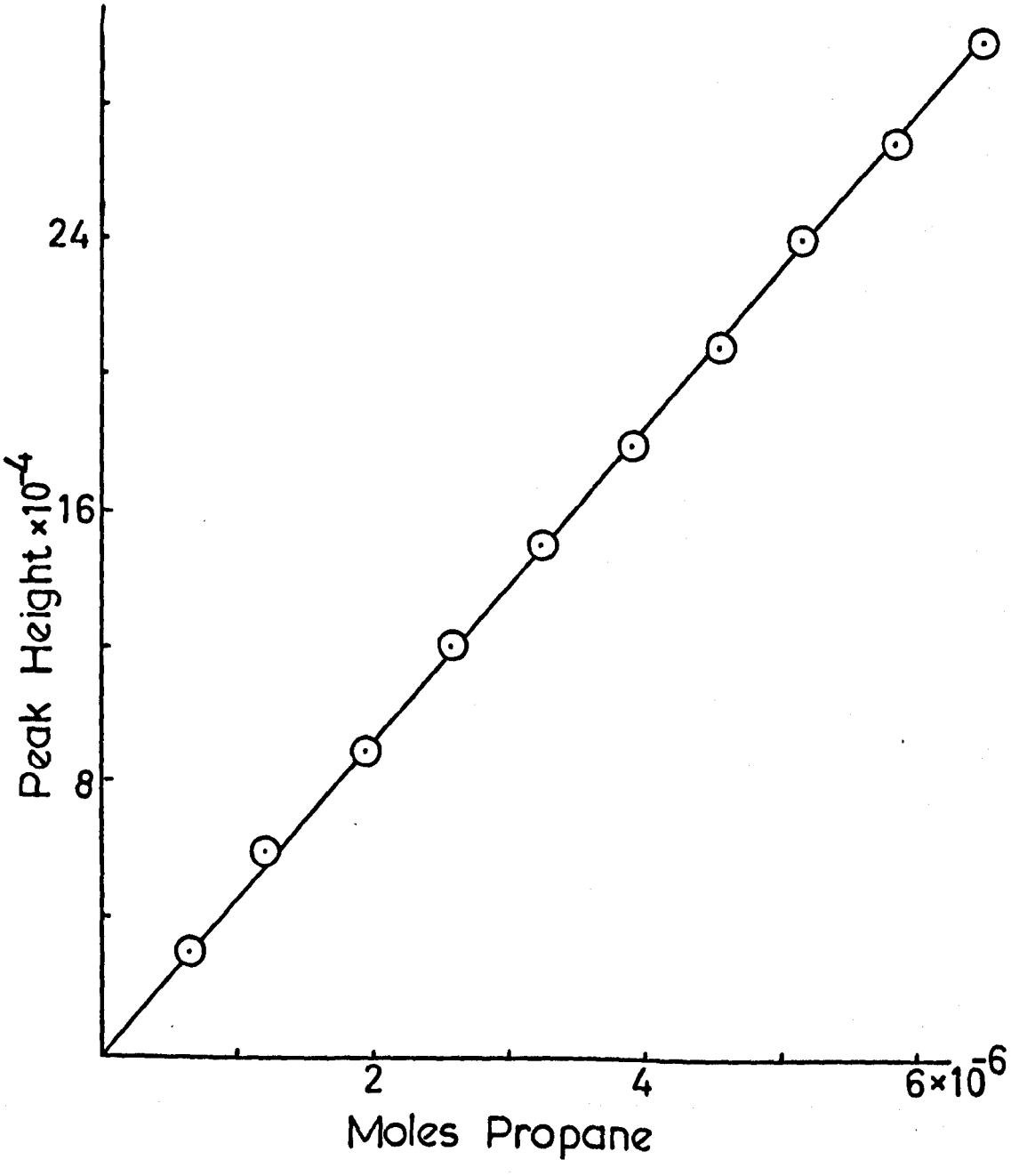

Figure 2.27

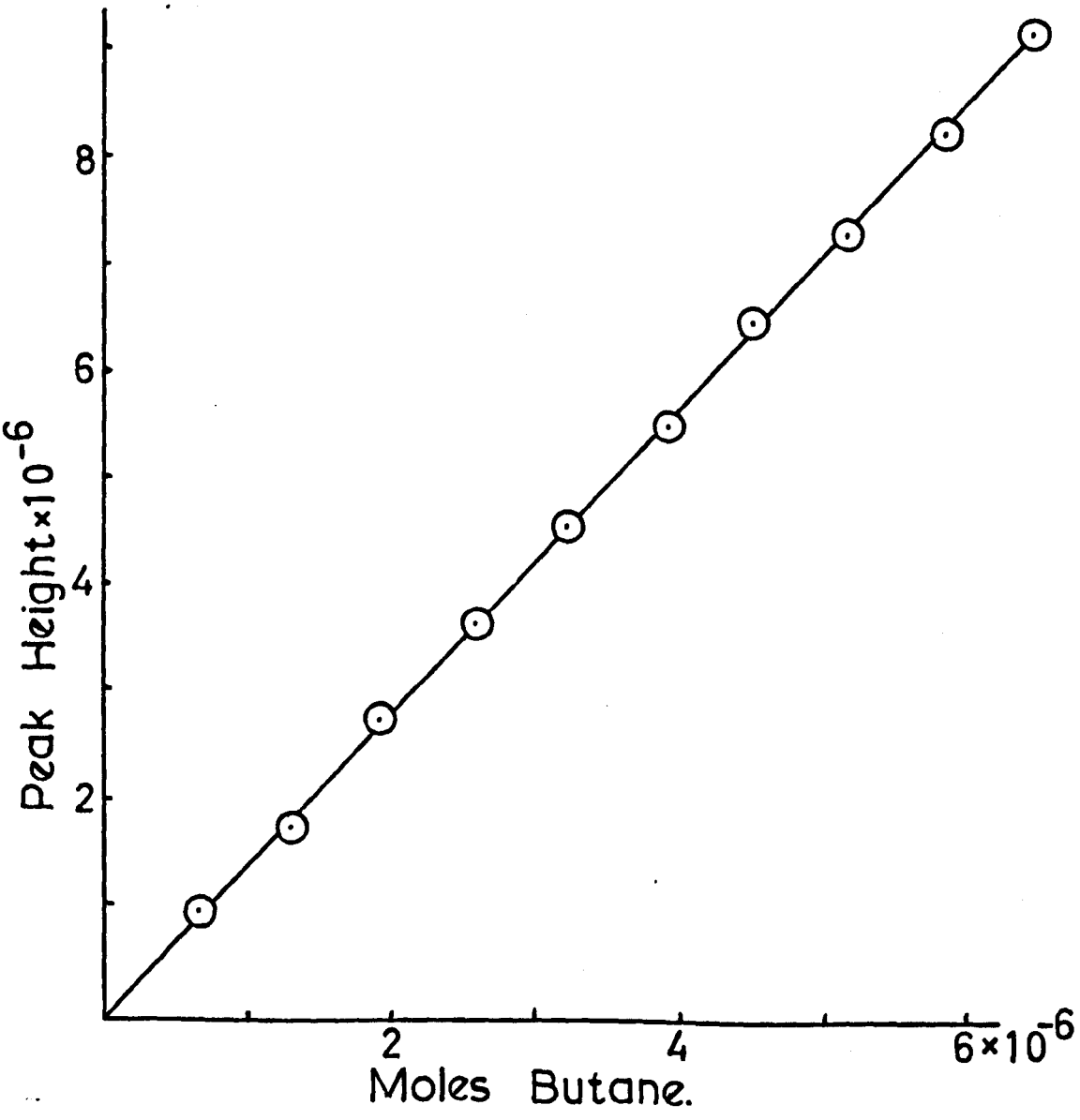

Infrared spectra were recorded on a Perkin-Elmer Model 221 I.R. Spectrometer, and ultraviolet transmission data and spectra were recorded on a Unicam S.P. 700 and S.P. 800. Electron microscopy was carried out at the National Physical Laboratories, Teddington and I am grateful to Dr. Stoddart for this service.

3. RESULTS

Tetramethyl Stannane

Irradiation of a sample of tetramethyl stannane with a filter of 2% acetic acid, 1 cm. thick, interposed between the lamp and the cell, resulted in no photochemical reactions, whereas without the filter in position a number of photochemical products were obtained. The presence of the filter which absorbs 1849 Å radiation (Section 2.5.2) indicated that 1849 Å was the exciting radiation and also that no mercury was present in the system, acting as a sensitiser since tetramethyl stannane is transparent to 2537 Å which is the main component of the light emitted from a low pressure mercury vapour lamp (Section 2.5.1, figure 2.11).

Initially when using the high pressure lamp and a mercury diffusion pump it was possible that mercury sensitisation could have been taking place resulting in some products being formed.

The products of irradiation at 1849 Å were ethane, methane and very small amounts of propane and ethylene. At higher temperatures trimethyl tin hydride, ethyl trimethyl stannane and hexamethyl distannane were observed. Table 3.1 shows the relative quantities of the products.

TABLE 3.1

25°C		100°C	
C_2H_6	1.0×10^{-7} moles/min.	C_2H_6	1.4×10^{-7} moles/min.
CH_4	3.0×10^{-9} moles/min.	CH_4	1.7×10^{-8} moles/min.
C_2H_4	1.8×10^{-10} moles/min.	$(CH_3)_3SnH$	2×10^{-9} moles/min.
		$(CH_3)_3SnSn(CH_3)_3$	8×10^{-10} moles/min.
		$C_2H_5Sn(CH_3)_3$	1×10^{-10} moles/min.

Refer to figures 3.1a and 1b for chromatograms of products.

Clearly from the nature of the products there is the possibility of free radical processes being involved and also the possibility of molecular elimination (Section 1.6). To help to distinguish between the various modes of formation of the products their dependence upon the variation of the following parameters was observed:

(1) Time

(2) Intensity

(3) Pressure of tetramethyl stannane

(4) Temperature

(5) Added Inert gases

(6) Added radical scavengers

(7) Temperature at 50% and 2% intensity

(8) Temperature in the presence of added radical scavengers

Figure 3.1a

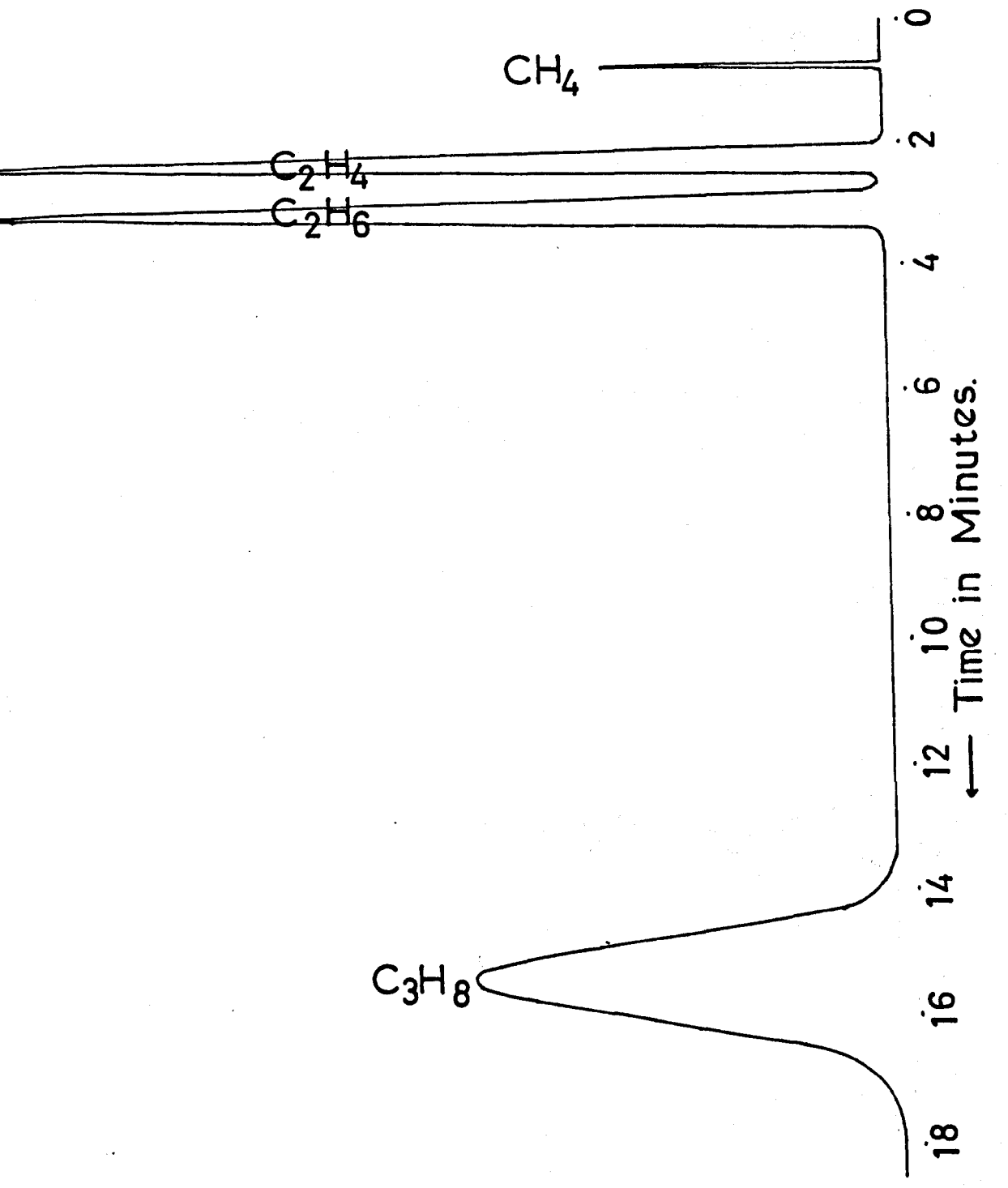

Figure 3.1b

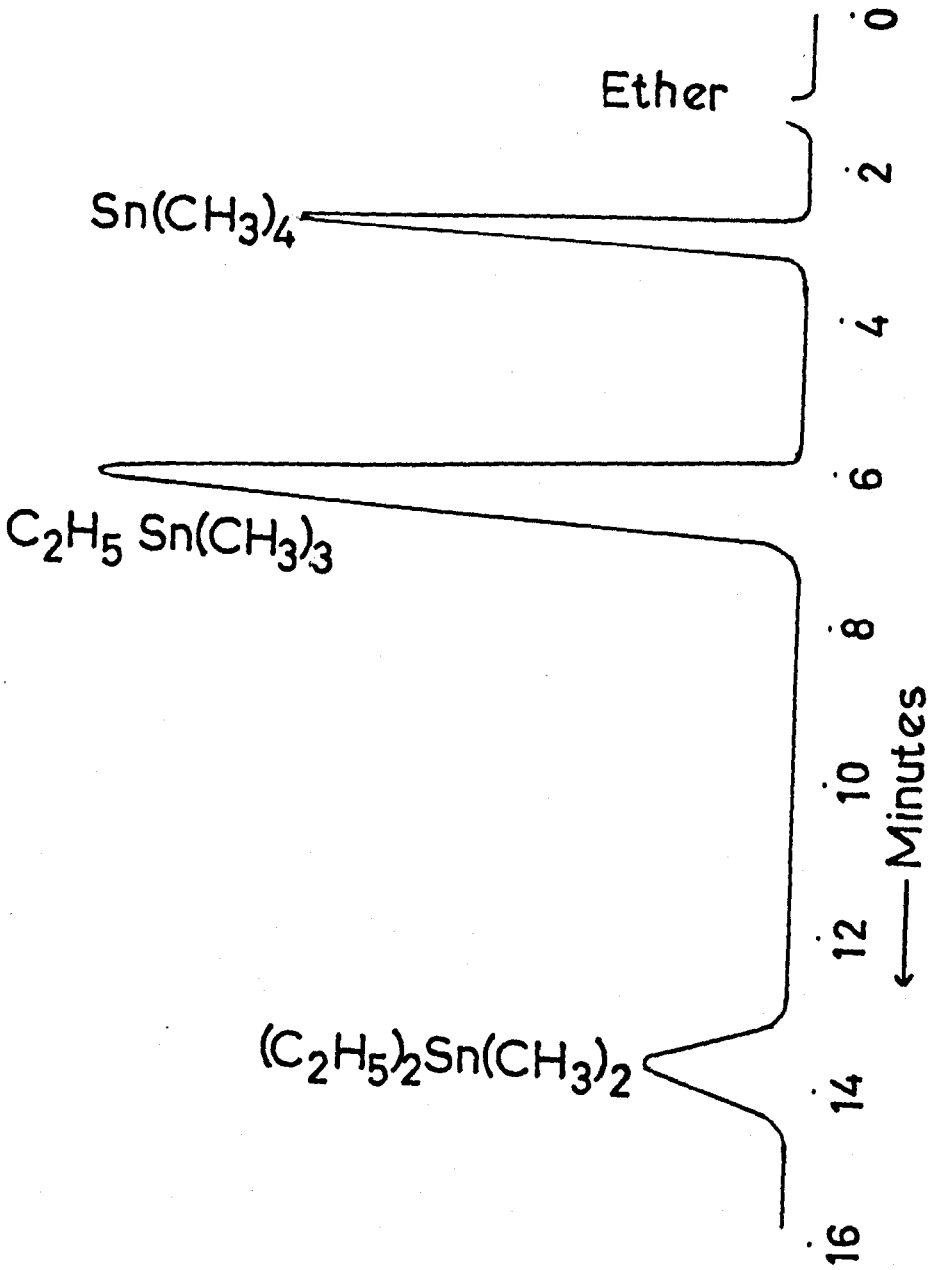
Ether
$Sn(CH_3)_4$
$C_2H_5\ Sn(CH_3)_3$
$(C_2H_5)_2Sn(CH_3)_2$
0
2
4
6
8
10
12
14
16
Minutes

(9) Time and high temperatures

Irradiations were generally of fifteen minutes duration resulting in less than 0.1% decomposition of tetramethyl stannane. The formation of hexamethyl distannane, trimethyl tin hydride and ethyl trimethyl stannane could only be detected after long irradiations at 100 - 150°C.

The pressure of tetramethyl stannane in the reaction cell was always sufficient to absorb greater than 99% of the 1849 Å radiation.

$$\log \frac{I}{I_o} = \varepsilon.c.l.$$

Using the above formula it is possible to calculate the absorption or transmission for a known path length versus pressure e.g. Figure 3.1c. The effect of varying the parameters 1 - 9 is given in Sections 3.1 to 3.9. In Section 3.1 product yields are given in moles, in the remaining sections they are expressed in rates of formation and quantum yields ϕ where

$$\phi = \frac{\text{Number of molecules formed per second}}{\text{Amount of light absorbed per second}}$$

and the amount of light absorbed was determined by ethylene actinometry (Section 2.10).

Figure 3.1c

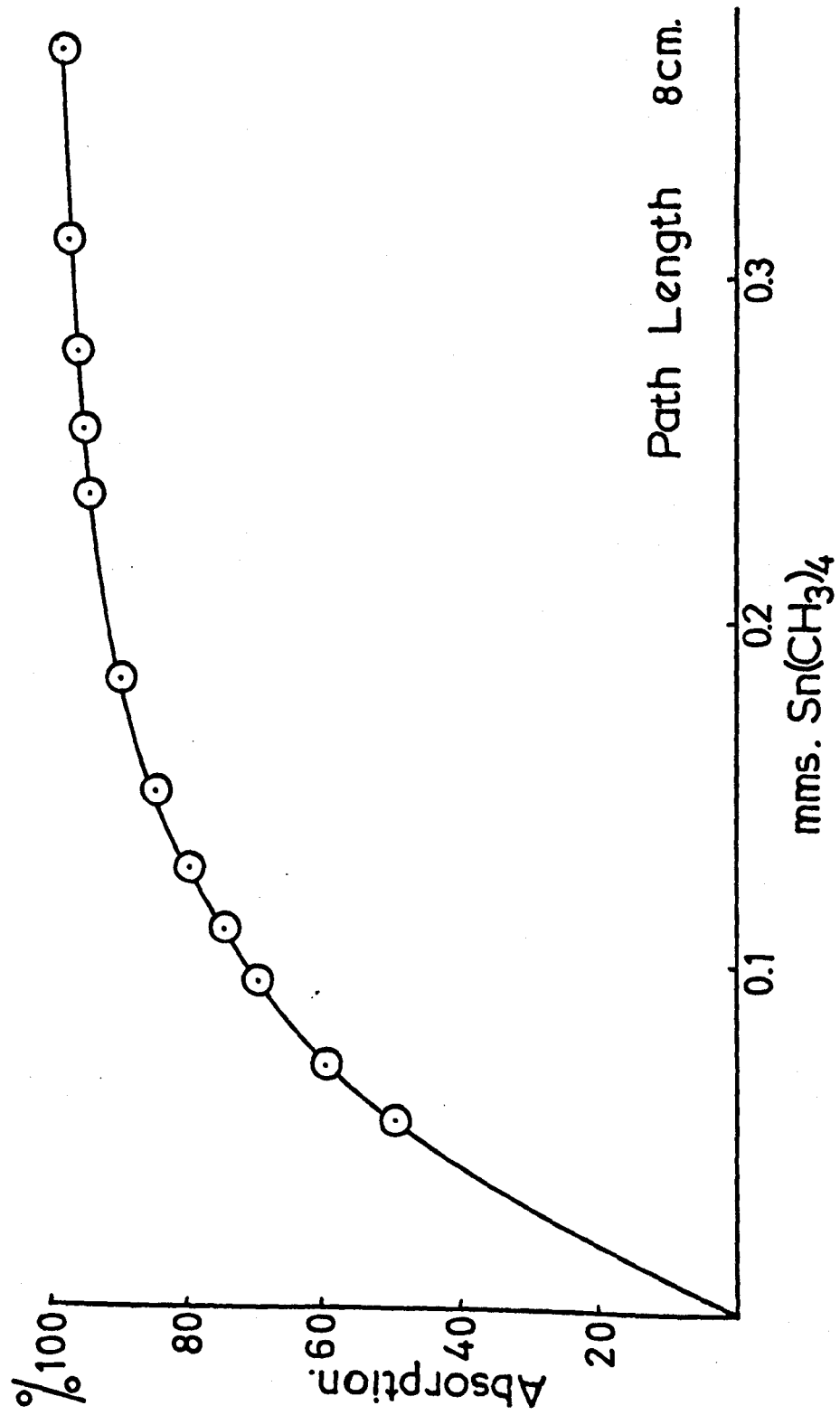

3.1 The effect of Time Variation

The variation of yields of methane and ethane with time are given in figures 3.2 and 3.3. At room temperature the rates of formation are approximately linear up to fifteen minutes after which the rates were progressively reduced. Examination of the cell window revealed that on irradiation of longer than ten minutes the transmission was gradually reduced due to the formation of a solid product on the window. The solid could be removed with dilute acids and it was found necessary, even with irradiation periods of fifteen minutes, to change the front spectrosil window after every experiment. This meant that time had to be allowed, prior to entrance of the sample to the cell, for complete pumping down of the cell.

Formation of a film on the window was the cause of irrepetitive results when using the high pressure mercury vapour lamp. However the film produced under these conditions was entirely different to that in the case of using the low pressure lamp. It could not be removed by dilute acids, only slowly with concentrated acids and was insoluble in organic solvents. Aqua regia was necessary to remove the film at a noticeable rate.

Figures 3.4 and 3.5 show the ethane and methane yields versus time using the high pressure lamp at 75^{o}C. Conversion was small even at this temperature and was presumably due to the fact that the film formed still contained Sn-C bonds and released only one or two methyl

groups per molecule of stannane. Figure 3.6 gives the absorption of the film after an irradiation period of two hours. The strong absorption in the region 54000 cm^{-1} indicates the presence of metal carbon bonds and the colour of the film i.e. red-brown is also indicative of a polymer containing Sn-C bonds.[29,69].

TABLE 3.2

Product yields as a function of time

Figures 3.2 and 3.3

Irradiation conditions: low pressure Hg-lamp

$Sn(Me)_4$ 20 mm.

Temperature, 25°C

Irradiation time, 0 - 50 minutes

Analytical conditions: Detector, flame ionisation

Column, Poropak Q

Temperature, 50°C

Nitrogen, 20 p.s.i.

Time	Moles Methane	Ethane	Ethylene
30 Mins.	8.66×10^{-8}	2.97×10^{-6}	3.64×10^{-9}
10 "	3.11×10^{-8}	1.28×10^{-6}	1.77×10^{-9}
25 "	-	2.61×10^{-6}	3.21×10^{-9}
15 "	4.82×10^{-8}	2.00×10^{-6}	2.43×10^{-9}
40 "	11.75×10^{-8}	3.23×10^{-6}	3.74×10^{-9}
20 "	6.10×10^{-8}	2.12×10^{-6}	-
50 "	15.32×10^{-8}	3.65×10^{-6}	3.98×10^{-9}
	3.2	3.3	3.3a

TABLE 3.3

Figures 3.4 and 3.5

Irradiation conditions: high pressure Hg-lamp
$Sn(CH_3)_4$, 20 mm.
Temperature, 75°C
Irradiation time, 0 - 105 minutes

Analytical conditions: Detector, flame ionisation
Column, Ap-L on Celite
Temperature, 100°C
Nitrogen, 20 p.s.i.

	3.5	Moles	3.4
Time	Methane		Ethane
45 Mins.	3.59×10^{-8}		6.76×10^{-8}
75 "	4.44×10^{-8}		10.77×10^{-8}
60 "	3.48×10^{-8}		8.06×10^{-8}
30 "	2.29×10^{-8}		3.98×10^{-8}
90 "	5.95×10^{-8}		12.93×10^{-8}
105 "	6.07×10^{-8}		15.14×10^{-8}

Figure 3.2

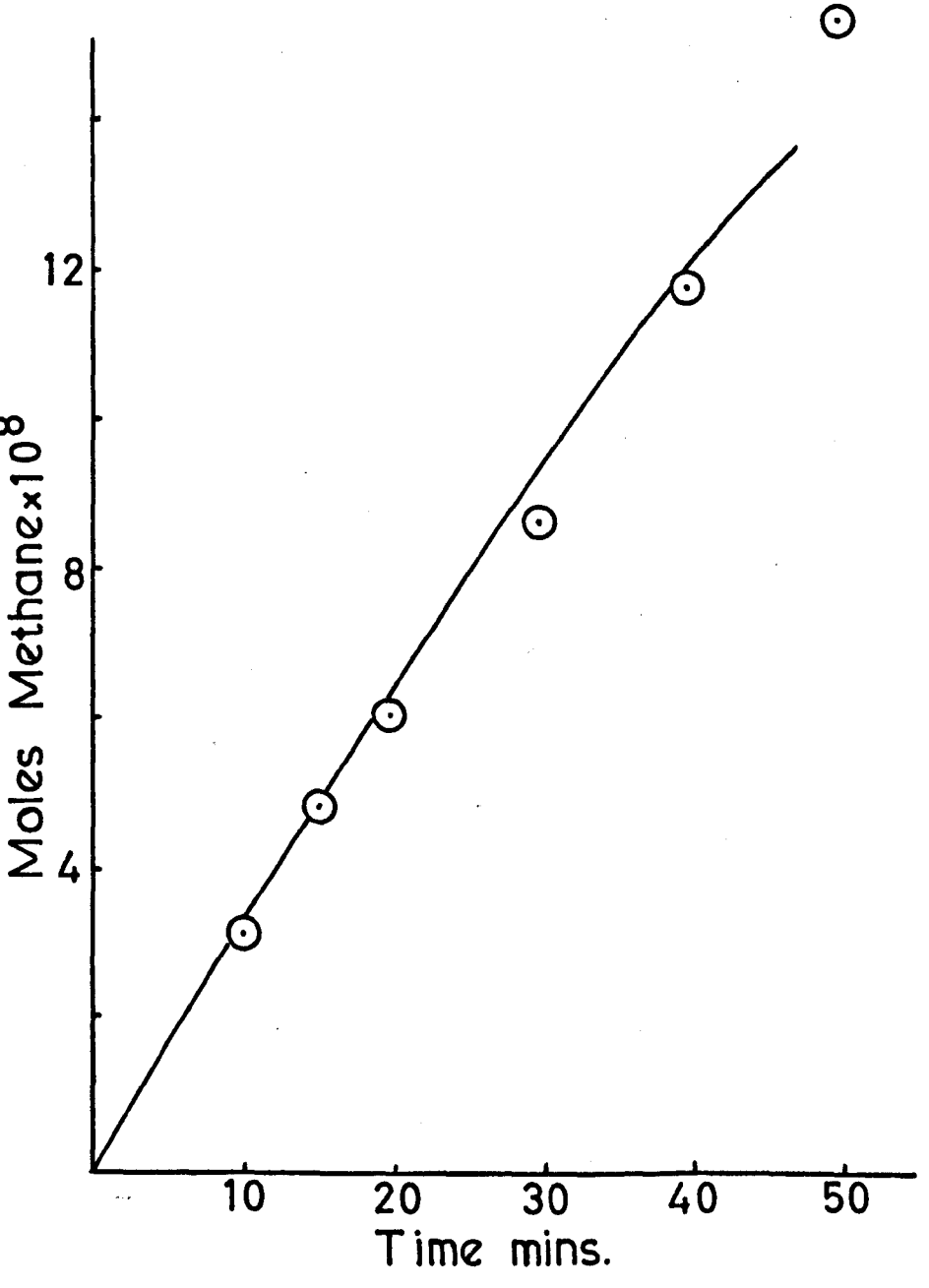

Figure 3.3

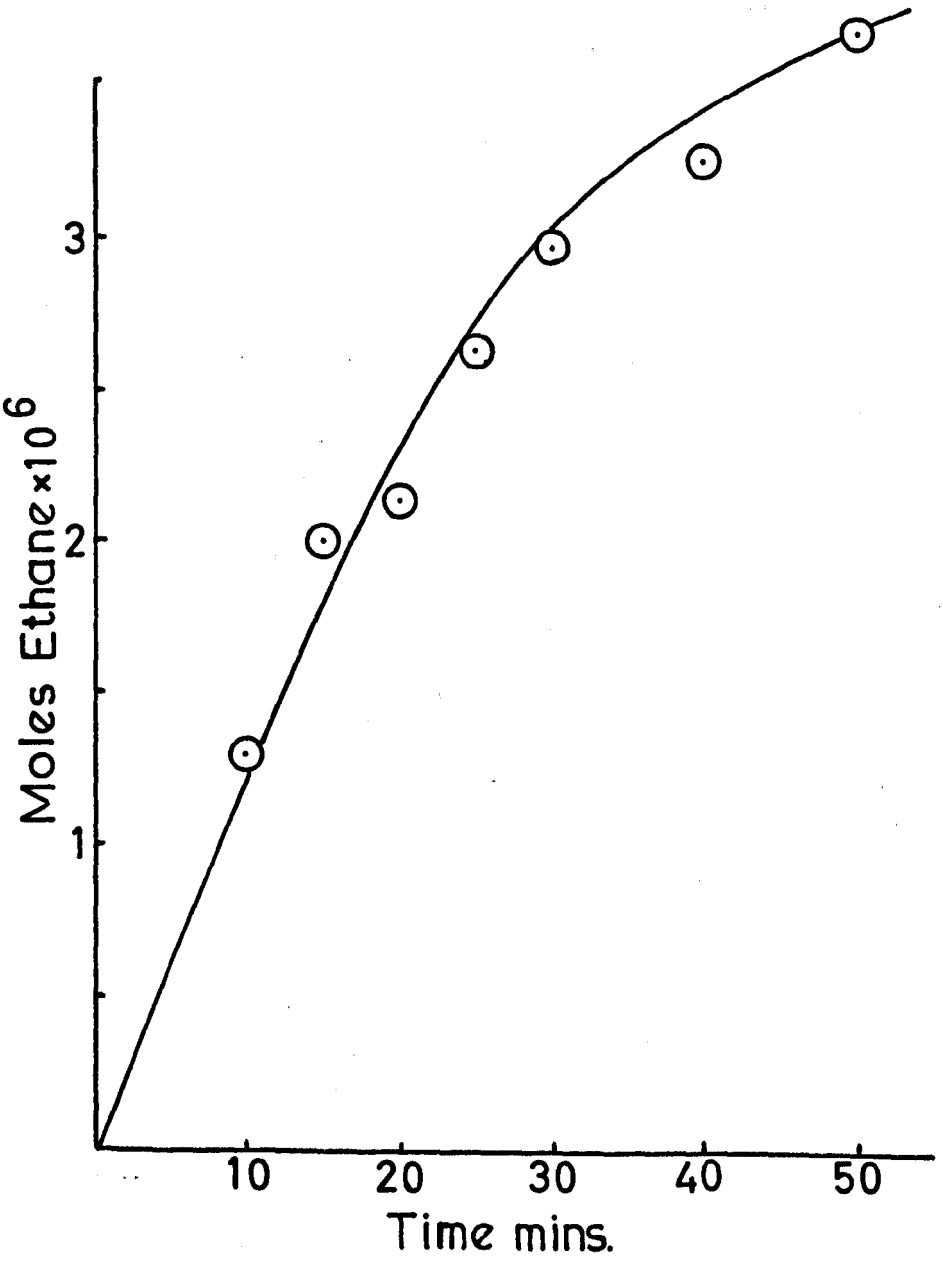

Figure 3.3a

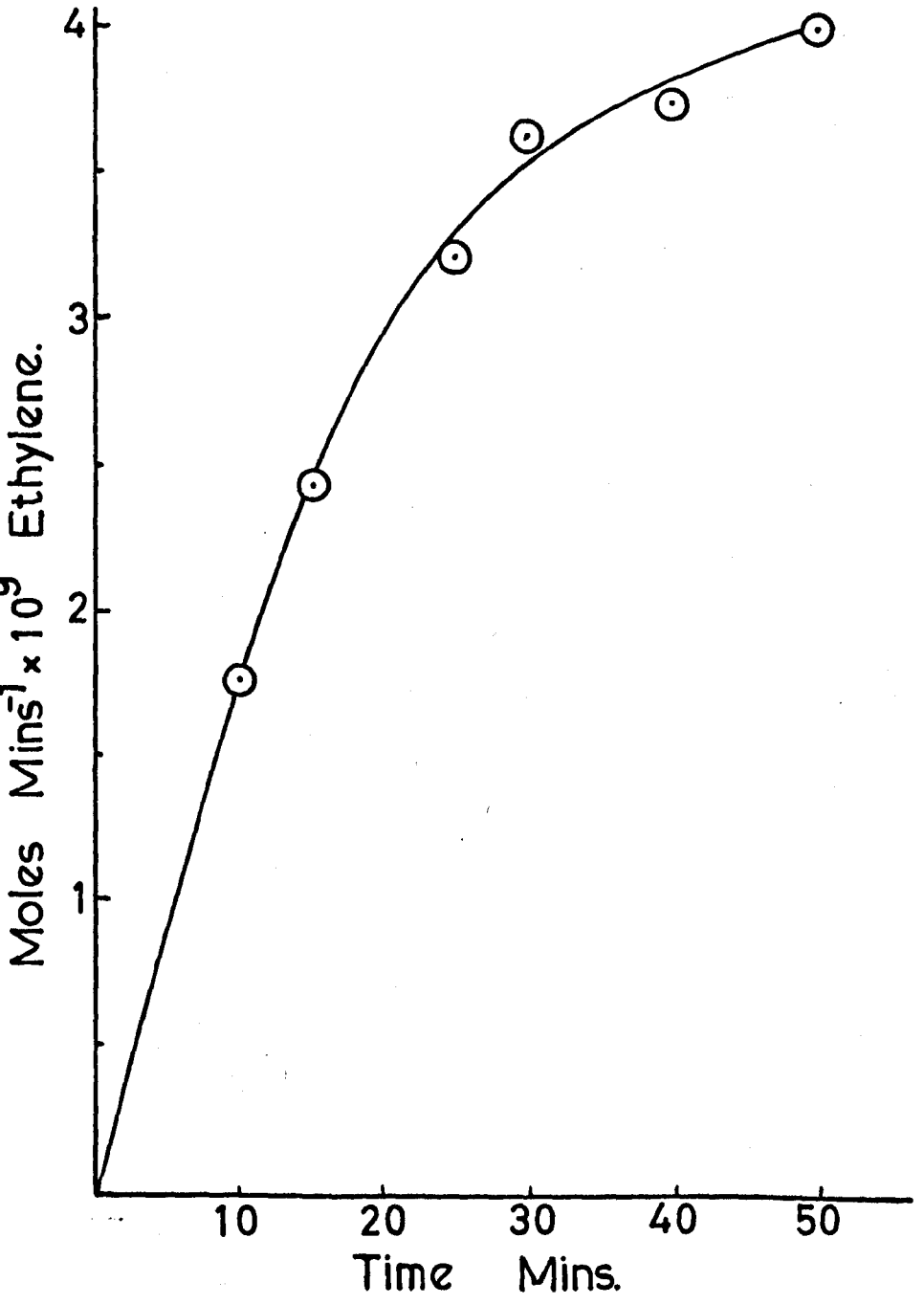

Figure 3.4

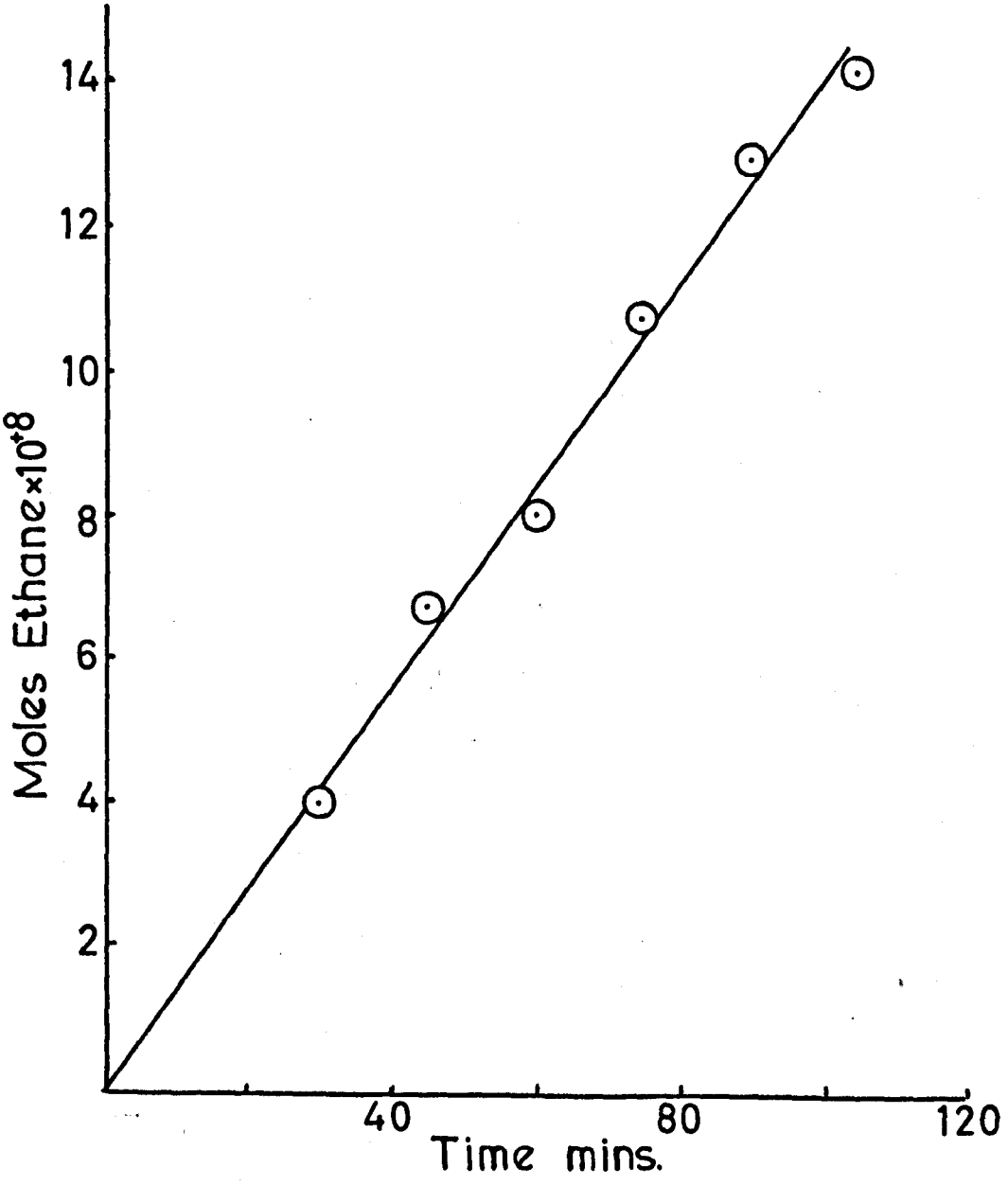

Figure 3.5

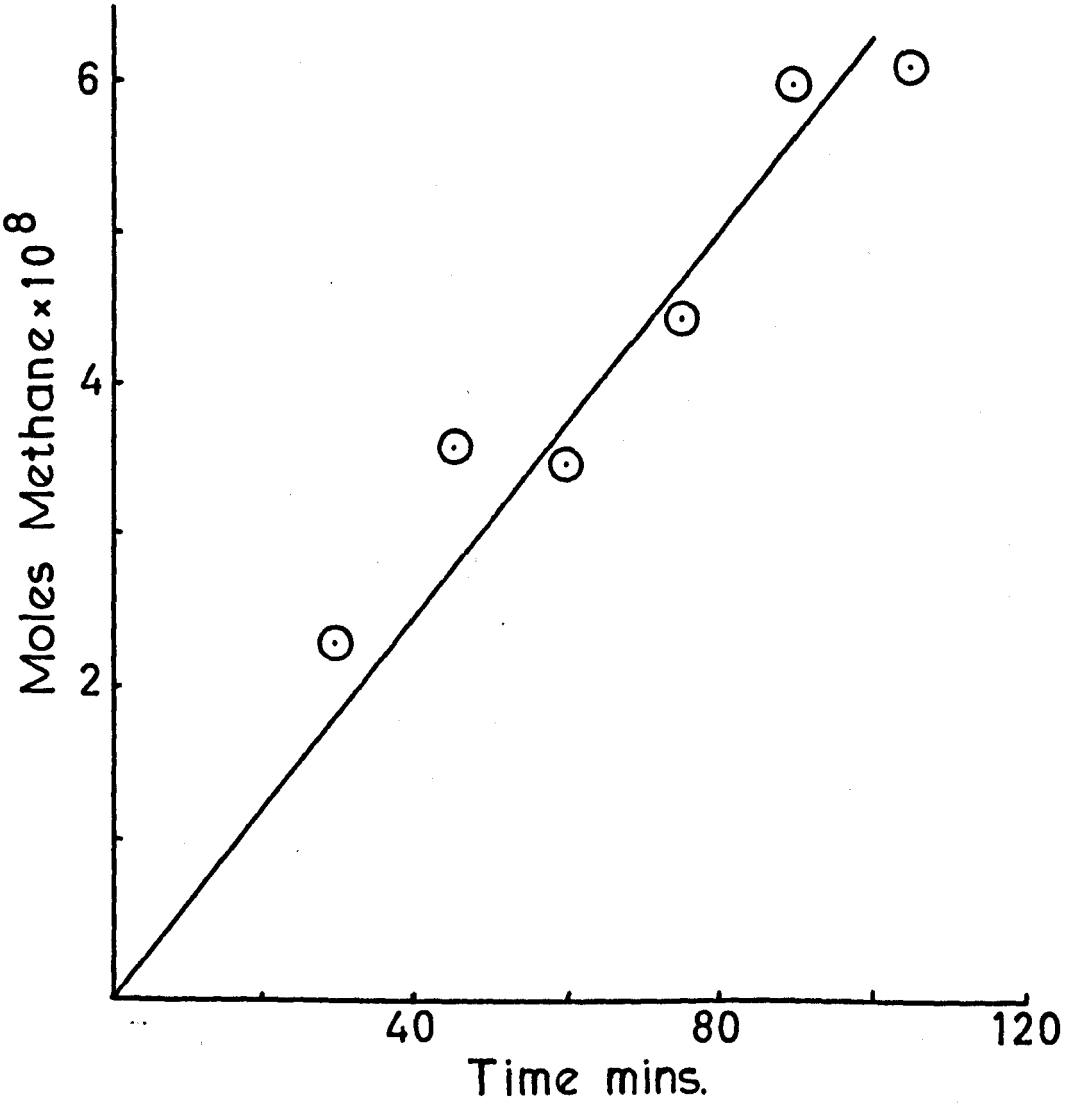

Figure 3.6

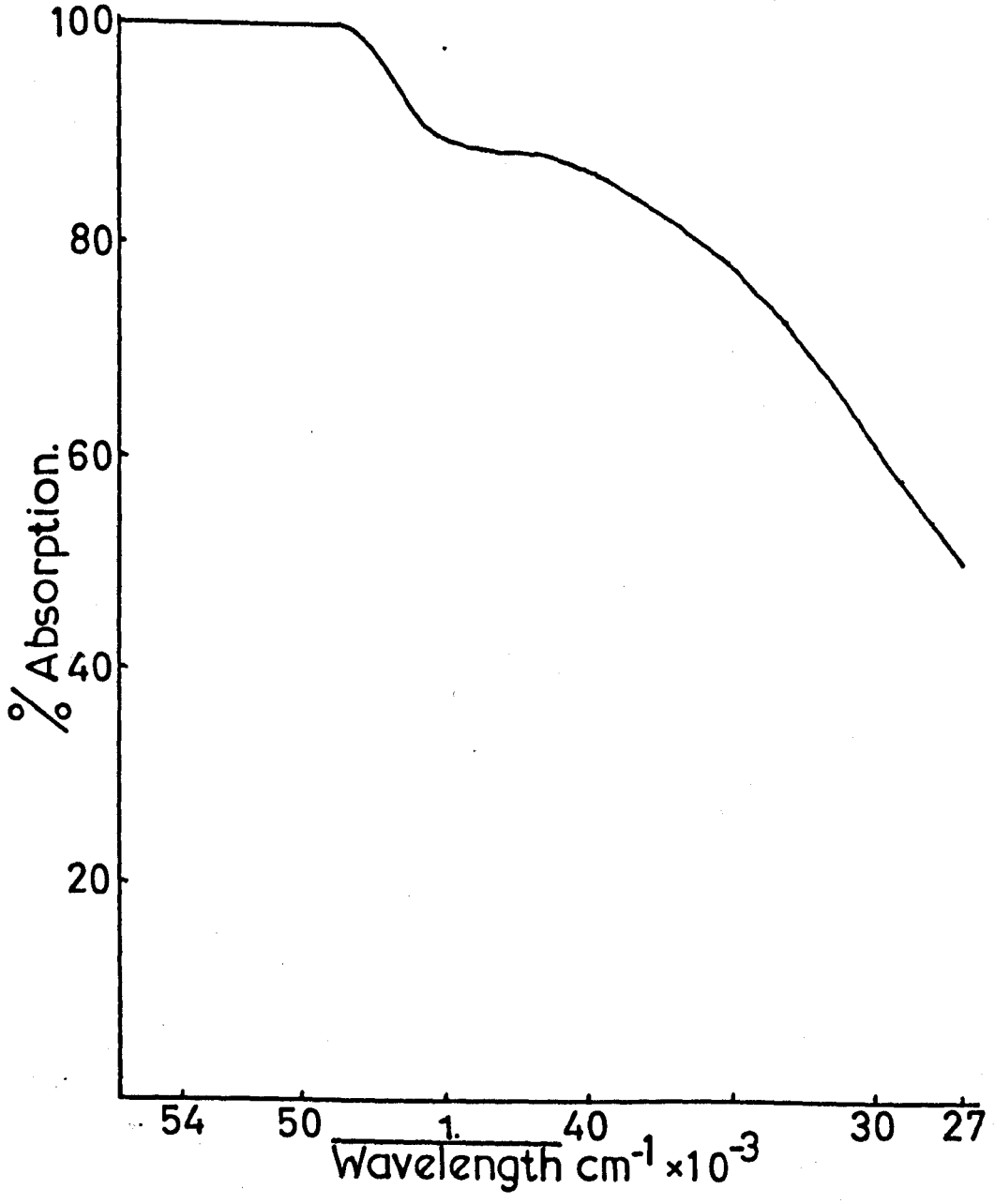

3.2 The effect of Intensity Variation

Using intensity stops of blackened copper gauge placed between the lamp and the cell, an eightfold variation in intensity could be obtained (Section 2.5.2). Figures 3.7 and 3.8 illustrate that the ratio of formation of the products are directly proportional to the intensity at room temperature.

TABLE 3.4

Product rates of formation as a function of intensity

Irradiation Conditions: $Sn(CH_3)_4$, 5 mm.
Temperature, 25°C
Irradiation time, 15 minutes

Analytical Conditions: Detector, flame ionisation
Column, Poropak Q
Temperature, 50°C
Nitrogen, 20 p.s.i.

	3.7	3.8
	Moles/minute	
Intensity	Methane	Ethane
100%	3.21×10^{-9}	9.6×10^{-8}
35.8	1.15×10^{-9}	3.5×10^{-8}
52.4	1.72×10^{-9}	5.05×10^{-8}
12.6	0.40×10^{-9}	1.20×10^{-8}
42.6	1.37×10^{-9}	4.05×10^{-8}
16.4	0.50×10^{-9}	1.60×10^{-8}

Figure 3.7

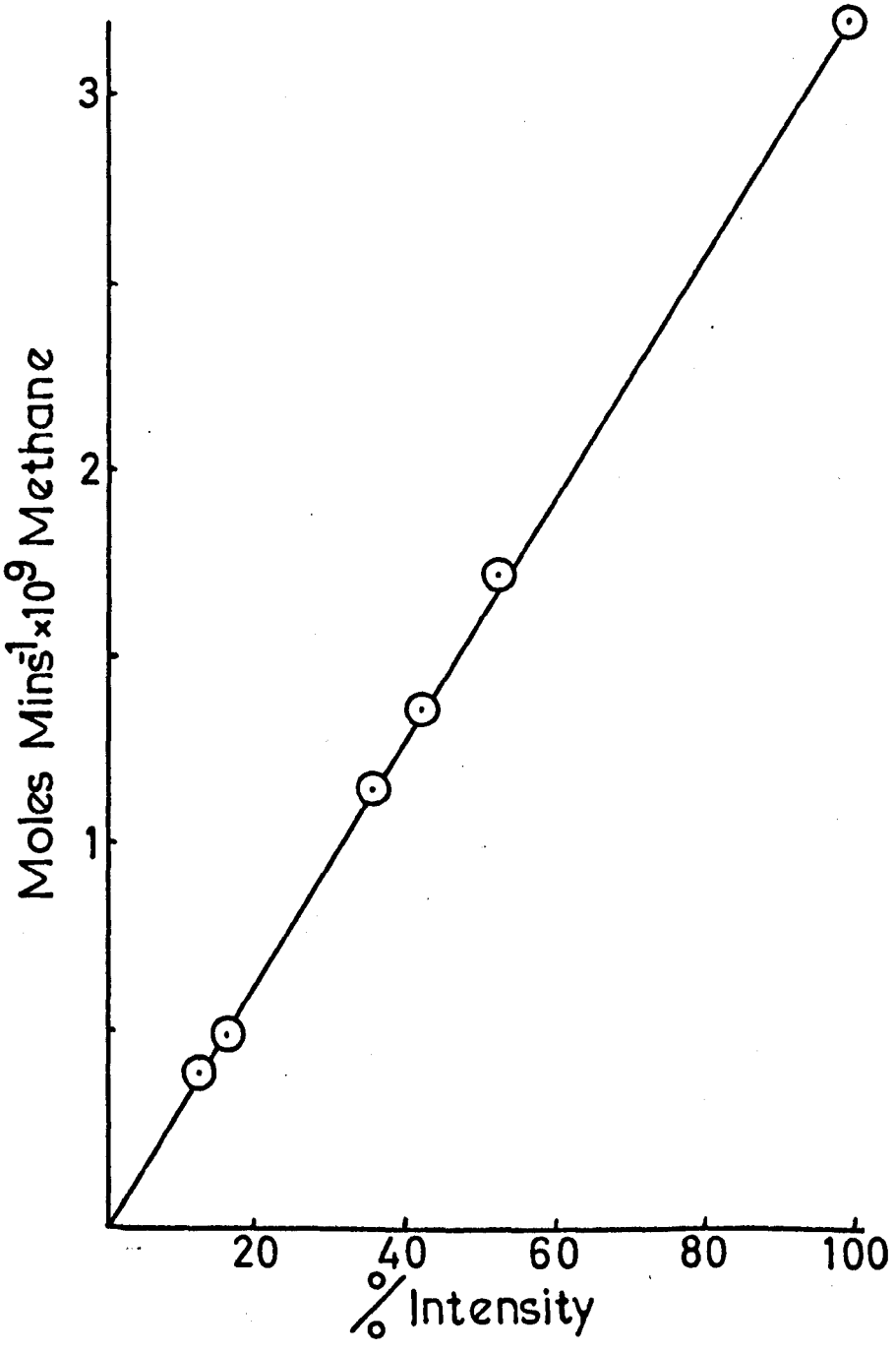

Figure 3.8

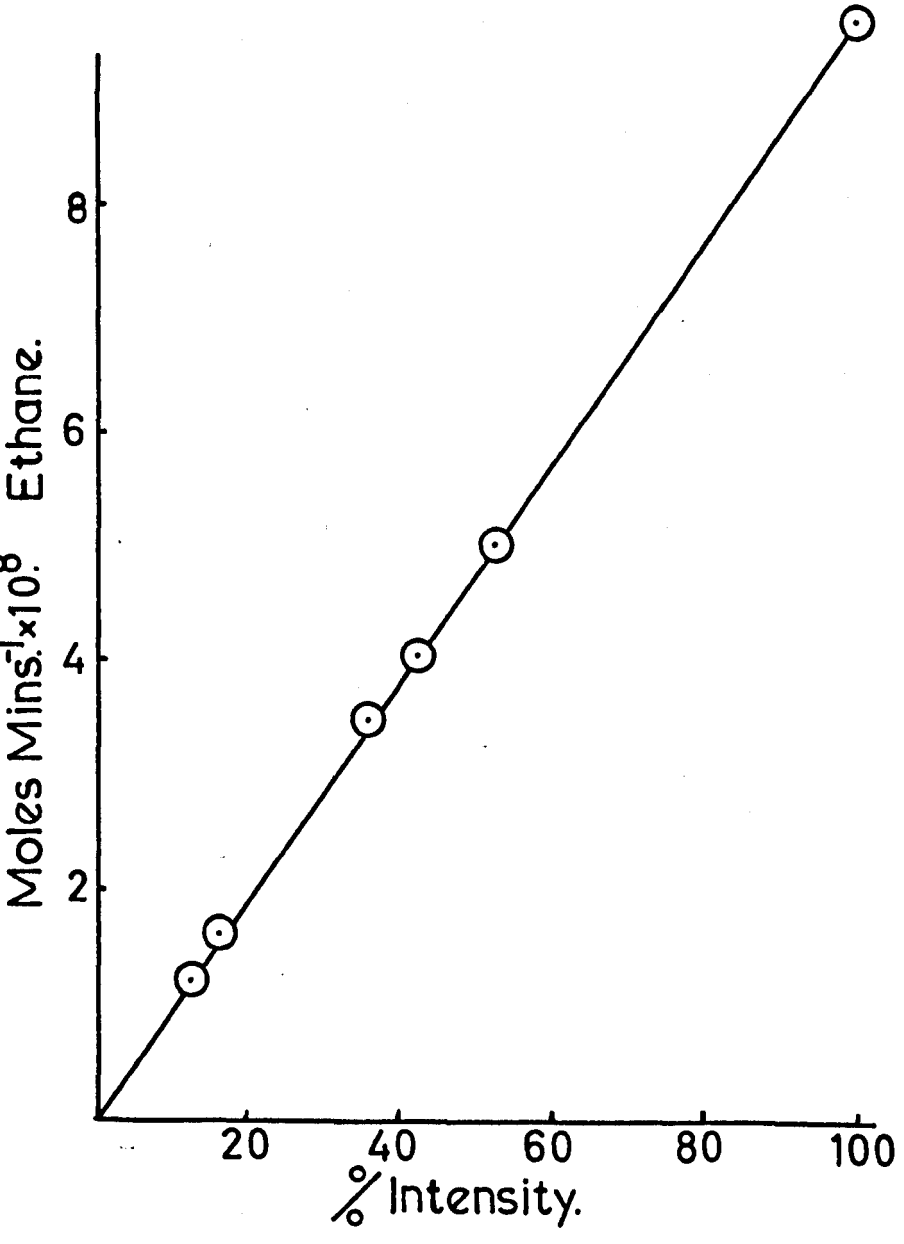

3.3 Effect of Variation of Tetramethyl Stannane Pressure

The effect of variation of tetramethyl stannane pressure upon the rates of formation of methane and ethane are shown in figures 3.9 and 3.10. The plots show that increasing the pressure above 5 mm. increases the rates linearly and in fact increases above a quantum yield of 2 in the ethane rate.

TABLE 3.5

Rates of formation as a function of $Sn(CH_3)_4$ pressure

Irradiation Conditions: $Sn(CH_3)_4$, 0 - 60 mm.
Temperature, 25°C
Irradiation Time, 15 minutes

Analytical Conditions: Detector, flame ionisation
Column, Poropak Q
Temperature, 50°C
Nitrogen, 20 p.s.i.

	3.9	3.10	
	Moles/minute		
Pressure	Methane	Ethane	Ethylene
15 mm	3.18×10^{-9}	11.1×10^{-8}	1.62×10^{-10}
40 mm	3.90×10^{-9}	12.2×10^{-8}	1.68×10^{-10}
10 mm	3.07×10^{-9}	10.8×10^{-8}	1.62×10^{-10}
50 mm	4.19×10^{-9}	12.9×10^{-8}	1.75×10^{-10}
30 mm	3.61×10^{-9}	11.7×10^{-8}	1.62×10^{-10}
60 mm	4.64×10^{-9}	13.4×10^{-8}	1.68×10^{-10}
5 mm	3.08×10^{-9}	9.6×10^{-8}	1.55×10^{-10}
20 mm	3.28×10^{-9}	11.3×10^{-8}	1.62×10^{-10}
2 mm	1.98×10^{-9}	7.9×10^{-8}	-
1 mm	1.33×10^{-9}	6.2×10^{-8}	-

Figure 3.9

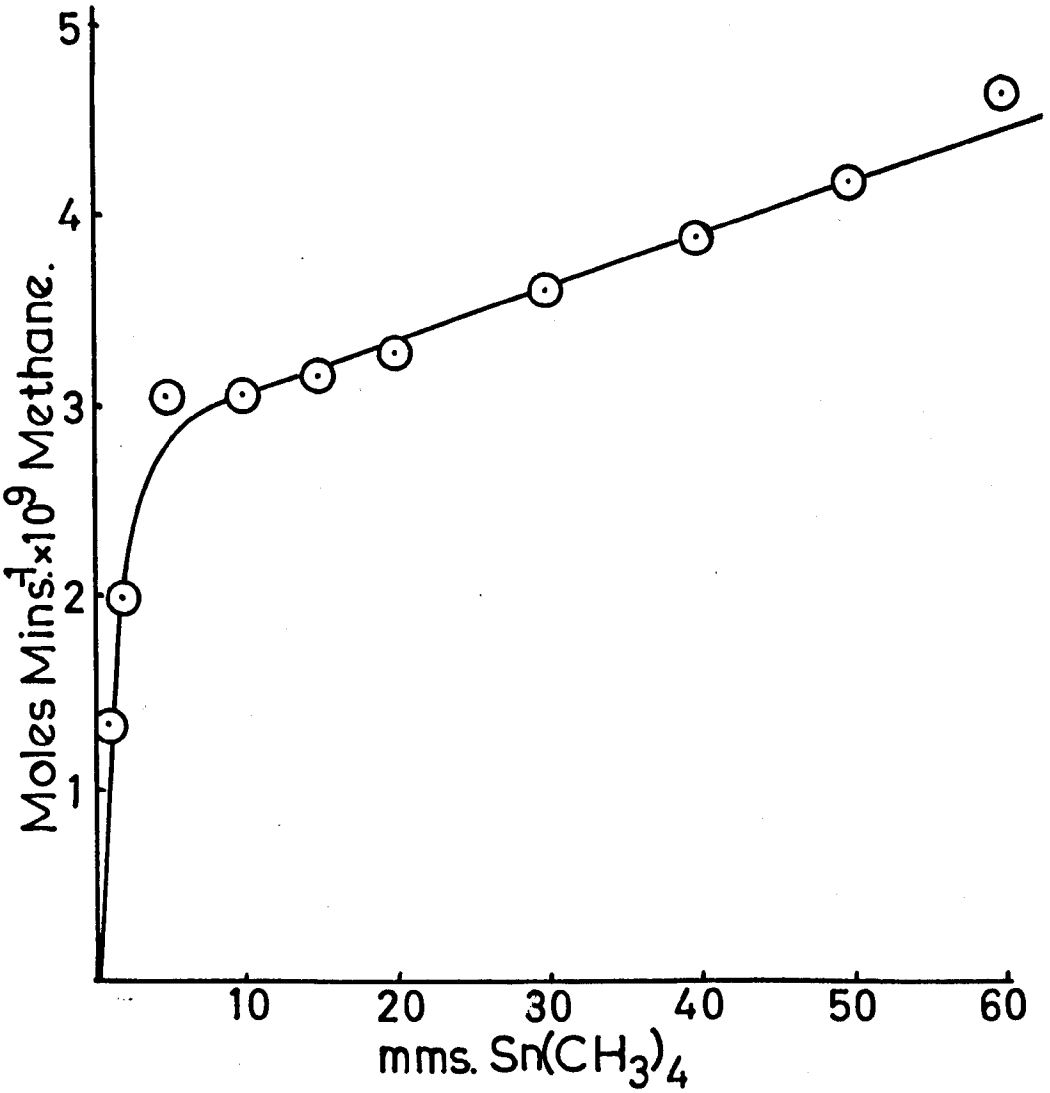

Figure 3.10

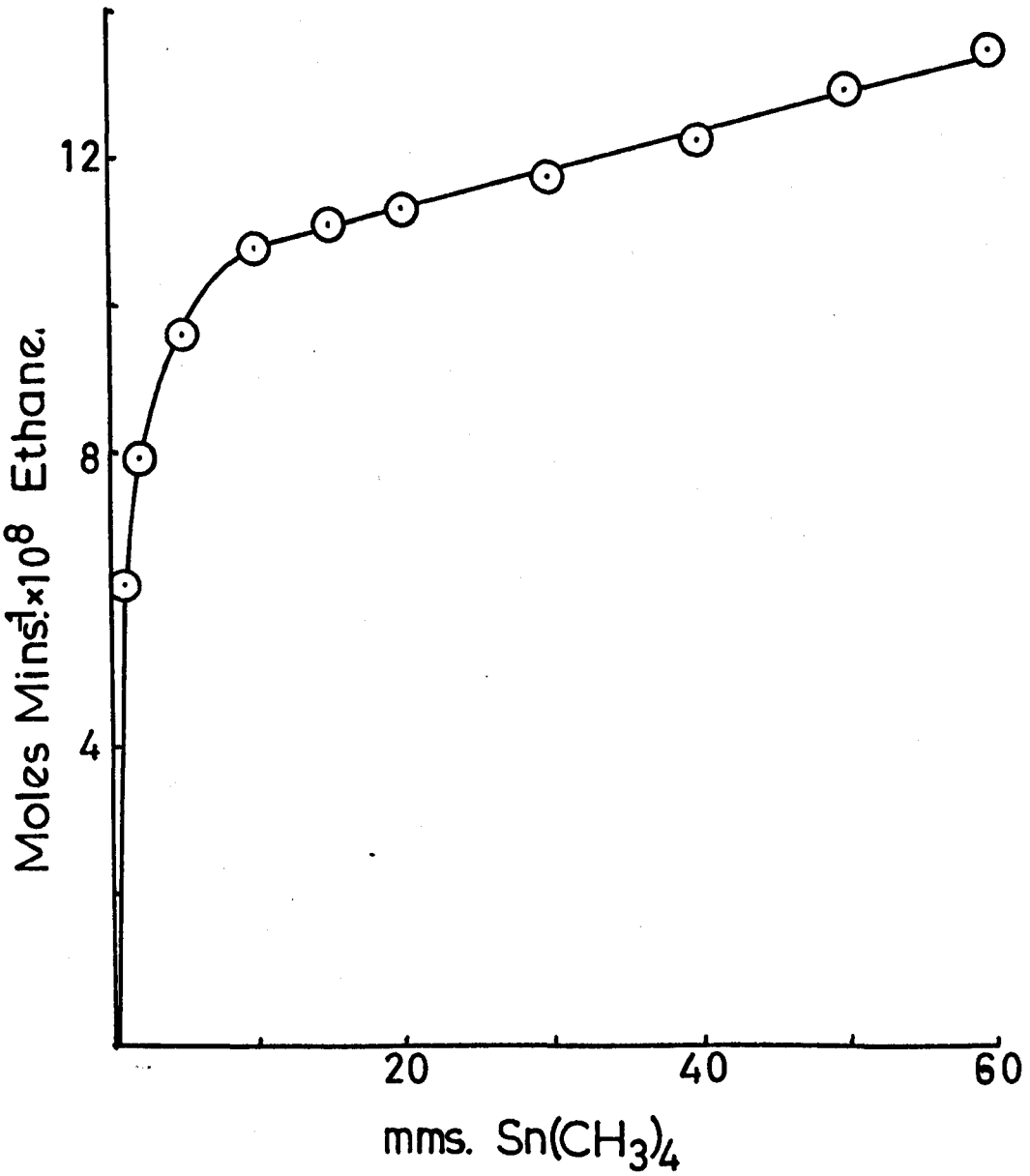

3.4 The effect of Temperature Variation

Irradiations were carried out at six temperatures, 25, 50, 75, 100, 125 and 150°C. It can be seen from figures 3.11 and 3.12 there was a drop in ethane yield and an increase in methane yield. Since the two did not match up it was thought that something must be wrong with the apparatus and it was found that because the lamp was inside the thermostat the electrodes were being heated. This resulted in less light being emitted through internal absorption by more mercury being present in the gas phase in the lamp. On correcting this by removing the lamp outside the thermostat and the electrodes kept at room temperature both yields increased as shown in figures 3.13 and 3.14.

TABLE 3.6

Rates of formation as a function of temperature

Irradiation Conditions: Pressure of $Sn(CH_3)_4$, 5 mm.
Temperature, 25, 50, 75, 100, 125 and 150°C
Irradiation time, 15 minutes

Analytical Conditions: Detector, flame ionisation
Column, Poropak Q
Temperature, 50°C
Nitrogen, 20 p.s.i.

	3.11	3.12	3.13	3.14
Temperature	Methane	Ethane	Methane	Ethane
25°C	3.03×10^{-9}	9.6×10^{-8}	3.27×10^{-9}	9.6×10^{-8}
50°C	3.25×10^{-9}	6.85×10^{-8}	4.33×10^{-9}	11.0×10^{-8}
75°C	4.20×10^{-9}	5.22×10^{-8}	7.97×10^{-9}	12.6×10^{-8}
100°C	6.07×10^{-9}	3.78×10^{-8}	17.54×10^{-9}	14.0×10^{-8}
125°C	13.35×10^{-9}	1.52×10^{-8}	37.18×10^{-9}	15.8×10^{-8}
150°C	28.54×10^{-9}	1.00×10^{-8}	71.09×10^{-9}	17.87×10^{-8}

Figures in moles/minute

Figure 3.11

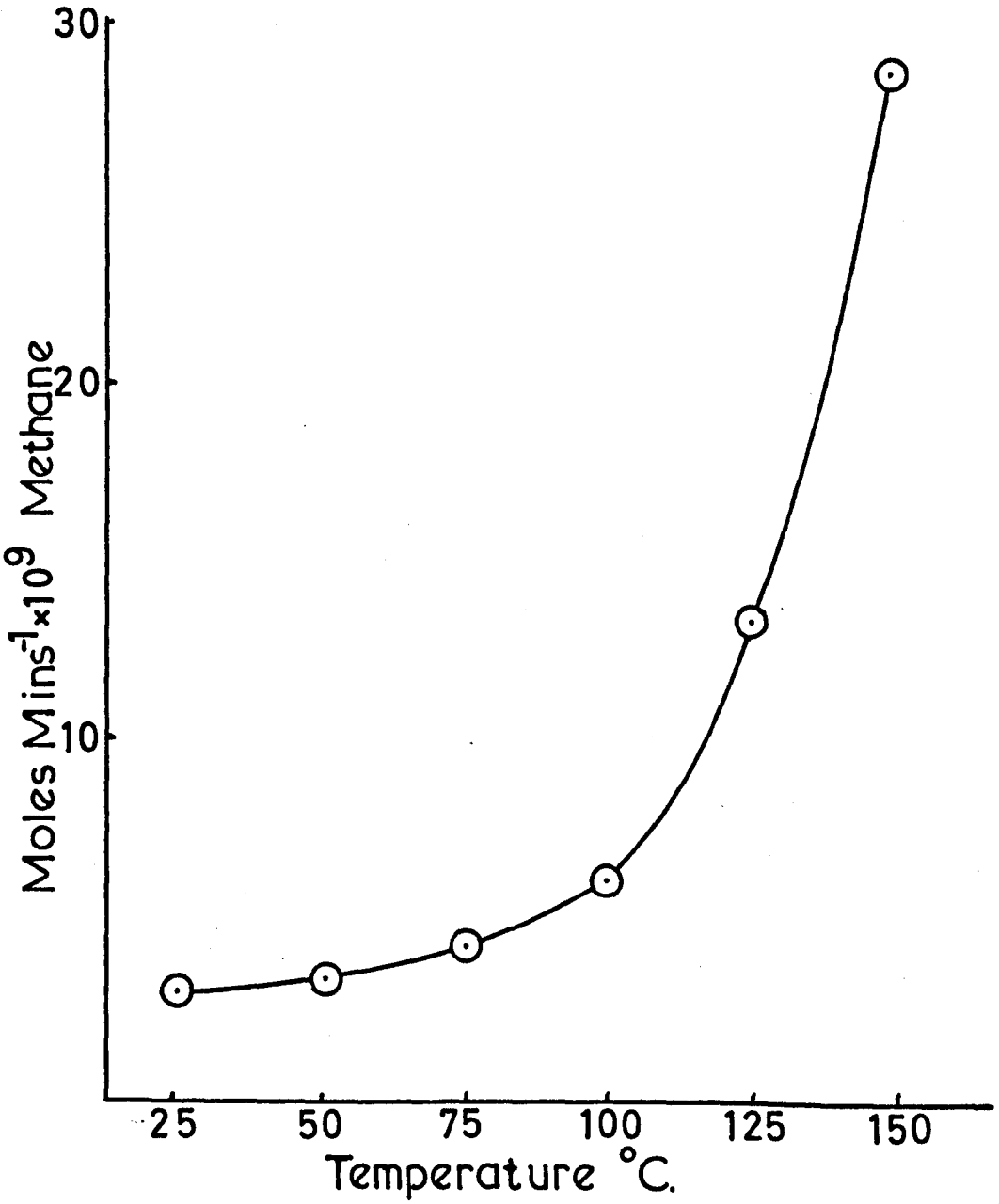
30
20
10
Moles Mins^{-1} x10^{9} Methane
25
50
75
100
125
150
Temperature °C.

Figure 3.12

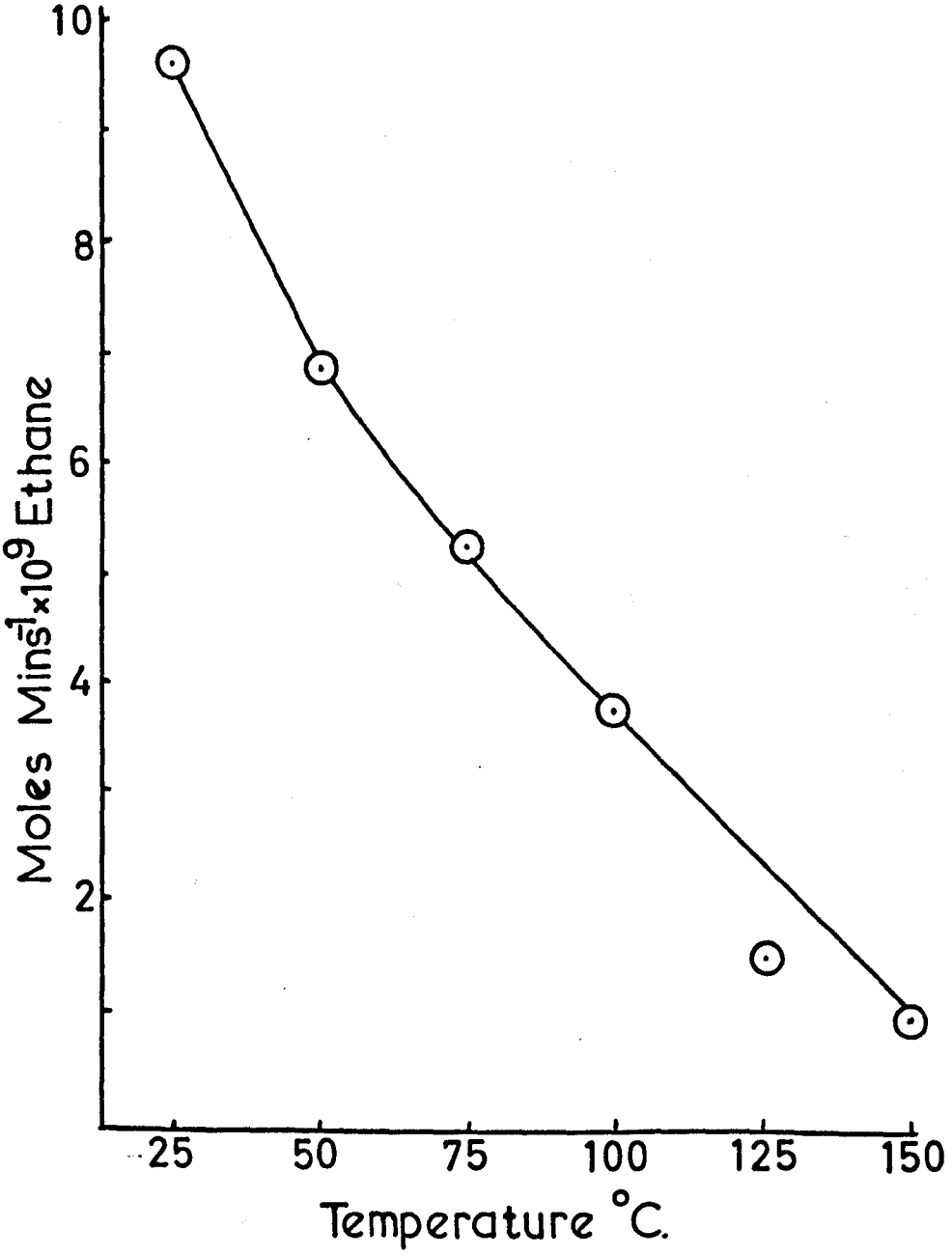
10
8
6
4
2
Moles $Mins^{-1} \times 10^9$ Ethane
25
50
75
100
125
150
Temperature °C.

Figure 3.13

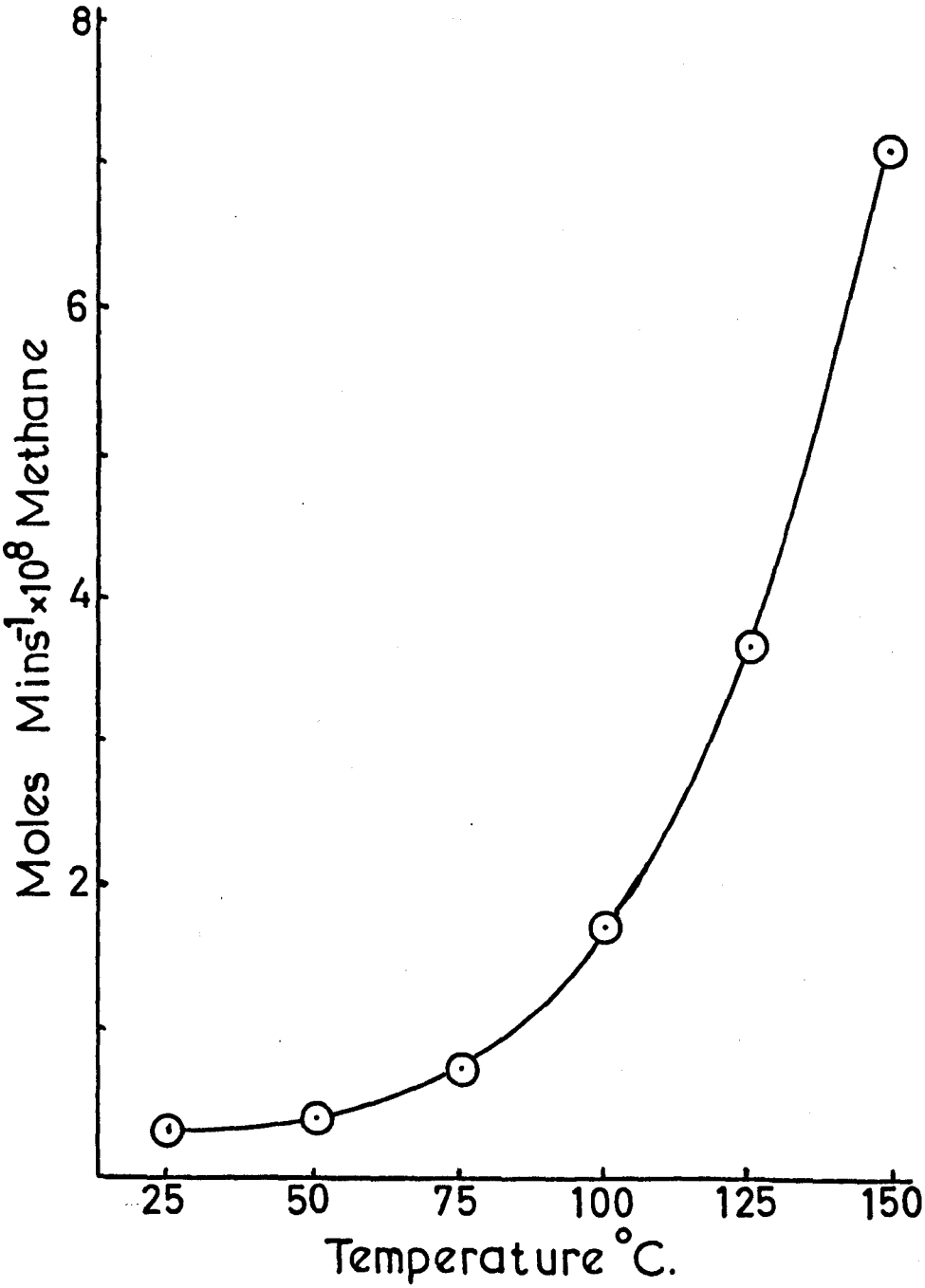
8
6
4
2
Moles Mins^{-1}x10^{8} Methane
25
50
75
100
125
150
Temperature °C.

Figure 3.14

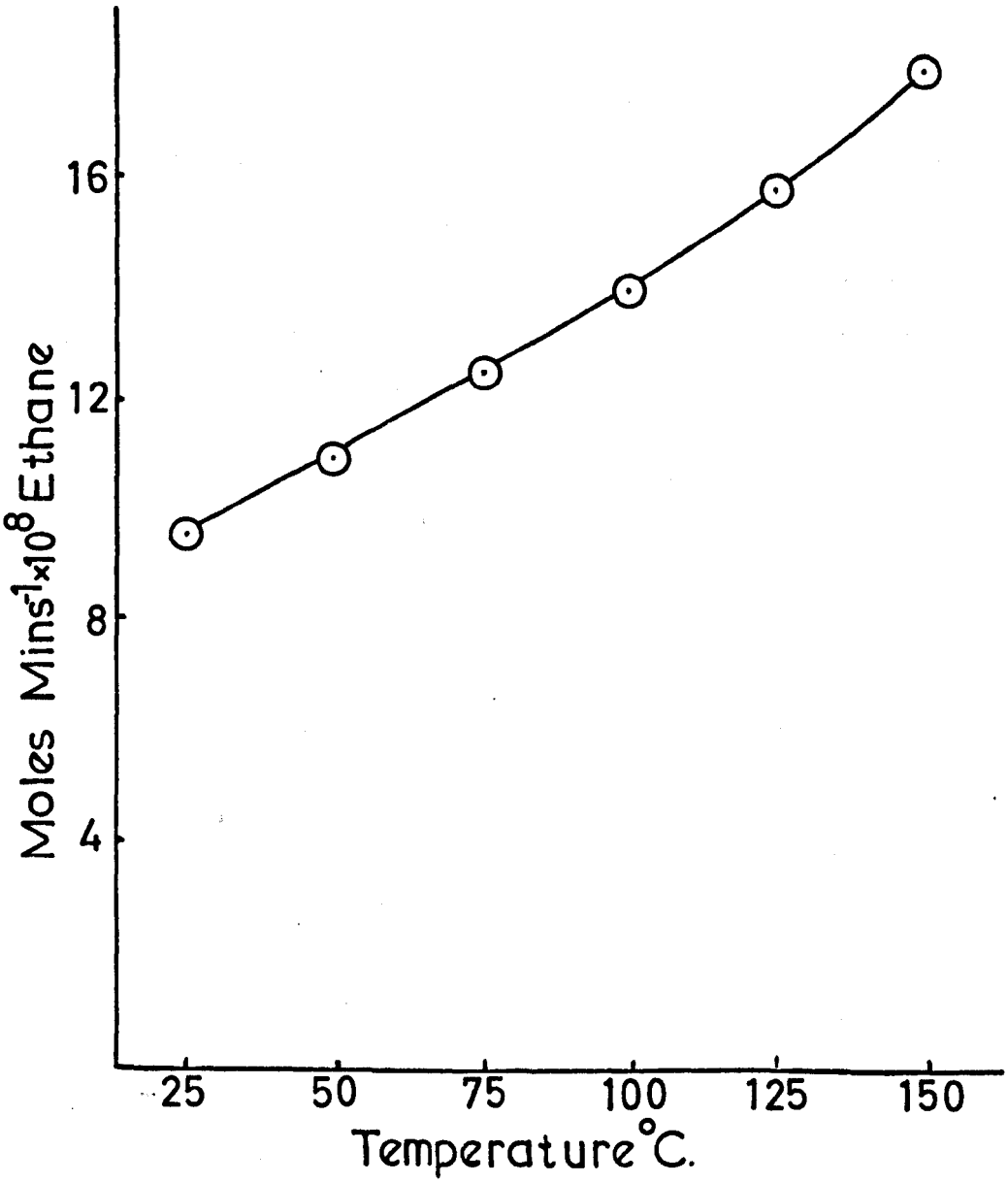
16
12
8
4
Moles Mins^{-1}x10^{8} Ethane
25
50
75
100
125
150
Temperature °C.

3.5 Effect of Pressure of Inert Gases

The effects of adding differing pressures of nitrogen, carbon dioxide and octafluorocyclobutane to a fixed pressure of tetramethyl stannane are illustrated in figure 3.13 to 3.18. The result of increasing the pressure of additive gas was a reduction in the rates of formation which is different to that obtained with increasing the pressure of tetramethyl stannane. The pressure of inert gases required to give a constant rate is surprisingly low and increase of pressure to several hundred mm's still gives this constant value.

TABLE 3.7

Rates of formation as a function of added gases

Irradiation Conditions: Pressure of $Sn(CH_3)_4$, 5 mm.
Temperature, 25°C
Irradiation time, 15 minutes

Analytical Conditions: Detector, flame ionisation
Column, Poropak Q
Temperature, 50°C
Nitrogen, 20 p.s.i.

	3.15	3.16
Nitrogen	Methane	Ethane
0 mm.	3.21×10^{-9}	9.6×10^{-8}
3 mm.	2.67×10^{-9}	5.21×10^{-8}
5.3 mm.	1.58×10^{-9}	4.55×10^{-8}
11.3 mm.	1.19×10^{-9}	3.94×10^{-8}
16 mm.	1.16×10^{-9}	3.82×10^{-8}
30 mm.	1.12×10^{-9}	3.79×10^{-8}
31.6 mm.	1.12×10^{-9}	3.79×10^{-8}
51.7 mm.	1.15×10^{-9}	3.82×10^{-8}

Figures in moles/minute

	3.17	3.18
Carbon Dioxide	Methane	Ethane
0 mm.	3.21×10^{-9}	9.6×10^{-8}
7.2 mm.	2.31×10^{-9}	4.81×10^{-8}
12.3 mm.	1.33×10^{-9}	4.75×10^{-8}
19.0 mm.	1.15×10^{-9}	3.95×10^{-8}
24.0 mm.	1.15×10^{-9}	3.76×10^{-8}
35.0 mm.	1.08×10^{-9}	3.78×10^{-8}
50.0 mm.	1.08×10^{-9}	3.78×10^{-8}
70.0 mm.	1.08×10^{-9}	3.78×10^{-8}

	3.19	3.20
C_4F_8	Methane	Ethane
0 mm.	3.21×10^{-9}	9.6×10^{-8}
8½ mm.	1.83×10^{-9}	7.24×10^{-8}
35 mm.	1.61×10^{-9}	7.24×10^{-8}
69 mm.	1.60×10^{-9}	7.18×10^{-8}
20 mm.	1.61×10^{-9}	7.27×10^{-8}
90 mm.	1.61×10^{-9}	7.18×10^{-8}
110 mm.	1.61×10^{-9}	7.20×10^{-8}

Figures in moles/minute

Figure 3.15

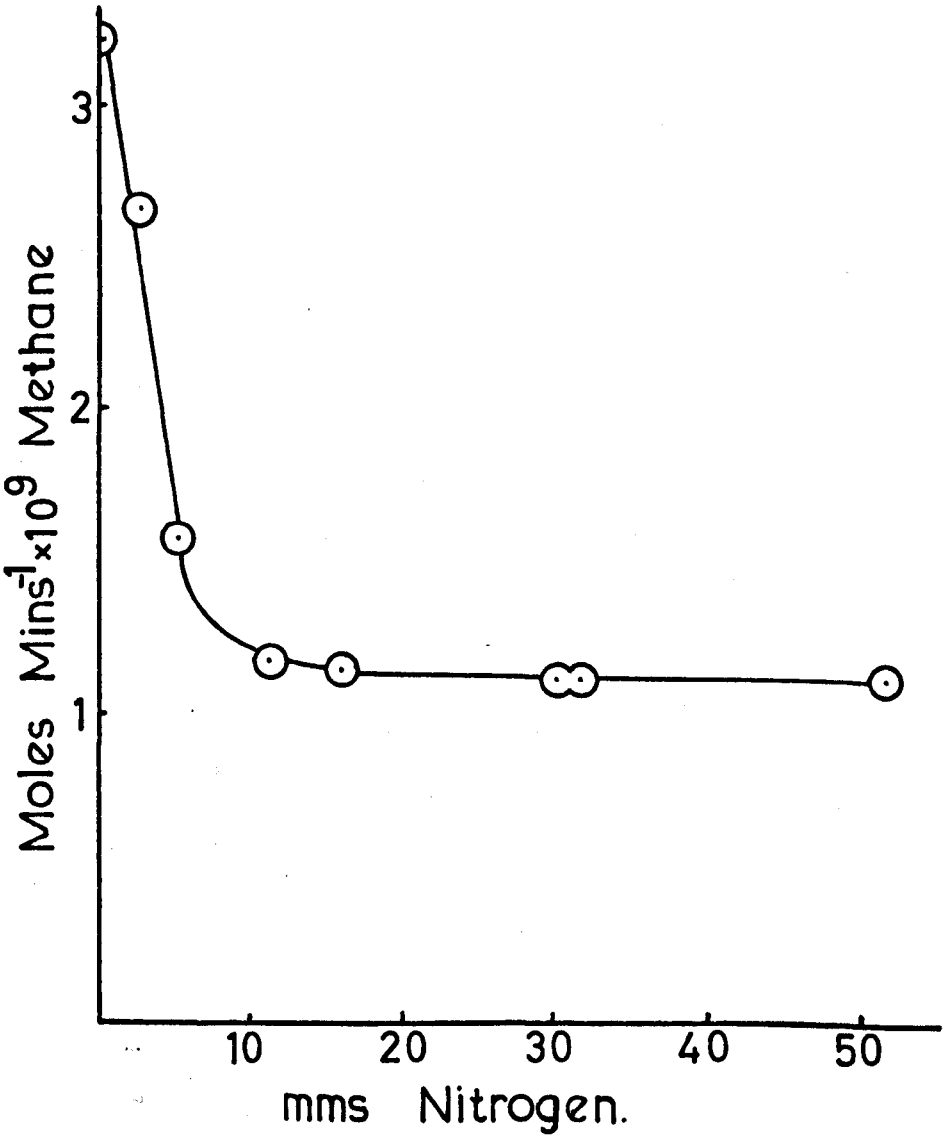

Figure 3.16

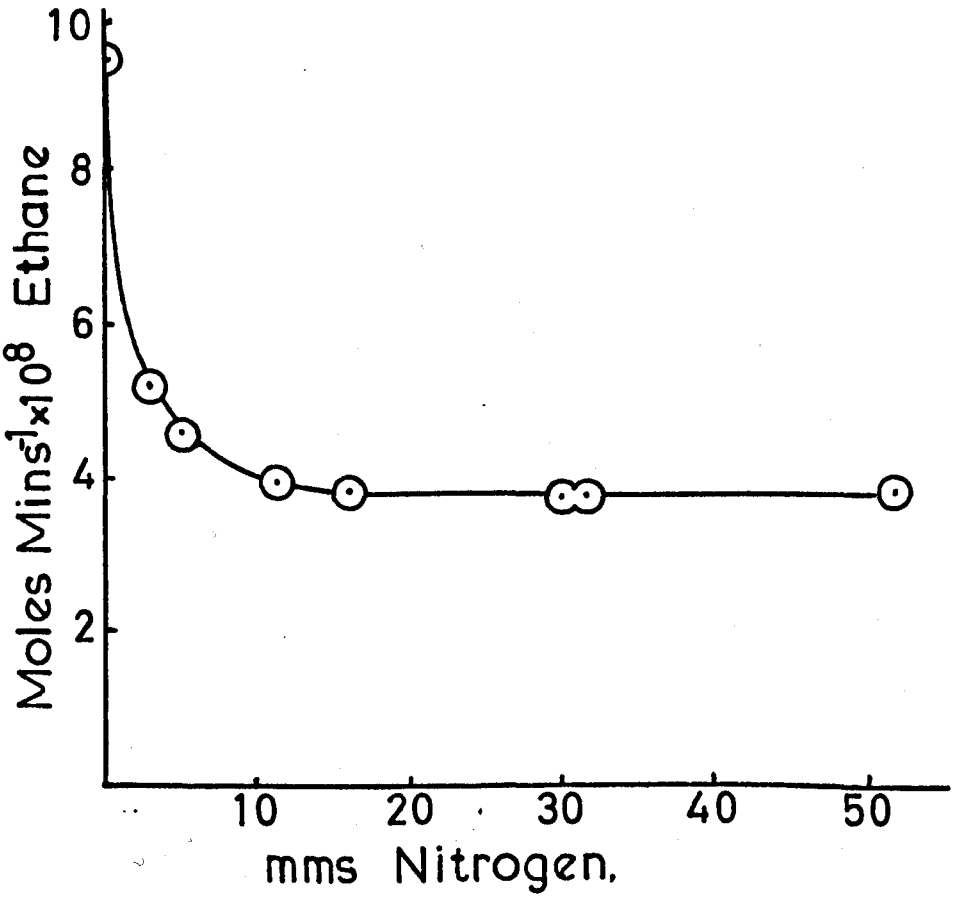

Figure 3.17

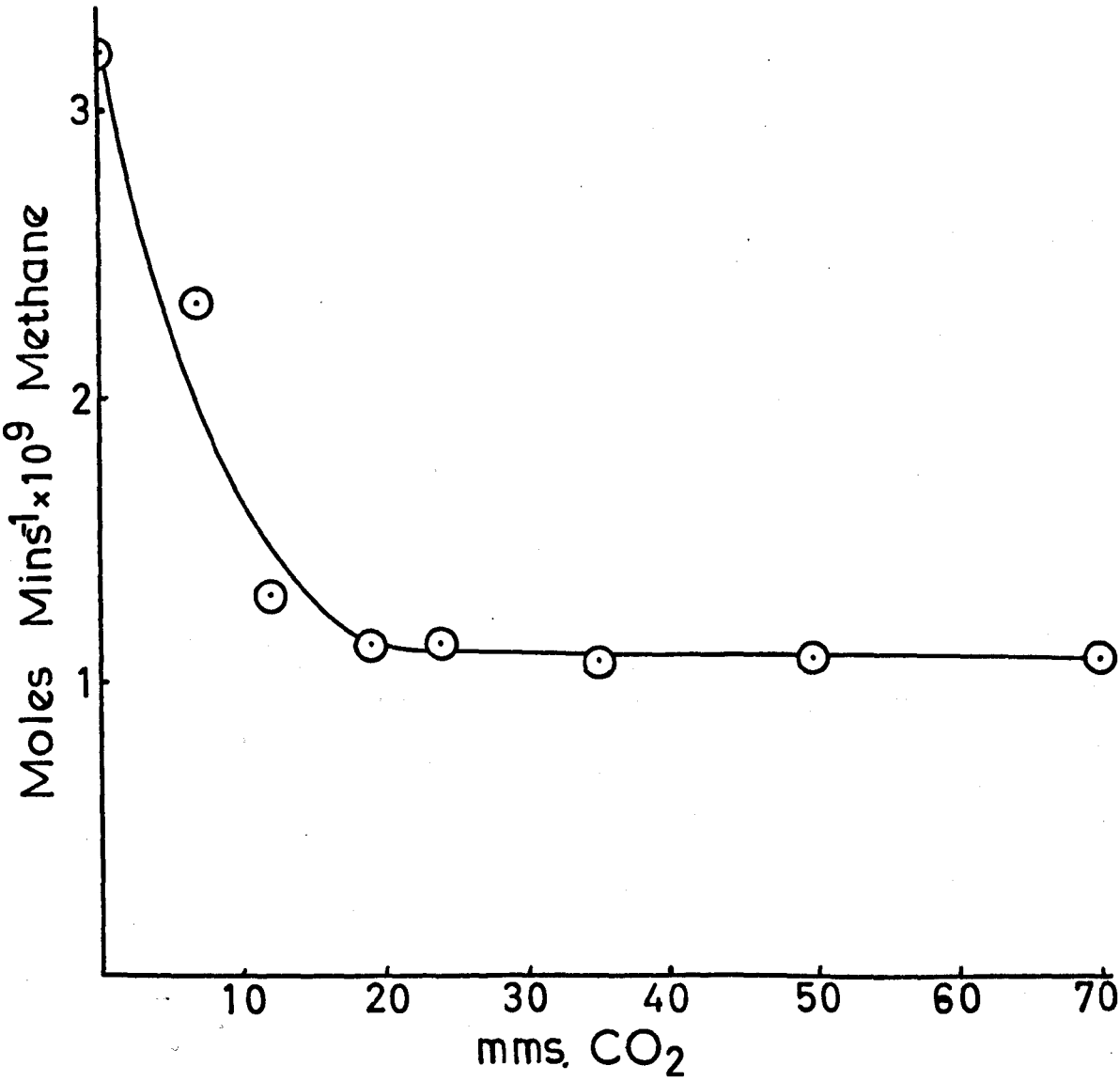

Figure 3.18

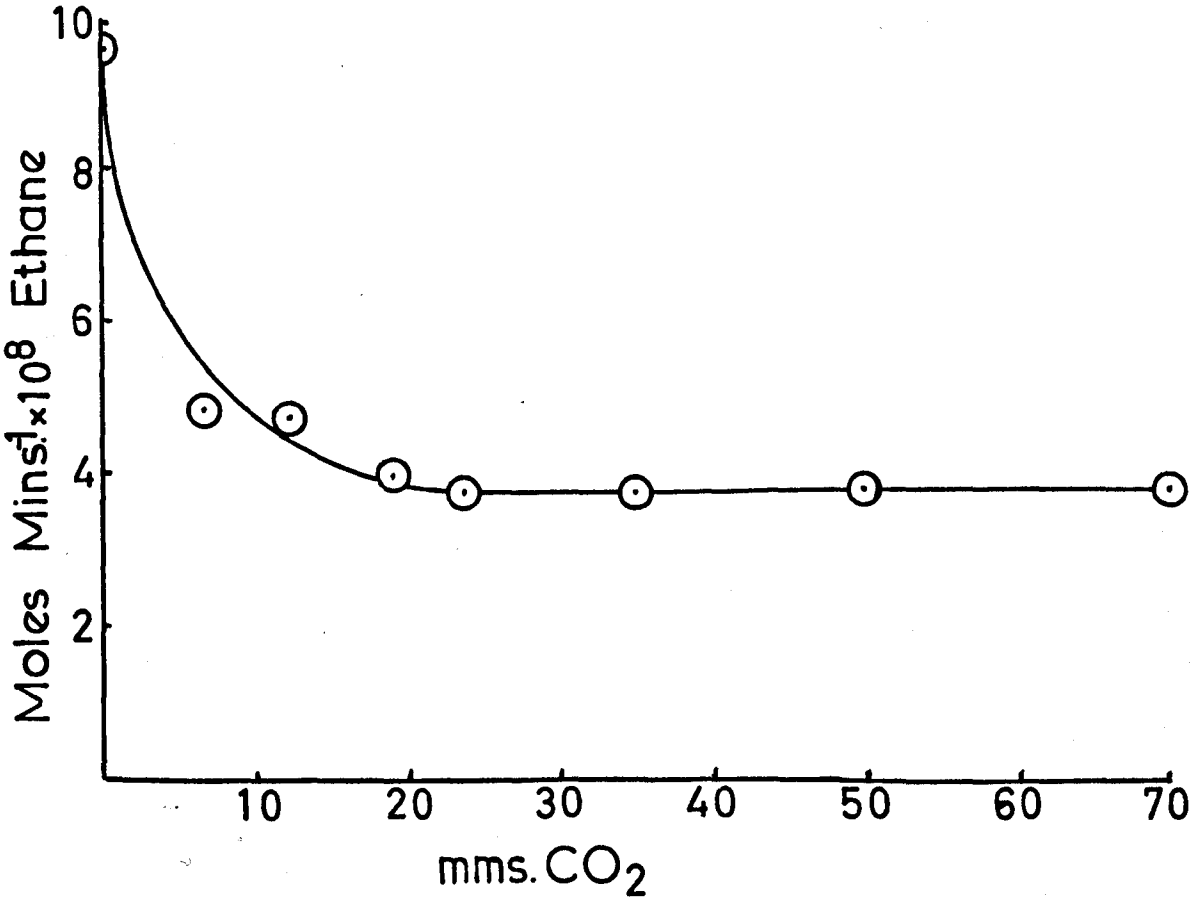

Figure 3.19

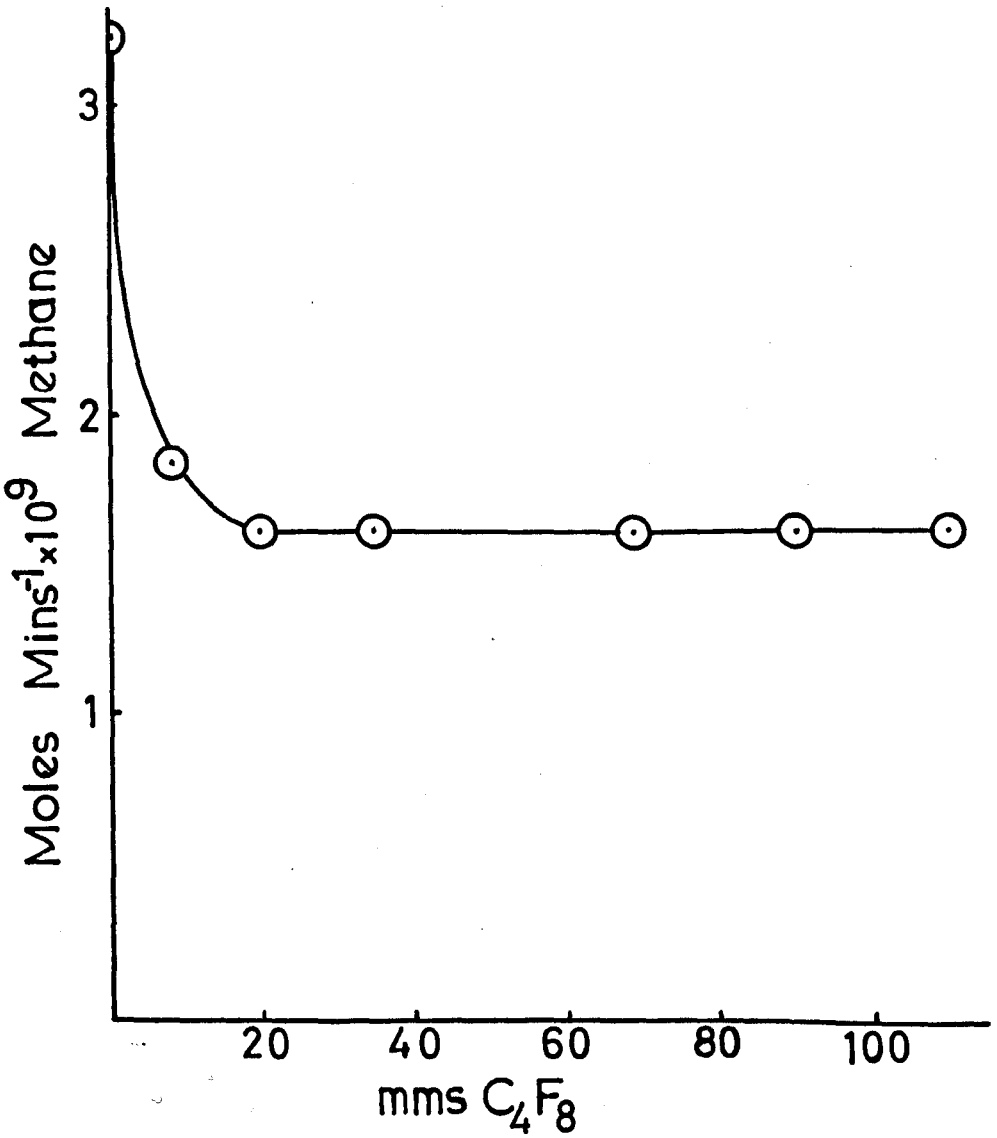

Figure 3.20

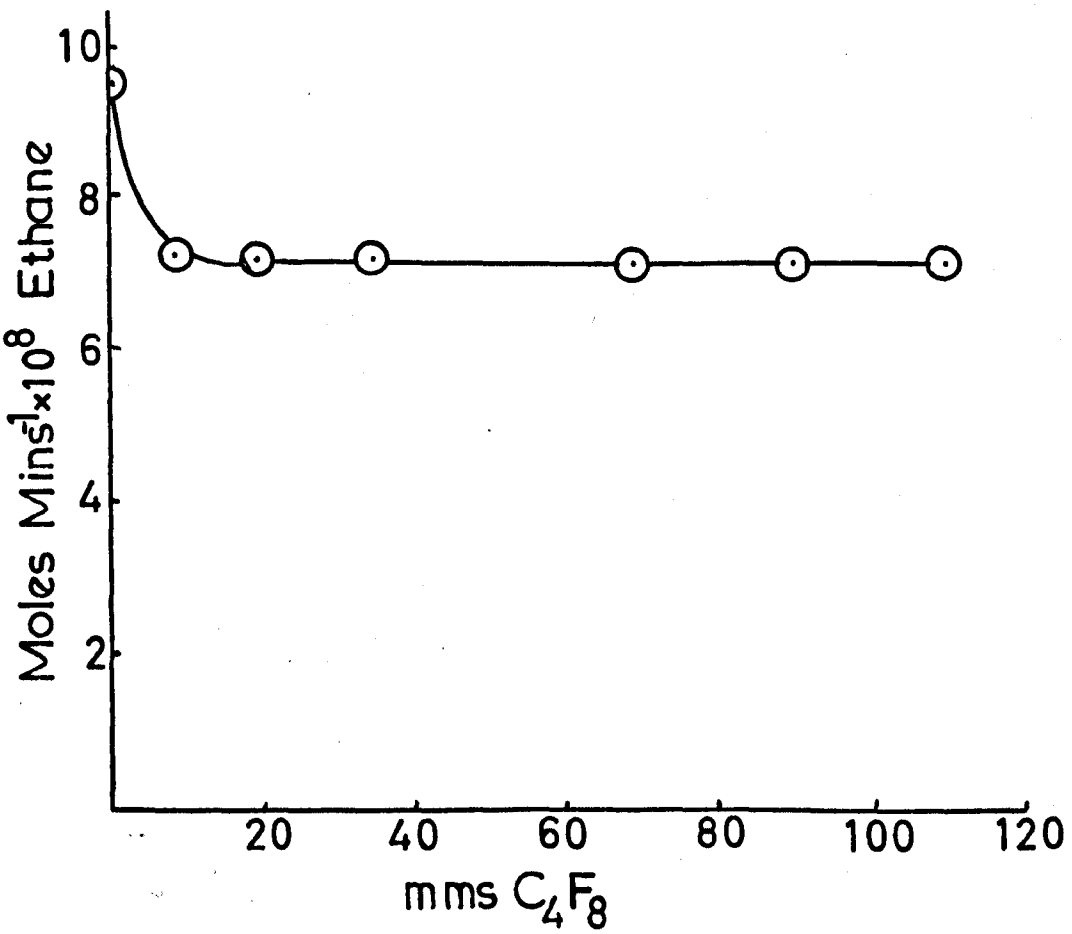

3.6 Effect of added Radical Scavengers

The addition of nitric oxide or oxygen, gases which have been used as radical scavengers in similar systems, resulted in the almost complete removal of ethane. In fact, the yield of ethane in the case of oxygen was brought down to the yield of methane and the methane yield was hardly effected. With nitric oxide the methane was depressed to the level of the inert gas effect and ethane was brought down to this rate. The effects can be seen in the figures 3.21 to 3.24.

TABLE 3.8

Rates of formation as a function of added radical scavengers

Irradiation Conditions: Pressure of $Sn(CH_3)_4$, 5 mm.
Temperature, 25°C
Irradiation time, 15 minutes

Analytical Conditions: Detector, flame ionisation
Column, Poropak Q
Temperature, 50°C
Nitrogen, 20 p.s.i.

	3.21	3.22
Oxygen	Methane	Ethane
0 mm.	3.21×10^{-9}	96.0×10^{-9}
18 mm.	3.21×10^{-9}	4.54×10^{-9}
9 mm.	3.21×10^{-9}	4.54×10^{-9}
22 mm.	2.96×10^{-9}	4.18×10^{-9}
7 mm.	3.18×10^{-9}	4.55×10^{-9}
37 mm.	2.89×10^{-9}	4.21×10^{-9}
51 mm.	2.56×10^{-9}	4.06×10^{-9}

Figures in moles/minute

	3.23	3.24
Nitric Oxide	Methane	Ethane
0 mm.	3.21×10^{-9}	96.0×10^{-9}
11.5 mm.	1.95×10^{-9}	1.69×10^{-9}
35 mm.	1.25×10^{-9}	1.08×10^{-9}
29 mm.	1.26×10^{-9}	1.02×10^{-9}
55 mm.	1.13×10^{-9}	1.13×10^{-9}
118 mm.	0.84×10^{-9}	0.96×10^{-9}

Figures in moles/minute

Figure.3.21

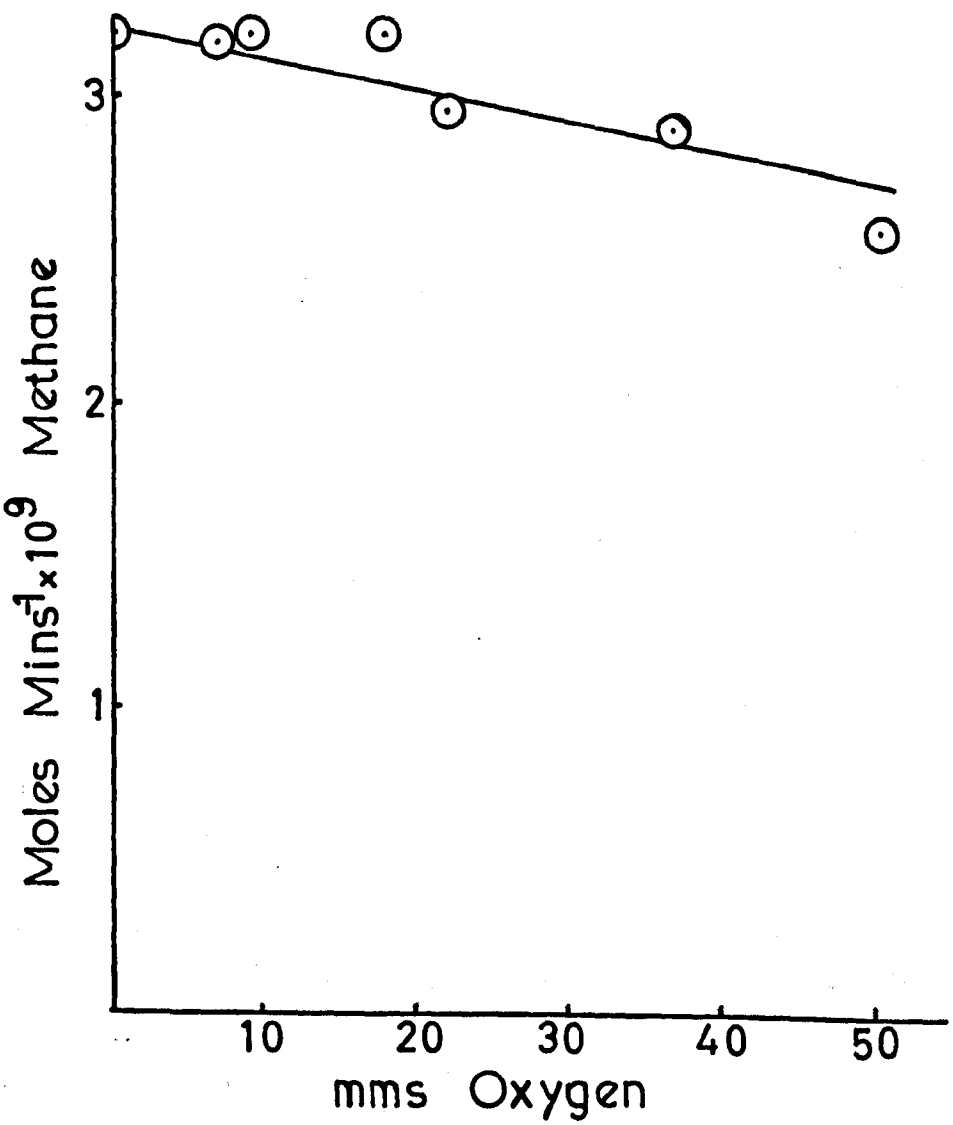

Figure 3.22

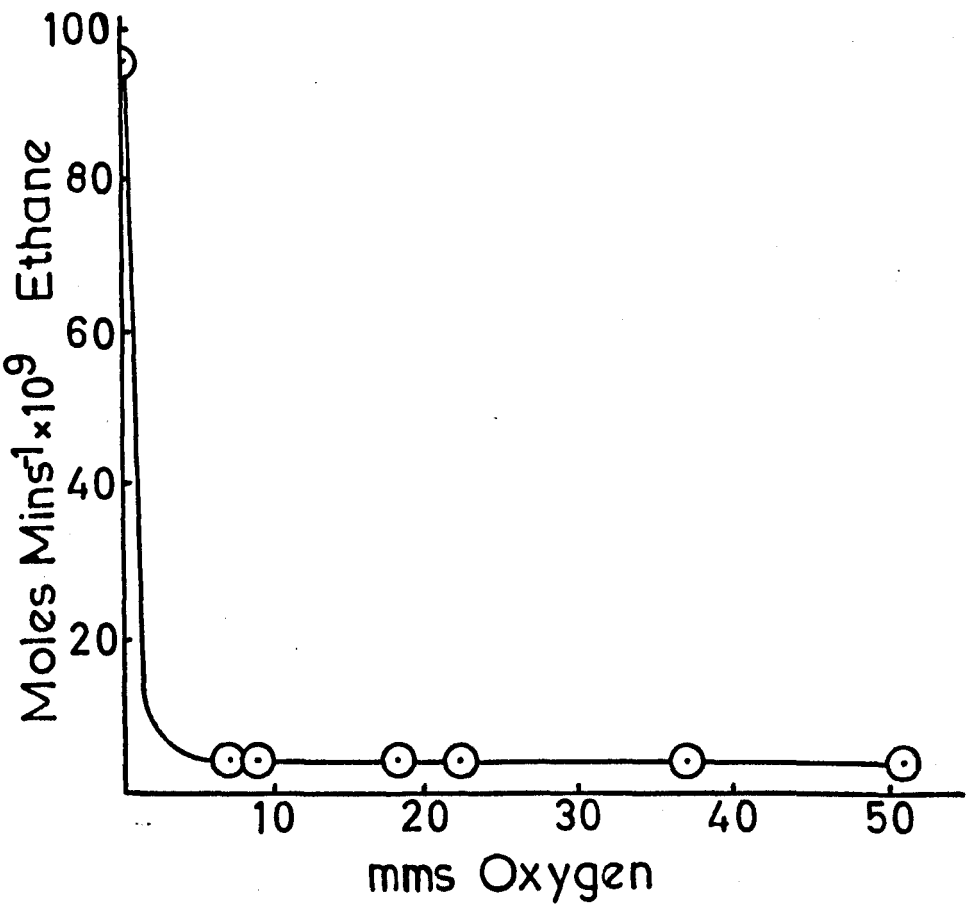
100
80
60
40
20
Moles Mins^{-1} x10^{9} Ethane
10
20
30
40
50
mms Oxygen

Figure 3.23

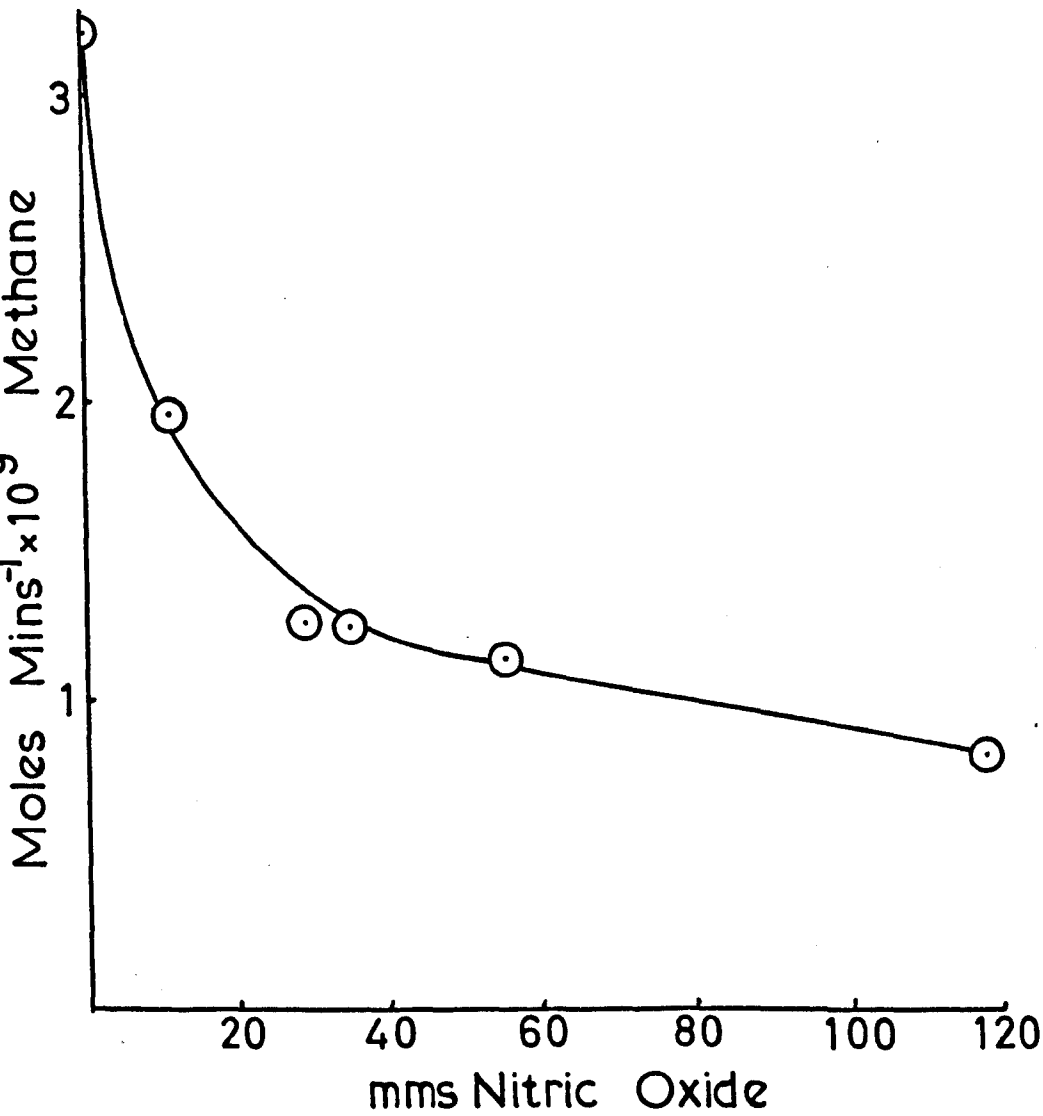
Moles Mins^{-1} x 10^{9} Methane
3
2
1
20
40
60
80
100
120
mms Nitric Oxide

Figure 3.24

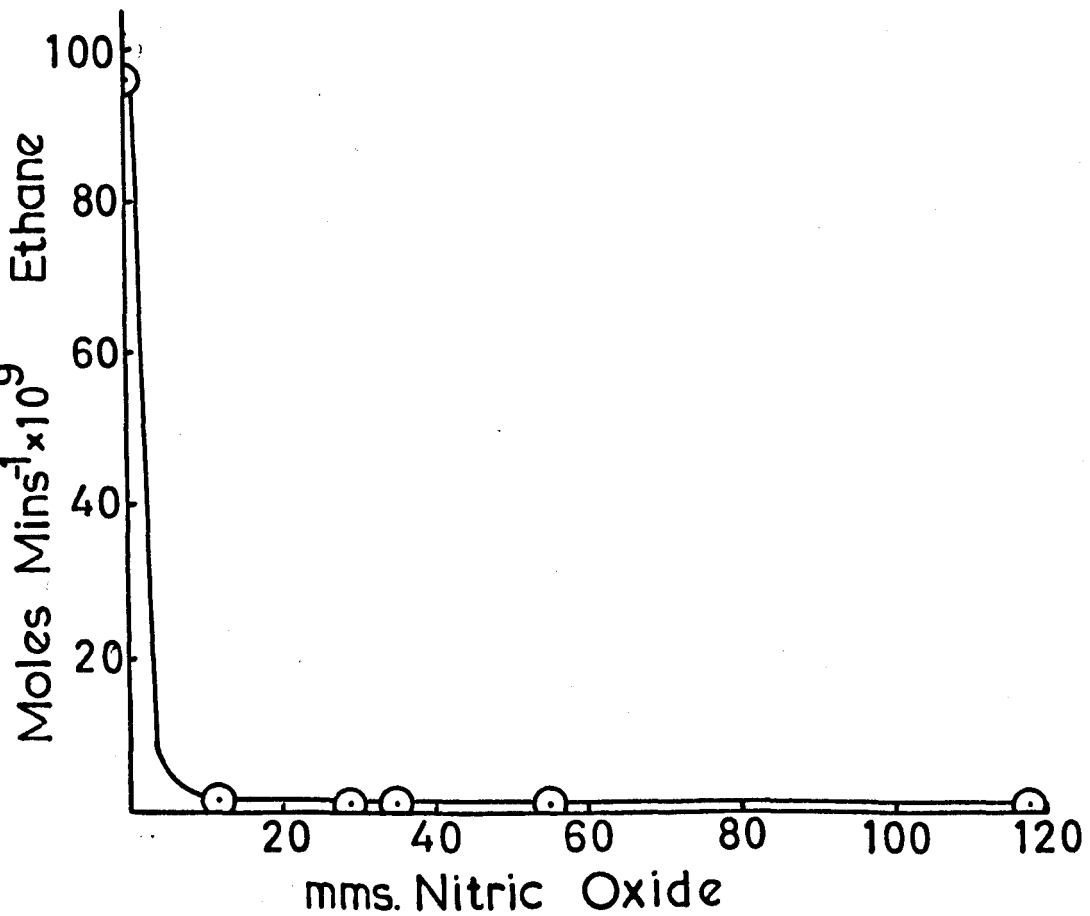
100
80
60
40
20
Moles Mins^{-1}x10^{9} Ethane
20
40
60
80
100
120
mms. Nitric Oxide

3.7 Variation of Temperature at 52.4% and 1.98% Intensity

In experiments carried out in Section 3.2, it was shown that both ethane and methane formation were directly proportional to intensity. This is a somewhat rather curious result if radical reactions are the cause of formation of both products. The methane rate should in fact have been proportional to $I^{\frac{1}{2}}$ and the ethane rate proportional to I. It was thus decided to carry out this set of experiments to see if increasing the temperature would show other dependences on intensity than could be gained at room temperature. The results are shown in Figures 3.25 to 3.32.

TABLE 3.9

Rates of formation as a function of temperature at different intensities

Irradiation Conditions: Pressure of $Sn(CH_3)_4$, 5 mm.
Irradiation time, 15 minutes
Temperature, 25, 50, 75, 100, 125, 150°C
Intensity, 52.4% and 1.98%

Analytical Conditions: Detector, flame ionisation
Column, Poropak Q
Temperature, 50°C
Nitrogen, 20 p.s.i.

	3.25	3.27	3.26	3.28
Temperature	Methane	% of I = 100%	Ethane	% of I = 100%
25°C	1.68×10^{-9}	52.4%	5.03×10^{-8}	52.4%
50°C	2.26×10^{-9}	52.4%	5.76×10^{-8}	52.4%
75°C	4.26×10^{-9}	53.4%	6.68×10^{-8}	53.0%
100°C	10.2×10^{-9}	58.8%	7.57×10^{-8}	54.1%
125°C	25.3×10^{-9}	68.0%	9.01×10^{-8}	57.0%
150°C	57.2×10^{-9}	80.4%	11.01×10^{-8}	61.6%

Figures in moles/minute

I = 52.4%

	3.29	3.31	3.30	3.32
Temperature	Methane	% of I = 100%	Ethane	% of I = 100%
25°C	0.665×10^{-10}	2.0%	1.72×10^{-9}	1.8%
50°C	1.91×10^{-10}	4.41%	2.03×10^{-9}	1.85%
75°C	7.58×10^{-10}	9.51%	3.22×10^{-9}	2.56%
100°C	19.38×10^{-10}	11.0%	4.44×10^{-9}	3.17%
125°C	48.04×10^{-10}	12.92%	6.53×10^{-9}	4.13%
150°C	124.0×10^{-10}	17.44%	7.56×10^{-9}	4.23%

Figures in moles/minute

I = 1.98%

Figure 3.25

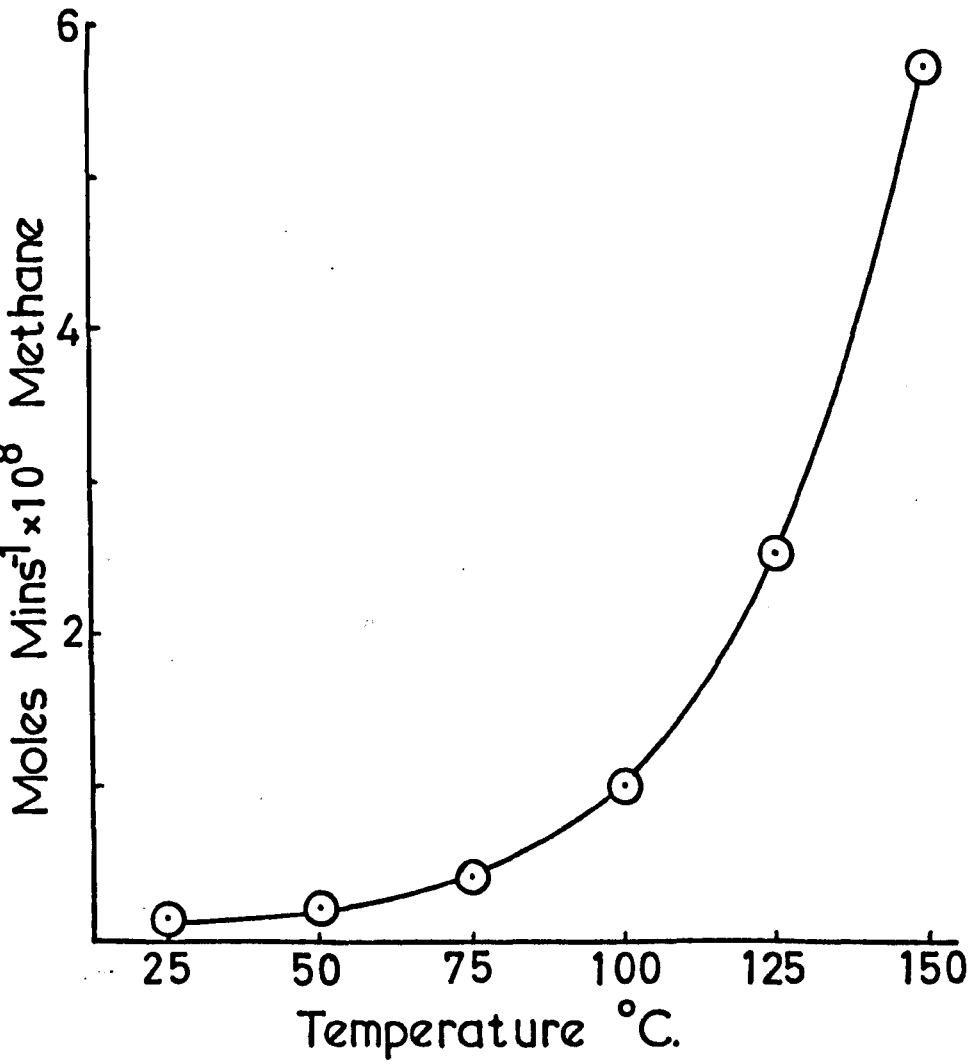
6
4
2
Moles Mins^{-1} x10^{8} Methane
25
50
75
100
125
150
Temperature °C.

Figure 3.26

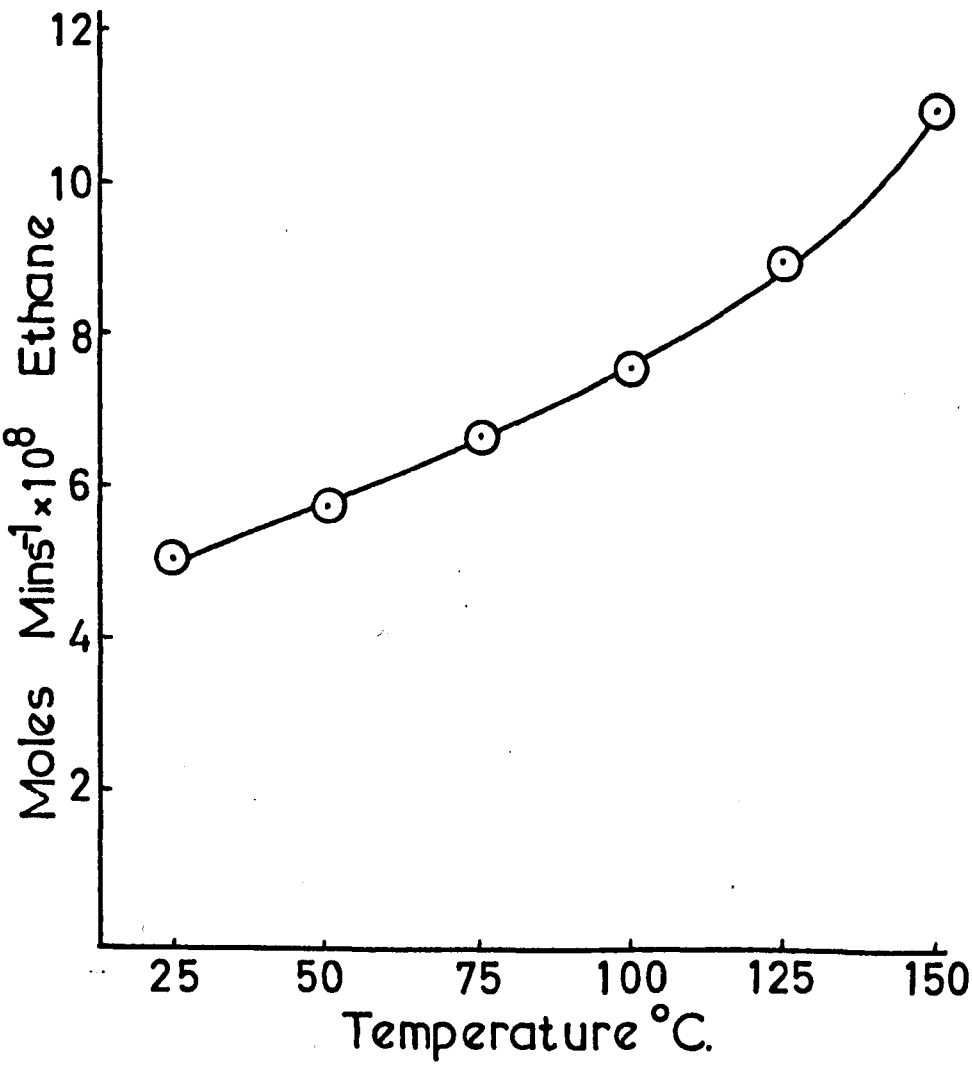
12
10
8
6
4
2
Moles Mins^{-1} x 10^{8} Ethane
25
50
75
100
125
150
Temperature °C.

Figure 3.27

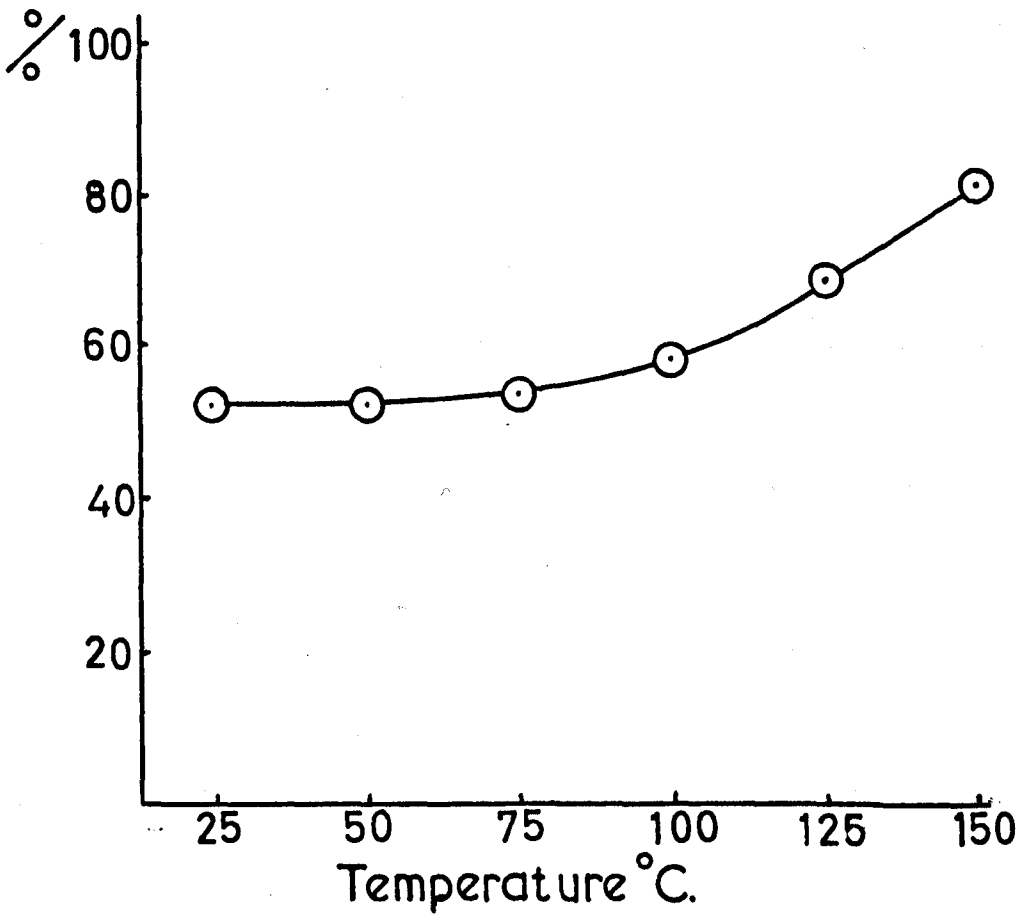

Figure 3.28

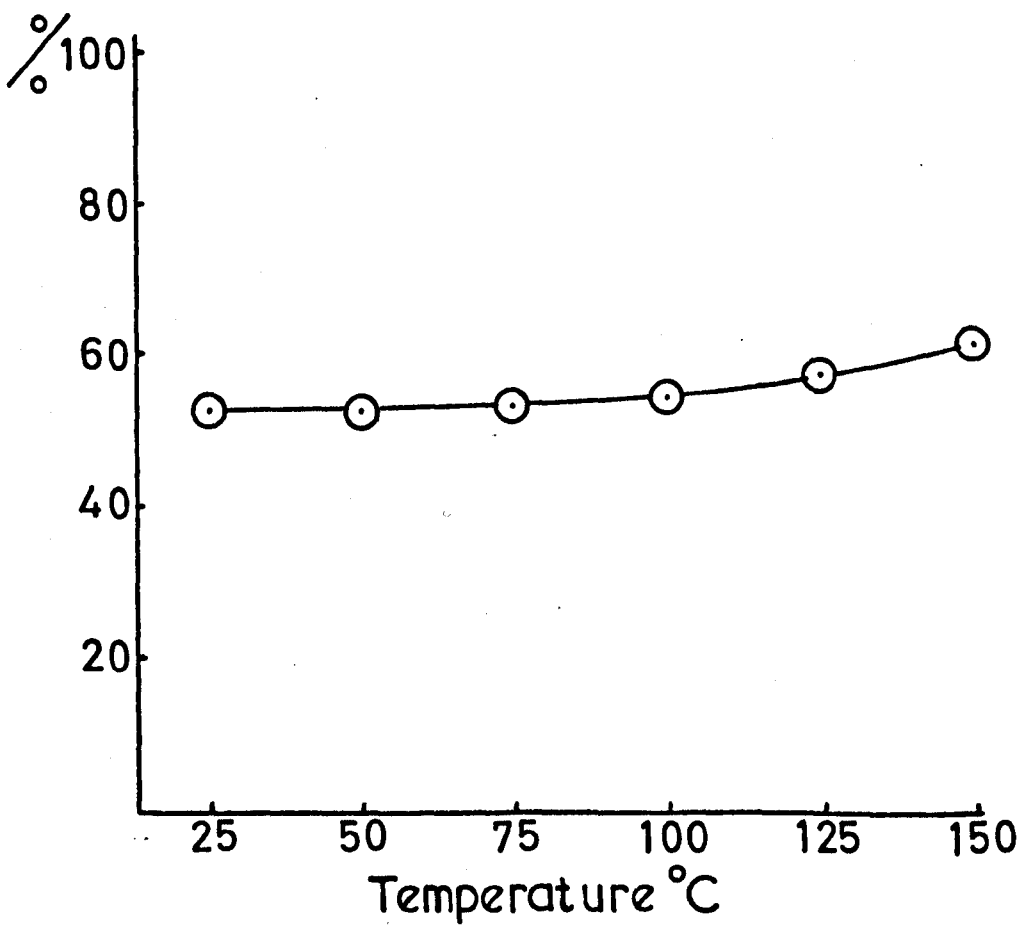

Figure 3.29

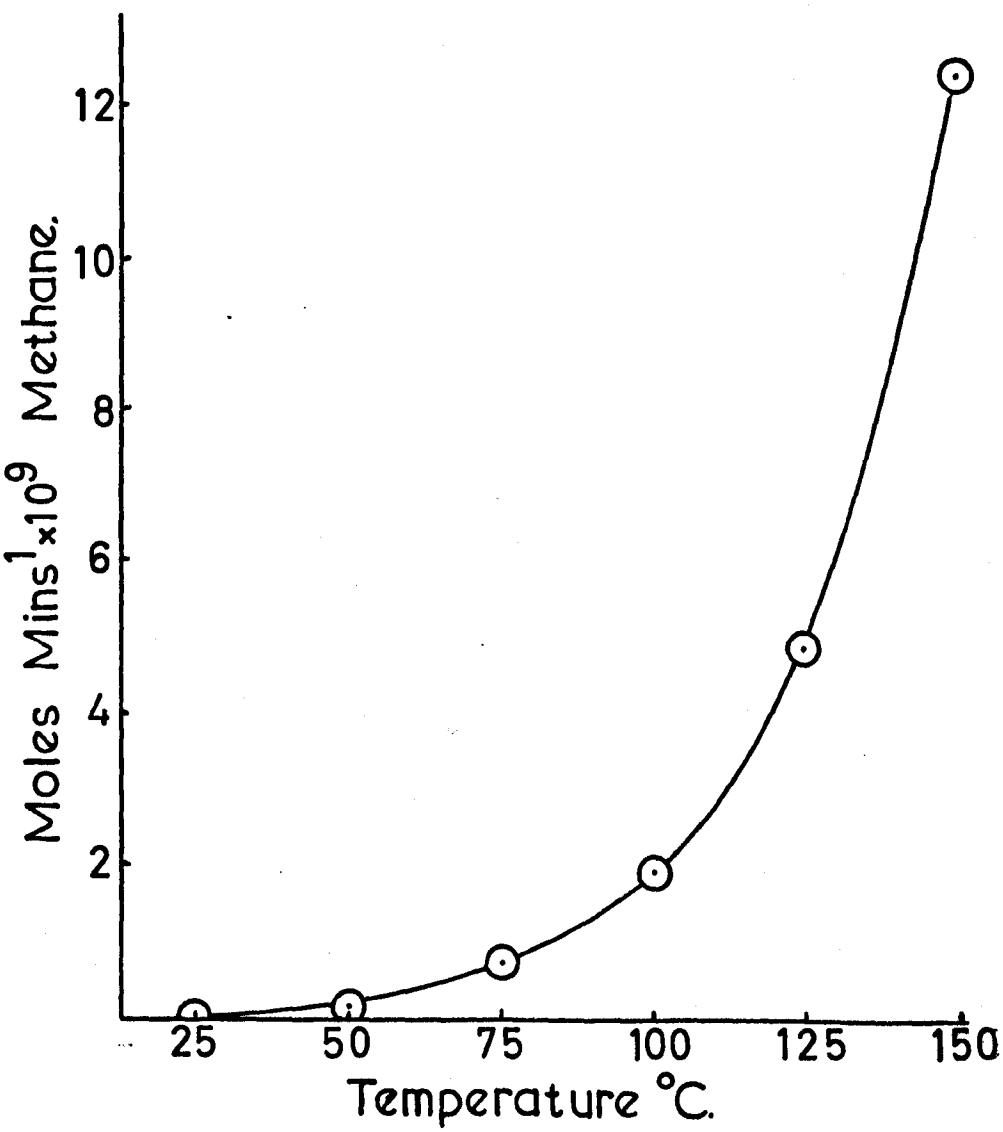
Moles Mins^{1} x10^{9} Methane.
12
10
8
6
4
2
25
50
75
100
125
150
Temperature °C.

Figure 3.30

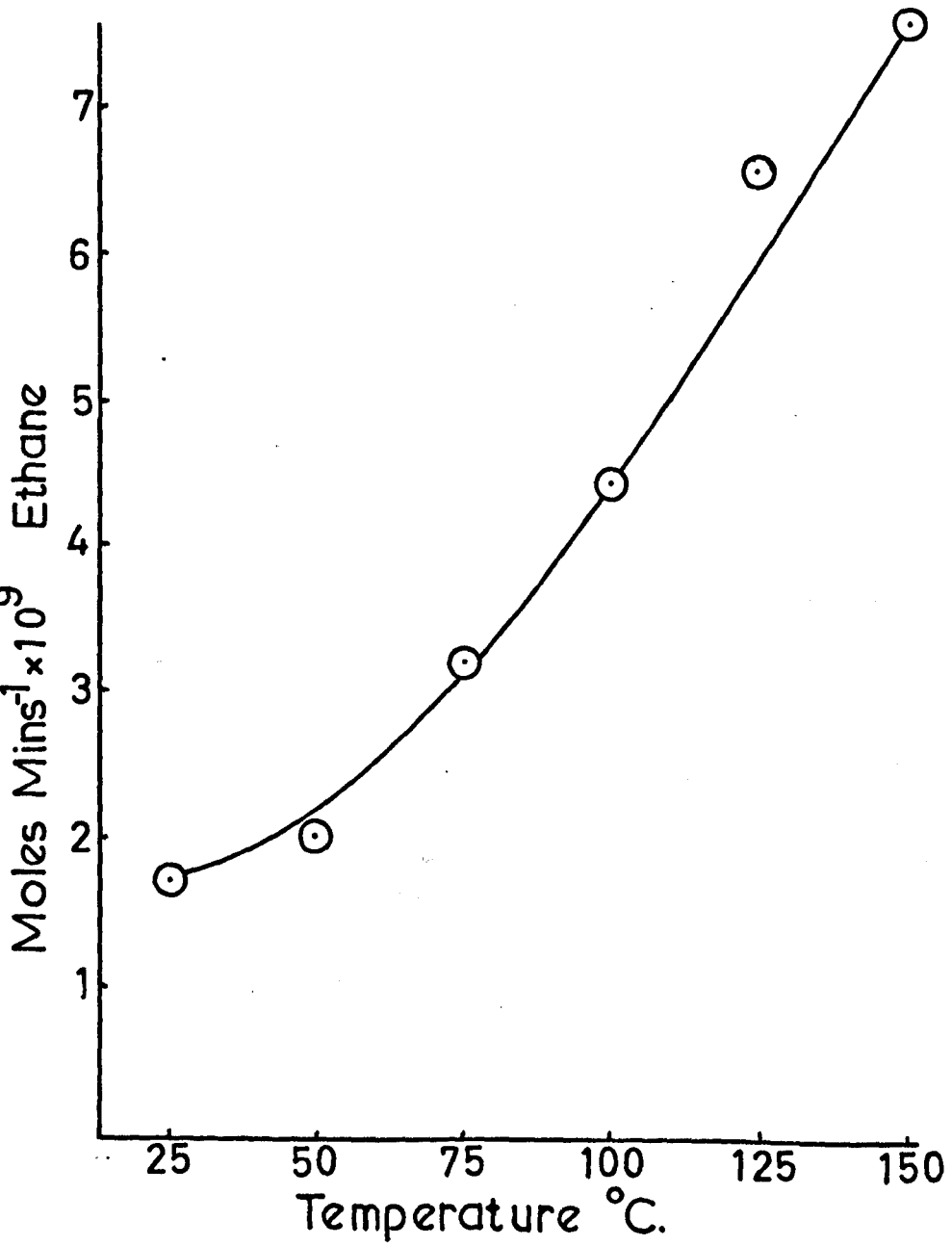
Moles Mins^{-1} x10^{9} Ethane
1
2
3
4
5
6
7
25
50
75
100
125
150
Temperature °C.

Figure 3.31

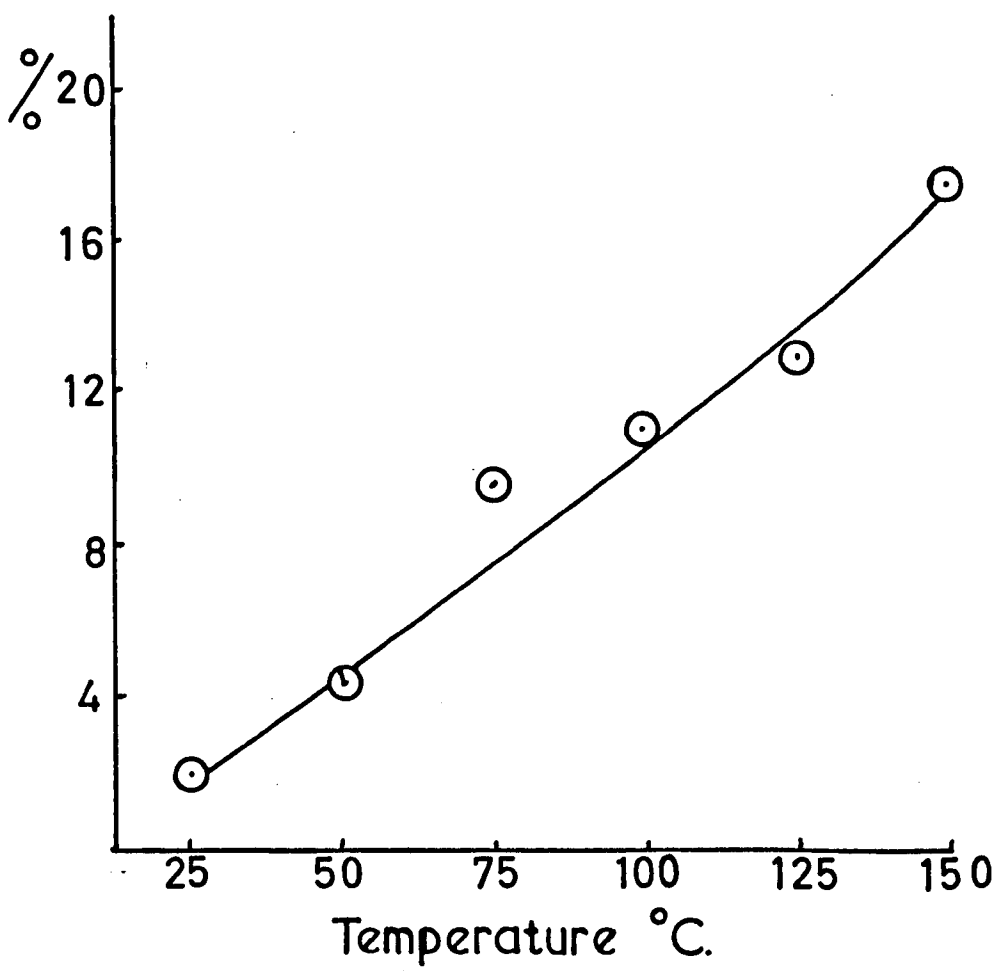

Figure 3.32

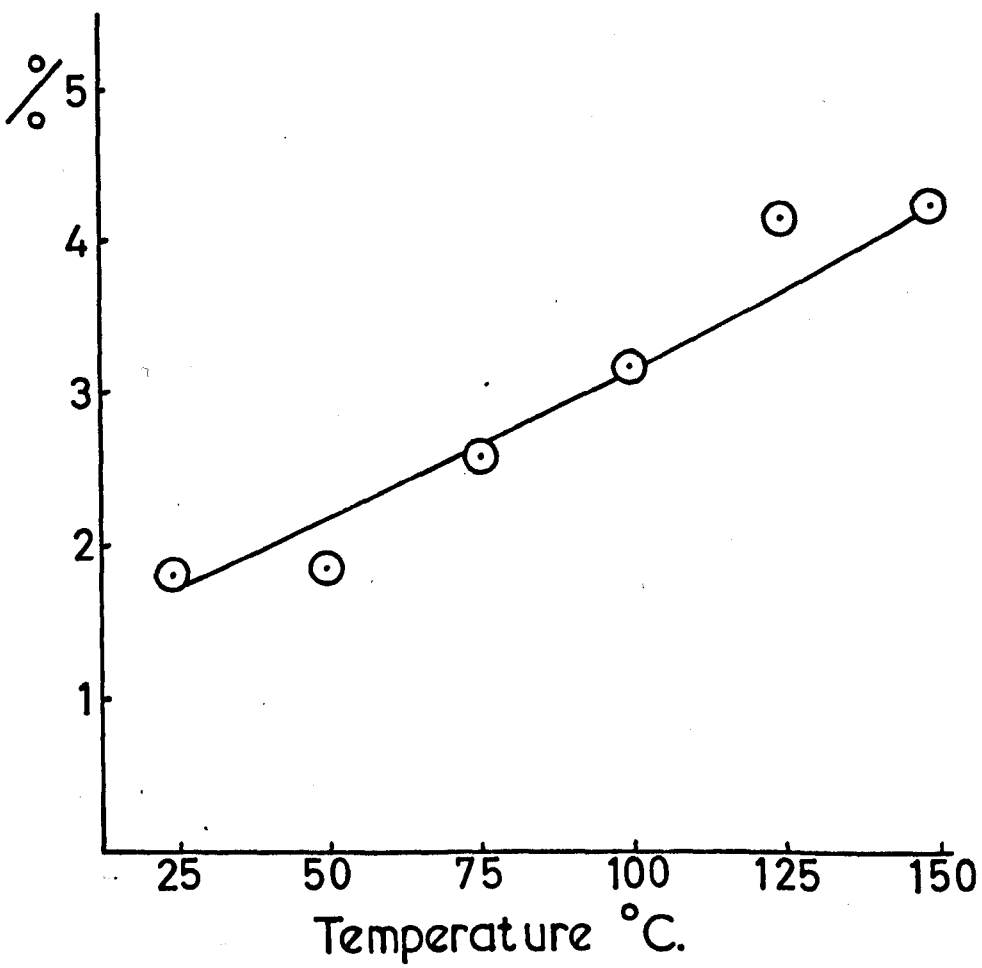

3.8 Variation of temperature with added Radical Scavenger

The fraction of products remaining after the addition of nitric oxide is thought to be molecular and to be so it would have to be a primary reaction. Primary reactions have no temperature coefficient and thus this set of experiments will give an idea on the extent of the primary nature of these products. Figure 3.33.

TABLE 3.10

Rate of formation as a function of temperature with added radical scavenger

Irradiation Conditions: Pressure of $Sn(CH_3)_4$, 5 mm.
Pressure of NO, 11.2 mm.
Temperature, 25, 50, 75, 100, 125, 150°C
Irradiation time, 15 minutes

Analytical Conditions: Detector, flame ionisation
Column, Poropak Q
Temperature 50°C
Nitrogen 20 p.s.i.
3.33

Temperature	Methane	Ethane
25°C	1.95×10^{-9}	1.60×10^{-9}
50°C	2.09×10^{-9}	1.69×10^{-9}
75°C	2.45×10^{-9}	1.69×10^{-9}
100°C	3.10×10^{-9}	1.69×10^{-9}
125°C	4.37×10^{-9}	1.69×10^{-9}
150°C	22.44×10^{-9}	1.69×10^{-9}

Figures in moles/minute

Figure 3.33

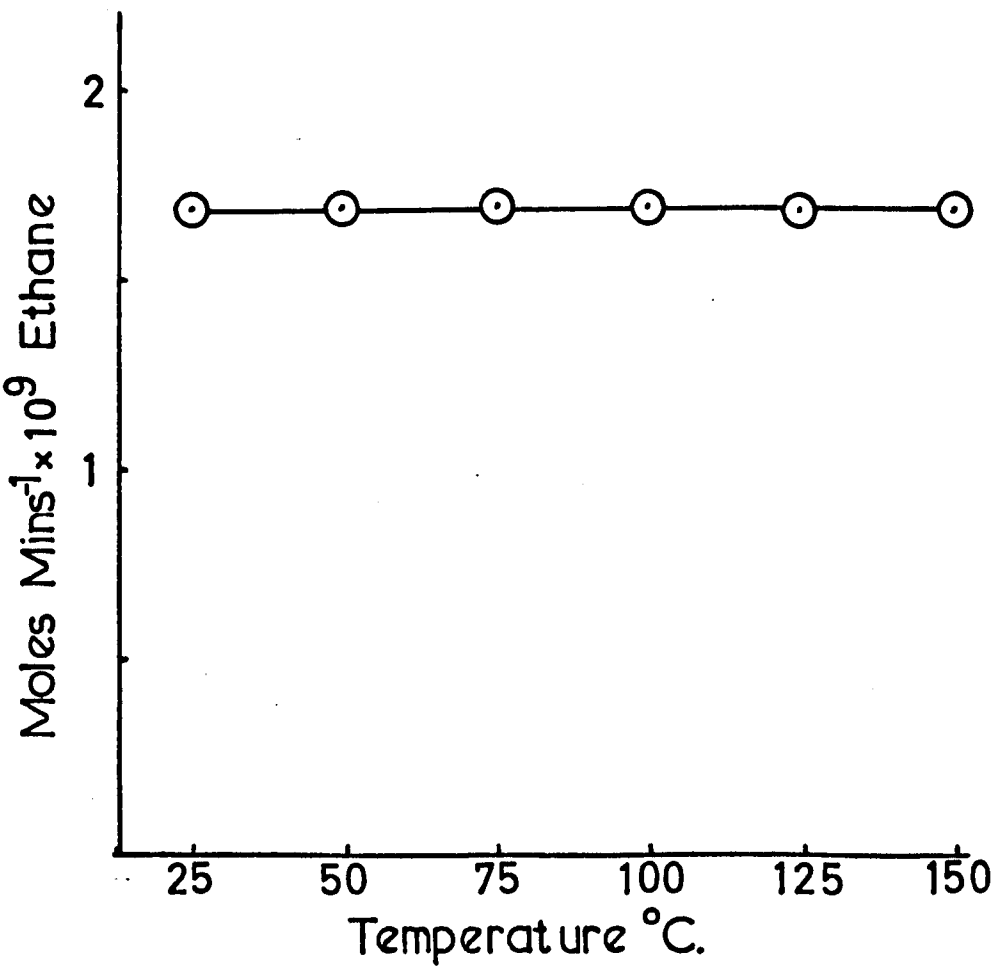

Another experiment was carried out with nitrogen present.

$Sn(CH_3)_4$	Nitrogen	Temperature	Methane	Ethane
5 mm.	500 mm.	25°C	1.33×10^{-9}	3.10×10^{-8}
5 mm.	500 mm.	100°C	4.66×10^{-9}	3.98×10^{-8}

Figures in moles/minute.

3.9 Variation of time at High Temperatures

Ordinary experiments carried out at room temperatures did not show any products other than methane, ethane, ethylene and propane. It was decided to carry out experiments at 100°C to show that other products could be formed and two further products were found, i.e. hexamethyl distannane and trimethyl tin hydride. Their yields as a function of time are shown in Figures 3.34 and 3.35.

TABLE 3.11

Product yields as a function of time at 100°C

Irradiation Conditions: Pressure of $Sn(CH_3)_4$, 5 mm.
Temperature, 100°C
Irradiation 0 - 3½hrs.

Analytical Conditions: Detector, flame ionisation
Column, Ap-L on Celite
Temperature, 100°C
Nitrogen, 20 p.s.i.

	3.34	3.35
Time	$Me_3SnSnMe_3$ Moles	Me_3SnH
30 mins.	0.77×10^{-8}	3.32×10^{-8}
60 mins.	1.53×10^{-8}	4.98×10^{-8}
90 mins.	2.04×10^{-8}	6.23×10^{-8}
120 mins.	2.52×10^{-8}	6.65×10^{-8}
150 mins.	2.88×10^{-8}	7.32×10^{-8}
187 mins.	3.22×10^{-8}	7.68×10^{-8}

Figure 3.34

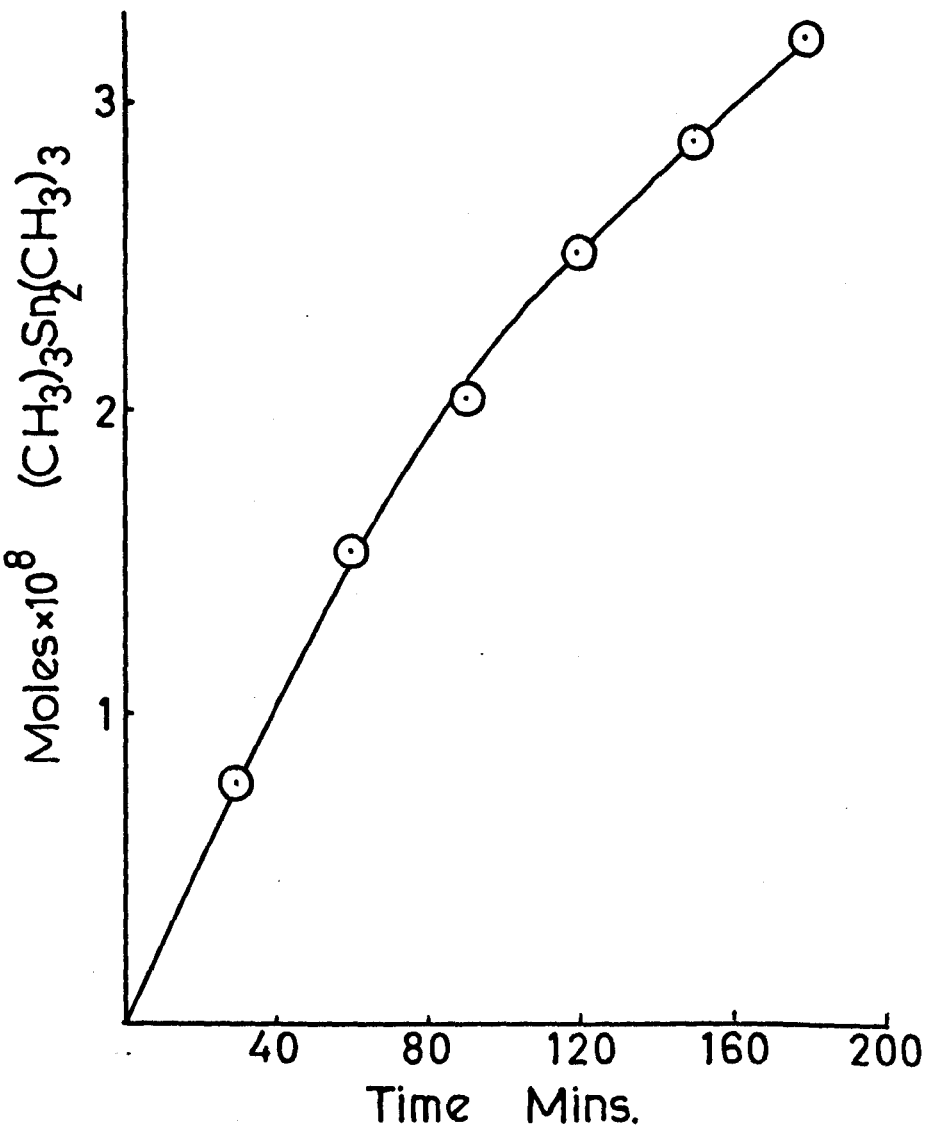

Figure 3.35

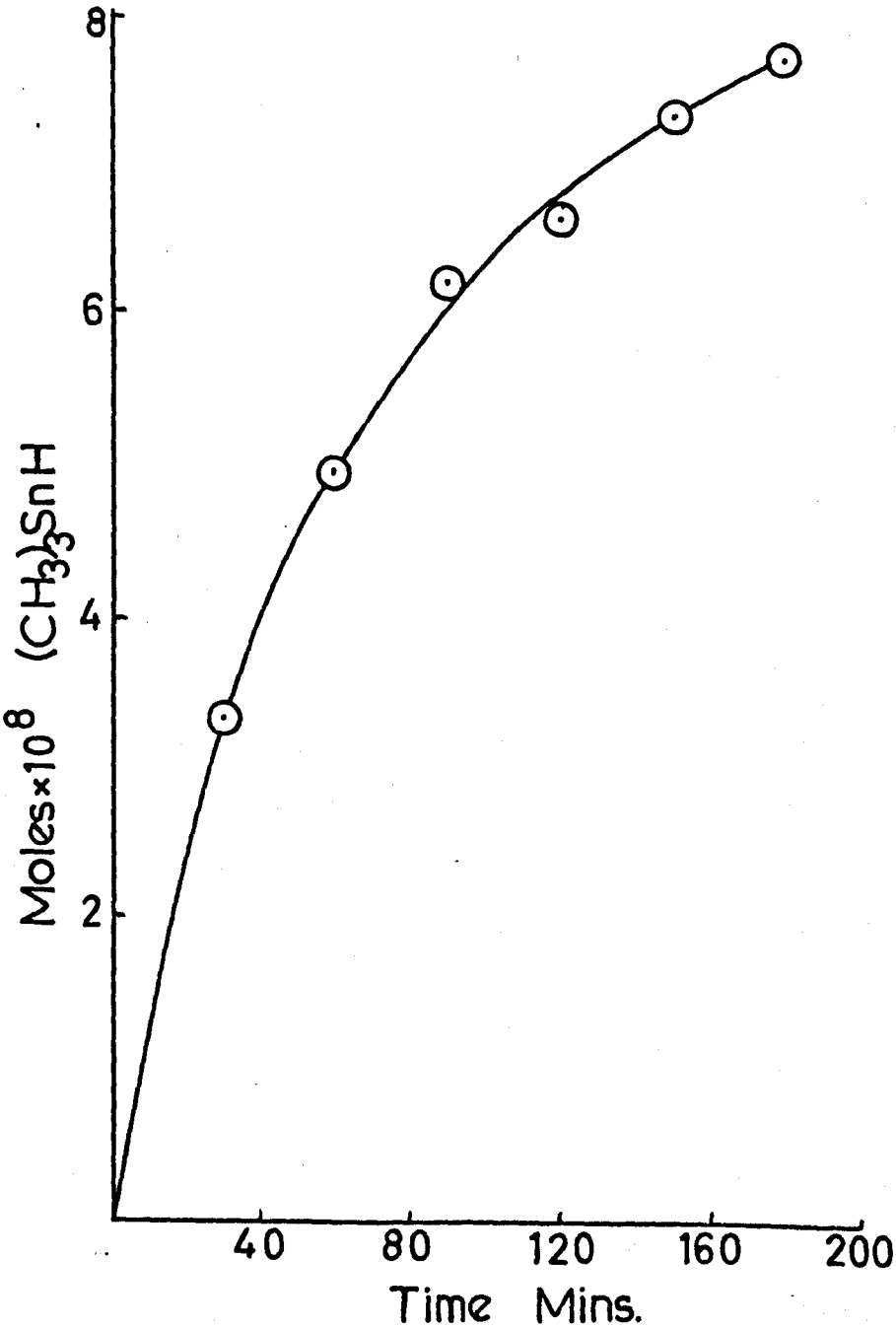

3.10 Film formation

In the original apparatus where a high pressure lamp was used, no attempt was made to analyse quantitatively the film formed. In the second case the film dissolved in dilute acids but not organic solvents. Once dissolved this gave positive tests for tin.

Over longer periods of irradiation, i.e. 20-30 hrs it was obvious that all the film could not be removed by dilute HCl or chromic acid and required, as for the high pressure lamp experiments, aqua regia to remove all traces. The absorption of the film remaining after washing with dilute HCl was similar to that from longer wavelength irradiation.

Polarography was used to analyse the amount of tin on the window of the cell. The film was dissolved in HCl and made up to 50 mls containing 0.005 grms/ml Gelatine, 0.1 M KCl in normal HCl. Figure 2.17 gives the standard graph from which the amount of tin can be determined. In the first case 5 mms of tetramethyl stannane was irradiated for 30 minutes and the window removed and the polarography carried out.

Analysis was impossible although 10^{-6} moles of tin would be formed. 20 mms of tetramethyl stannane was irradiated for four hours and a value of tin on the front window was obtained i.e. 7×10^{-7} moles Sn. Approximately 6×10^{-6} moles should have been formed. A further experiment was carried out using a quartz cell. 20 mm of $Sn(CH_3)_4$ was irradiated for 24 hrs and gave 37.86×10^{-6} moles of ethane which comes from 18.93×10^{-6} moles Sn. The total tin obtained by washing the vessel with HCl gave 4.178×10^{-6} moles Sn.

Figure 3.36 gives the absorption of the film formed versus the time irradiated.

TABLE 3.12

Film absorption as a function of time

Time	Absorption %
0 mins	7
10 mins	28
20 mins	32.5
30 mins	36.3
50 mins	46.25
60 mins	56.39

A repeat experiment in the brass vessel gave the following results similar to the previous ones. Ethane formed 36.74×10^{-6} moles, Tin formed 3.946×10^{-6} moles.

Long irradiations showed that no ethyl trimethyl stannane or ; hexamethyl stannane were formed even after periods of 24 hrs.

Figure 3.36

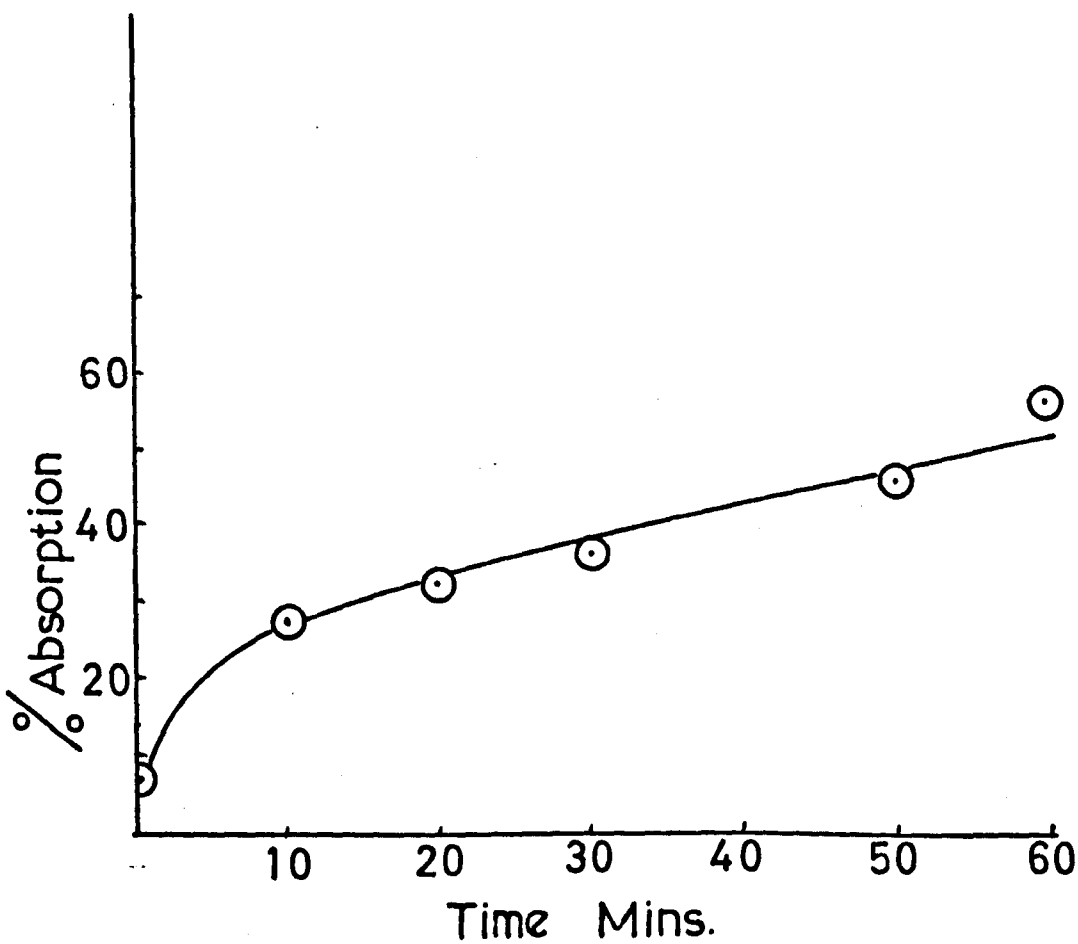

3.11 Identification of Ethyl Trimethyl Stannane

It was first thought possible that the compound ethyl trimethyl stannane which could be formed by addition of a methyl radical to a trimethyl stannyl methylene radical could be analysed by mass spectroscopy. This however proved difficult in that the mass spectrometer (Section 2.8) built from a MS10 kit did not have very good resolution and the number of tin isotopes confused analysis of the spectrum. An indication of the presence of ethyl trimethyl stannane was all that could be obtained from the spectra. Figure 3.37 shows the mass range 110 - 126 of two samples

a) $Sn(CH_3)_4$

b) $Sn(CH_3)_4$ irradiated for 2 hrs at 125°C at 50 μamps and 10 μamp trap current.

Figures 3.38, 3.39, 3.40 and 3.41 show the mass spectra of $Sn(Me)_4$, $EtSnMe_3$, Et_2SnMe_2 and $SnEt_4$ obtained on a Perkin Elmer RMU 6 spectroscope and these show the complexity of the spectra involved. Certainly a large proportion of product is required before resolution by mass spectroscopy can be achieved.

Whilst carrying out long duration experiments at 100°C for the mass spectroscope, samples of the gas were analysed by gas chromatography and it became apparent that carbon balances could be obtained and also another peak was obtained on the tail of the $Sn(CH_3)_4$ peak. Comparison of this peak with an authentic sample of $EtSn(Me)_3$

showed that the compound had in fact been formed. However no quantitative values have in fact been carried out.

Figure 3.37

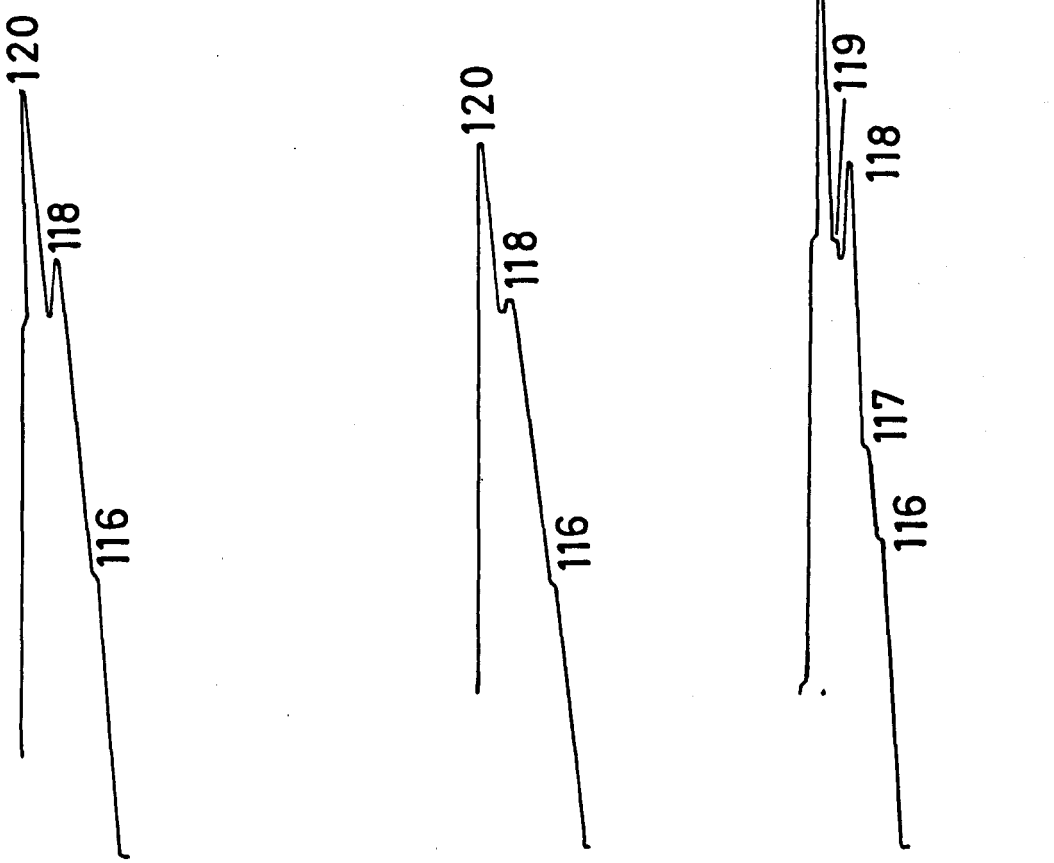

$Sn(CH_3)_4$

a. 50 uamps b. 10 uamps

90 Mins at 125°C.

Figure 3.38

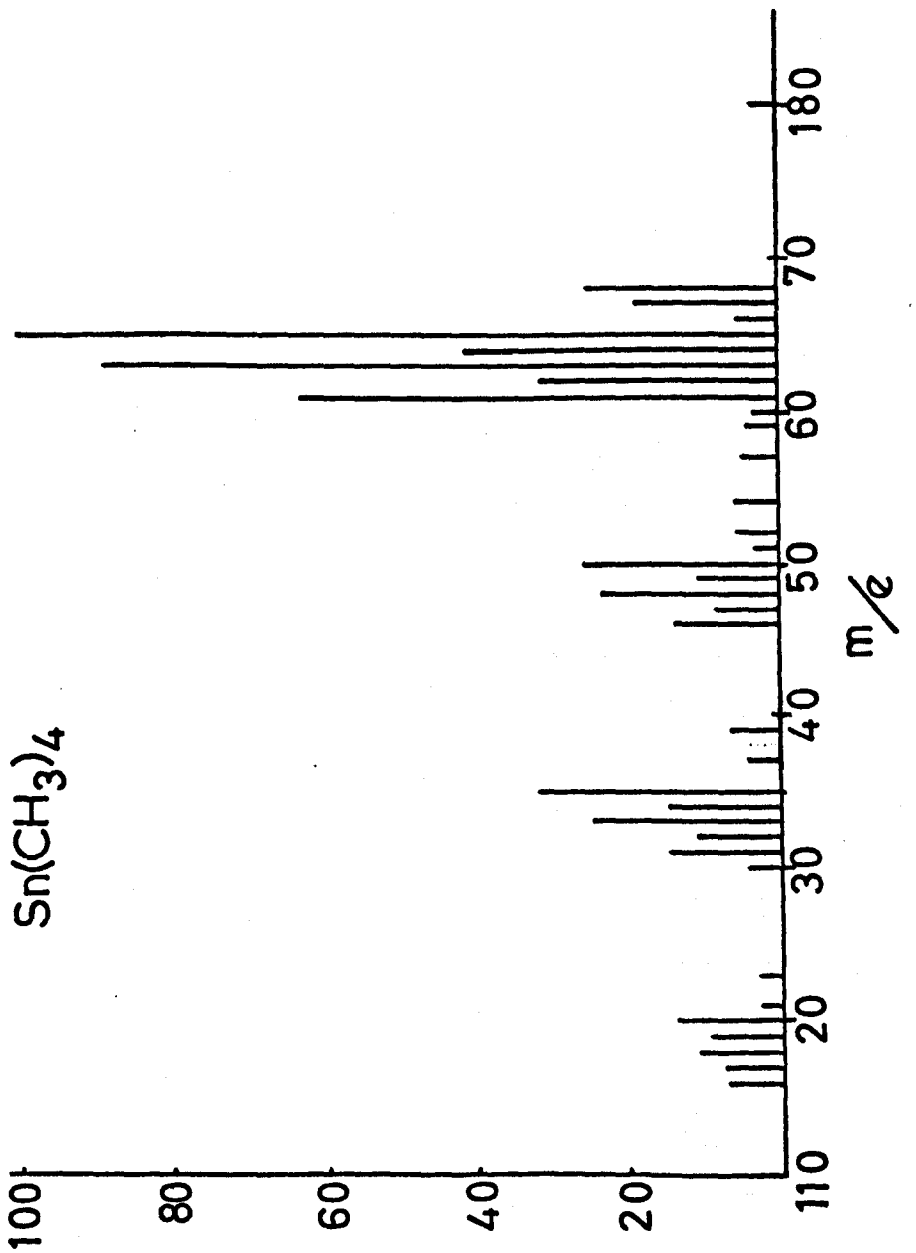

Figure 3.39

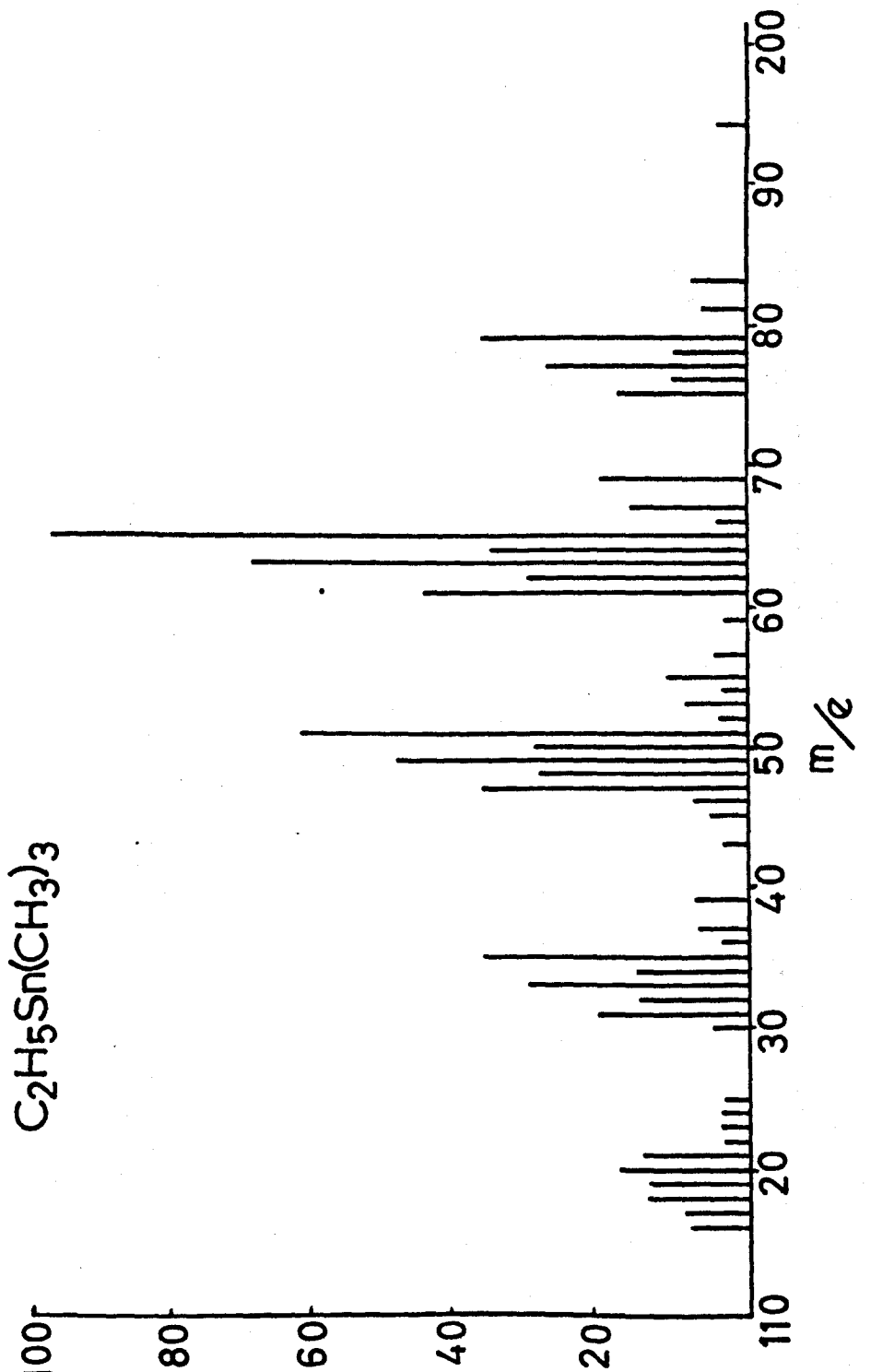

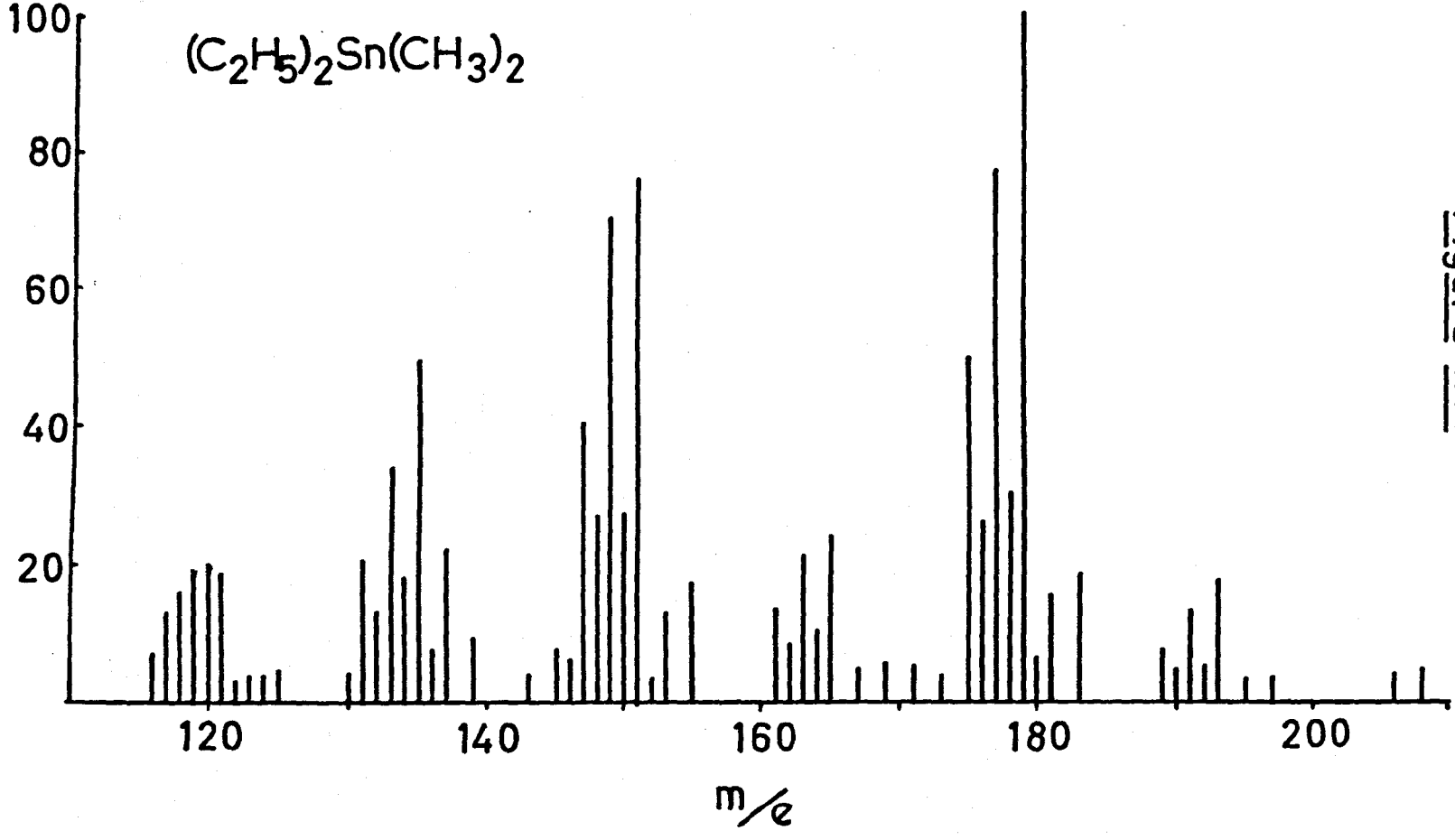

Figure 3.40

Figure 3.41

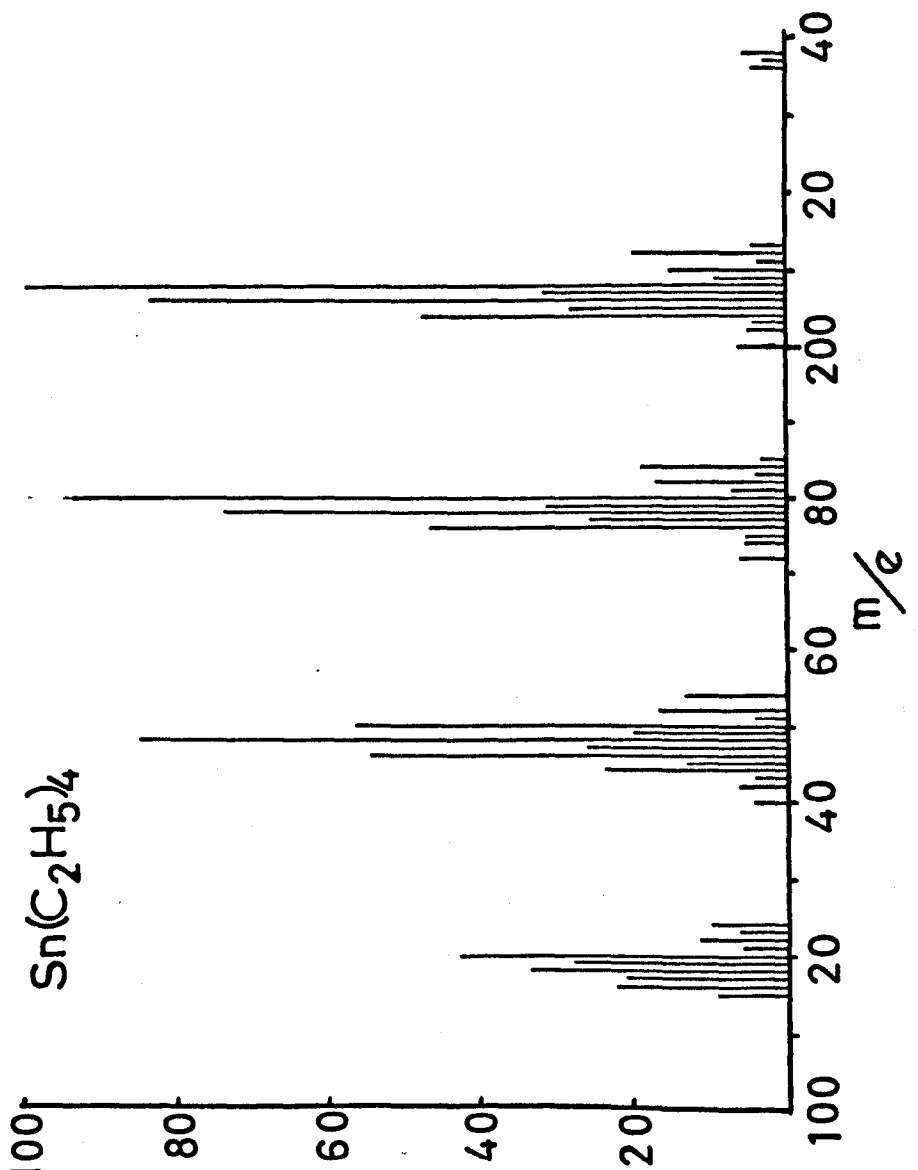

3.12 Carbon and Hydrogen Balance

Two experiments were carried out, one at 100°C and the other at 125°C.

TABLE 3.13

°C	Time	$Sn(CH_3)_4$	CH_4	C_2H_6	Me_3SnH	$EtSnMe_3$	$Me_3SnSnMe_3$	%error C	%error H
100	3 hrs	4.39×10^{-6}	1.55×10^{-6}	7.75×10^{-6}	1.8×10^{-8}	1.0×10^{-8}	2.8×10^{-9}	1.77	0.75
125	$2\frac{1}{2}$hrs	4.39×10^{-6}	2.01×10^{-6}	7.44×10^{-6}	2.39×10^{-8}	1.84×10^{-8}	1.6×10^{-9}	3.13	0.46

Yields in Moles

As can be seen the error in the C & H balance is quite reasonable and it may be assumed that these products are the major ones in the reactions.

3.13 Actinometry

The rate of hydrogen production from ethylene (Section 2.10) was measured and found to be 3.88×10^{-8} moles/minute.

The rates of production of the products at room temperature (Section 3.1) were found to be

$$\text{Ethane:} \quad \frac{1.278 \times 10^{-7}}{3.88 \times 10^{-8}} \times 0.61 = 2.01$$

$$\text{Methane:} \quad \frac{3.03 \times 10^{-9}}{3.88 \times 10^{-8}} \times 0.61 = 0.05$$

3.14 Preparation of Trimethyl Stannyl Chloride

The second compound to be studied was ethyl trimethyl tin and to prepare this it was necessary to prepare the intermediate compound trimethyl tin chloride. It was at first thought that a direct alkylation using methyl magnesium iodide replacing three of the chlorine atoms on stannic chloride was feasible, but attempts failed to yield any of the trimethyl tin chloride. It was found necessary to complete the alkylation of stannic chloride and react the tetramethyl stannane with more stannic chloride to give a redistribution reaction and thus trimethyl tin chloride.

The preparation of tetramethyl stannane was carried out in dry-ether and under an atmosphere of nitrogen. Attempts to prepare it in tetrahydrofuran failed. 78.3 grms of Mg turnings were placed in a 5-litre, round bottom, three-necked flask fitted with a stirrer, condenser and a nitrogen inlet. The magnesium turnings were covered with ether and the Grignard reaction started by adding neat methyl iodide after a crystal of iodine. The reaction was continued by addition of 1:1 methyl iodide ether mixture until a total of 457 grms MeI had been added. The whole was refluxed on a steam bath for half an hour to ensure completion of the reaction. The steam bath was removed and a water-ice bath placed in position. Time was allowed for the Grignard solution to cool to $0^{o}C$ and then anhydrous stannic chloride was added dropwise whilst the Grignard solution was stirred. The cooling of the

diethyl ether solution reduces the formation of etherate which stannic chloride easily forms. A total of 80 mls (167 grms) $SnCl_4$ was added and the stoichiometry of the reaction was

$$SnCl_4 + 5\ CH_3MgI$$

Excess Grignard was used to give complete methylation.

On completion of the addition of stannic chloride the solution was refluxed for 2 hrs and then distilled through a glass helices column yielding approximately 100 mls of tetramethyl stannane solution in ether. (Approximately two-thirds of the solution was $Sn(CH_3)_4$).

To this solution was added 20 mls $SnCl_4$ and the whole refluxed for 4 hrs under nitrogen by which time any ether remaining in solution had been removed by the nitrogen flow and the solution was refluxing at 154°C. The boiling point of $(CH_3)_3SnCl$ is 154°C. Gas chromatography showed that pure $(CH_3)_3SnCl$ had been formed and no $Sn(CH_3)_4$ was present. A small amount of $(CH_3)_2SnCl_2$ was also present.

Trimethyl ethyl stannane was then prepared by the action of ethyl Grignard reagent on trimethyl tin chloride. Separation from the solvent and purification was carried out by distillation through a 2 ft. glass helices column. Subsequent preparative gas phase chromatography yielded ~100% pure ethyl trimethyl tin of approximately 10 mls in volume.

Similarly n-propyl trimethyl stannane was prepared for Section 5.

4. RESULTS

Ethyl Trimethyl Stannane

Irradiation of a sample of ethyl trimethyl stannane with a filter of 2% Acetic Acid, 1 cm. thick, interposed between the lamp and the cell, resulted in no photochemical reaction whereas without the filter a number of photochemical products were obtained. The presence of the filter which absorbs 1849 Å (Section 2.5.2) indicated that this was the exciting wavelength and also that no mercury was present acting as a sensitiser since it is expected, from the U.V. absorption of similar compounds (Section 1.2), that the compound is transparent to 2537 Å which is the main component of the light emitted from a low pressure mercury vapour lamp (Section 2.5.1 Figure 2.11).

The products of irradiation at 1849 Å were methane, ethylene, ethane, propane and butane at room temperature.

TABLE 4.1

Product	Yield
Methane	3.52×10^{-9} moles/min.
Ethylene	2.41×10^{-8} moles/min.
Ethane	3.20×10^{-8} moles/min.
Propane	7.44×10^{-8} moles/min.
Butane	3.12×10^{-8} moles/min.

Clearly from the nature of the products there is the possibility, as in Section 3, of free radical processes being involved and possibly some molecular elimination processes.

To help distinguish between the modes of formation of the products, their dependence upon the variation of the following parameters was measured.

(1) Pressure of ethyl trimethyl stannane

(2) Time

(3) Intensity

(4) Added inert gases

(5) Added radical scavengers

(6) Temperature

(7) Time at high temperatures

Irradiations were generally of ten minutes duration resulting in <0.1% decomposition of ethyl trimethyl stannane. The pressure of ethyl trimethyl stannane in the reaction cell was always sufficient to absorb >99% of the 1849 Å radiation. The effects of varying the parameters 1 - 7 are given in the Section 4.1 - 7. In Section 4.2 the product yields are in moles and in the remainder they are expressed in rates of formation i.e. moles/minute, and quantum yields ϕ where

$$\phi = \frac{\text{Number of molecules formed per second}}{\text{Amount of light absorbed per second}}$$

and as in Section 3.1 the light absorbed was determined by ethylene actinometry (Section 2.10).

4.1 The effect of variation of Ethyl Trimethyl Stannane Pressure

The effect of variation of ethyl trimethyl stannane pressure on the product yields are shown in Figure 4.1 - 4 and it can be seen that increasing the pressure over the range shown linearly increases the rates of formation.

TABLE 4.2

Product yields as a function of variation of $C_2H_5Sn(CH_3)_3$ pressure

Irradiation Conditions: Pressure $C_2H_5Sn(CH_3)_3$, 0 - 30 mm.
Temperature, 25°C
Irradiation time, 5 minutes

Analytical Conditions: Detector, flame ionisation
Column, Ap-L on Celite
Temperature, 65°C
Nitrogen, 20 p.s.i.

	4.1	4.2	4.3	4.4
Pressure	C_2H_6	C_2H_4	C_3H_8	C_4H_{10}
5 mm.	3.11×10^{-8}	2.35×10^{-8}	7.94×10^{-8}	3.31×10^{-8}
15 mm.	3.45×10^{-8}	2.60×10^{-8}	9.64×10^{-8}	6.61×10^{-8}
10 mm.	3.34×10^{-8}	2.52×10^{-8}	8.82×10^{-8}	4.63×10^{-8}
20 mm.	3.77×10^{-8}	2.84×10^{-8}	9.89×10^{-8}	7.31×10^{-8}
30 mm.	4.34×10^{-8}	3.27×10^{-8}	12.98×10^{-8}	10.51×10^{-8}
28 mm.	4.20×10^{-8}	3.17×10^{-8}	12.47×10^{-8}	9.19×10^{-8}
23 mm.	3.91×10^{-8}	2.95×10^{-8}	11.28×10^{-8}	8.02×10^{-8}

Figures in moles/minute

Figure 4.1

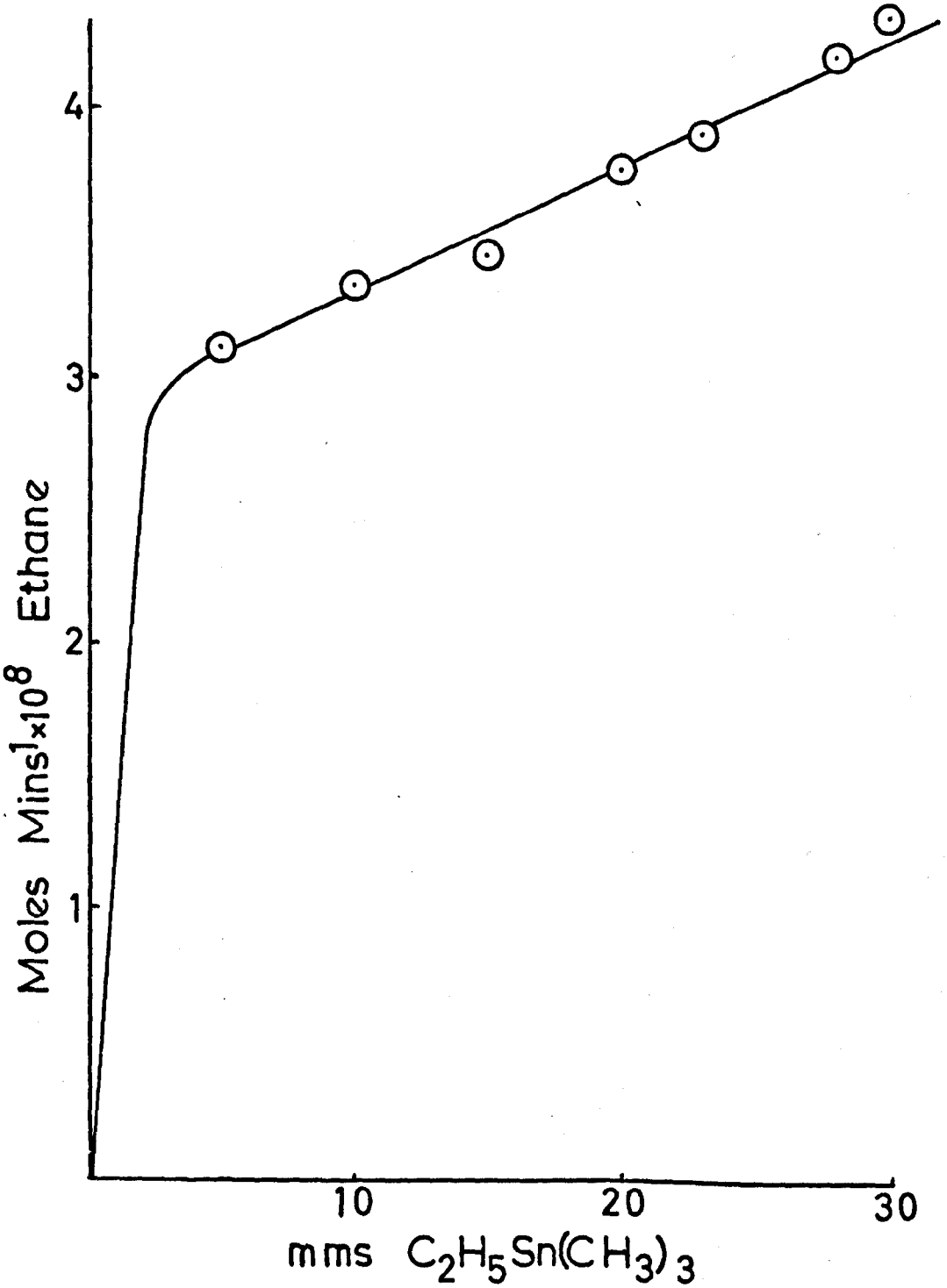

Figure 4.2

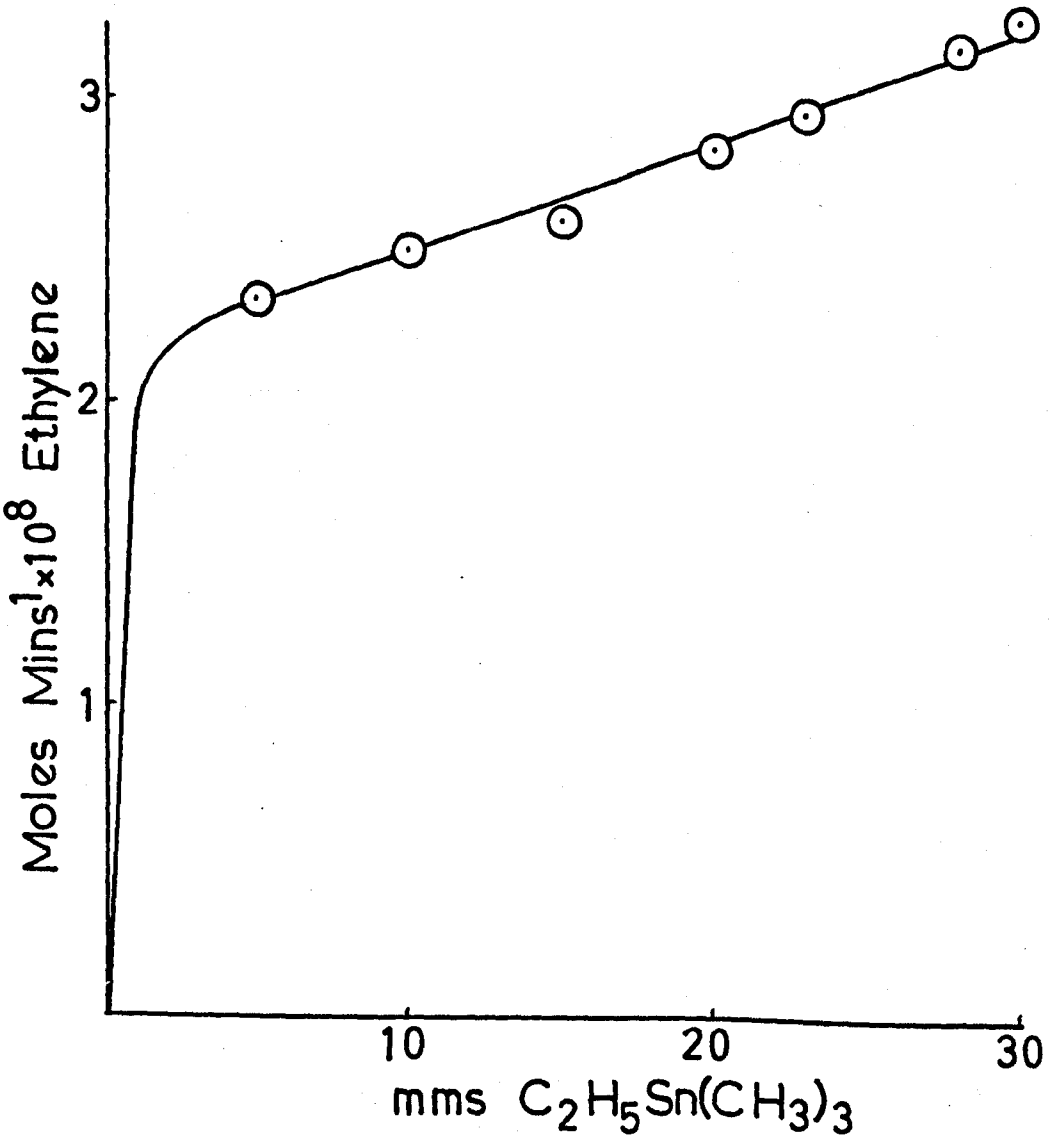

Figure 4.3

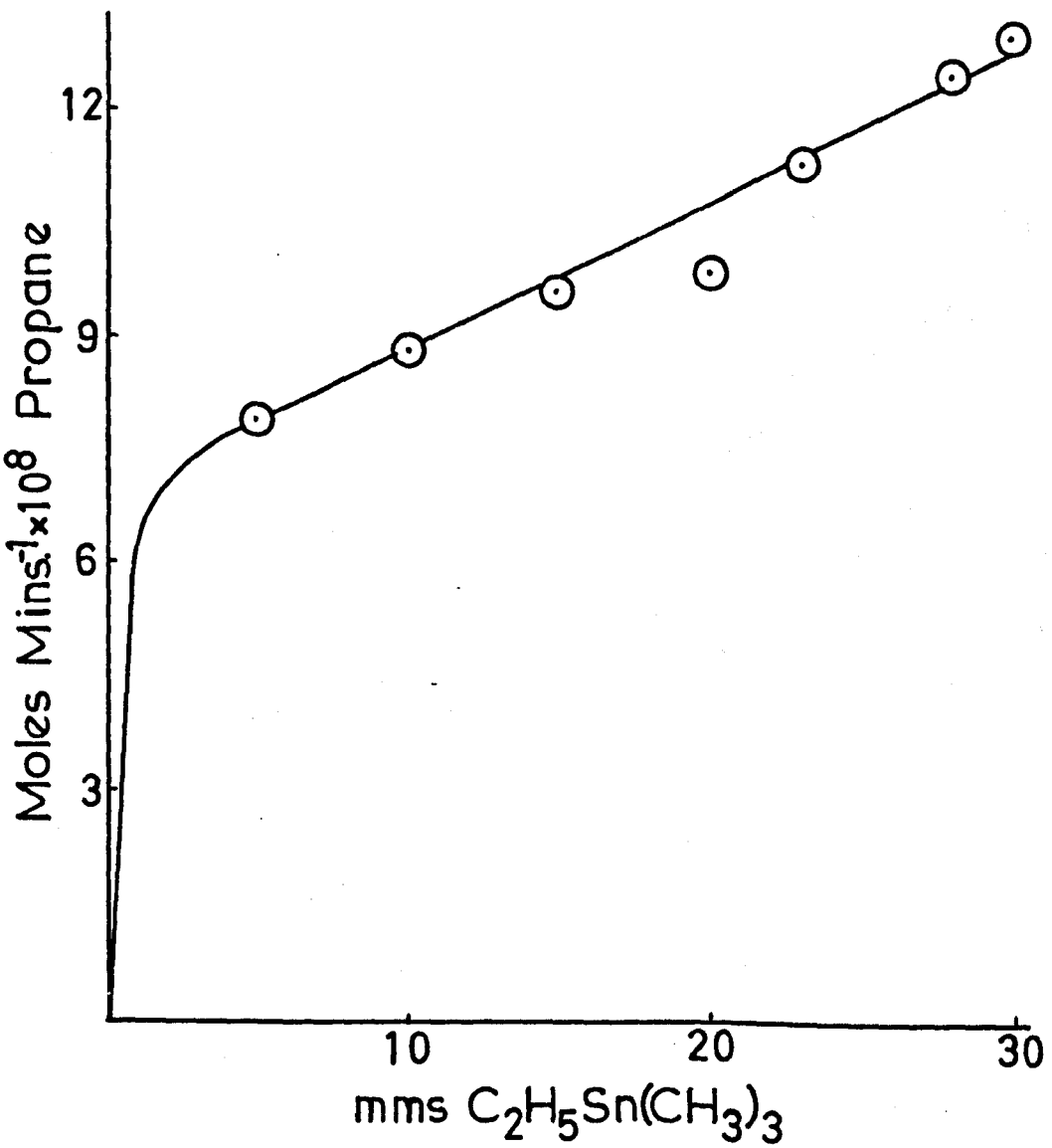

Figure 4.4

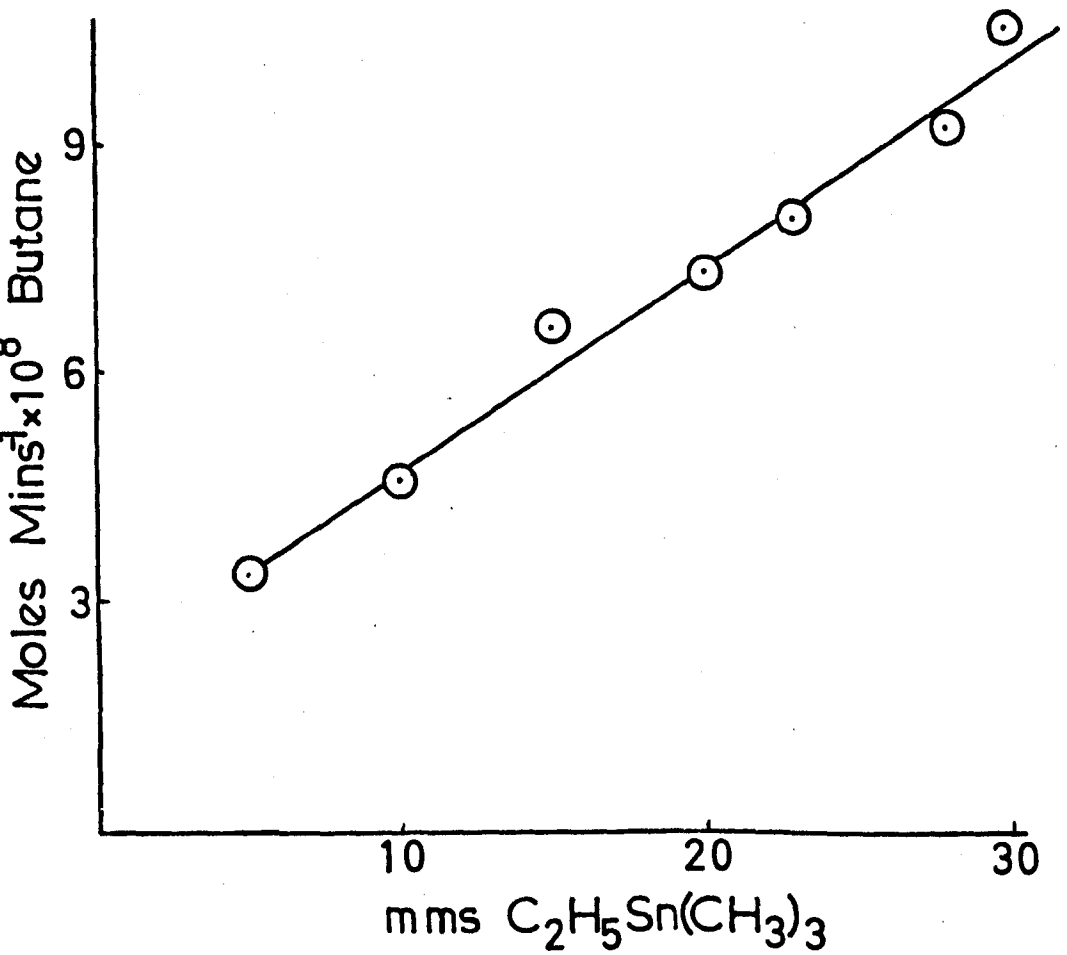

4.2 Effect of Time of Irradiation

On increasing the irradiation time the yields of the products increased linearly up to about 10 minutes and then the rate began to fall off, due again to the formation of a solid on the cell window. The variation of product yields are given in Figures 4.5 - 8.

TABLE 4.3

Effect of irradiation time on the product yields

Irradiation Conditions: $C_2H_5Sn(CH_3)_3$, 10 mm.
Temperature, 25°C
Irradiation time, 0 - 140 minutes

Analytical Conditions: Detector, flame ionisation
Column, Ap-L on Celite
Temperature, 65°C
Nitrogen 20 p.s.i.

Time	MOLES			
	C_2H_6	C_2H_4	C_3H_8	C_4H_{10}
5 mins.	16.7×10^{-8}	12.6×10^{-8}	44.1×10^{-8}	23.1×10^{-8}
10 mins.	32×10^{-8}	24.1×10^{-8}	74.4×10^{-8}	31.2×10^{-8}
30 mins.	80.8×10^{-8}	60.86×10^{-8}	203.1×10^{-8}	97.9×10^{-8}
140 mins.	187.4×10^{-8}	141.1×10^{-8}	384.2×10^{-8}	130.4×10^{-8}
90 mins.	153×10^{-8}	115.2×10^{-8}	337.0×10^{-8}	125.8×10^{-8}
62 mins.	133.7×10^{-8}	100.7×10^{-8}	314.9×10^{-8}	124.0×10^{-8}
40 mins.	102.3×10^{-8}	77.0×10^{-8}	244.1×10^{-8}	106.5×10^{-8}
125 mins.	166.3×10^{-8}	125.2×10^{-8}	366.1×10^{-8}	128.4×10^{-8}
	4.5	4.6	4.7	4.8

Figure 4.5

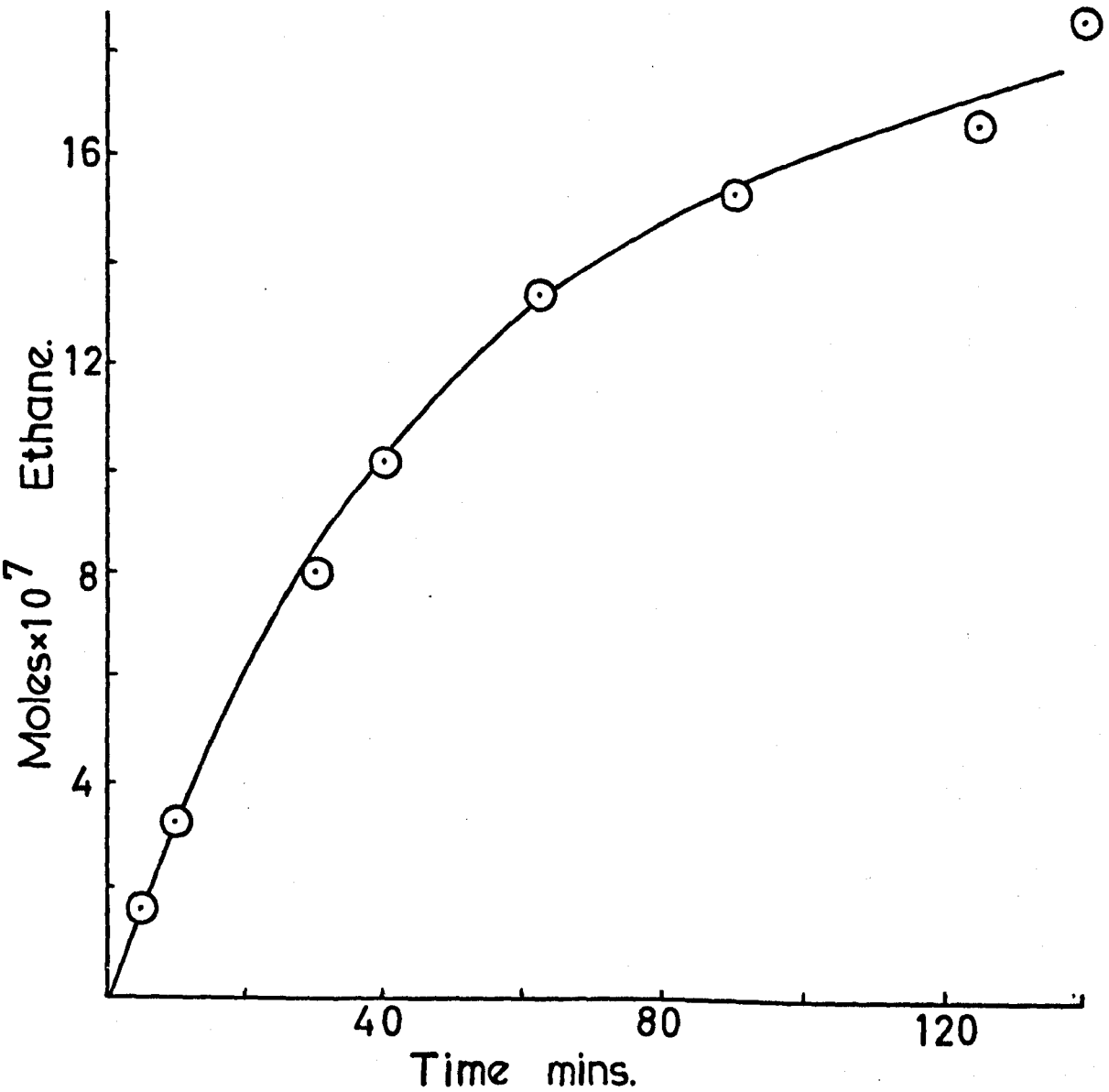

Figure 4.6

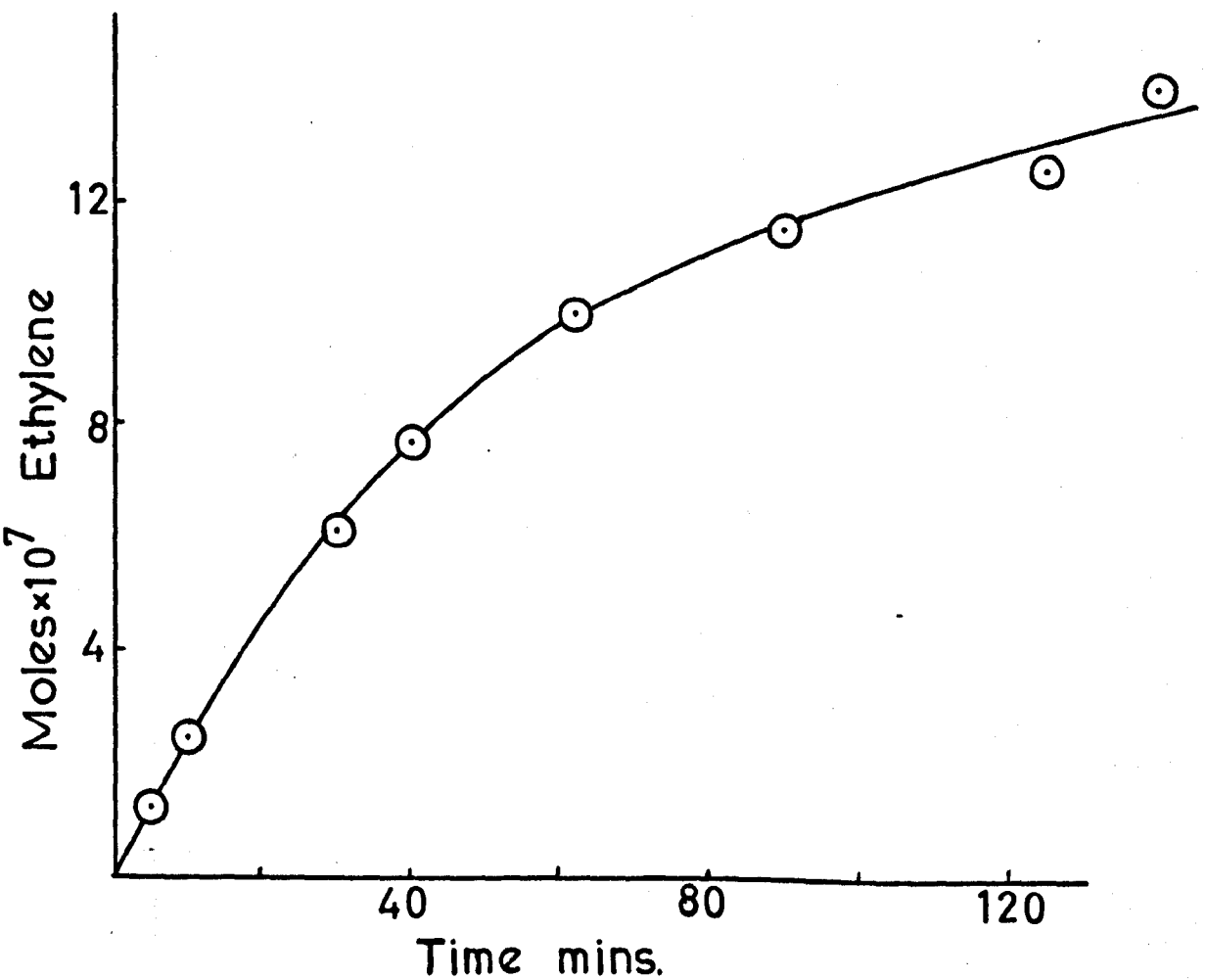

Figure 4.7

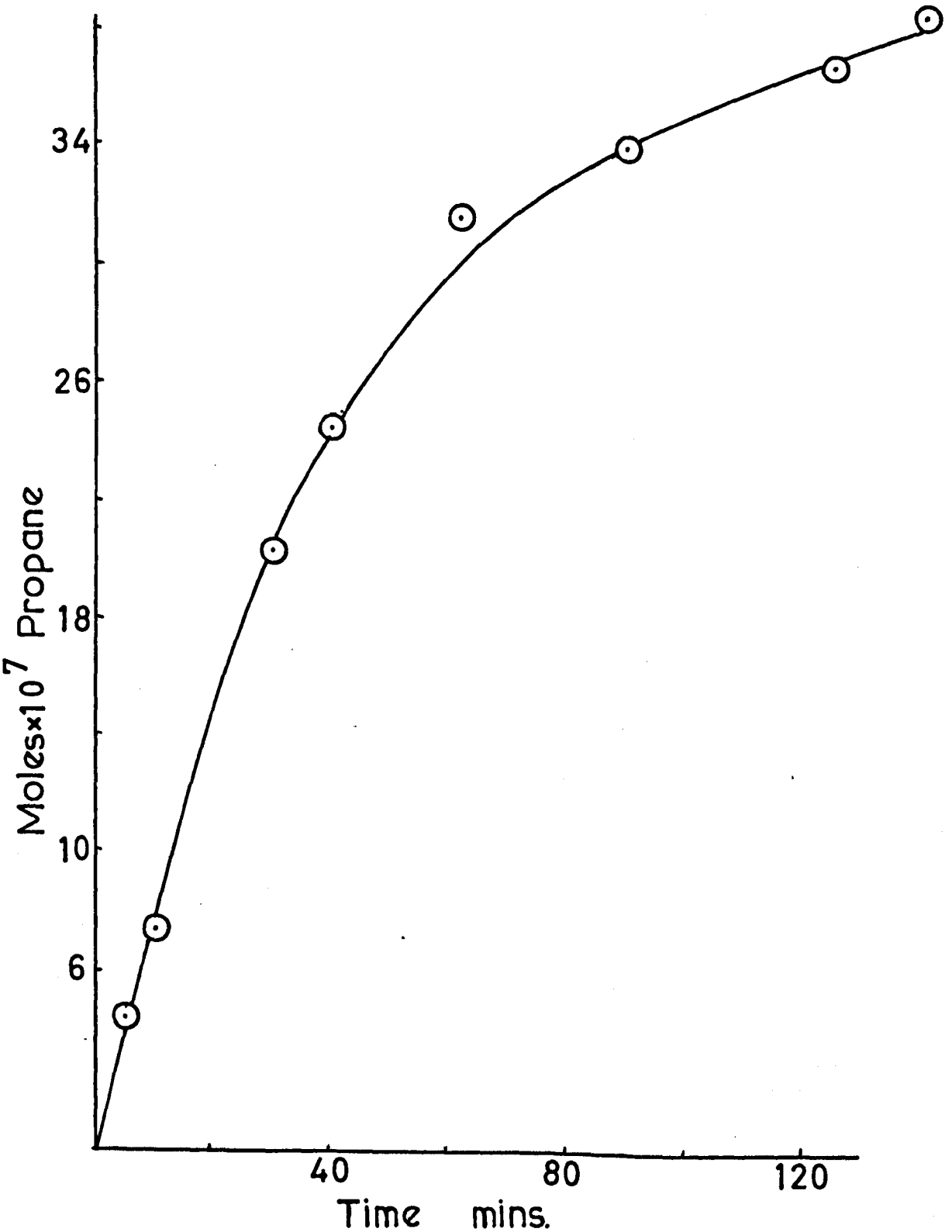

Figure 4.8

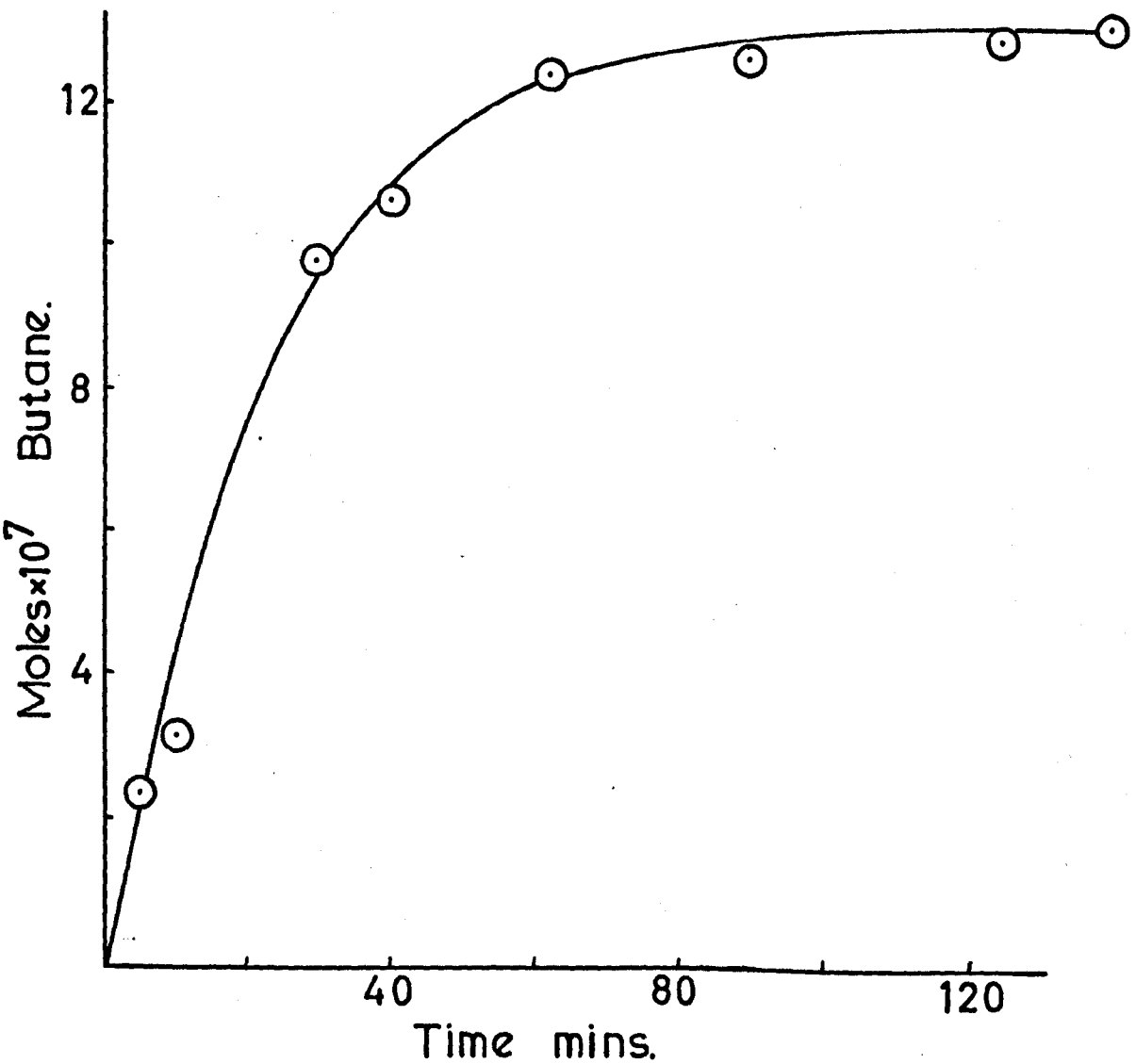

4.3 Effect of Variation of Intensity

Using intensity stops placed between the lamp and the cell, as in Section 3.2, an eight-fold variation of intensity could be obtained (Section 2.5.2). The variation of the rates of formation of the products are shown in Figures 4.9 - 13 and show that all the products are linearly dependent on intensity.

TABLE 4.4

Rates of formation of products as a function of intensity

Irradiation Conditions: $C_2H_5Sn(CH_3)_3$, 10 mm.
Temperature, 25°C
Irradiation time, 10 minutes

Analytical Conditions: Detector, flame ionisation
Column, Ap-L on Celite and Poropak Q
Temperature, 65°C or 50°C
Nitrogen, 20 p.s.i.

	4.12	4.9	4.10	4.11	4.13
Intensity	CH_4	C_2H_6	C_2H_4	C_3H_8	C_4H_{10}
100%	3.52×10^{-9}	3.2×10^{-8}	2.41×10^{-8}	7.44×10^{-8}	3.12×10^{-8}
52.4%	1.85×10^{-9}	1.63×10^{-8}	1.19×10^{-8}	3.31×10^{-8}	1.63×10^{-8}
16.4%	0.51×10^{-9}	0.697×10^{-8}	0.51×10^{-8}	1.32×10^{-8}	0.51×10^{-8}
35.8%	1.27×10^{-9}	1.12×10^{-8}	0.82×10^{-8}	2.70×10^{-8}	1.12×10^{-8}
12.6%	0.41×10^{-9}	0.40×10^{-8}	0.29×10^{-8}	0.84×10^{-8}	0.39×10^{-8}
42.6%	1.52×10^{-9}	1.35×10^{-8}	0.98×10^{-8}	3.24×10^{-8}	1.33×10^{-8}

Figures in moles/minute

Figure 49

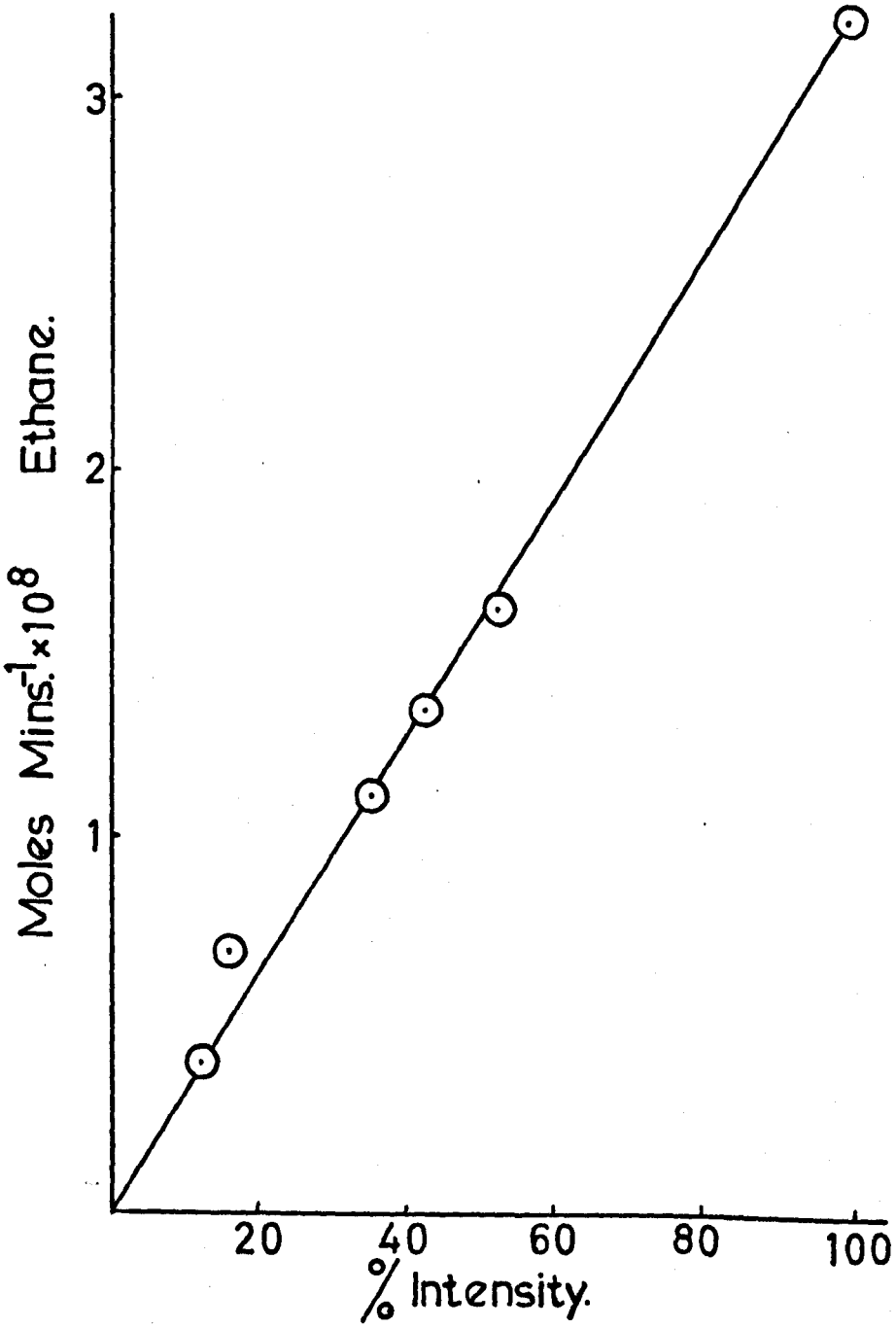

Figure 4.10

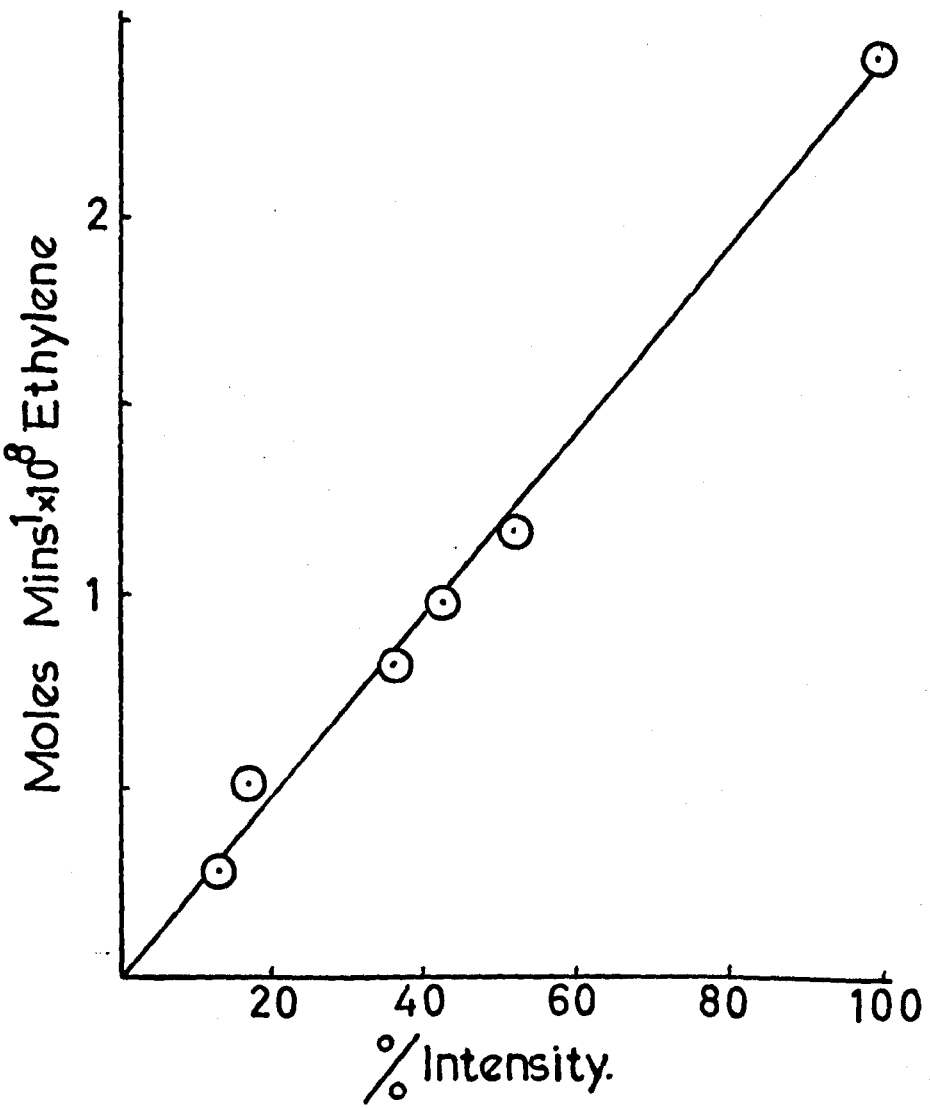

Figure 4.11

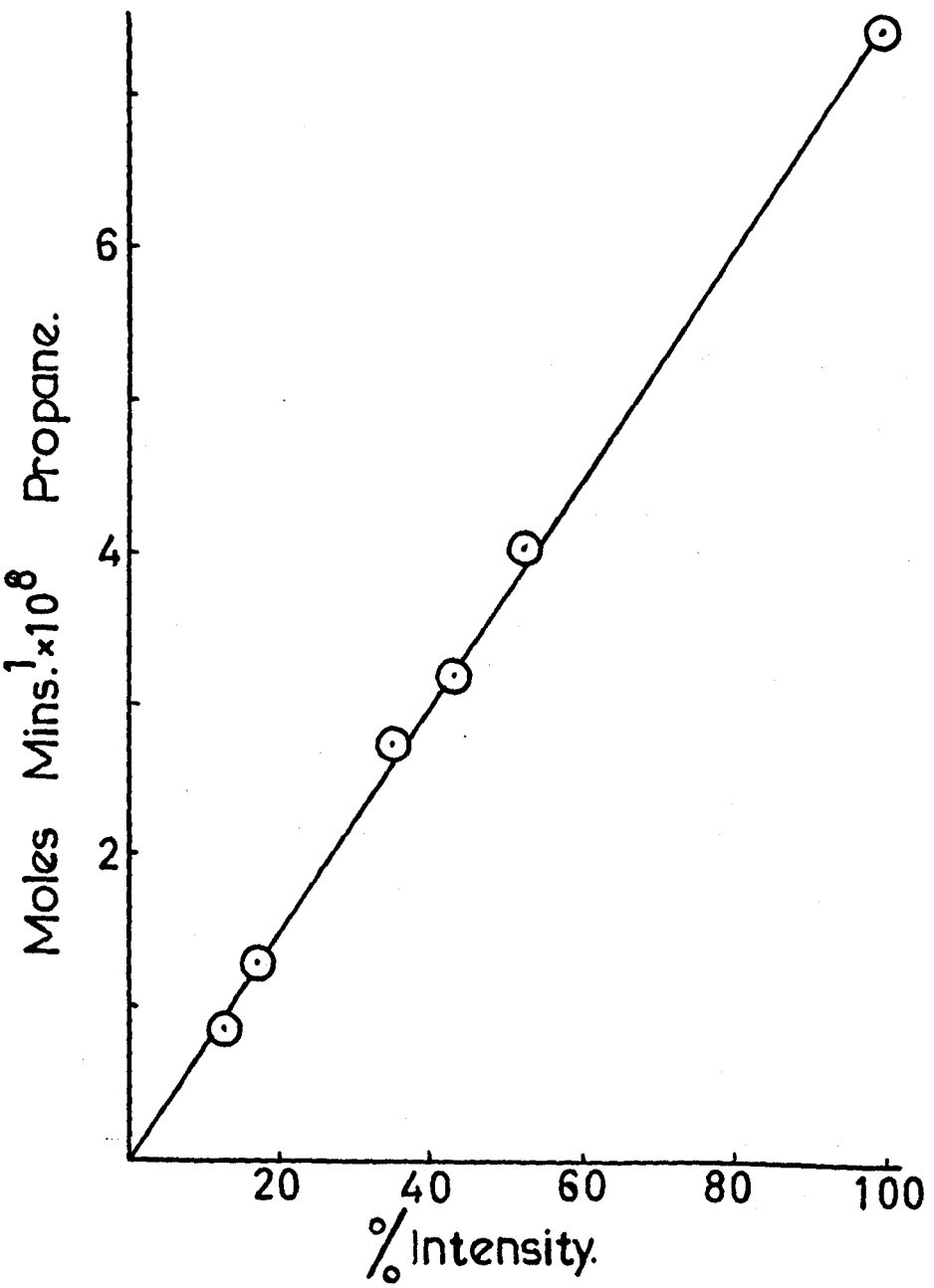

Figure 4.12

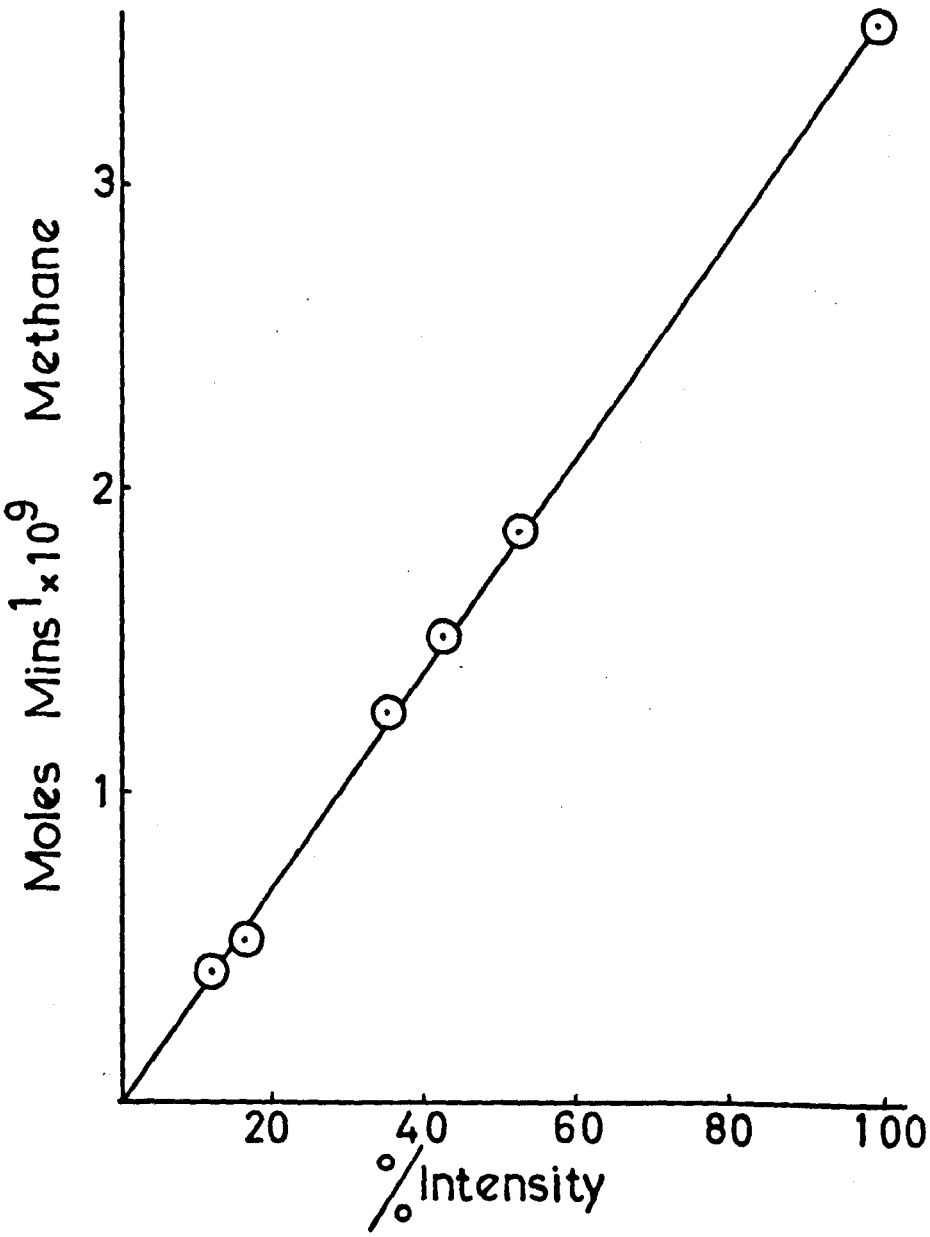

Figure 4.13

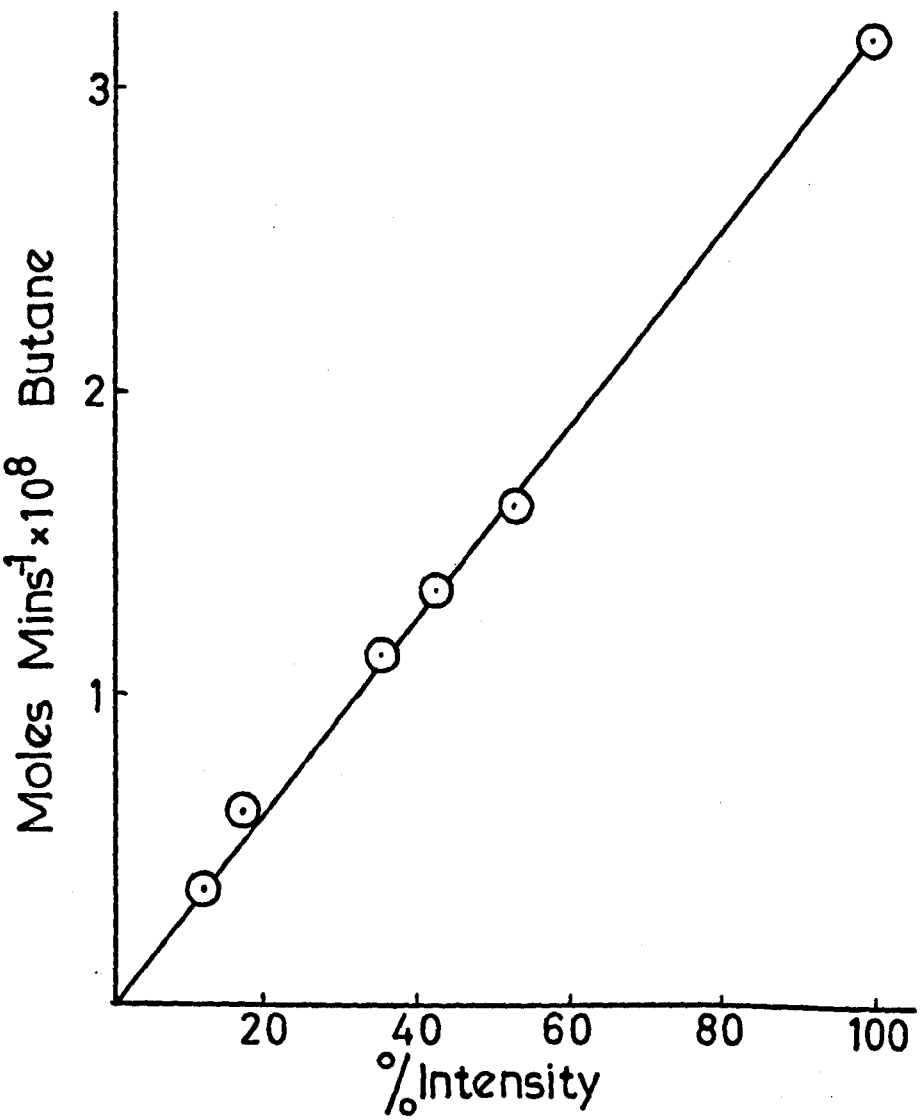

4.4 Effect of Added Inert Gases

On adding inert gases, nitrogen and argon, the yields of all the products were decreased. The effect of both gases appeared to be about the same and the results are illustrated in Figures 4.14 - 22.

TABLE 4.5

Effect on rates of formation of added nitrogen

Irradiation Conditions: $C_2H_5Sn(CH_3)_3$, 10 mm.
Temperature, 25°C
Irradiation time, 10 minutes

Analytical Conditions: Detector, flame ionisation
Column, Ap-L on Celite and Poropak Q
Temperature, 65°C or 50°C
Nitrogen, 20 p.s.i.

	4.18	4.14	4.15	4.17	4.16
Nitrogen	CH_4	C_2H_6	C_2H_4	C_3H_8	C_4H_{10}
0	3.52×10^{-9}	3.20×10^{-8}	2.41×10^{-8}	7.44×10^{-8}	3.12×10^{-8}
7½ mm.	-	8.72×10^{-9}	6.57×10^{-9}	2.00×10^{-8}	8.45×10^{-9}
44 mm.	-	5.11×10^{-9}	3.85×10^{-9}	1.13×10^{-8}	3.64×10^{-9}
490 mm.	-	3.9×10^{-9}	2.94×10^{-9}	7.09×10^{-9}	2.30×10^{-9}
90 mm.	6.77×10^{-10}	5.73×10^{-9}	3.93×10^{-9}	7.32×10^{-9}	-
290 mm.	4.87×10^{-10}	4.91×10^{-9}	3.28×10^{-9}	6.20×10^{-9}	-
22 mm.	9.47×10^{-10}	7.80×10^{-9}	5.20×10^{-9}	10.40×10^{-9}	-
650 mm.	4.33×10^{-10}	3.87×10^{-9}	2.82×10^{-9}	6.20×10^{-9}	-

Figures in moles/minute

TABLE 4.6

Effect on rates of formation of added argon

	4.20	4.19	4.21	4.22
Argon	C_2H_6	C_2H_4	C_3H_8	C_4H_{10}
0	3.20×10^{-8}	2.41×10^{-8}	7.44×10^{-8}	3.12×10^{-8}
7½ mm.	9.2×10^{-9}	6.9×10^{-9}	1.78×10^{-8}	5.4×10^{-9}
79 mm.	4.6×10^{-9}	3.4×10^{-9}	8.2×10^{-9}	2.0×10^{-9}
660 mm.	2.5×10^{-9}	1.9×10^{-9}	4.3×10^{-9}	1.1×10^{-9}
350 mm.	4.2×10^{-9}	3.2×10^{-9}	6.2×10^{-9}	1.6×10^{-9}
190 mm.	4.5×10^{-9}	3.4×10^{-9}	7.0×10^{-9}	1.8×10^{-9}

Figures in moles/minute

Figure 4.14

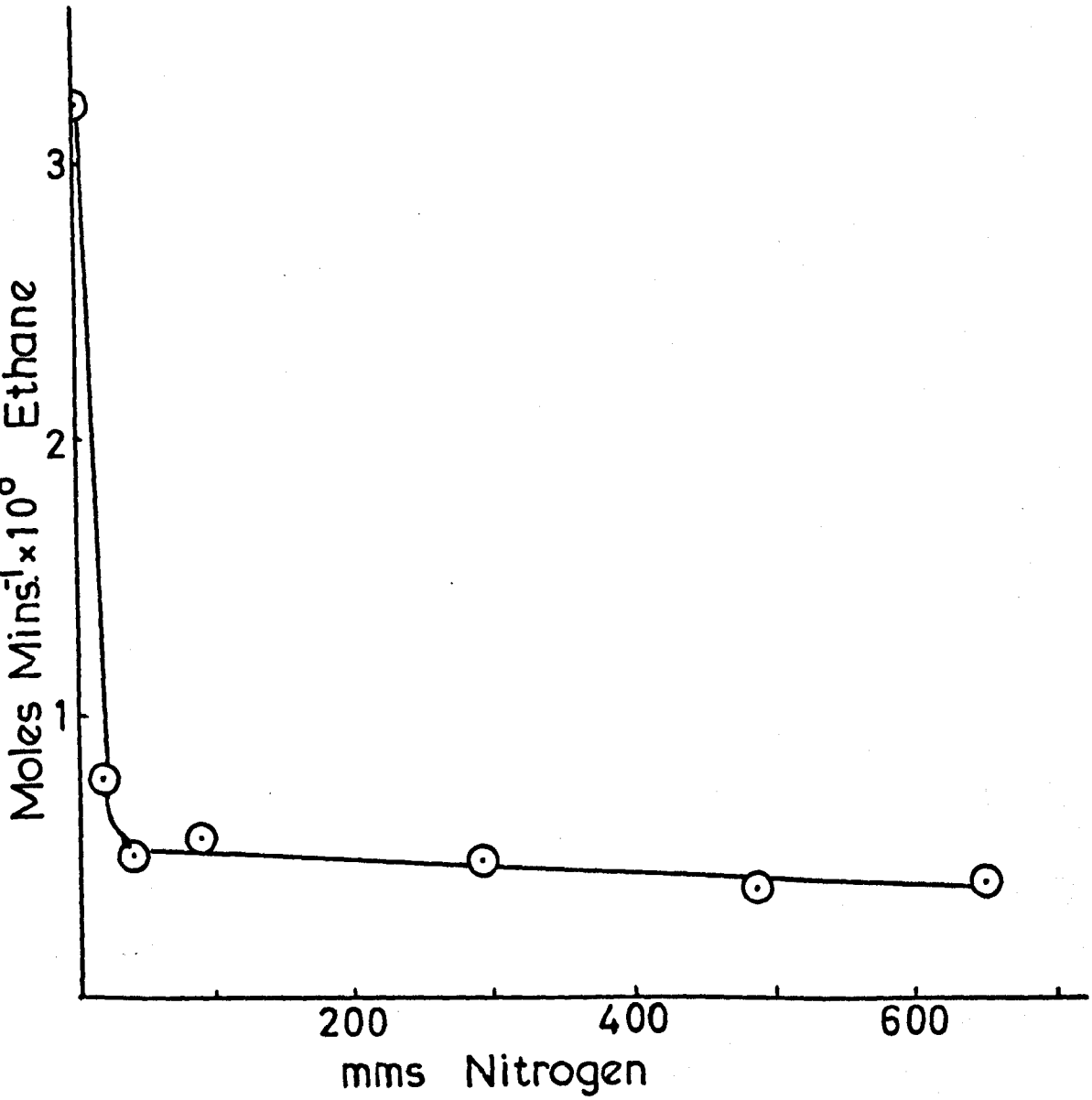

Figure 4.15

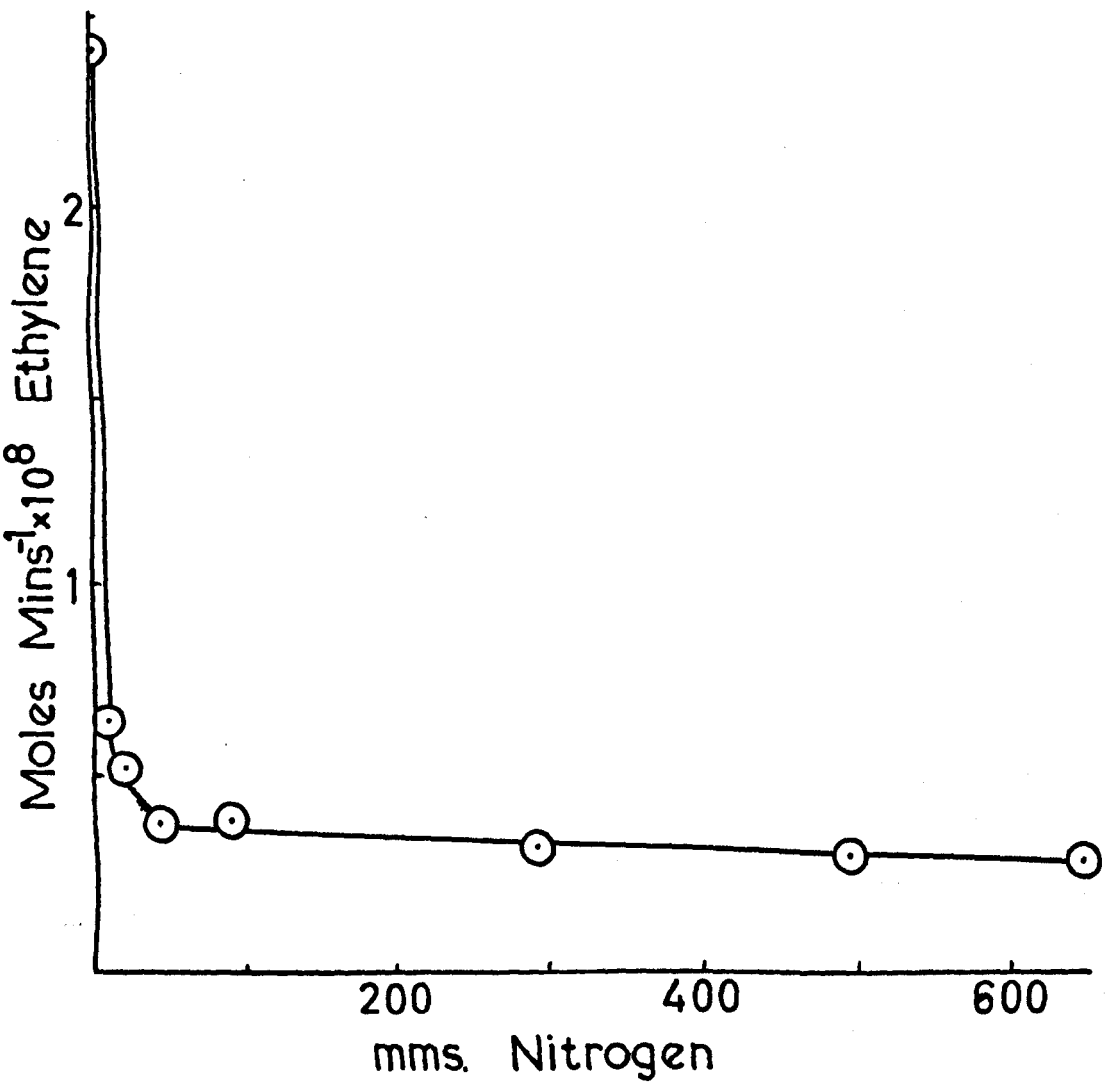

Figure 4.16

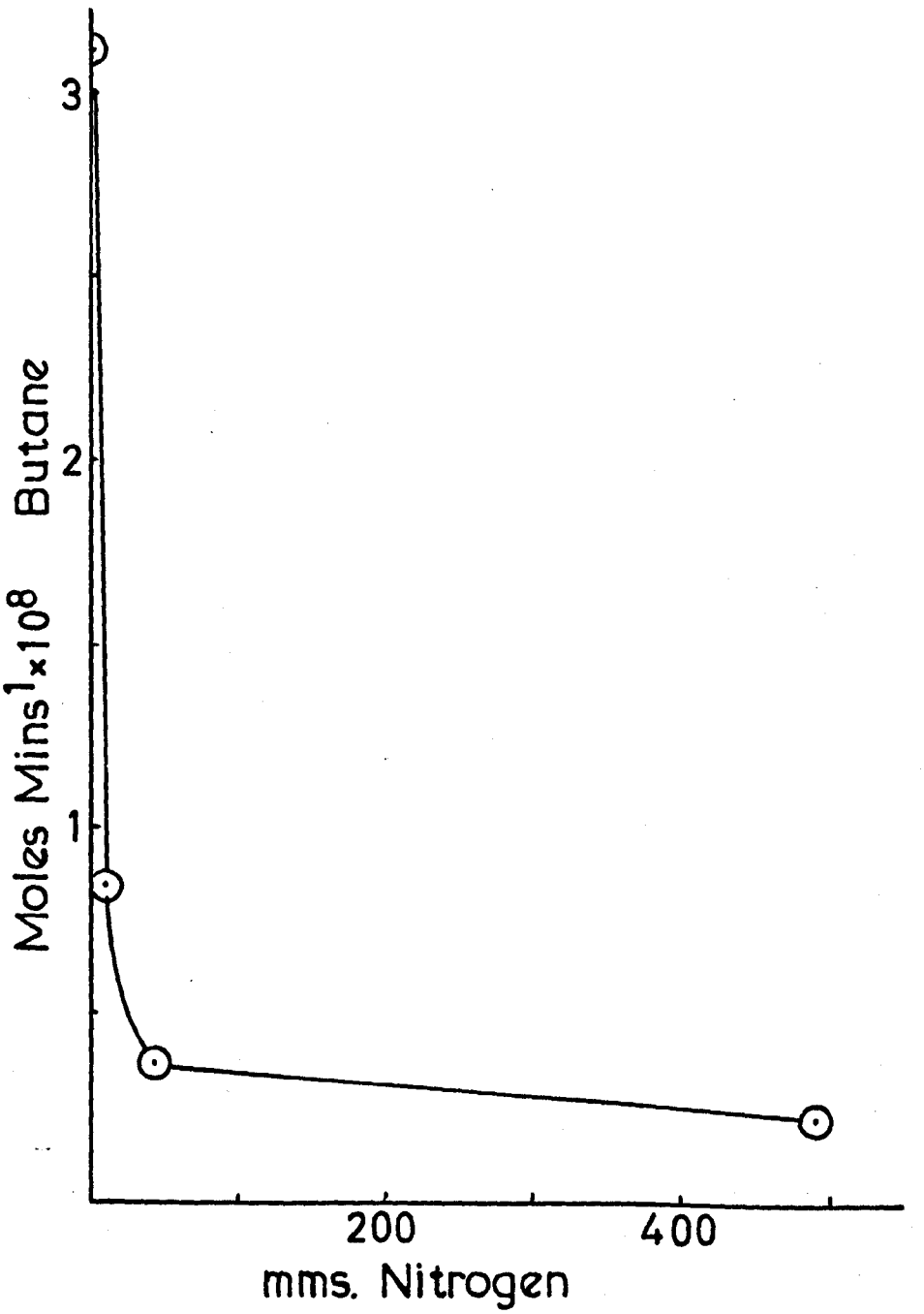

Figure 4.17

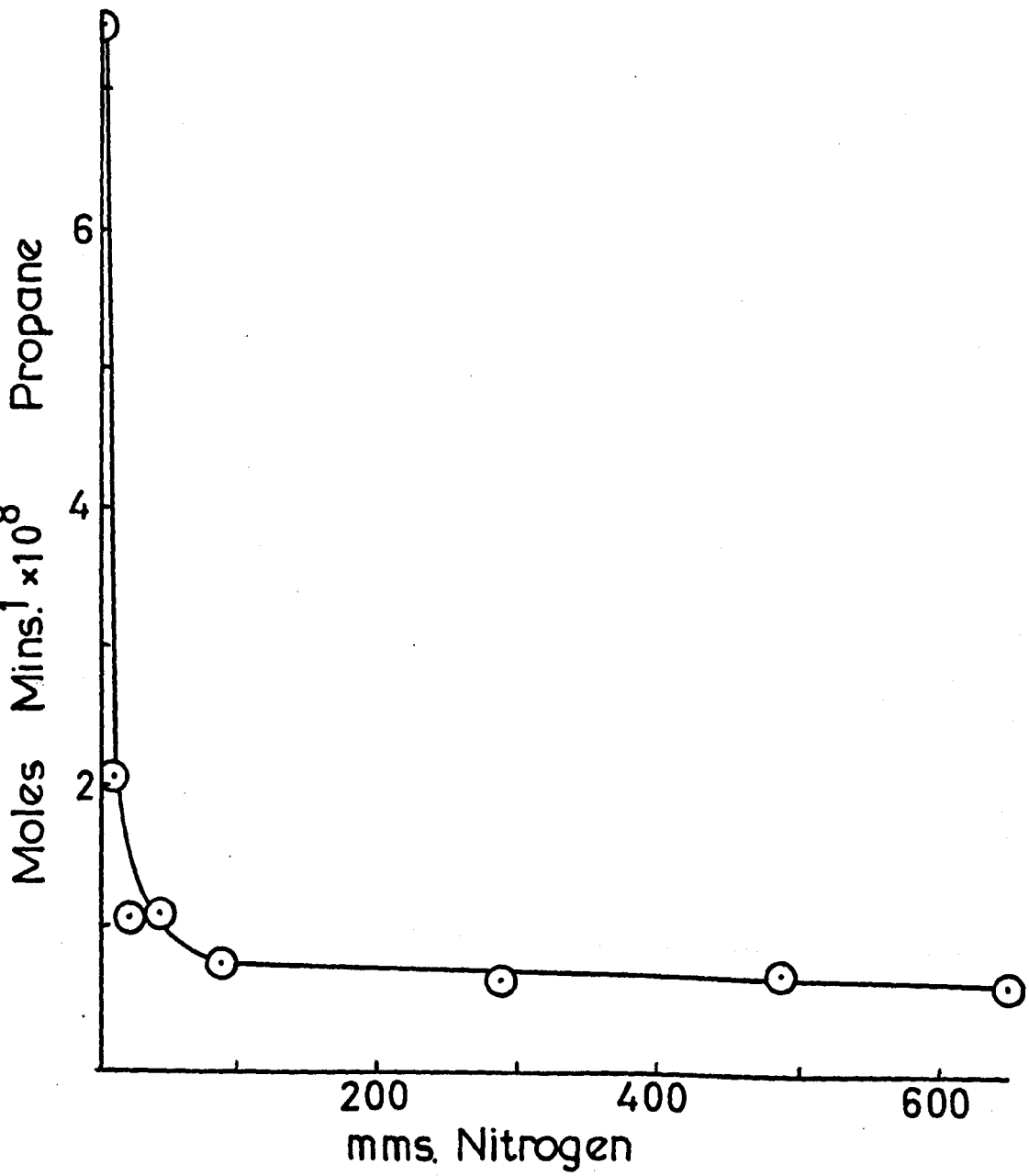

Figure 4.18

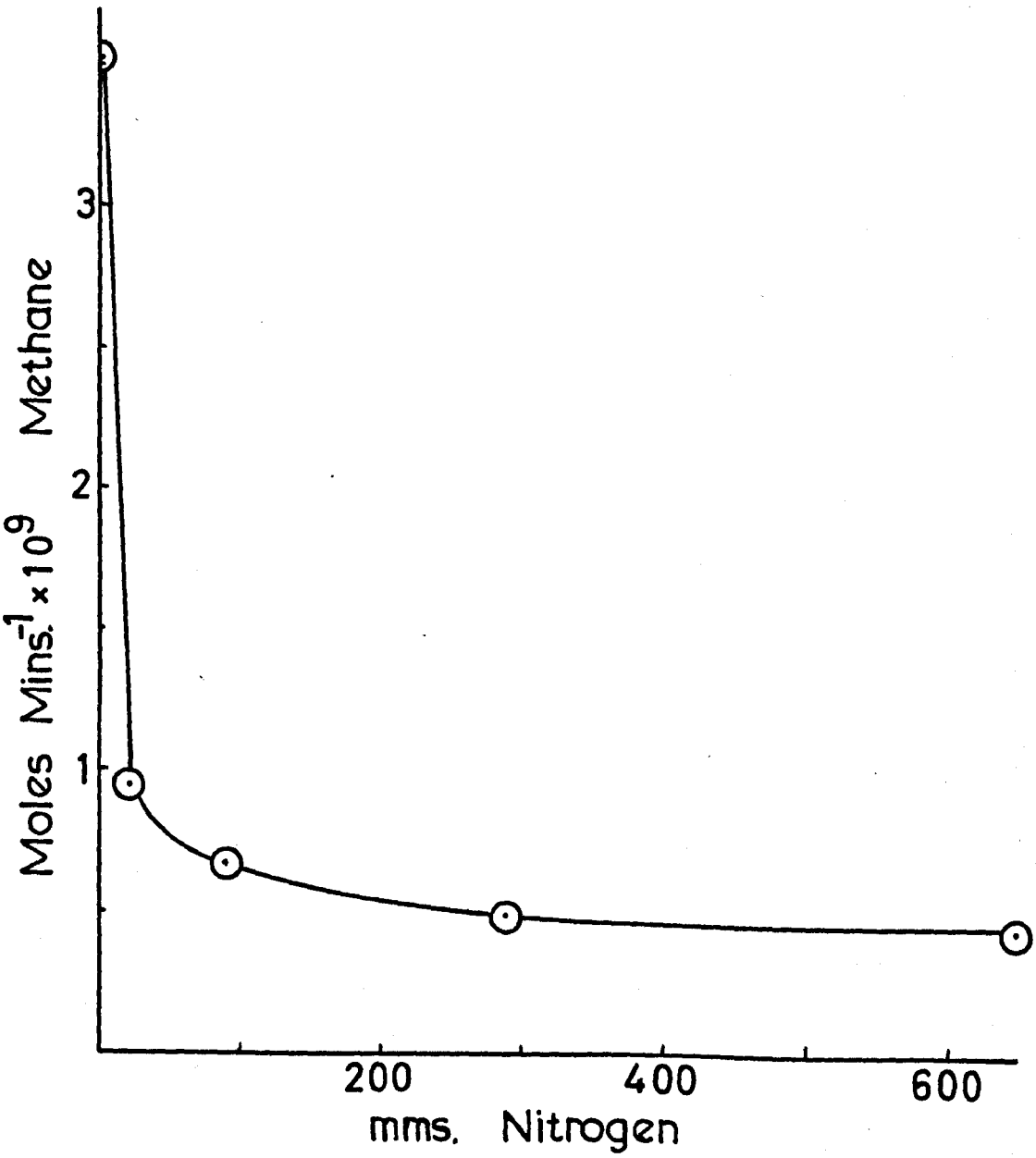

Figure 4.19

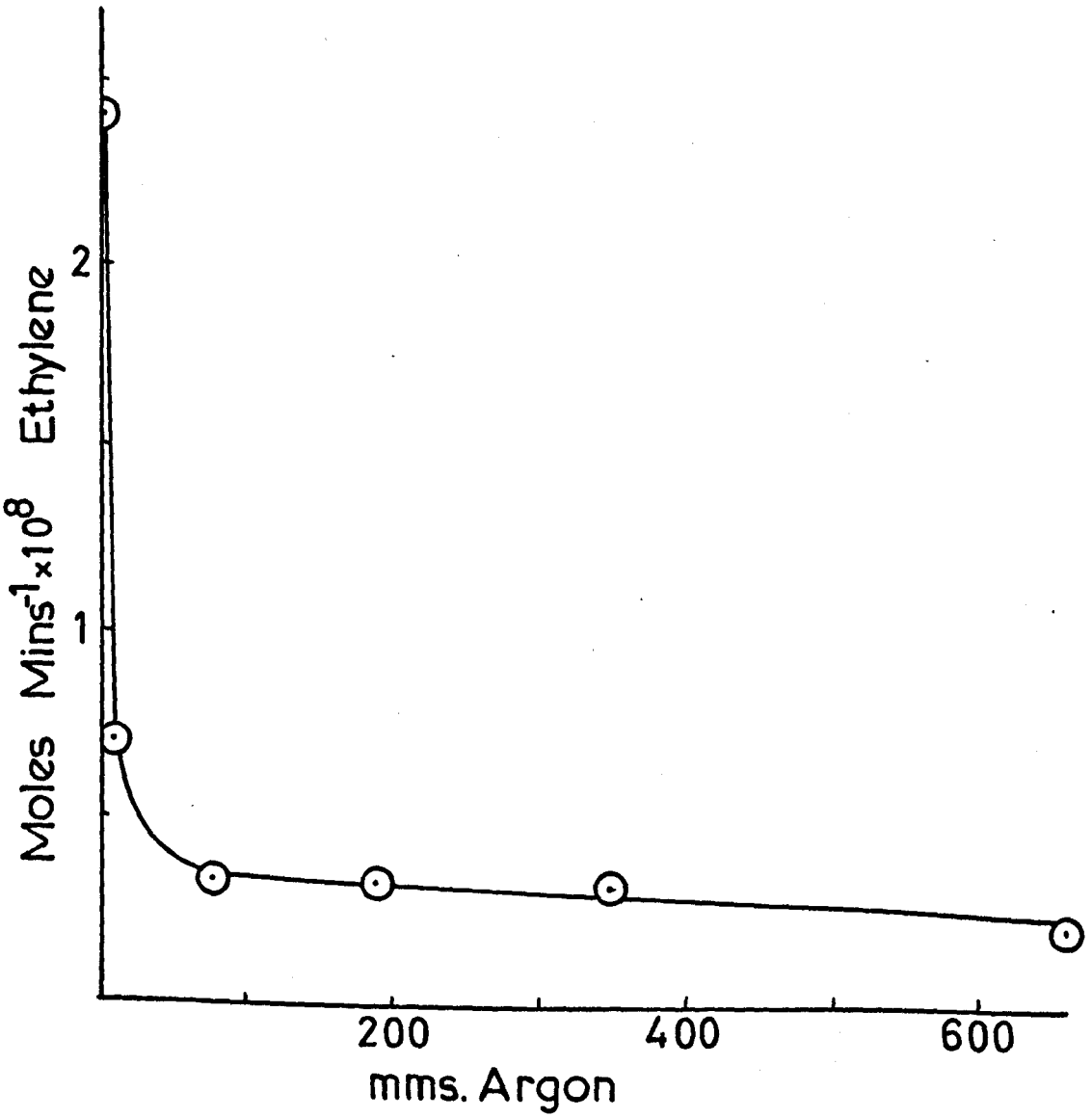

Figure 4.20

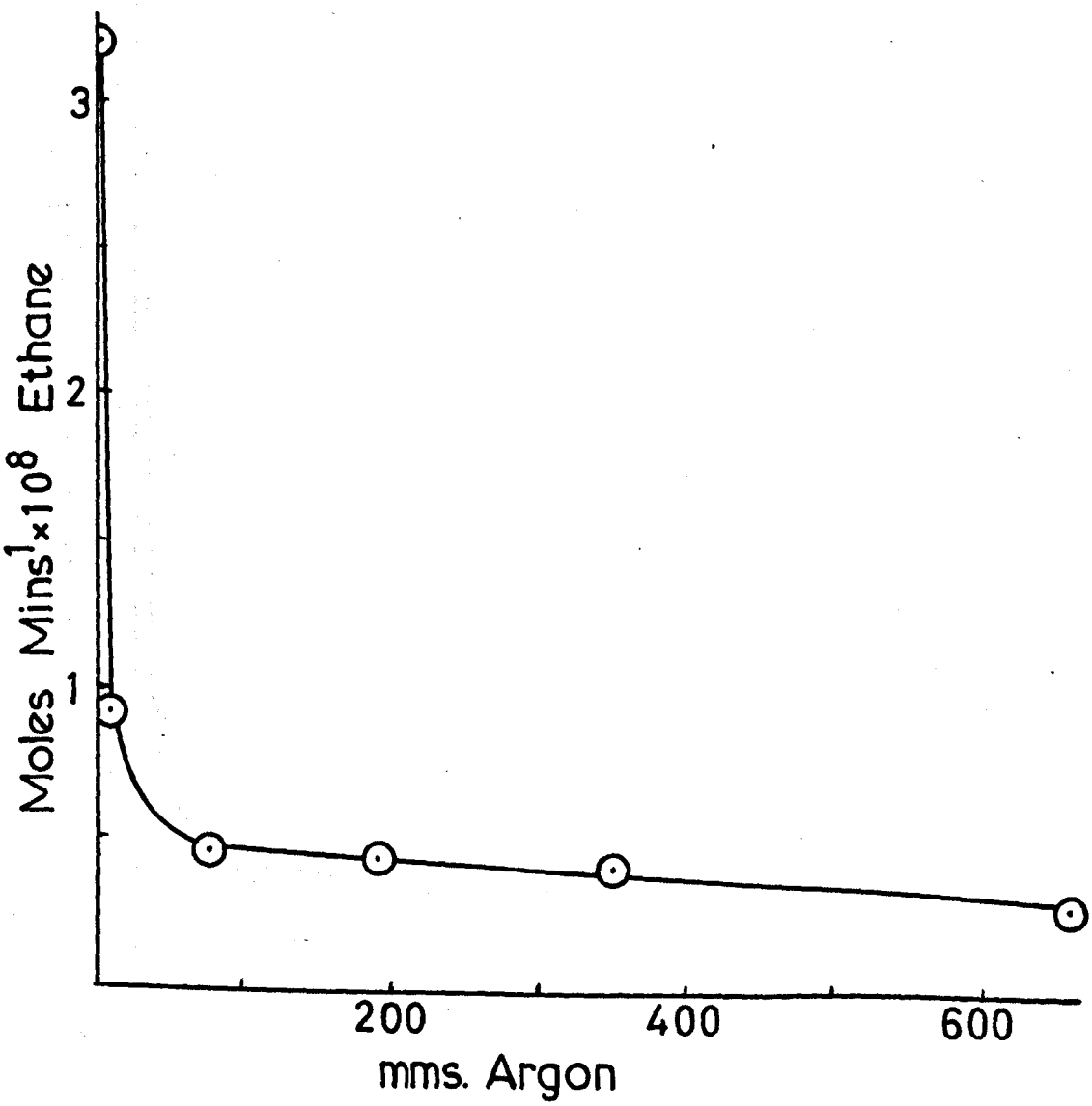

Figure 4.21

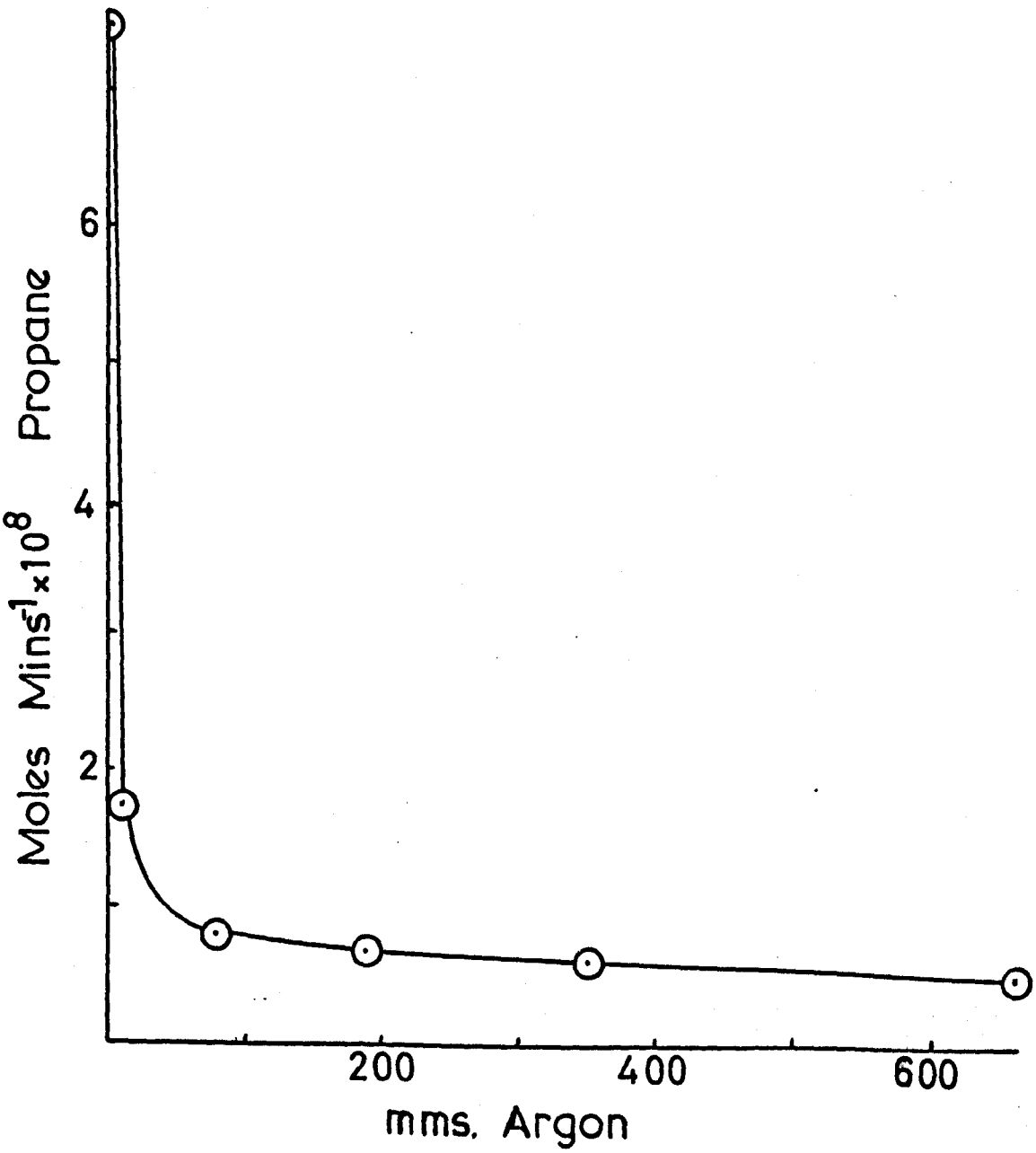

Figure 4.22

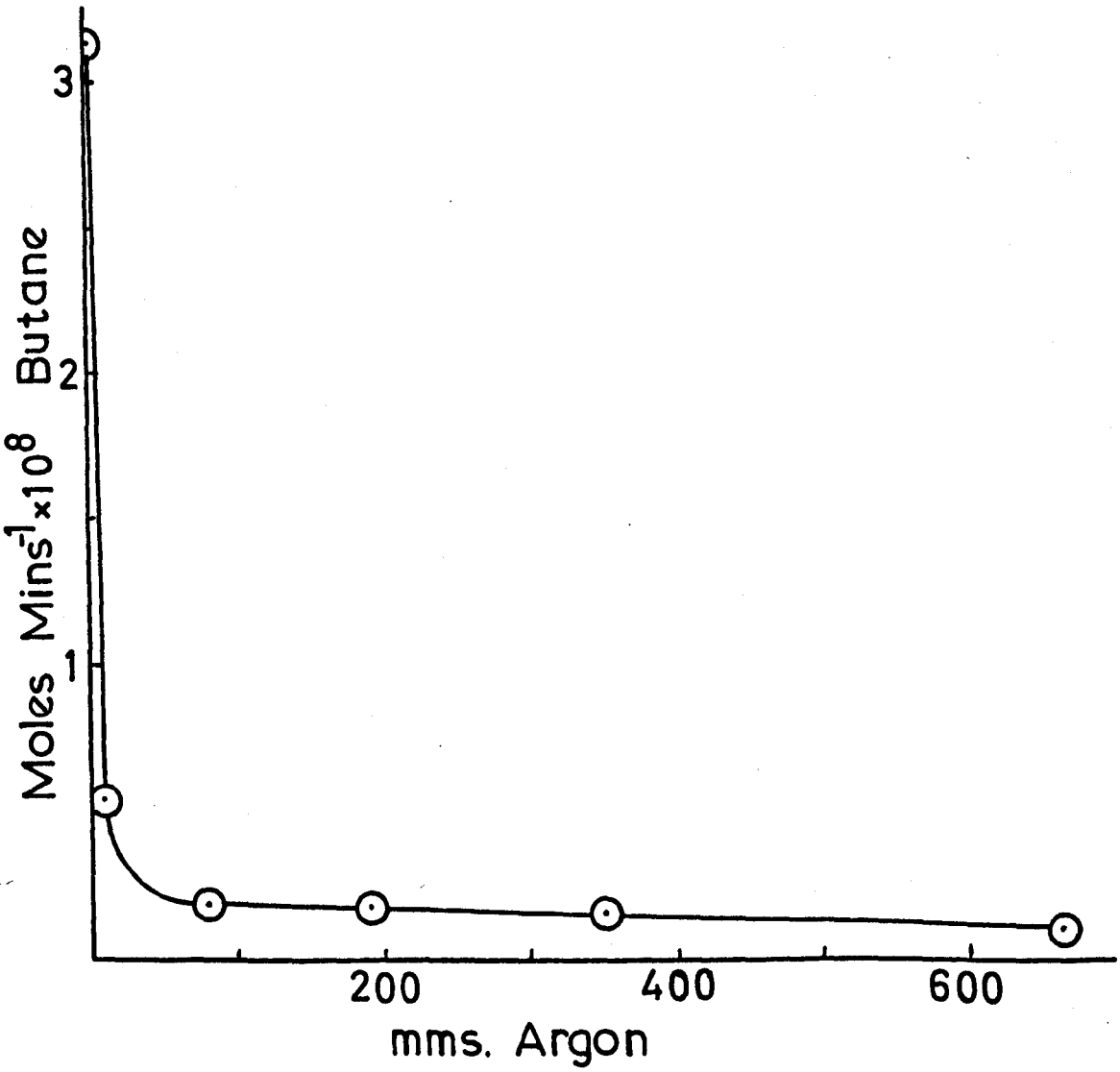

4.5 Effect of Added Radical Scavengers

On addition of oxygen the yields of all the products were decreased and those of propane and butane completely eliminated. However, there still remained a certain amount of ethane although small compared to the original rate, it still justifies the conclusion that a portion of the ethane is molecularly formed. The ethylene rate is effected more so than in the cases of nitrogen and argon and so can be said to be formed molecularly and radically. Methane is similarly effected by oxygen as by nitrogen and the same conclusion can be adopted. Nitric oxide affects the products to the same extent as oxygen up to a pressure of approximately 50 mm and then appears to act as a chain initiator in that the yields of ethylene and methane increase, ethylene to the extent of fifty times the rate at 40 mm in the presence of 150 mm nitric oxide.

TABLE 4.7

Effect on rates of formation of added oxygen.

Irradiation Conditions: $C_2H_5Sn(CH_3)_3$, 10 mm
Temperature, 25°C
Irradiation time, 10 minutes

Analytical Conditions: Detector, flame ionisation
Column, Ap-L on Celite and Poropak Q
Temperature, 65°C and 50°C
Nitrogen, 20 p.s.i.

	4.25	4.23	4.24
Oxygen	CH_4	C_2H_4	C_2H_6
0 mm.	3.52×10^{-9}	2.41×10^{-8}	3.2×10^{-8}
7½mm.	1.09×10^{-9}	0.99×10^{-8}	0.08×10^{-8}
51 mm.	0.63×10^{-9}	0.43×10^{-8}	0.051×10^{-8}
280 mm.	0.58×10^{-9}	0.28×10^{-8}	0.040×10^{-8}
650 mm.	0.27×10^{-9}	0.18×10^{-8}	0.043×10^{-8}
470 mm.	0.43×10^{-9}	0.24×10^{-8}	0.037×10^{-8}

Figures in moles/minute

TABLE 4.8

Effect of rates of formation of added nitric oxide

	4.26	4.27	4.28
NO	CH_4	C_2H_4	C_2H_6
0	3.52×10^{-9}	2.41×10^{-8}	3.20×10^{-8}
$7\frac{1}{2}$	0.87×10^{-9}	0.53×10^{-8}	0.051×10^{-8}
42	0.46×10^{-9}	0.40×10^{-8}	0.04×10^{-8}
150	0.7×10^{-9}	21.8×10^{-8}	0.04×10^{-8}
110	0.54×10^{-9}	14.2×10^{-8}	0.03×10^{-8}

Figures in moles/minute

Figure 4.23

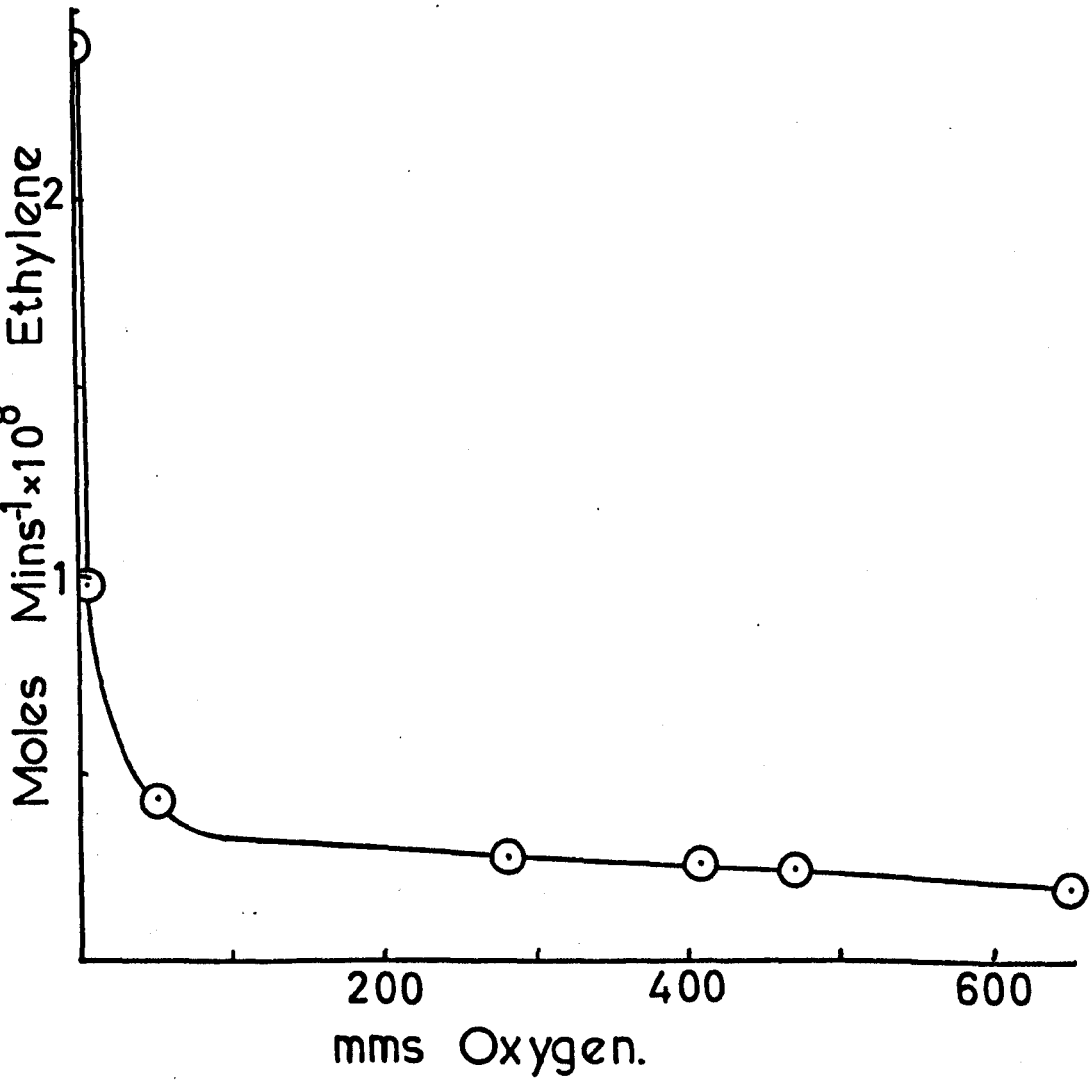

Figure 4.24

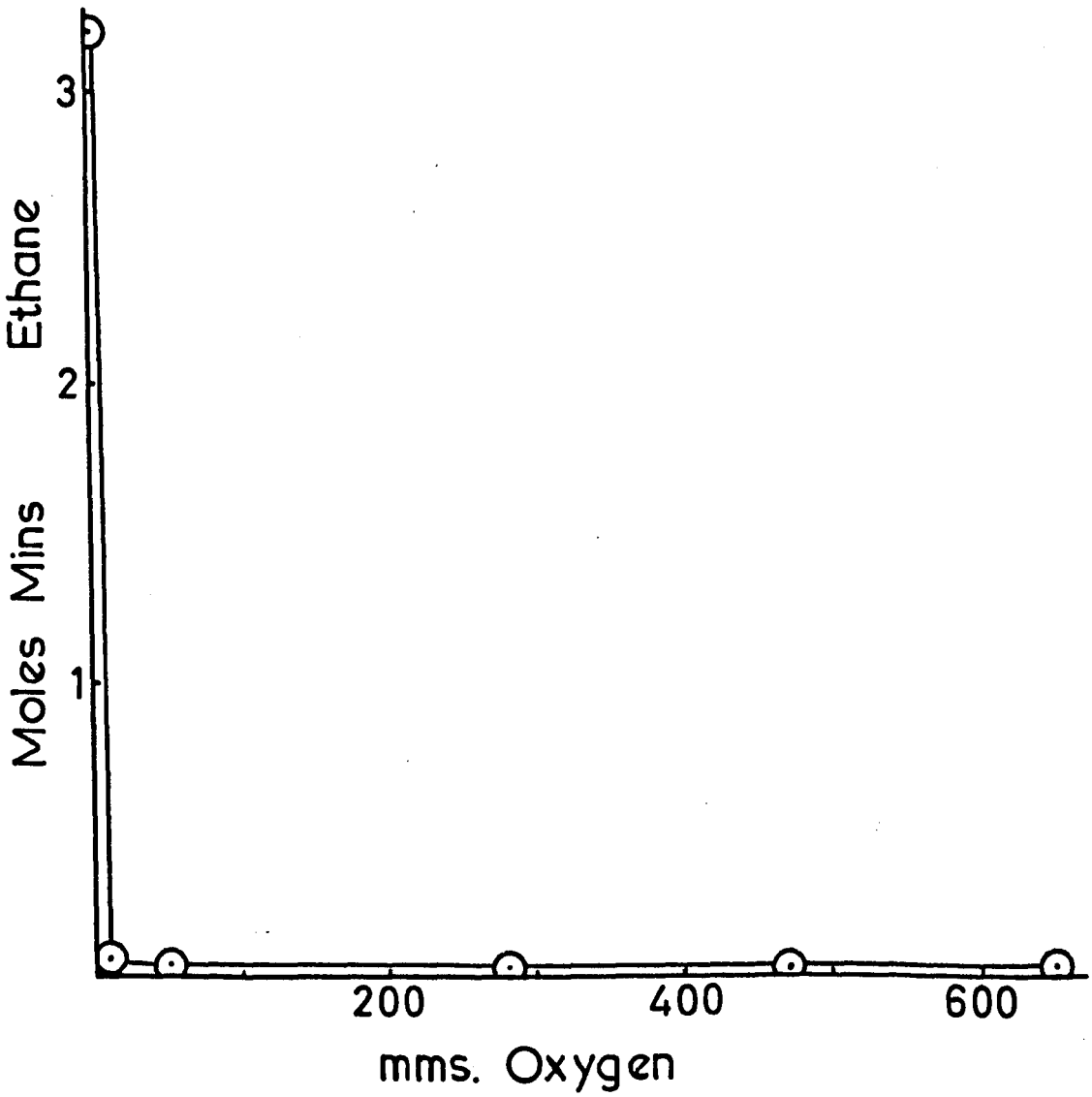

Figure 4.26

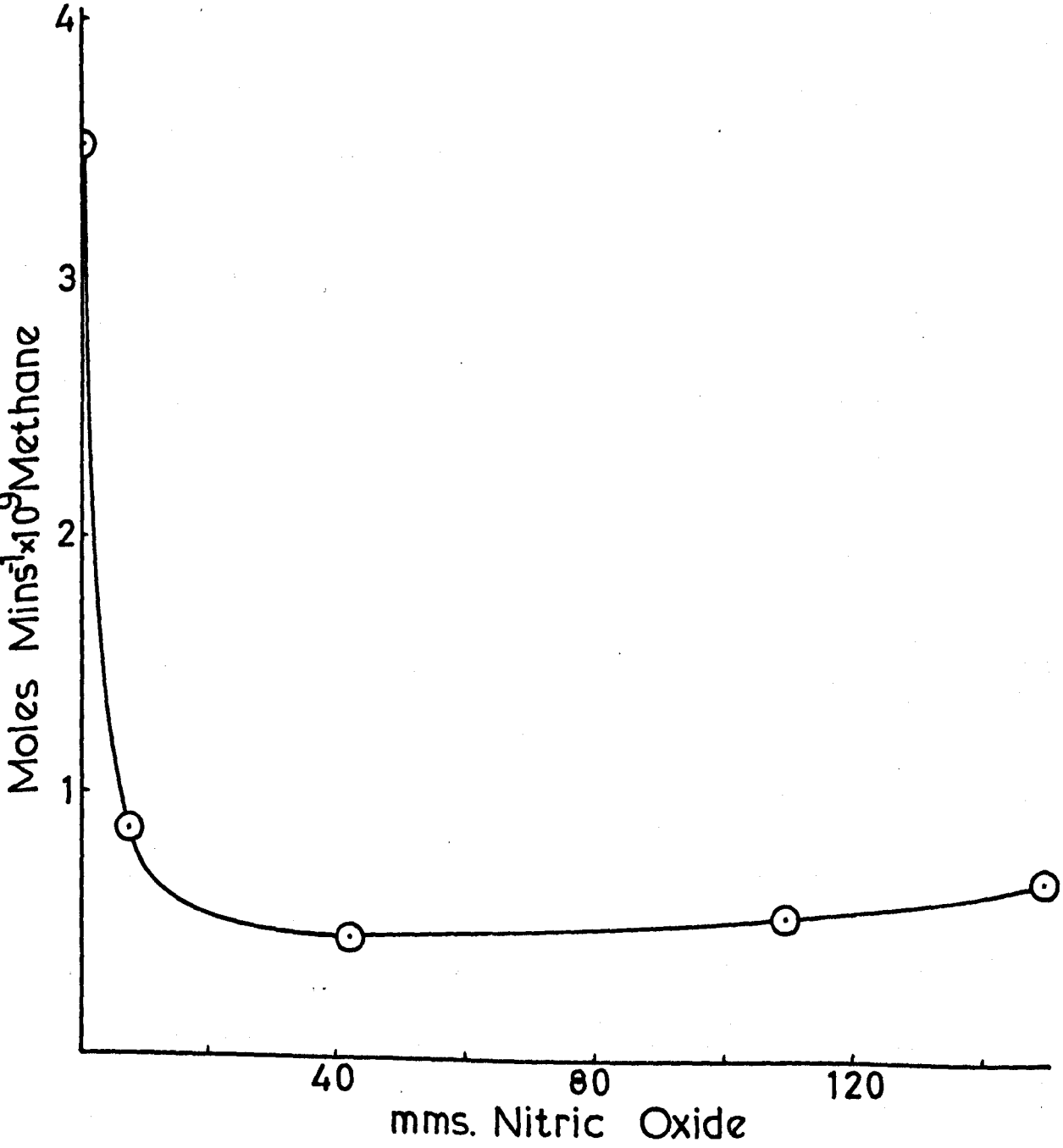

Figure 4.27

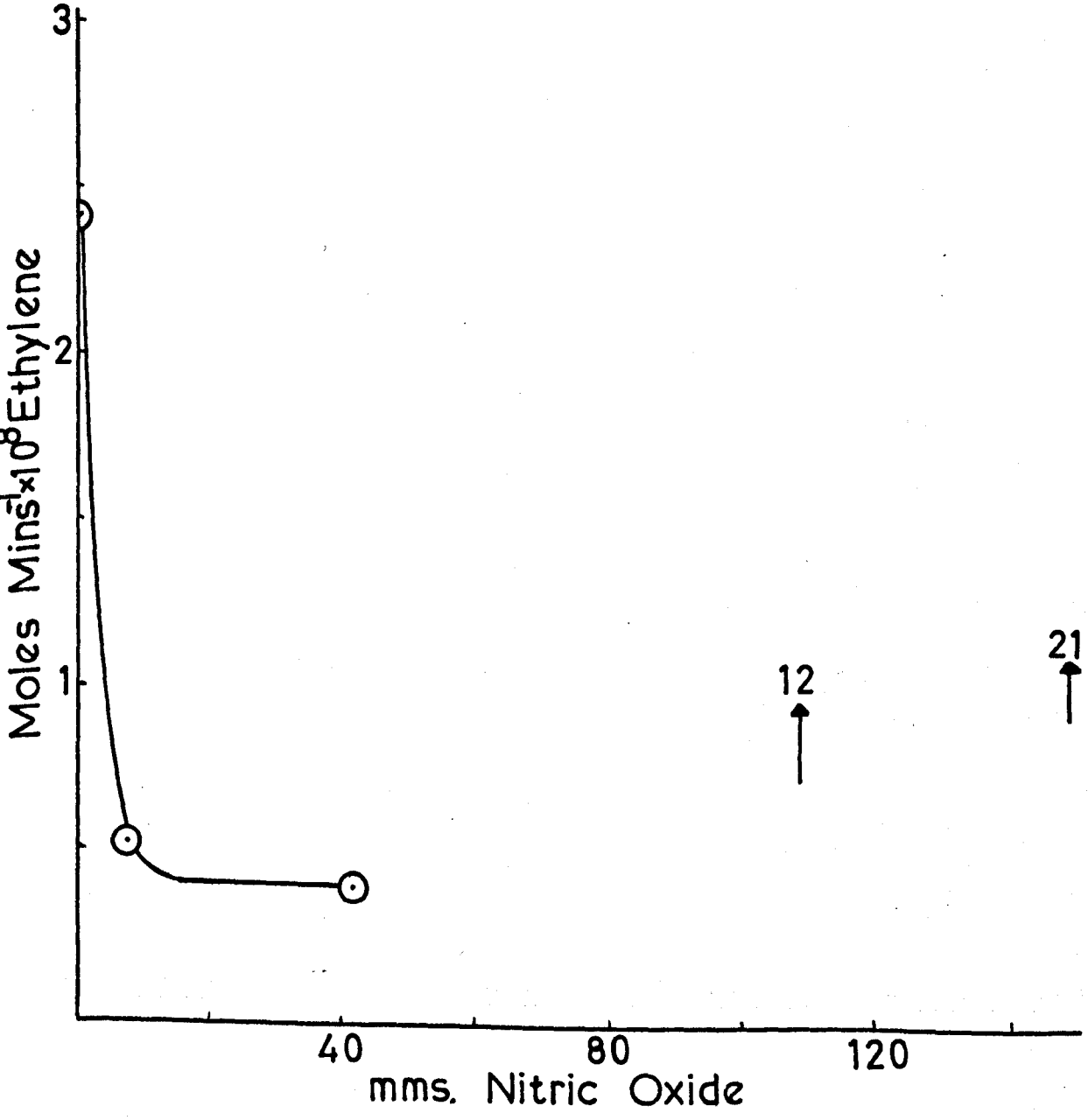
3
2
1
Moles Mins^{-1}x10^{8}Ethylene
12
21
40
80
120
mms. Nitric Oxide

Figure 4.28

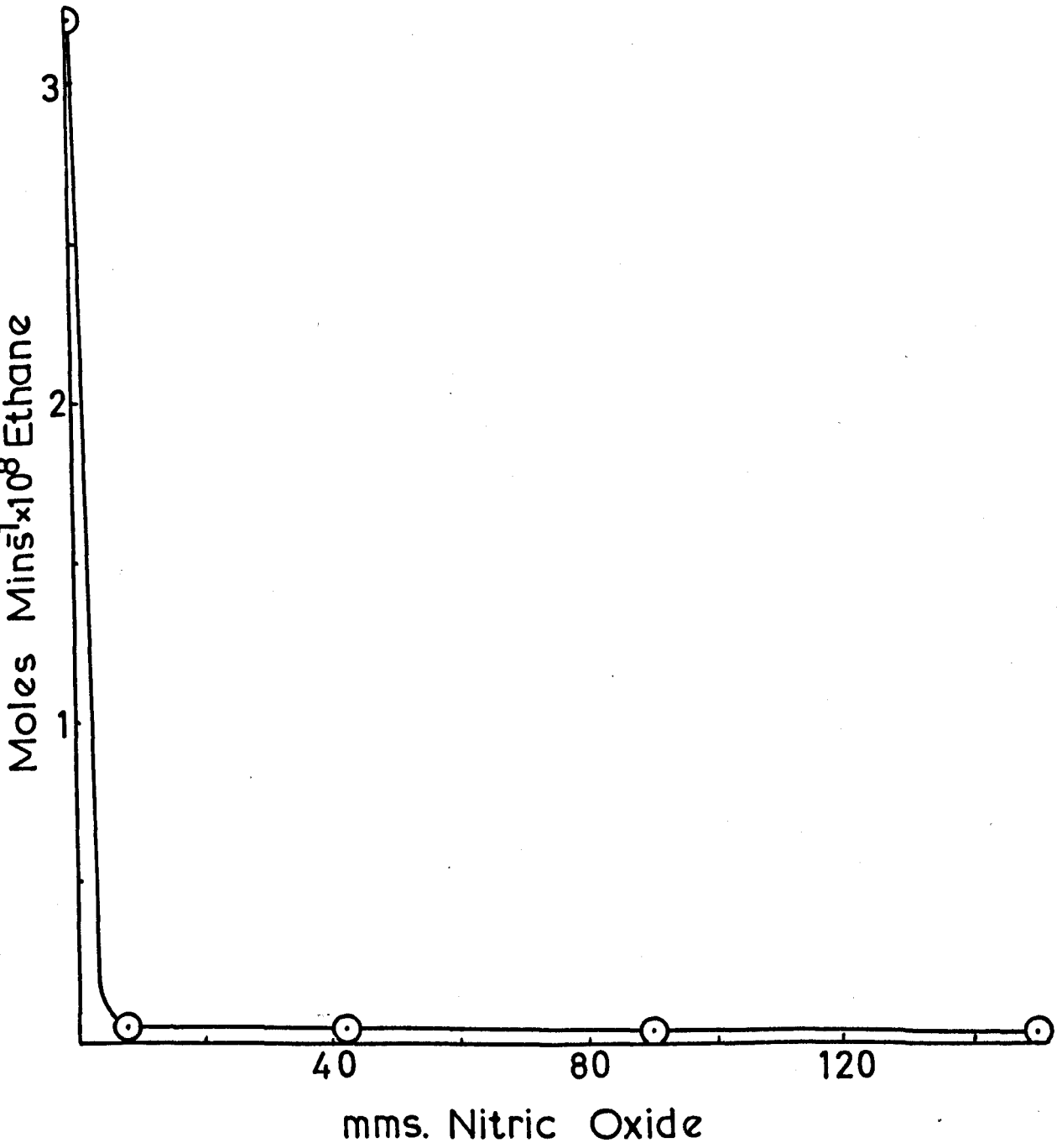

4.6 The Effect of Variation of Temperature

Irradiations were carried out at six different temperatures, 25°, 50°, 75°, 100°, 125° and 150°C. From the figures 4.29-33 can be seen the effect of temperature variation on the individual rates of formation. The methane rate increased by over a factor of forty whilst the propane rate dropped to approximately one quarter of its rate at room temperature and butane similarly dropped by a factor of fifteen.

Ethylene increased to a seemingly constant value whilst ethane increased to a maximum and then decreased. At 150°C butene was formed although no quantitative value was measured.

TABLE 4.9

Effect of variation on rates of formation

Irradiation Conditions: $C_2H_5Sn(CH_3)_3$, 10 mm.
Temperature, 25 - 150°C
Irradiation time, 10 mins.

Analytical Conditions: Detector, flame ionisation
Column, Ap-L on Celite and Poropak Q
Temperature, 65°C 50°C
Nitrogen, 20 p.s.i.

	4.29	4.30	4.31	4.32	4.33
Temperature	CH_4	C_2H_4	C_2H_6	C_4H_{10}	C_3H_8
25°C	3.52×10^{-9}	2.44×10^{-8}	3.2×10^{-8}	3.12×10^{-8}	7.44×10^{-8}
50°C	4.40×10^{-9}	2.76×10^{-8}	3.79×10^{-8}	2.98×10^{-8}	6.96×10^{-8}
75°C	6.68×10^{-9}	2.95×10^{-8}	4.45×10^{-8}	2.56×10^{-8}	6.38×10^{-8}
100°C	13.2×10^{-9}	3.05×10^{-8}	3.50×10^{-8}	2.16×10^{-8}	5.58×10^{-8}
125°C	26.9×10^{-9}	3.11×10^{-8}	3.17×10^{-8}	1.32×10^{-8}	4.20×10^{-8}
150°C	$160. \times 10^{-9}$	3.10×10^{-8}	2.71×10^{-8}	0.22×10^{-8}	1.81×10^{-8}

Figures in moles/minute

Figure 4.29

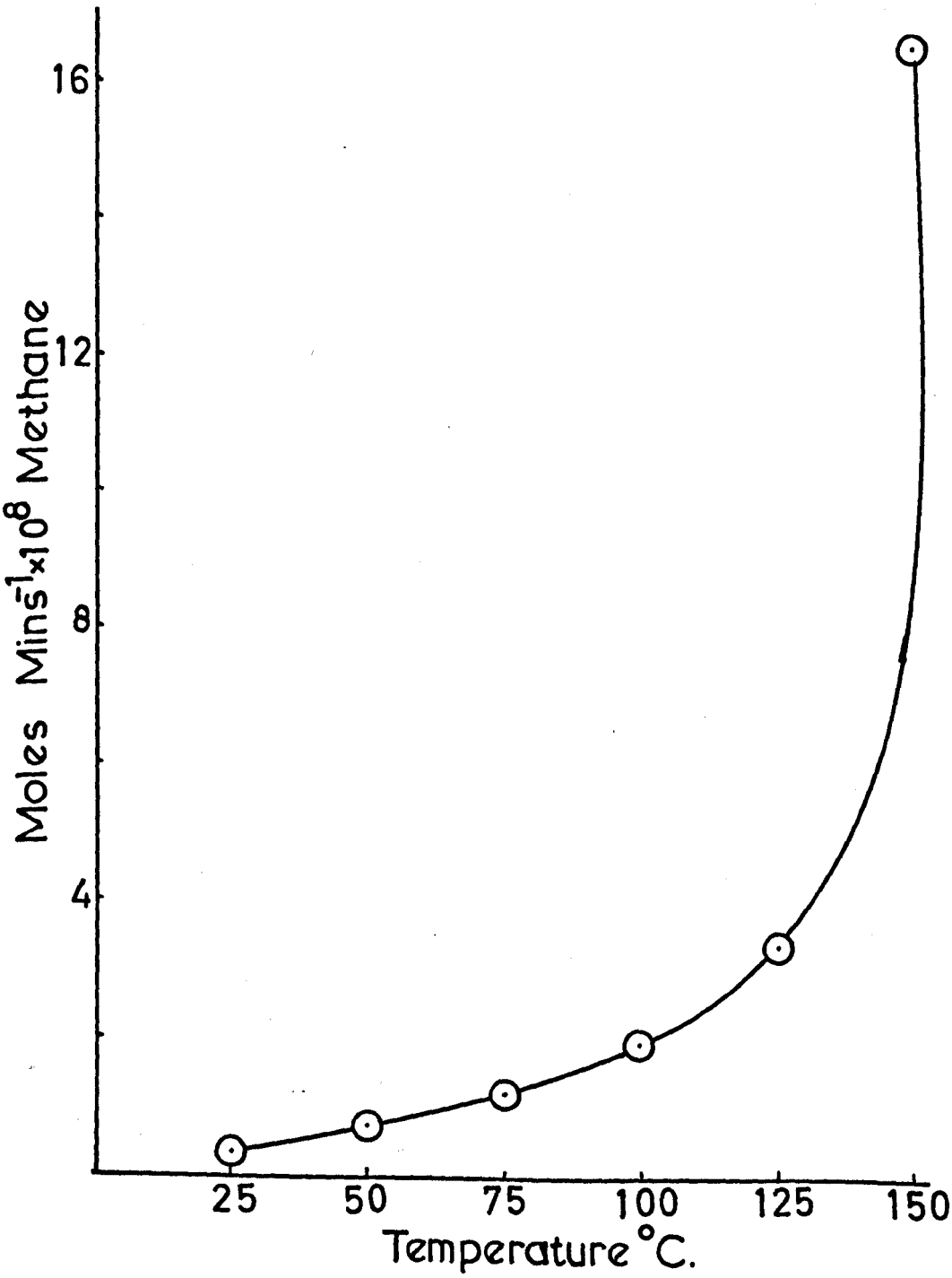
16
12
8
4
Moles Mins^{-1}x10^{8} Methane
25
50
75
100
125
150
Temperature °C.

Figure 4.30

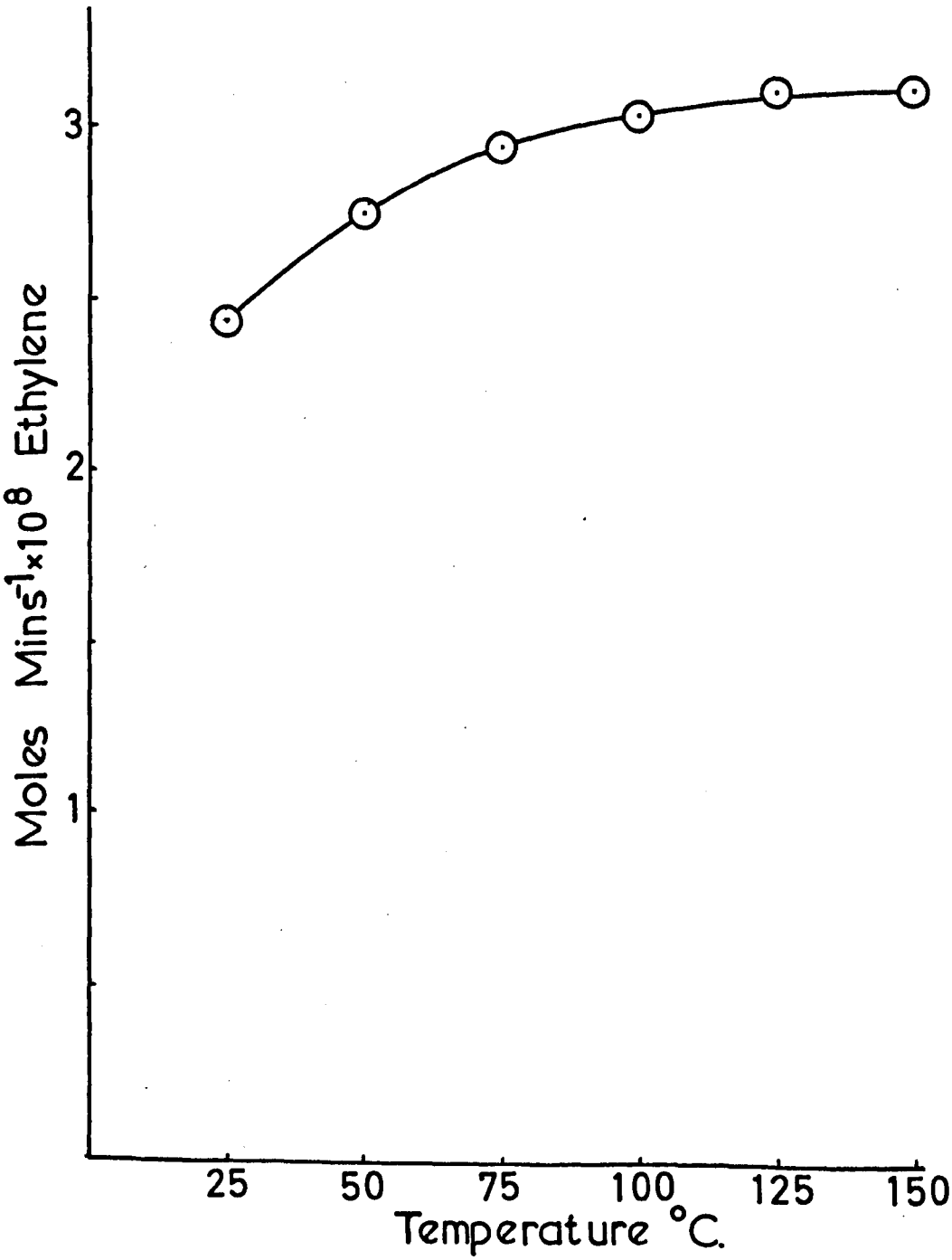
Moles Mins^{-1}x10^{8} Ethylene
3
2
1
25
50
75
100
125
150
Temperature °C.

Figure 4.31

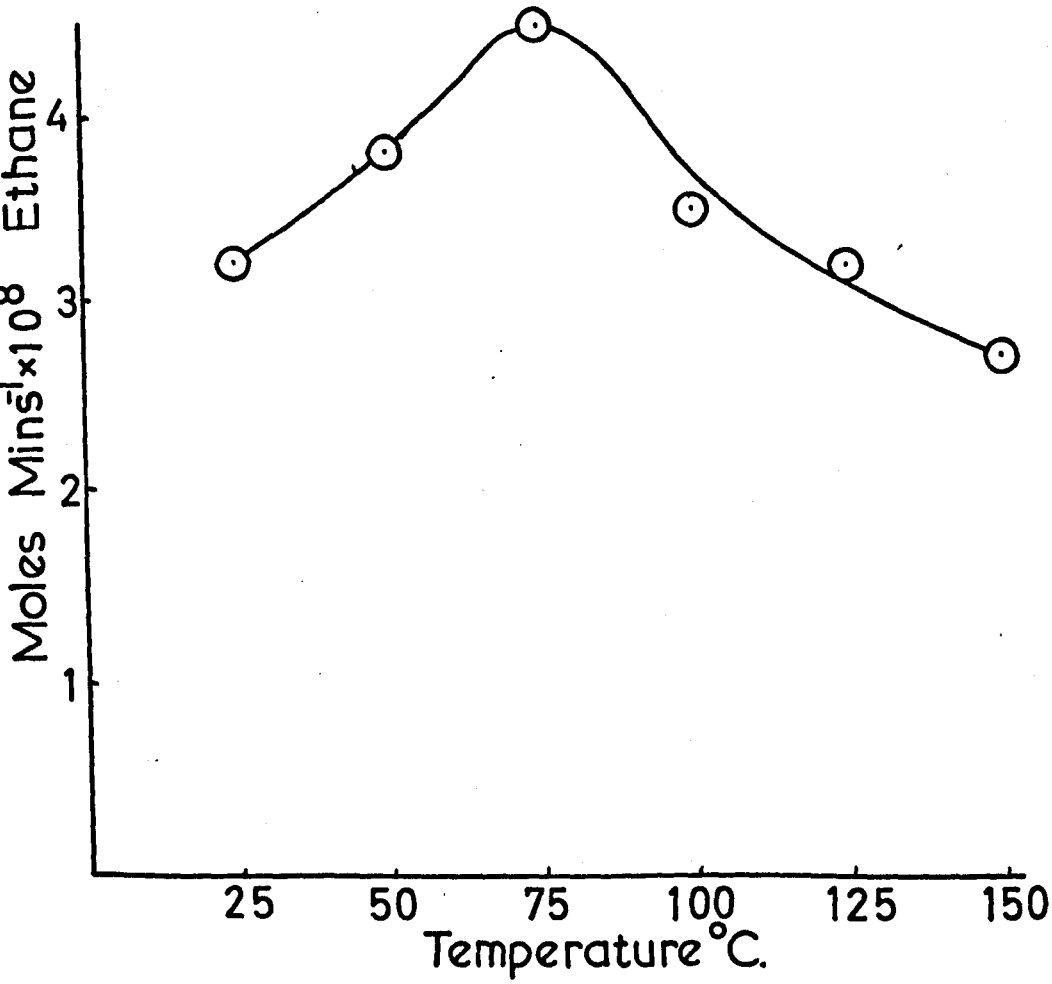
Moles Mins^{-1}×10^{8} Ethane
1
2
3
4
25
50
75
100
125
150
Temperature °C.

Figure 4.32

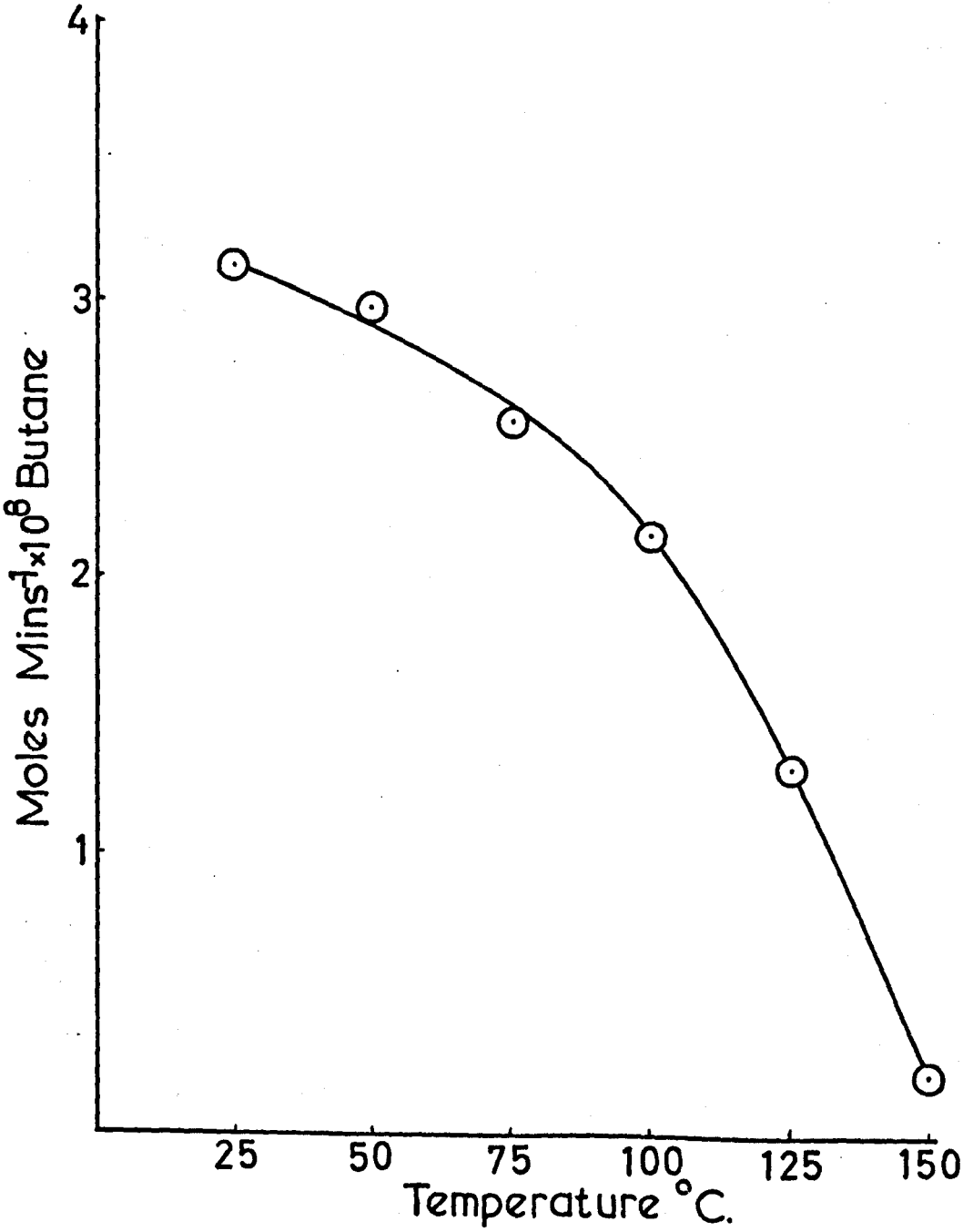
4
3
2
1
Moles Mins^{-1}x10^{8} Butane
25
50
75
100
125
150
Temperature °C.

Figure 4.33

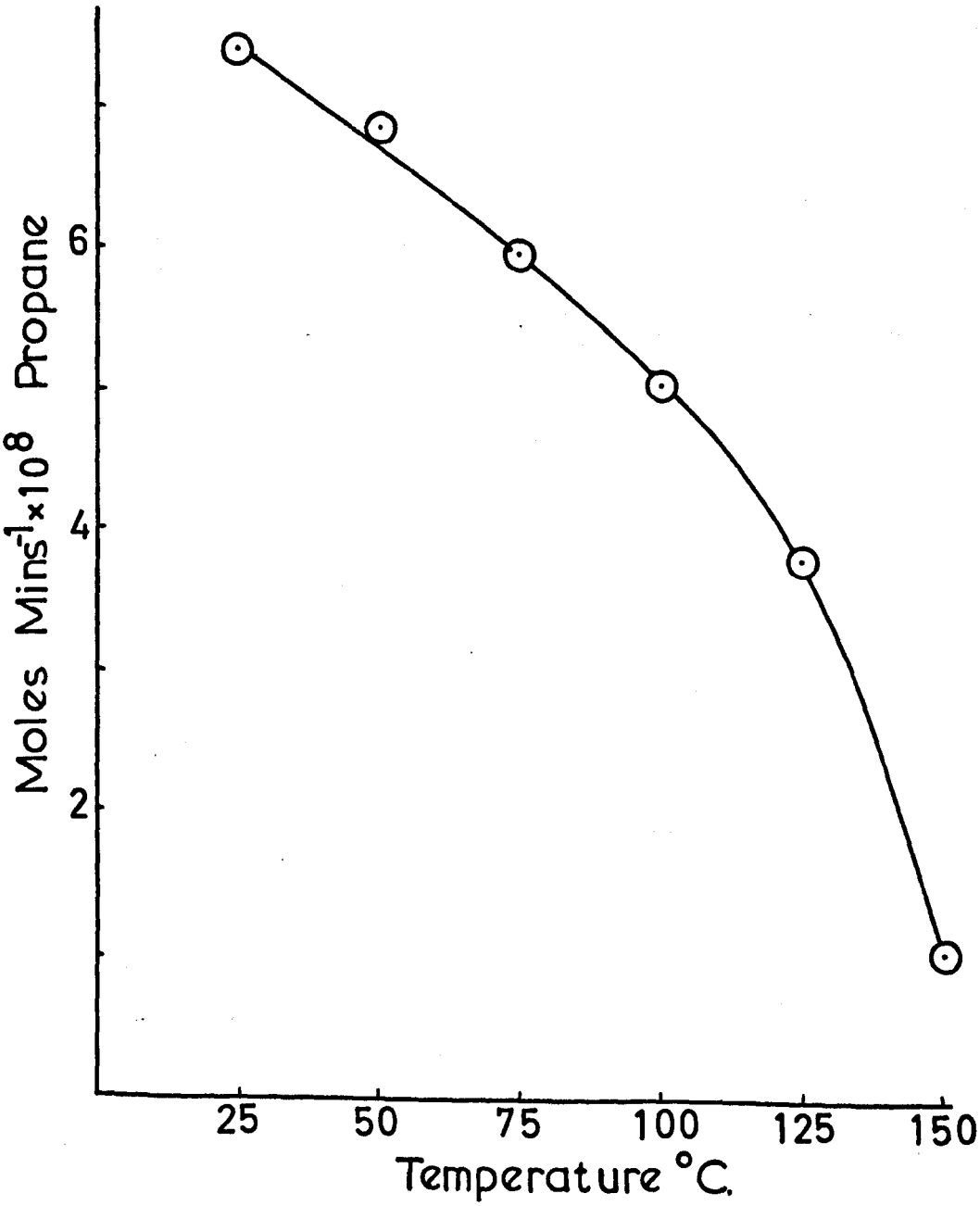
Moles Mins^{-1} x 10^{8} Propane
6
4
2
25
50
75
100
125
150
Temperature °C.

4.7 Effect of Time at High Temperatures

Irradiation periods up to 24 hrs showed that no further products other than those stated in the previous section were found. In Section 3 further products were obtained on irradiation for long periods at high temperatures and it may be expected that similar conditions may produce new compounds with ethyl trimethyl stannane. Irradiation of 10 mms of ethyl trimethyl stannane at 125^{o}C for a period of 2 hrs showed no further addition peaks after the parent peak. However a small amount of tetramethyl stannane was produced.

4.8 Effect of Long Irradiation at Room Temperature

The section was carried out to account for the total tin formed and compare it with the total hydrocarbons formed. A large amount of yellow polymeric material was observed on the window after 24 hrs irradiation and also some tetramethyl stannane detected.

The total tin analysis of polymer was carried out by dissolving the polymer in aqua regia and evaporating to dryness which leaves SnO_2 and water-soluble stannous salts. The soluble salts were dissolved in the polarographic solution and analysed. The remaining solid weighed and the analysis figures shown below.

Irradiation Conditions: $C_2H_5Sn(CH_3)_3$: 20 mms.
Temperature: 25°C
Irradiation time: 24 hrs.

Analytical Conditions: Detector: flame ionisation
Column: Poropak Q
Temperature: 50°C
Nitrogen: 20 p.s.i.

Hydrocarbon Analysis

	Moles
Methane:	4.86×10^{-6}
Ethylene:	1.069×10^{-5}
Ethane:	9.935×10^{-6}
Propane:	2.067×10^{-5}
Butane:	6.99×10^{-6}

Tin Analysis

Polarography	=	1.07×10^{-5} moles
SnO_2	=	3.60×10^{-5} moles
Total tin	=	4.67×10^{-5} moles

4.9 Actinometry

The change in geometry of the optical system required further actinometry to be carried out but did not alter the quantum input.

Rate of hydrogen formation 3.88×10^{-8} moles/min.

Quantum yields:

Ethane = $\frac{3.39 \times 10^{-8}}{3.88 \times 10^{-8}} \times 0.61 = 0.53$

Ethylene = $\frac{2.484 \times 10^{-8}}{3.88 \times 10^{-8}} \times 0.61 = 0.39$

Propane = $\frac{8.33 \times 10^{-8}}{3.88 \times 10^{-8}} \times 0.61 = 1.31$

Butane = $\frac{4.62 \times 10^{-8}}{3.88 \times 10^{-8}} \times 0.61 = 0.73$

Methane = $\frac{3.52 \times 10^{-9}}{3.88 \times 10^{-8}} \times 0.61 = 0.06$

Total ϕ = 3.02

5. RESULTS

n-Propyl Trimethyl Stannane

Irradiation of a sample of n-propyl trimethyl stannane with a filter of 2% acetic acid, 1 cm thick, interposed between the lamp and the cell, resulted in no photochemical reaction whereas without the filter a number of photochemical products were obtained. The filter absorbs 1849Å radiation (Section 2.5.2) indicating that this is the exciting wavelength and also that no mercury was present in the system acting as a sensitiser.

The products of irradiation by light of wavelength 1849Å were methane, ethylene, ethane, propylene, a small amount of propane, butane and n-hexane at room temperature.

TABLE 5.1

Product	Yield
CH_4	5.8×10^{-9} moles/minute
C_2H_4	8.20×10^{-9} "
C_2H_6	2.03×10^{-7} "
C_3H_6	2.61×10^{-8} "
C_4H_{10}	6.47×10^{-8} "
C_6	not analysed

Clearly from the nature of these products there is the possibility as in Sections 3 and 4 of free radical processes being involved and also molecular elimination processes.

The experiments carried out with this compound are limited to variation of pressure of n-propyl trimethyl stannane, variation of pressure of added nitrogen and variation of pressure of added oxygen. As in Sections 3 and 4 the actinometry was carried out using ethylene as an actinometer.

5.1 The Effect of Variation of n-Propyl Trimethyl Stannane Pressure

The effect of variation of the pressure of n-propyl trimethyl stannane is similar to those of ethyl trimethyl stannane and tetramethyl stannane in that an approximately linear dependence occurs above full absorption. Analysis for n-hexane proved difficult due to 0.002% of hexane in the n-propyl trimethyl stannane.

TABLE 5.2

Product yields as a function of variation of $n\text{-}C_3H_7Sn(CH_3)_3$ pressure

Irradiation Conditions: Pressure $n\text{-}C_3H_7Sn(CH_3)_3$, 0-11 mm.
Temperature, 25°C
Irradiation time, 10 minutes

Analytical Conditions: Detector, flame ionisation
Column, Poropak Q
Temperature, 150°C
Nitrogen, 20 p.s.i.

$n\text{-}C_3H_7Sn(CH_3)_3$	CH_4	C_2H_4	C_2H_6	C_3H_6	C_4H_{10}
5 mm.	5.82×10^{-9}	8.20×10^{-9}	3.84×10^{-8}	2.61×10^{-8}	6.47×10^{-8}
6 mm.	6.14×10^{-9}	8.64×10^{-9}	4.10×10^{-8}	2.76×10^{-8}	6.72×10^{-8}
7 mm.	6.55×10^{-9}	8.84×10^{-9}	4.40×10^{-8}	2.89×10^{-8}	7.00×10^{-8}
8 mm.	6.86×10^{-9}	9.20×10^{-9}	4.71×10^{-8}	3.06×10^{-8}	7.30×10^{-8}
9 mm.	7.31×10^{-9}	9.54×10^{-9}	5.05×10^{-8}	3.28×10^{-8}	7.57×10^{-8}
10 mm.	7.63×10^{-9}	9.81×10^{-9}	5.31×10^{-8}	3.37×10^{-8}	7.85×10^{-8}
11 mm.	8.08×10^{-9}	10.16×10^{-9}	5.58×10^{-8}	3.45×10^{-8}	8.06×10^{-8}

Moles/minute

Figure 5.1

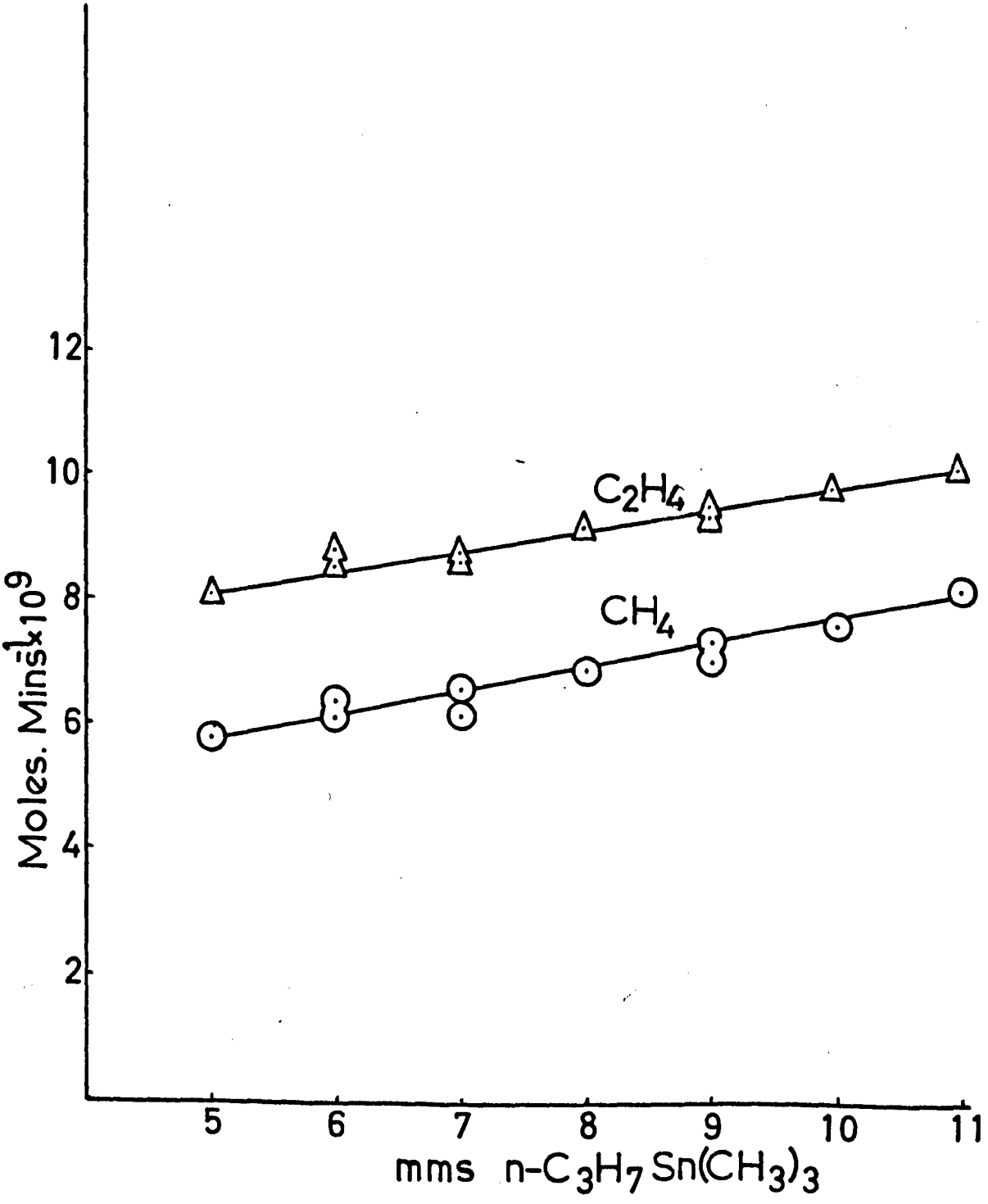
12
10
8
6
4
2
Moles. Mins^{-1}x10^9
C_2H_4
CH_4
5
6
7
8
9
10
11
mms n-$C_3H_7Sn(CH_3)_3$

Figure 5.2

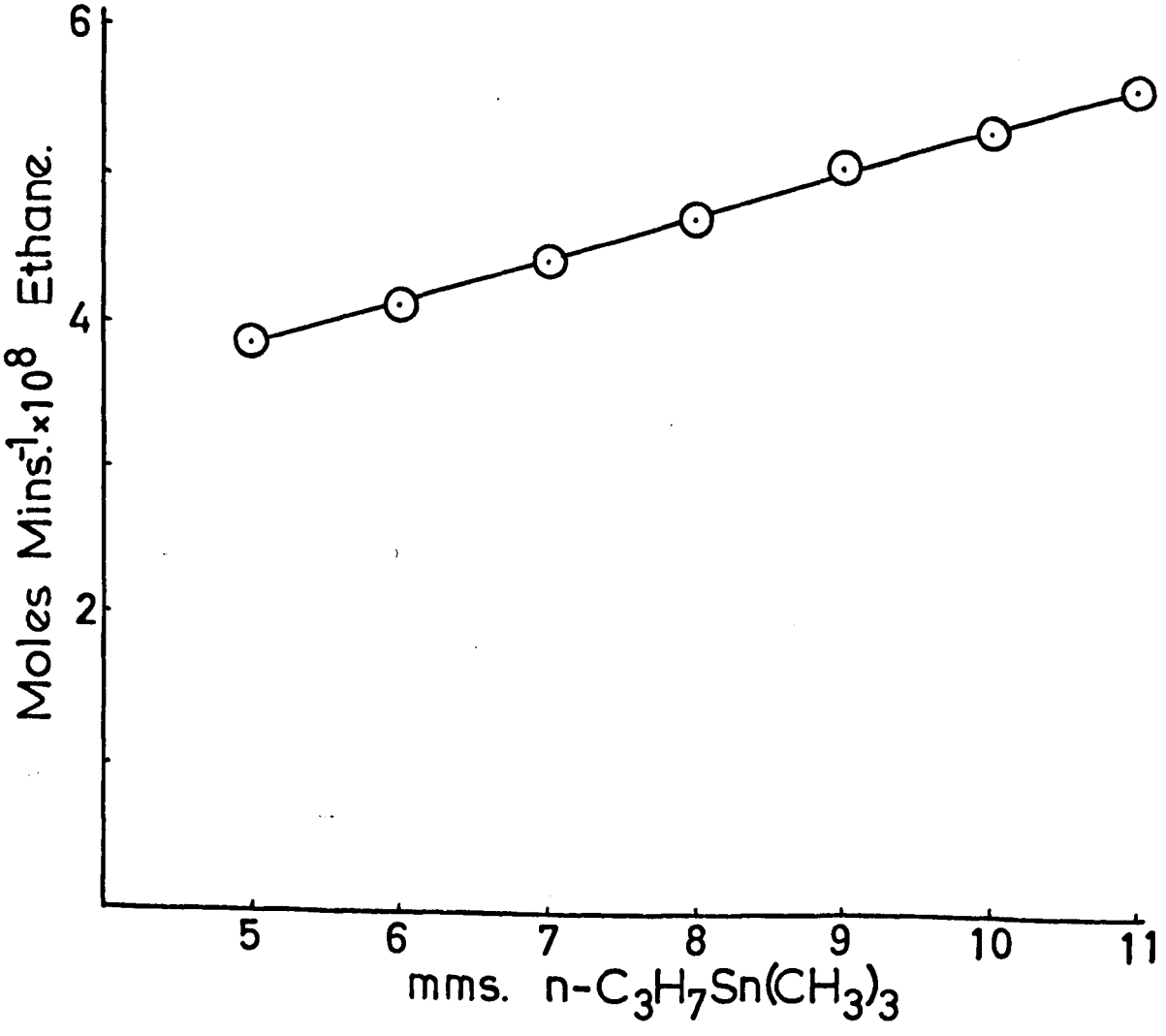

Figure 5.3

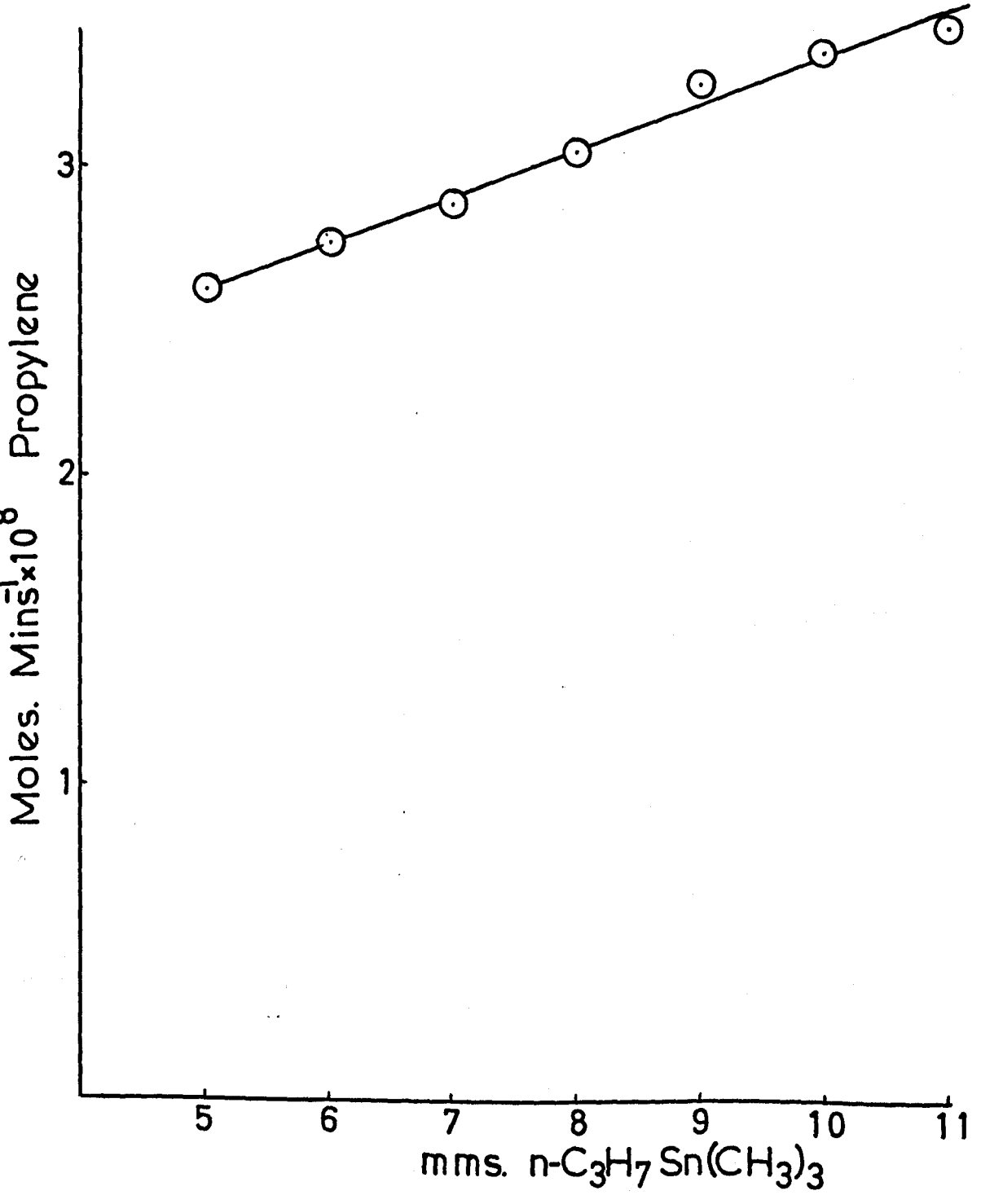

Figure 5.4

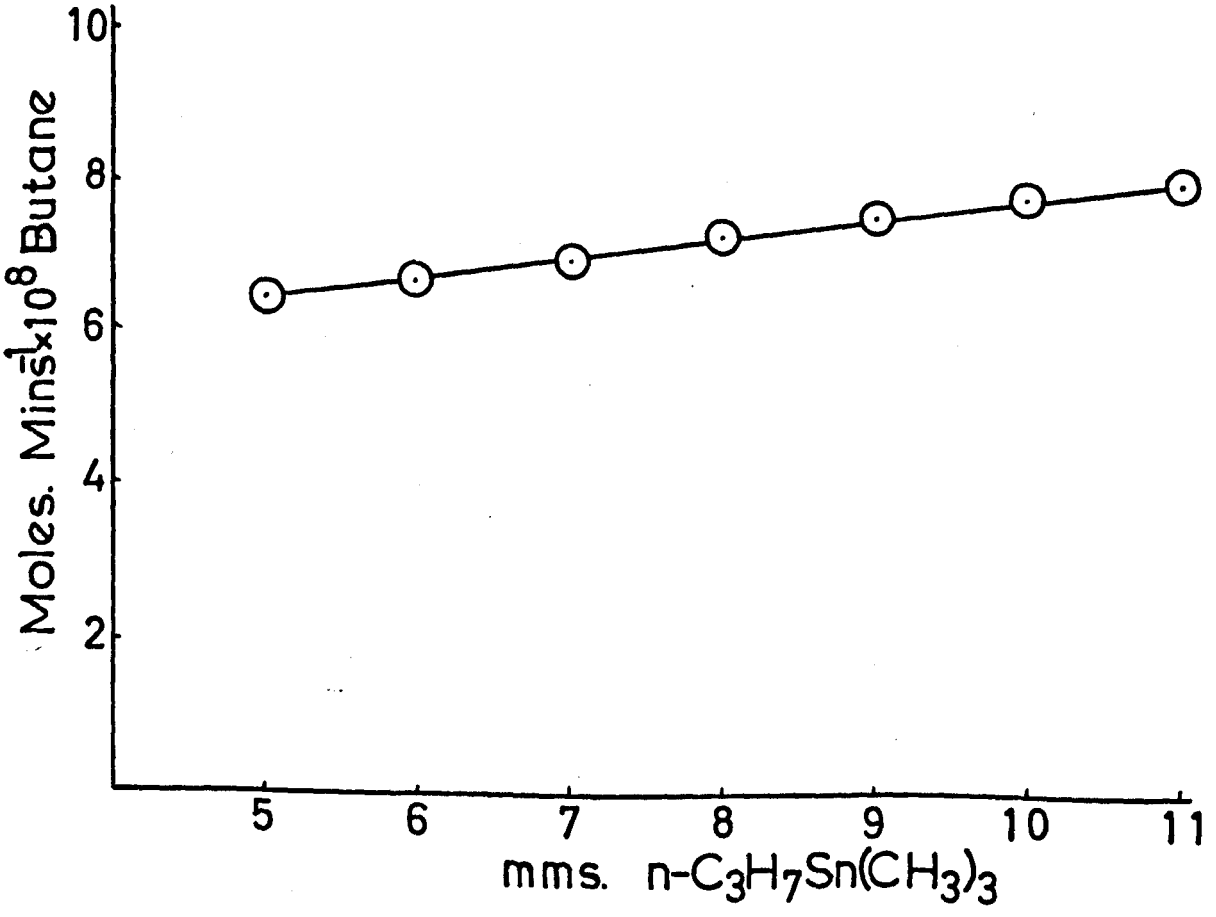

5.2 Effect of Variation of Added Nitrogen

Increasing the pressure of added nitrogen caused similar effects as in the case of ethyl trimethyl stannane. All the products decreased very markedly over a short range in pressure. The variation of product yields are given in Table 5.3 and Figures 5.5 to 5.8.

TABLE 5.3

Effect of variation of added nitrogen pressure

Irradiation Conditions: $n\text{-}C_3H_7Sn(CH_3)_3$, 6 mm.
Temperature, 25°C
Irradiation time, 10 mins.

Analytical Conditions: Detector, flame ionisation
Column, Poropak Q
Temperature, 150°C
Nitrogen, 20 p.s.i.

Nitrogen	CH_4	C_2H_4	C_2H_6	C_3H_6	C_4H_{10}
0 mm.	6.14×10^{-9}	8.64×10^{-9}	4.10×10^{-8}	2.76×10^{-8}	6.72×10^{-8}
$10\frac{1}{2}$ mm.	1.27×10^{-9}	1.59×10^{-9}	7.52×10^{-9}	3.43×10^{-9}	1.50×10^{-8}
66 mm.	0.93×10^{-9}	1.15×10^{-9}	5.84×10^{-9}	2.73×10^{-9}	1.07×10^{-8}
150 mm.	0.88×10^{-9}	0.83×10^{-9}	4.63×10^{-9}	2.26×10^{-9}	0.88×10^{-8}
384 mm.	0.84×10^{-9}	0.81×10^{-9}	4.35×10^{-9}	2.10×10^{-9}	0.83×10^{-8}
590 mm.	0.63×10^{-9}	0.52×10^{-9}	4.10×10^{-9}	2.00×10^{-9}	0.78×10^{-8}

Moles/minute

Figure 5.5

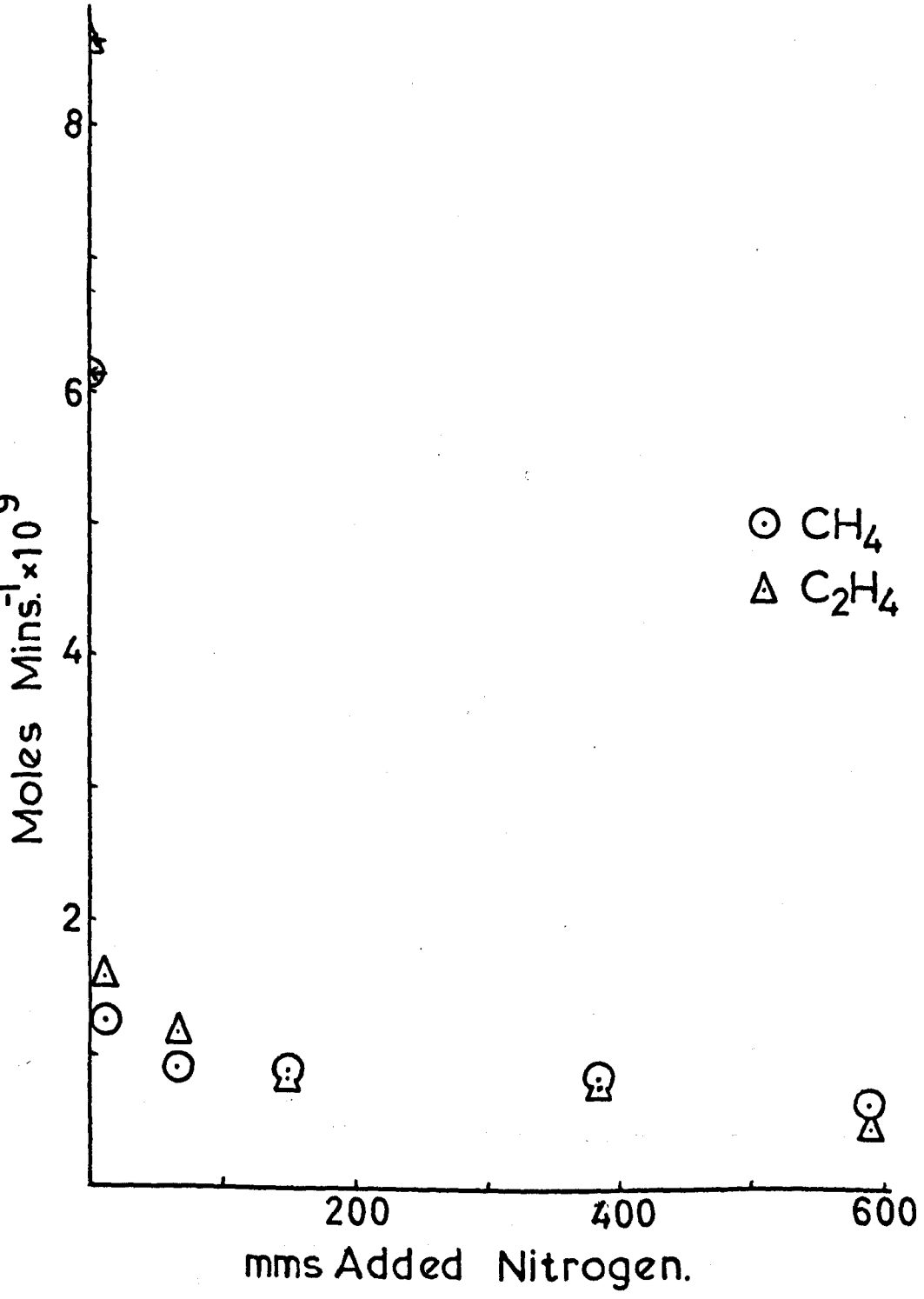
8
6
4
2
Moles Mins.$^{-1}$ x10^{9}
⊙ CH_4
Δ C_2H_4
200
400
600
mms Added Nitrogen.

Figure 5.6

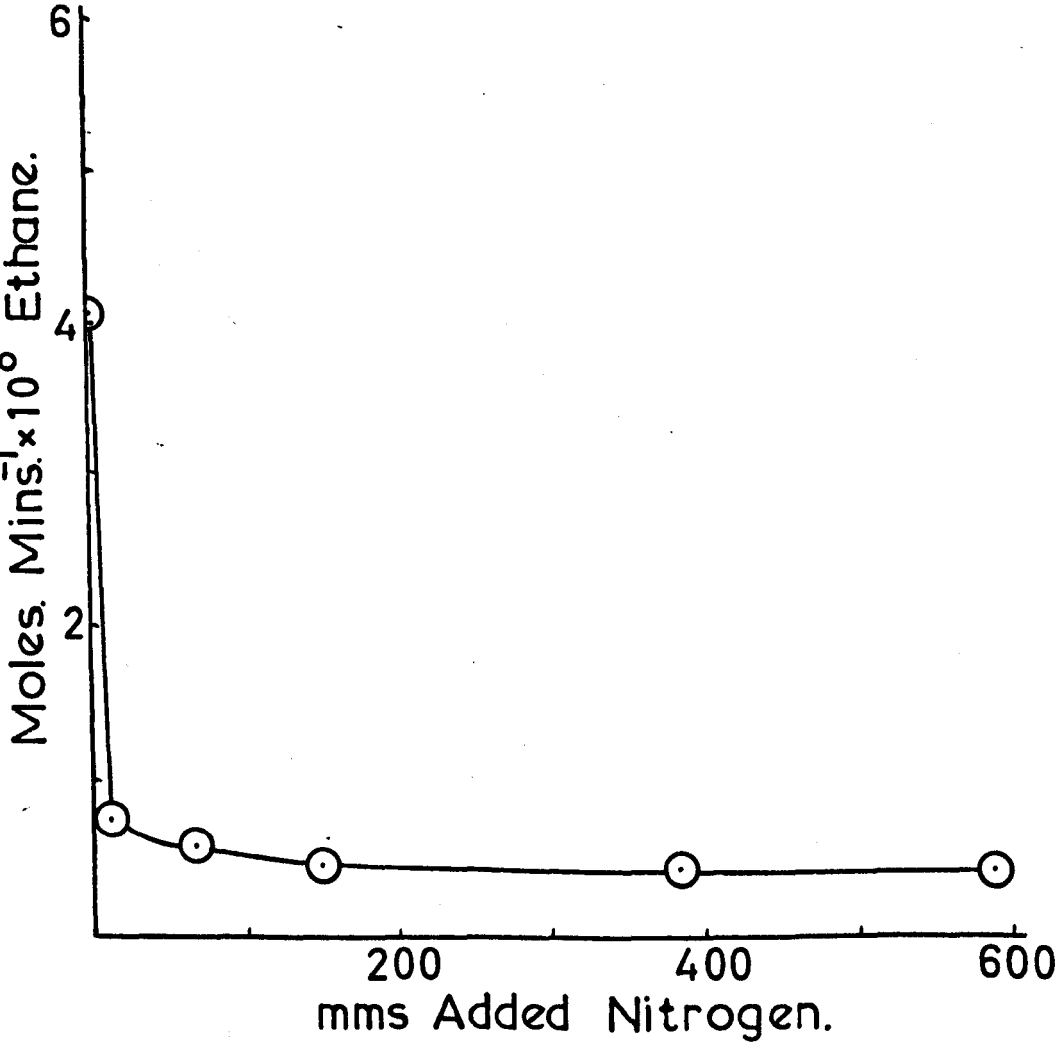

Figure 5.7

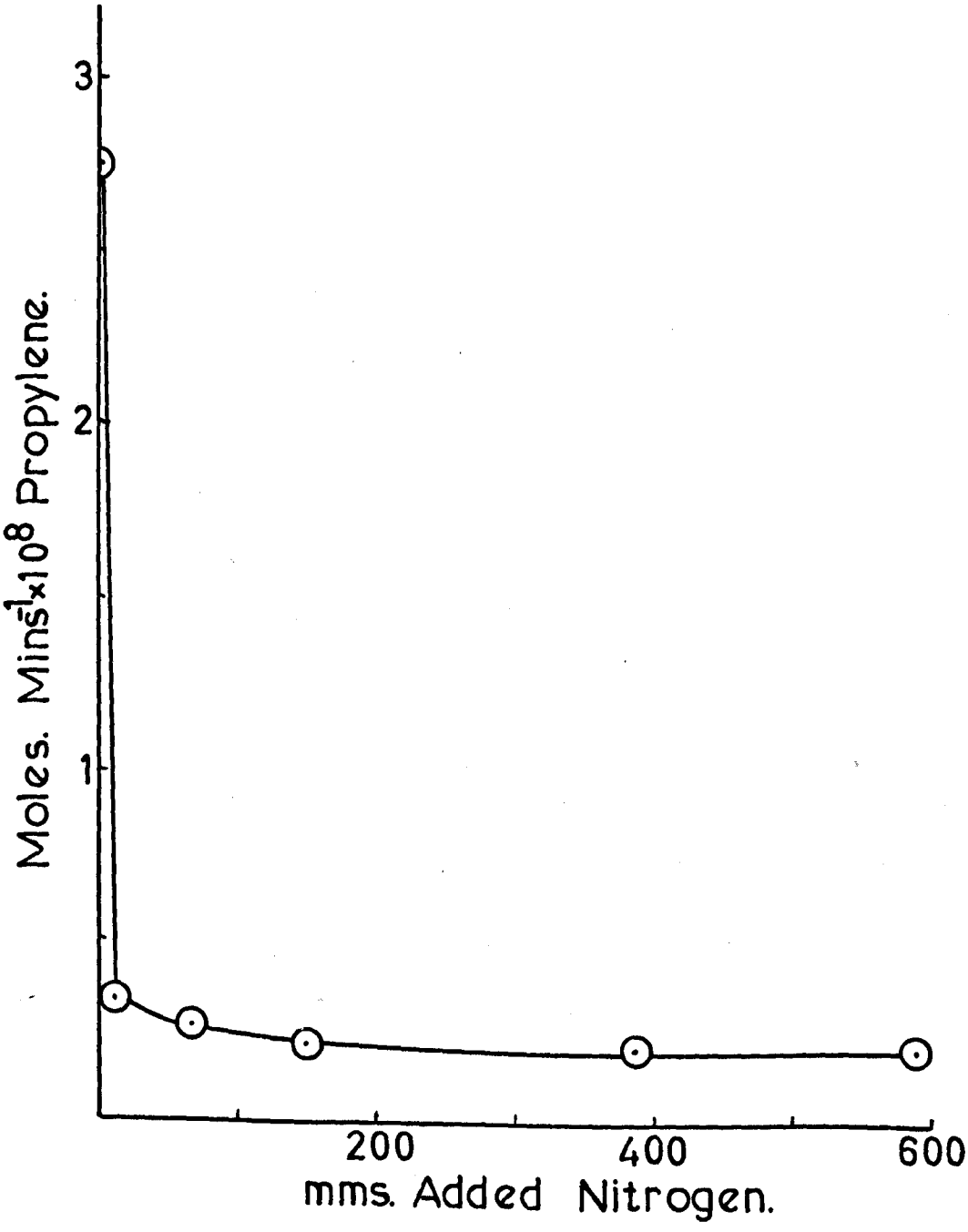
3
2
1
Moles. Mins^{-1}x10^{8} Propylene.
200
400
600
mms. Added Nitrogen.

Figure 5.8

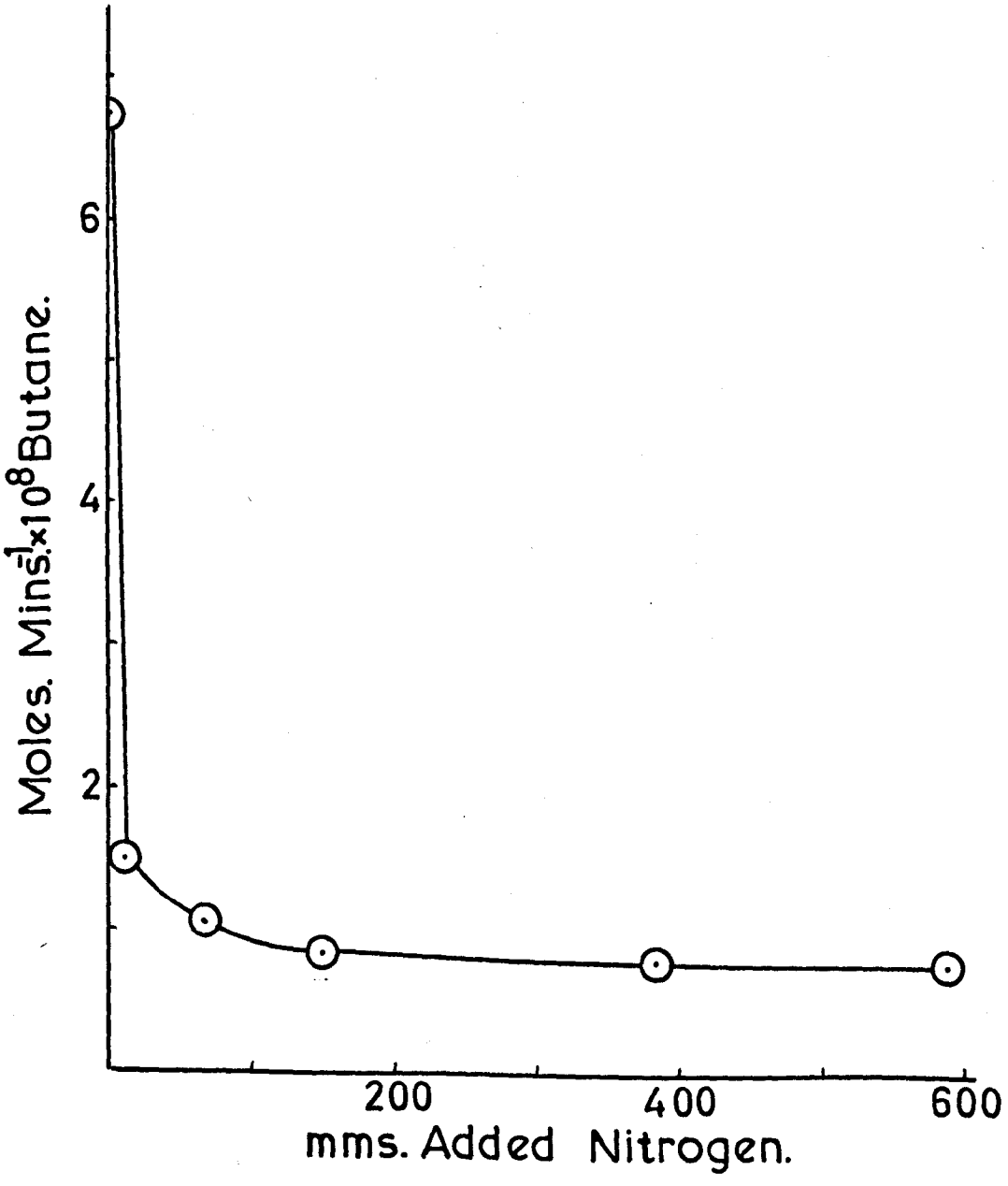

5.3 Effect of Variation of Added Oxygen Pressure

The addition of oxygen or nitric oxide, gases which have been used as radical scavengers in Sections 3 and 4, should show the proportion of the products that is molecularly formed. The products methane, ethylene, ethane, propylene and butane all showed a small amount of molecular formation. The n-hexane was apparently formed only by radical reactions. The rates of formation of the products versus pressure of added oxygen are shown in Figures 5.9 - 5.12.

TABLE 5.4

Effect of variation of added oxygen pressure

Irradiation Conditions: Pressure of n-$C_3H_7Sn(CH_3)_3$: 6 mm.
Temperature, 25°C
Irradiation time, 10 mins.

Analytical Conditions: Detector, flame ionisation
Column, Poropak Q
Temperature, 150°C
Nitrogen, 20 p.s.i.

Oxygen	CH_4	C_2H_4	C_2H_6	C_3H_6	C_4H_{10}
0	6.14×10^{-9}	8.64×10^{-9}	4.10×10^{-8}	2.76×10^{-8}	6.72×10^{-8}
11 mm.	1.01×10^{-9}	1.40×10^{-9}	6.72×10^{-10}	8.38×10^{-9}	1.58×10^{-9}
76 mm.	0.81×10^{-9}	1.02×10^{-9}	3.02×10^{-10}	3.07×10^{-9}	0.78×10^{-9}
170 mm.	0.65×10^{-9}	0.70×10^{-9}	2.76×10^{-10}	1.65×10^{-9}	0.55×10^{-9}
390 mm.	0.60×10^{-9}	0.52×10^{-9}	2.50×10^{-10}	1.50×10^{-9}	0.50×10^{-9}
600 mm.	0.40×10^{-9}	0.45×10^{-9}	2.35×10^{-10}	1.47×10^{-9}	0.35×10^{-9}

Moles/minute

Figure 5.9

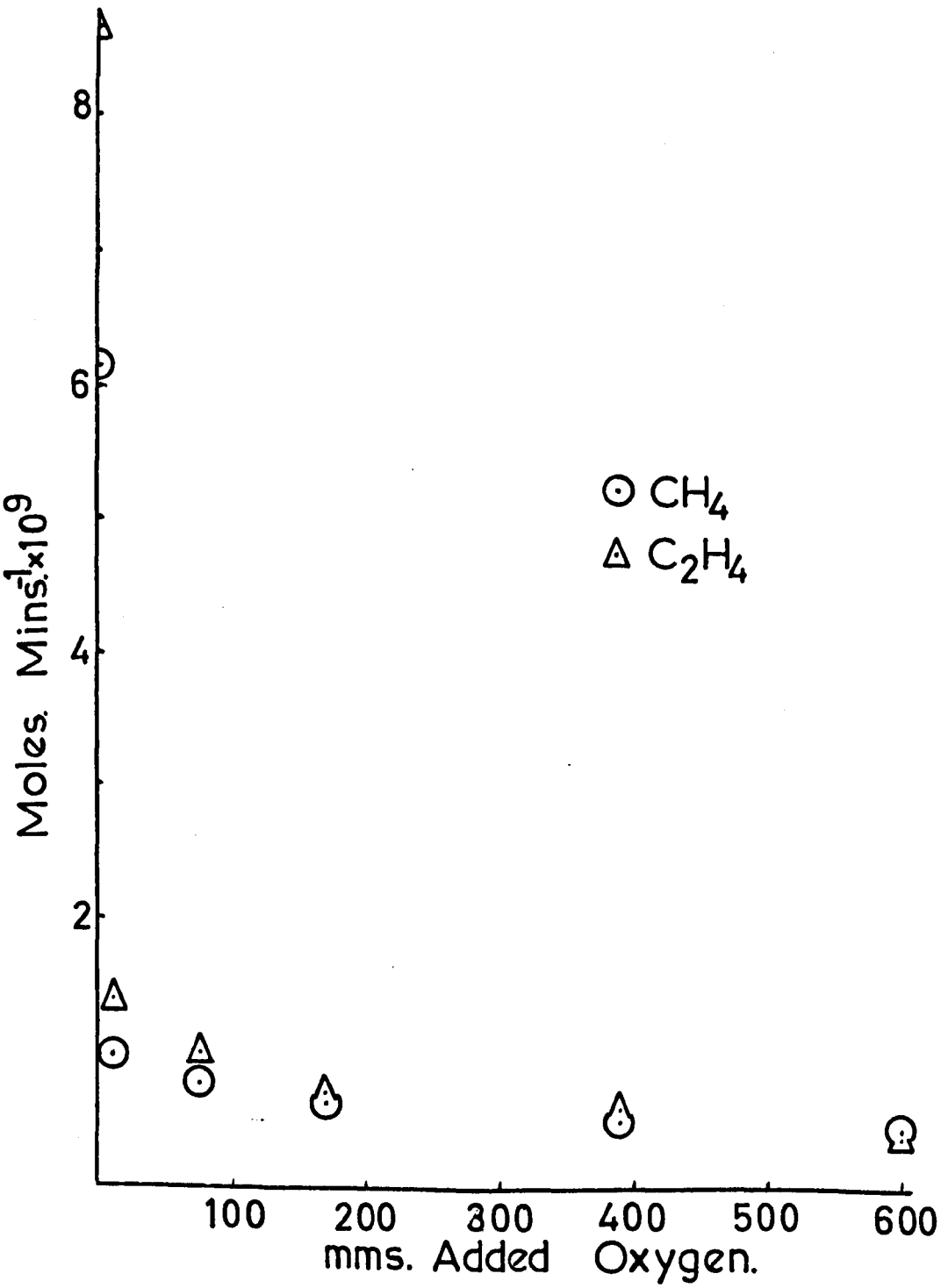
8
6
4
2
Moles. Mins.$^{-1}$x10^{9}
⊙ CH_4
△ C_2H_4
100
200
300
400
500
600
mms. Added Oxygen.

Figure 5.10

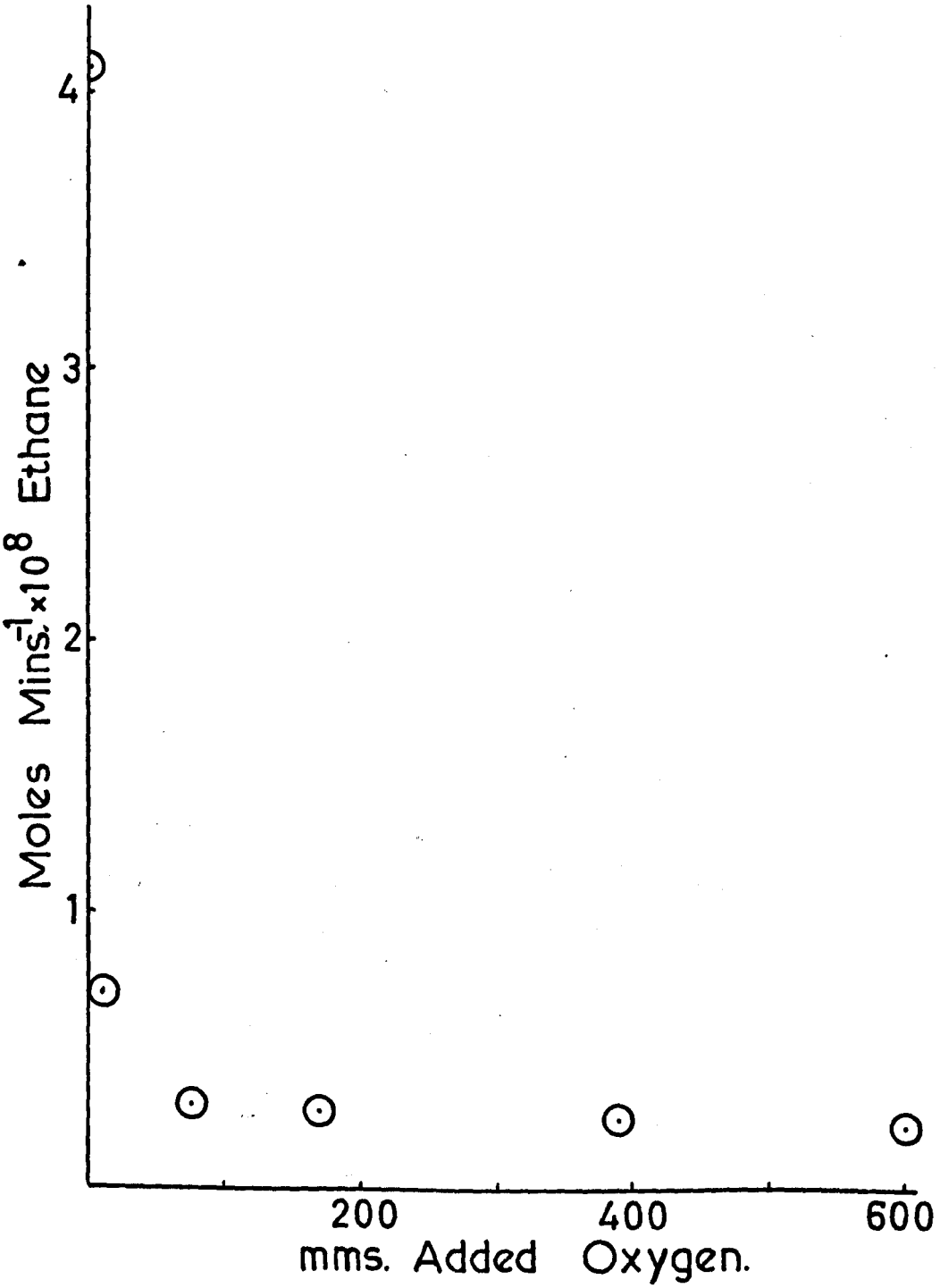

Figure 5.11

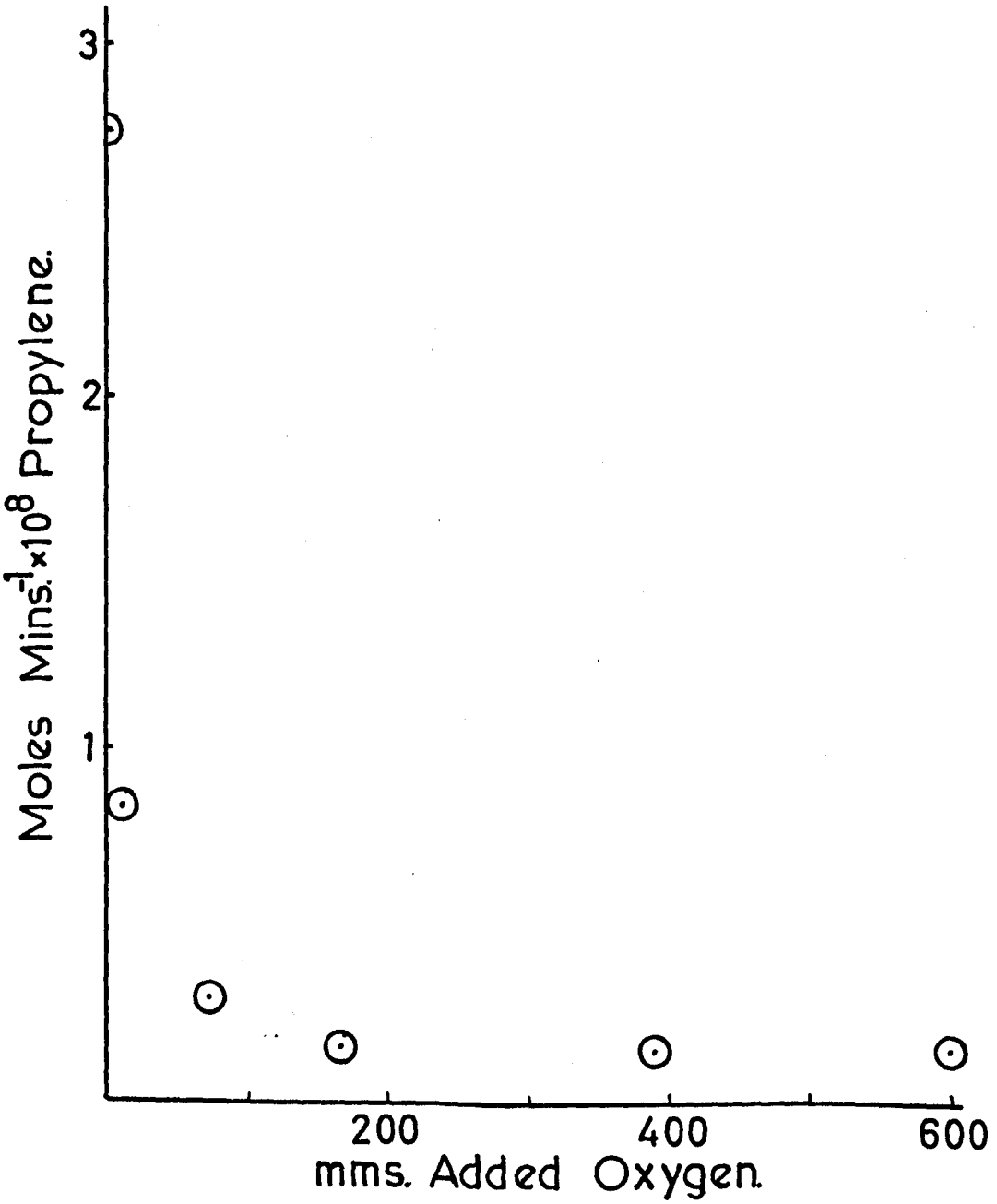

Figure 5.12

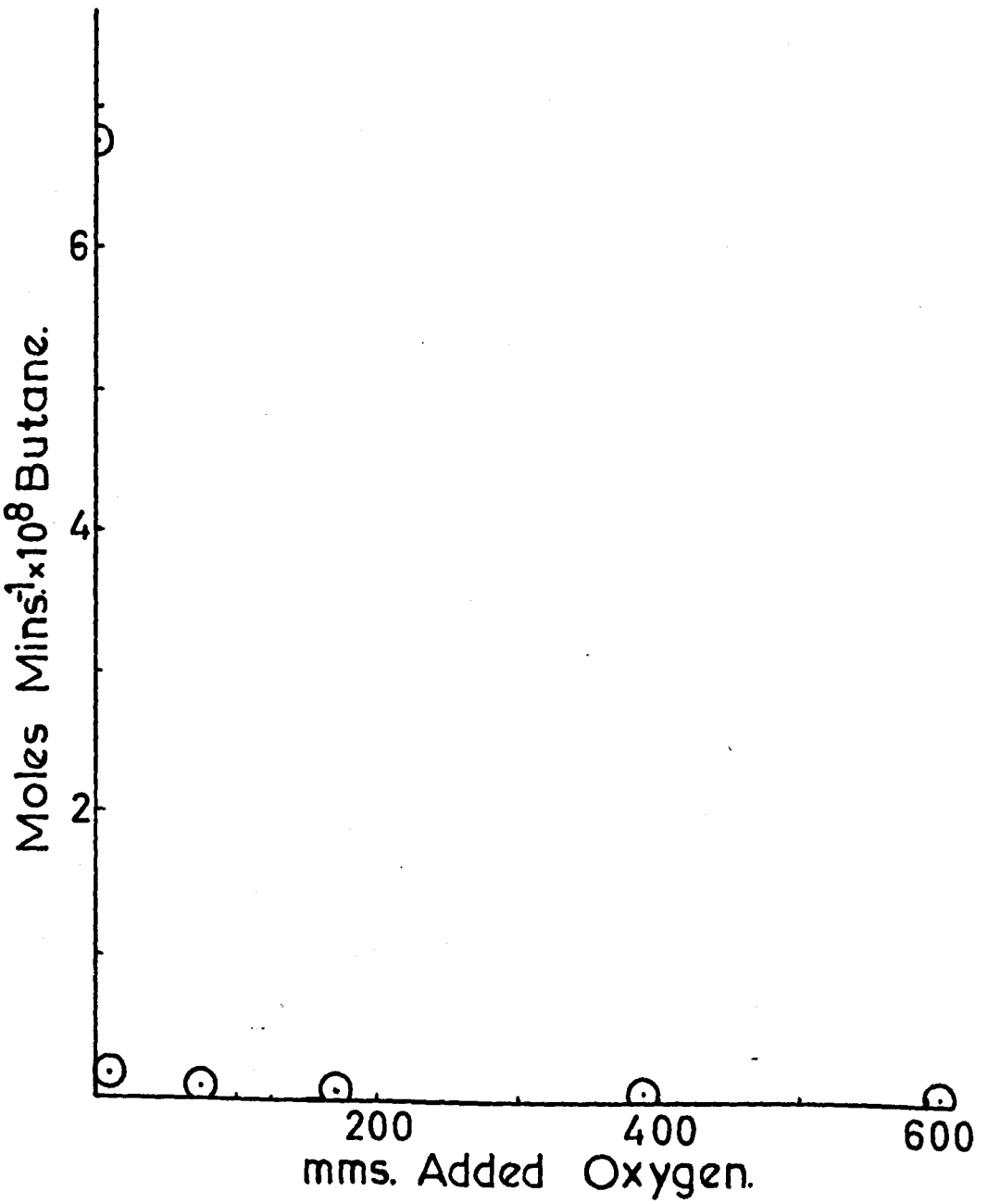

6. LIQUID PHASE PHOTOLYSIS

The experiments carried out in this section were initiated to try to ascertain the nature of the compounds which Razuvaev[69] formed in the liquid phase photolysis of tetramethyl stannane. If it is a polymer as he suggests it may be possible to follow its formation if it occurs through discreet dimers, trimers etc. of the nature of

$$CH_3-\left[-Sn(CH_3)_2-\right]_n-Sn(CH_3)_3$$

It is quite easy to elute hexamethyl distannane from an Apiezon-L on celite gas chromatograph column and the rates of formation of polymers may possibly be followed by gas chromatography.

Whilst conducting these experiments the nature of the solvent was varied, originally to see the effect of changing the nature of carbon-hydrogen bonds on the rates of formation of methane and ethane. However this proved impossible with the amounts of material available and the isomers of hexane were found to absorb in the region of absorption of tetramethyl stannane i.e. 2240 Å. This would have meant having tetramethyl stannane in excess of the hydrocarbon and as has been said this was impracticable. The solvents that were tried are as follows: cyclohexane, isopentane, 1-octane, 2methyl pentane, 3methyl pentane, methanol and tetramethyl stannane.

The apparatus used is shown in Figures 2.10 and 2.15 of Section 2.4.2. The experiments were, however, only conducted to see if a further research project could be started on the lines discussed above and so no quantum yields were measured and so the rates are only relative. Also with the apparatus used no variation in temperature could be applied due to the water jacket cooling system.

6.1 Cyclohexane

Initially 17.5 mls of cyclohexane were added to 7.5 mls tetramethyl stannane and placed into the reactor. Nitrogen was bubbled through the solution, via the sintered glass disc, to remove any oxygen in the solution. The water supply to the jacket and condenser was switched on and the sample irradiated for a known time after equilibration of temperature.

Four new peaks were observed in the gas chromatogram and their relative retentions are shown in Figures 6.1 and 6.2. Their yields versus time are shown in Figures 6.3 - 5. Only two of the peaks could be identified by comparative chromatography and were found to be methyl cyclohexane and hexamethyl distannane.

TABLE 6.1

Product yields as a function of time

Irradiation Conditions: 17.5 mls cyclohexane

7.5 mls $Sn(CH_3)_4$

Temperature 15°C

Irradiation time 0-12 hrs.

Analytical Conditions: Detector, flame ionisation

Column, Ap-L and Poropak

Temperature, 100, 130°C and 50°C

Nitrogen, 20 p.s.i.

Time	CH_3	C_2H_6	$C_6H_{11}CH_3$	$Me_3SnSnMe_3$	Peak 1	Peak 2
1 hr	4.73×10^{-4}	6.3×10^{-5}	3.88×10^{-5}	-	1.4×10^{2}	0.8×10^{2}
2 hrs	7.29×10^{-4}	9.71×10^{-5}	6.70×10^{-5}	1.85×10^{-5}	2.4×10^{2}	1.4×10^{2}
3½ hrs	9.06×10^{-4}	12.1×10^{-5}	7.93×10^{-5}	2.45×10^{-5}	3.0×10^{2}	1.6×10^{2}
5½ hrs	11.23×10^{-4}	15.0×10^{-5}	10.77×10^{-5}	3.24×10^{-5}	3.5×10^{2}	2.0×10^{2}
6½ hrs	11.82×10^{-4}	15.8×10^{-5}	11.80×10^{-5}	3.71×10^{-5}	3.9×10^{2}	2.2×10^{2}
10 hrs	13.93×10^{-4}	19.2×10^{-5}	13.63×10^{-5}	4.71×10^{-5}	4.4×10^{2}	2.4×10^{2}
12 hrs	14.26×10^{-4}	20.7×10^{-5}	14.23×10^{-5}	5.25×10^{-5}	4.9×10^{2}	2.78×10^{2}
	Moles	Moles	Moles	Moles	cms	cms

As well as the products listed in Table 6.1 a solid precipitate was formed and on filtration appeared yellow as did the filtrate. However on exposure to the atmosphere both solid and solution lost their colour. The mass spectrum of the solid after exposure is shown in Figure 6.6, the parent ion being approximately mass 330. Analysis of the solid gave

C	H	Sn
12.80%	2.80%	32.50%

If the remainder is oxygen the stoichiometry is approximately

$$SnC_4H_{10}O_{12}$$

Figure 6.1

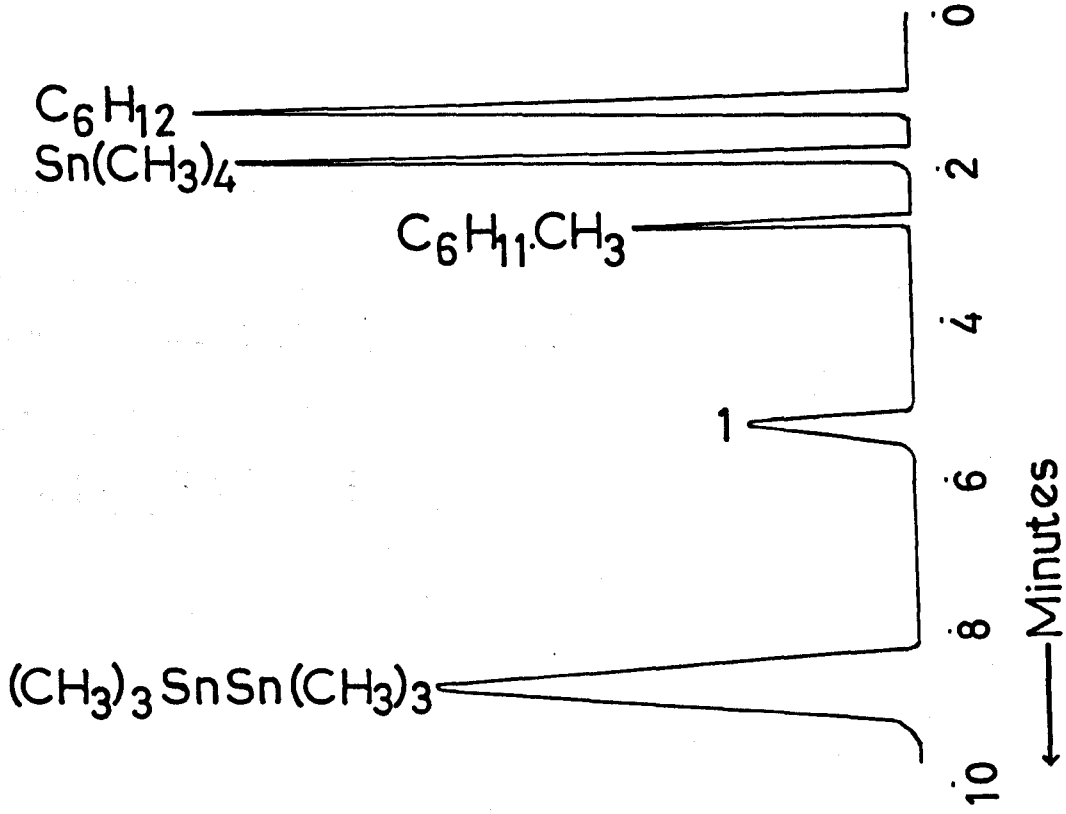

Ap-L 130°C.
N_2 20 p.s.i.

Figure 6.2

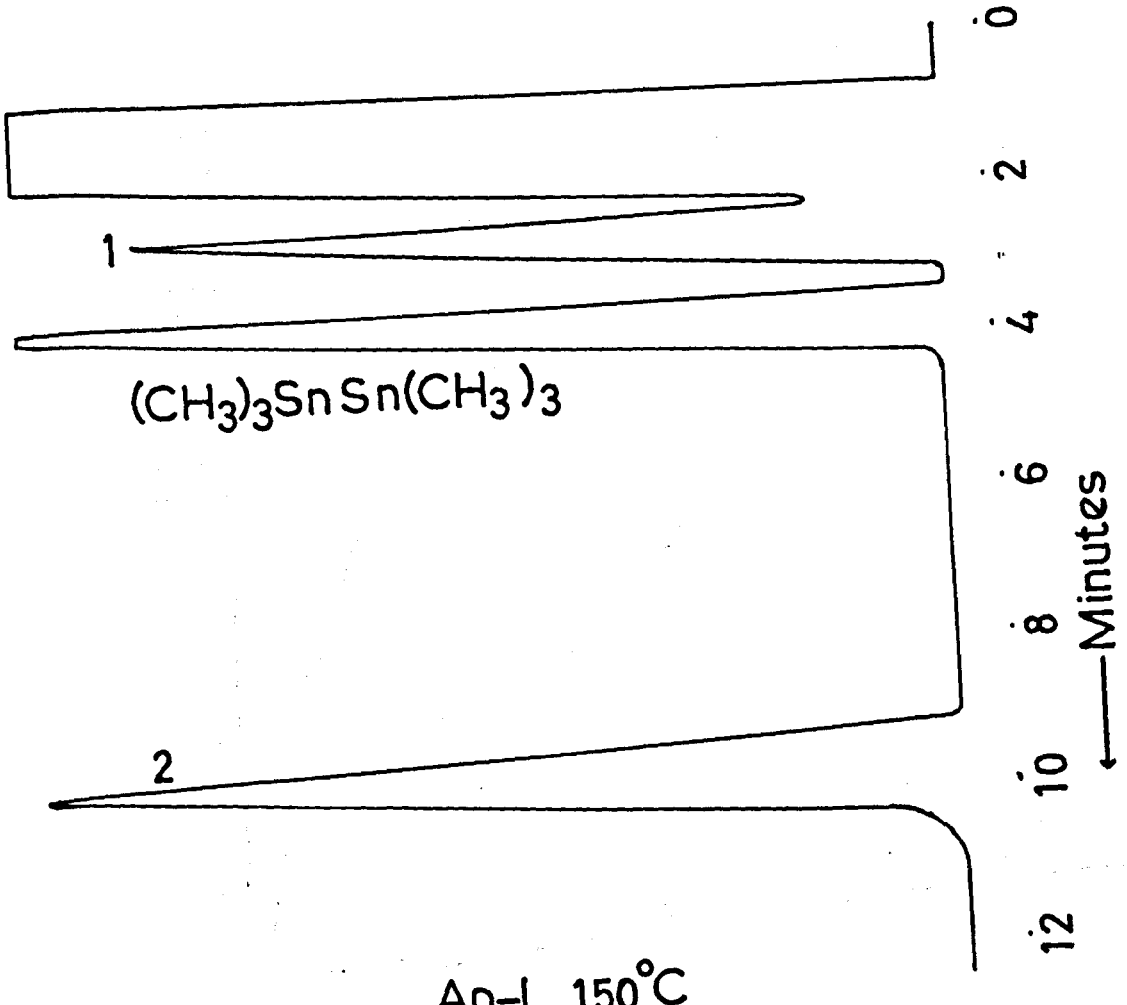

Figure 6.3

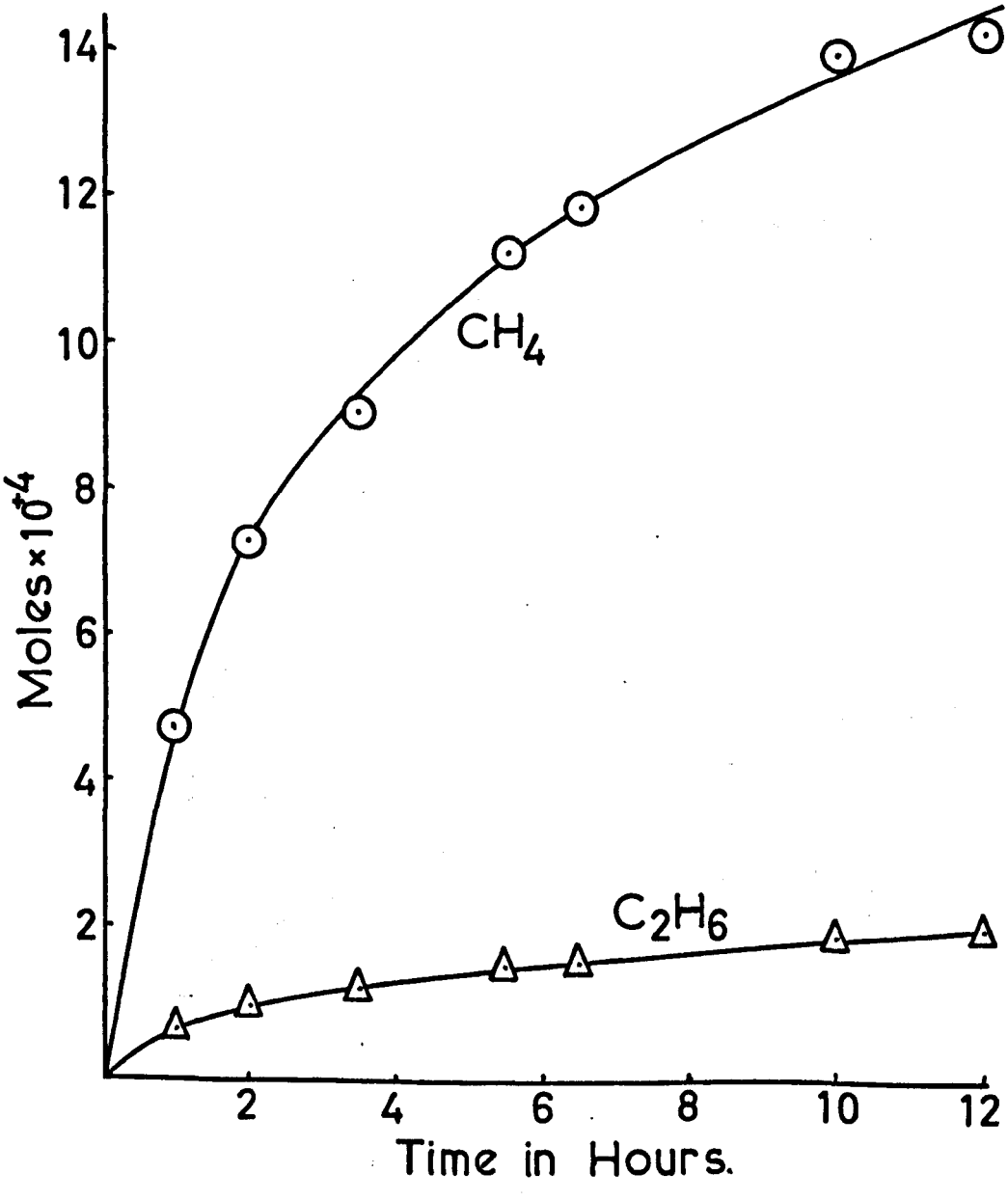

Figure 6.4

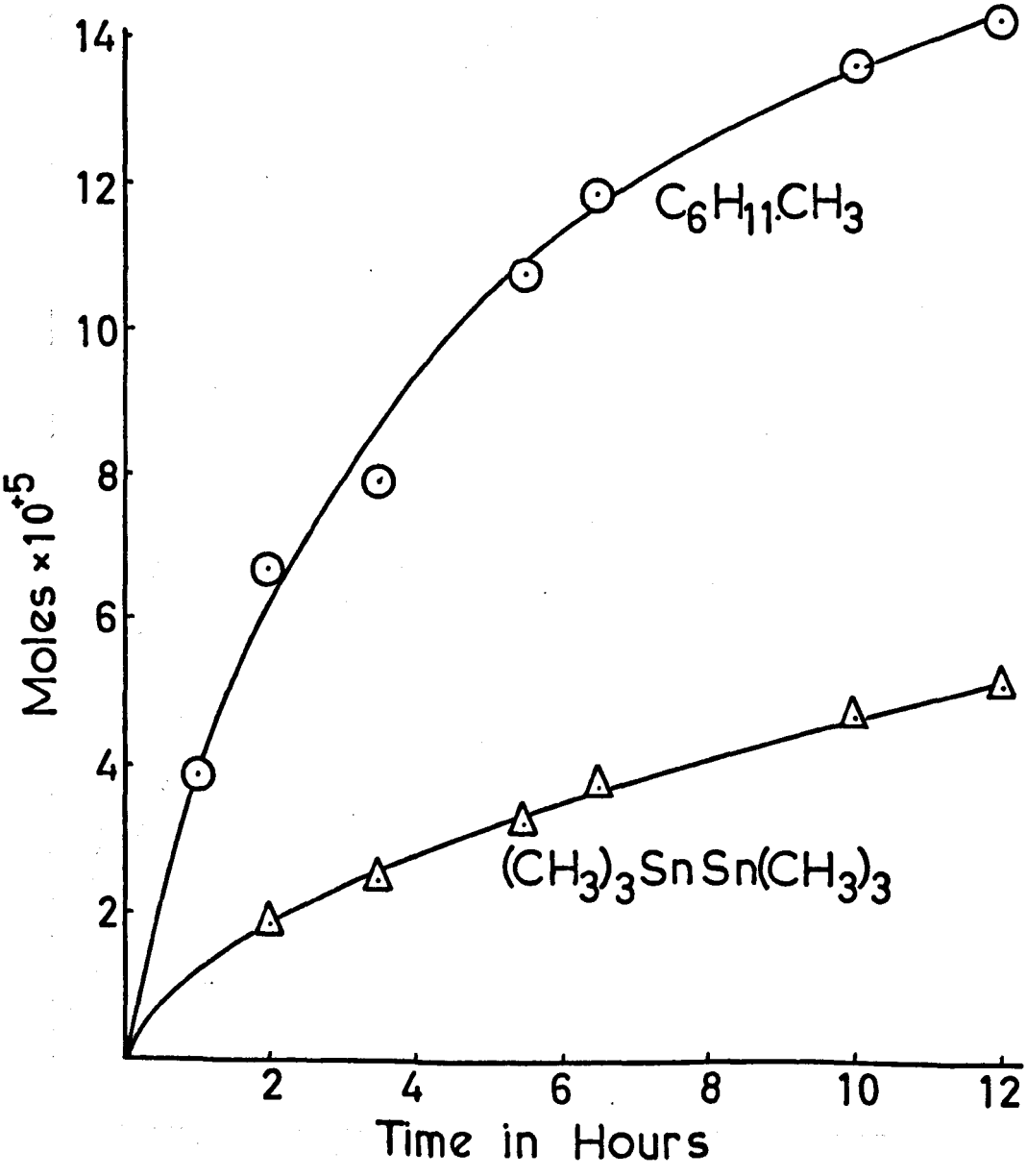
14
12
10
8
6
4
2
Moles x10+5
C6H11.CH3
(CH3)3Sn Sn(CH3)3
2
4
6
8
10
12
Time in Hours

Figure 6.5

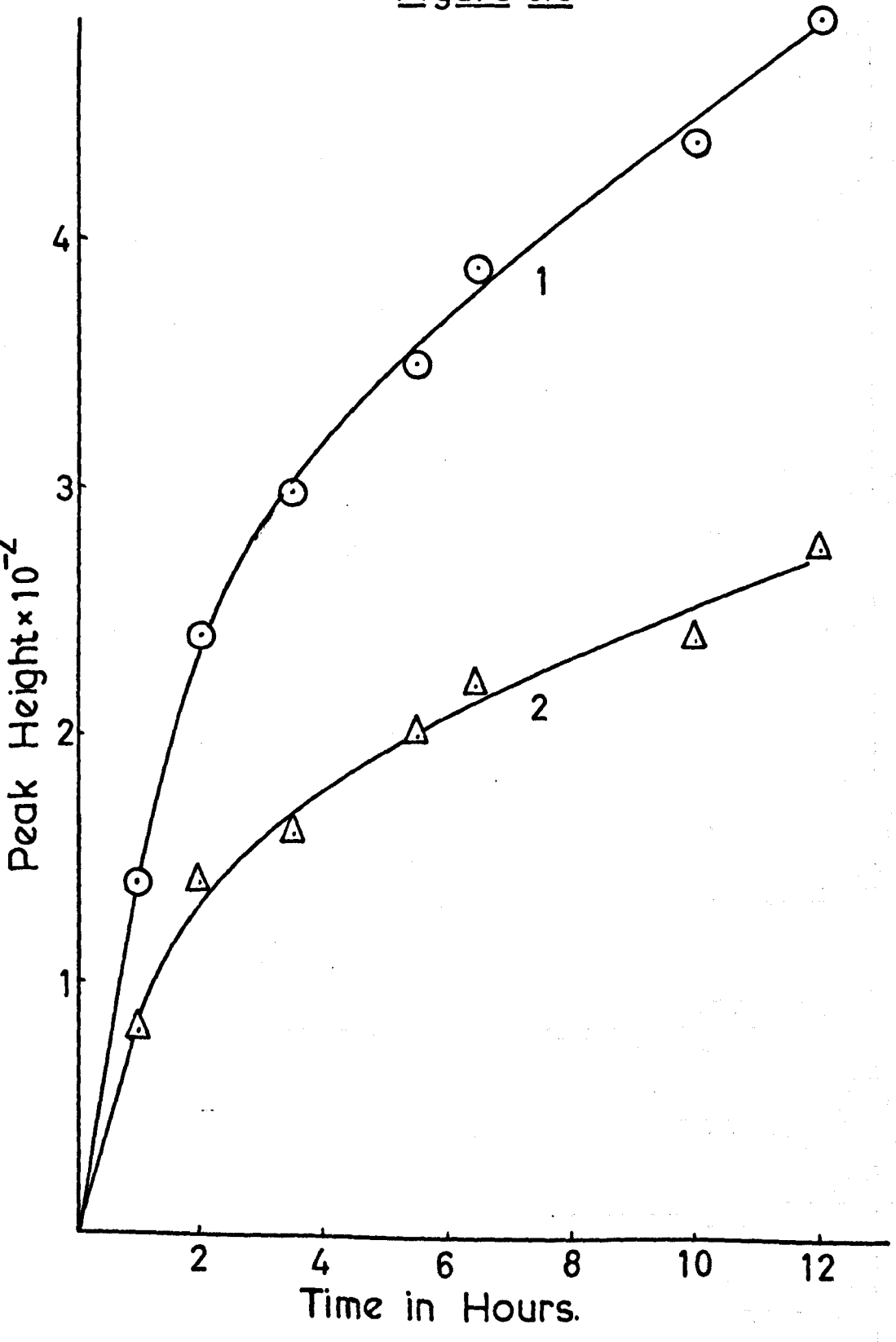

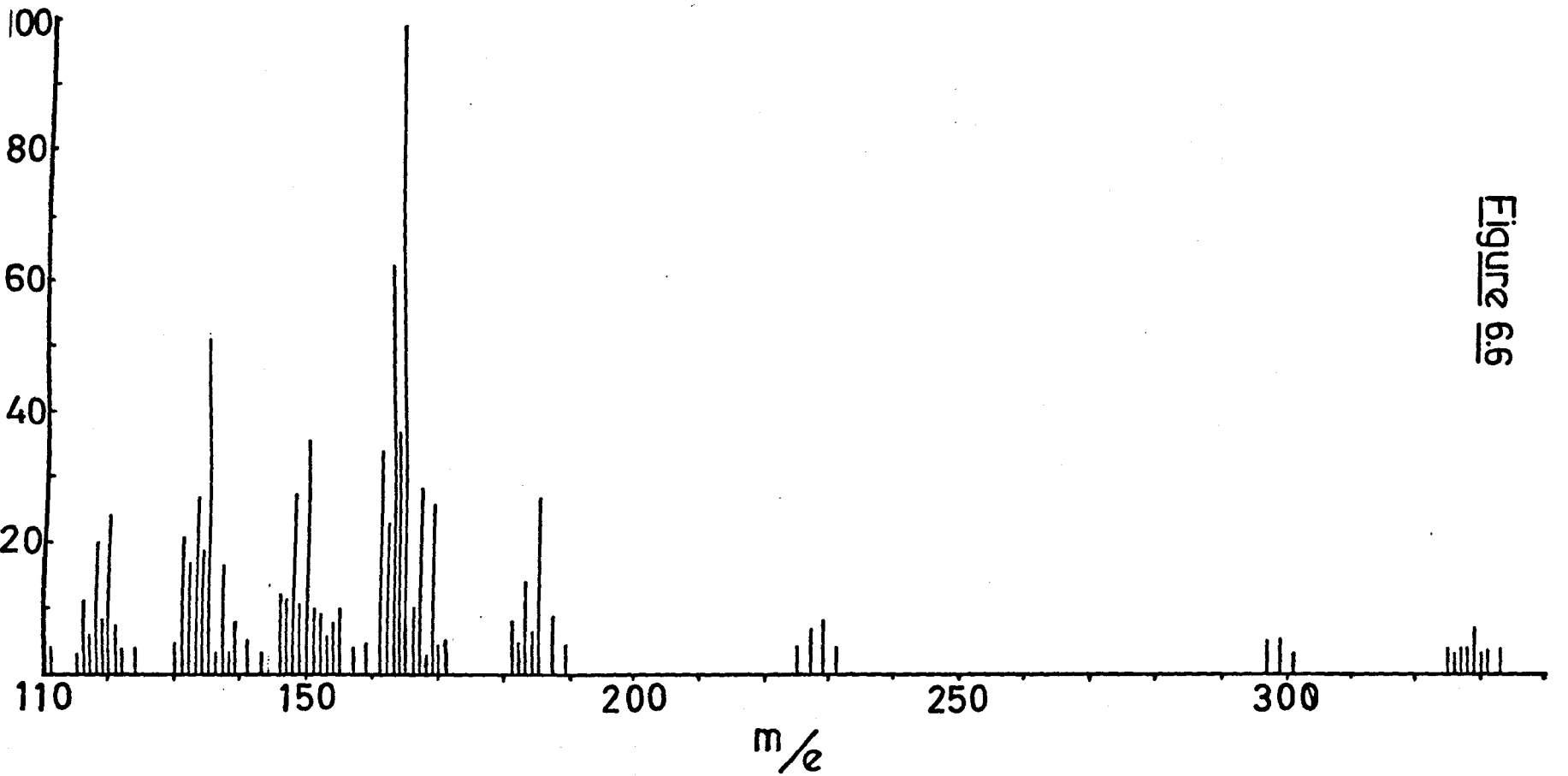

Figure 6.6

6.2 Iso Pentane

The experiment conditions were identical to those of the previous experiment, 12.5 mls isopentane and 7.5 mls tetramethyl stannane. Again four peaks were observed in the liquid phase, however, only one could be identified with assurance. The retention times of the production are shown in Figure 6.10. Again the solid precipitate was observed. Yields versus time are given in Figures 6.7 - 6.9.

TABLE 6.3

Irradiation Conditions: 17.5 mls iso pentane
7.5 mls tetramethyl stannane
Temperature 15°C
Irradiation time 0 - $8\frac{3}{4}$ hrs.

Analytical Conditions: Detector, flame ionisation
Column, Ap-L & Poropak Q
Temperature, 100, 130° and 50°C
Nitrogen 20, 30 p.s.a. and 20 p.s.i.

	6.7	6.7	6.8	6.9	6.9	6.9
Time	methane	ethane	$(CH_3)_3SnSn(CH_3)_3$	Peak 1	Peak 2	Peak 3
1 hr.	10.43×10^{-4}	7.32×10^{-5}	1.02×10^{-5}	2 x 50	3.2 x 50	2.10×10^{2}
2hrs7mins	15.85×10^{-4}	11.1×10^{-5}	2.79×10^{-5}	3.2 x 50	5.2 x 50	4.50×10^{2}
3 hrs	18.35×10^{-4}	12.9×10^{-5}	4.09×10^{-5}	4.5 x 50	7.2 x 50	6.0×10^{2}
5 hrs	23.78×10^{-4}	16.7×10^{-5}	5.32×10^{-5}	5.6 x 50	9.2 x 50	6.4×10^{2}
$8\frac{3}{4}$ hrs	28.37×10^{-4}	19.9×10^{-5}	7.12×10^{-5}	6.6 x 50	10.6 x 50	7.5×10^{2}
	moles	moles	moles	cms.	cms.	cms.

Figure 6.7

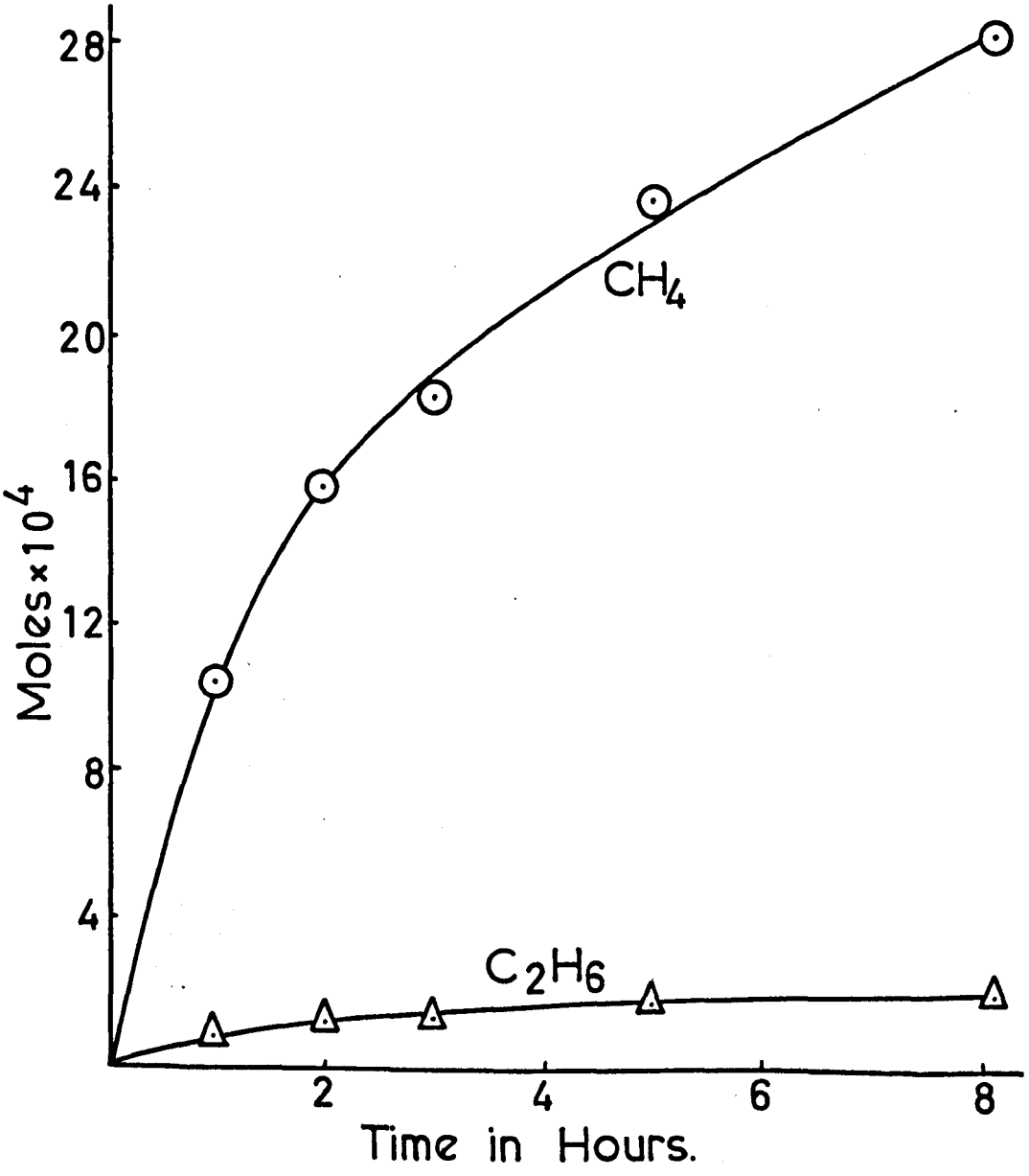

Figure 6.8

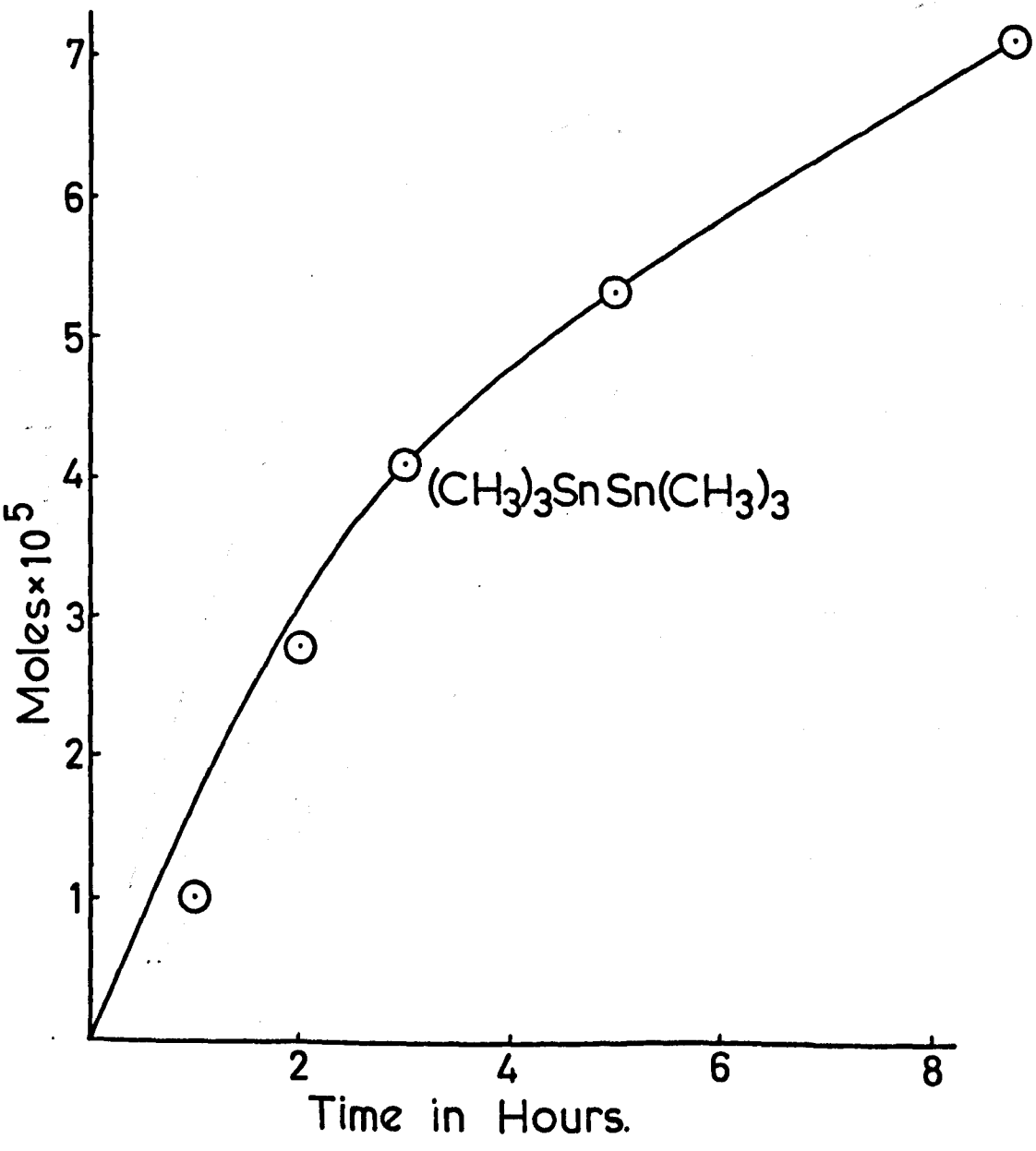

Figure 6.9

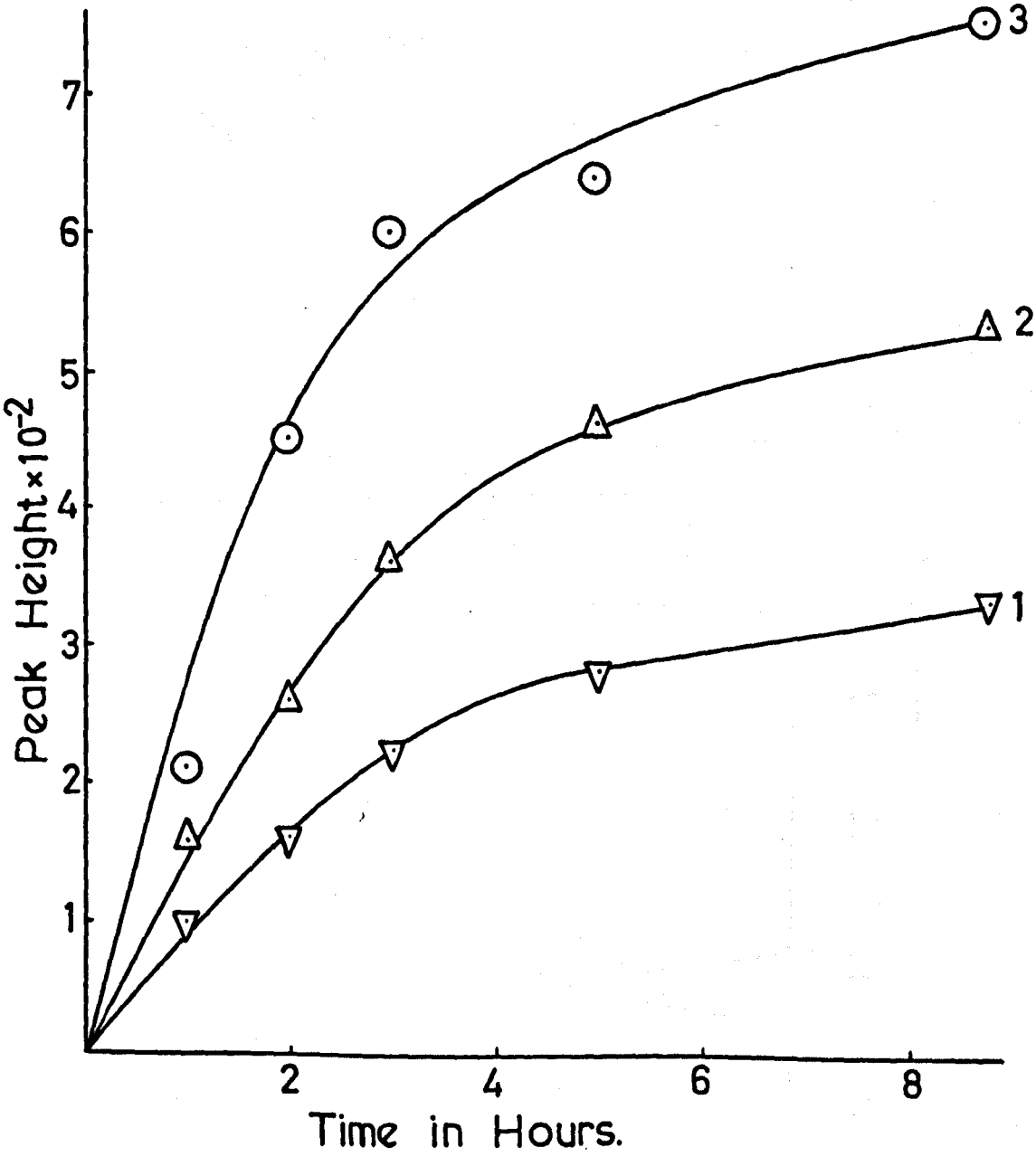

Figure 6.10

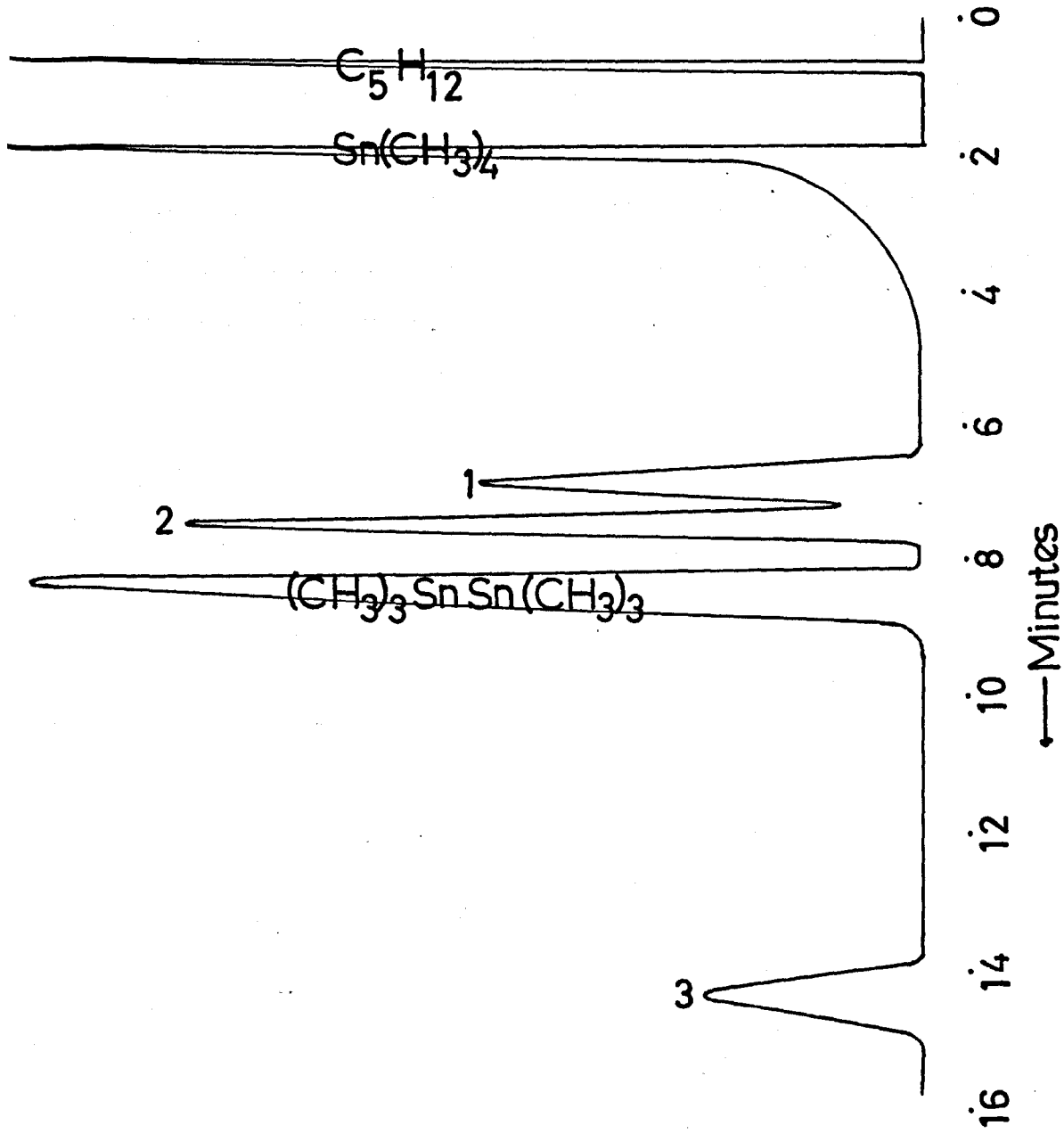

6.3 1-Octene

The experimental conditions were identical to those of the previous experiment, 17.5 mls 1-octene and 7.5 mls tetramethyl stannane. Three peaks were observed in the liquid phase and their retention times can be seen in Figure 6.11. One could be identified by comparative chromatography as hexamethyl distannane. The gas phase again consisted of a mixture of methane and ethane. The yellow solid precipitated out again after a period of time. The yields versus time are given in Figures 6.12 - 6.14.

TABLE 6.4

Irradiation Conditions: 17.5 mls 1-octene

7.5 mls tetramethyl stannane

Temperature 15°C

Irradiation time 0-13 hrs.

Analytical Conditions: Detector, flame ionisation

Column, Ap-L and Poropak Q

Temperature, 100, 130° & 50°C

Nitrogen, 20 p.s.i.

	6.12	6.12	6.13	6.14	6.14
Time	CH_4	C_2H_6	$(CH_3)_3SnSn(CH_3)_3$	Peak 1	Peak 2
1 hr	3.56×10^{-4}	4.63×10^{-5}	8.1×10^{-6}	1.74×10^{3}	1.02×10^{4}
2 hrs	5.44×10^{-4}	8.10×10^{-5}	13.4×10^{-6}	3.0×10^{3}	1.77×10^{4}
3½ hrs	8.55×10^{-4}	12.7×10^{-5}	23.3×10^{-6}	5.22×10^{3}	2.92×10^{4}
4 hrs	10.10×10^{-4}	15.0×10^{-5}			
5 hrs	11.65×10^{-4}	17.4×10^{-5}			
6 hrs	13.60×10^{-4}	20.3×10^{-5}	38.4×10^{-6}	7.95×10^{3}	4.25×10^{4}
8 hrs	16.32×10^{-4}	24.3×10^{-5}	51.6×10^{-6}	10.60×10^{3}	5.4×10^{4}
10 hrs	18.84×10^{-4}	28.1×10^{-5}			
12 hrs	20.4×10^{-4}	30.4×10^{-5}			
13 hrs	20.8×10^{-4}	31.0×10^{-5}	75.8×10^{-6}	13.4×10^{3}	6.83×10^{4}

Figure 6.11

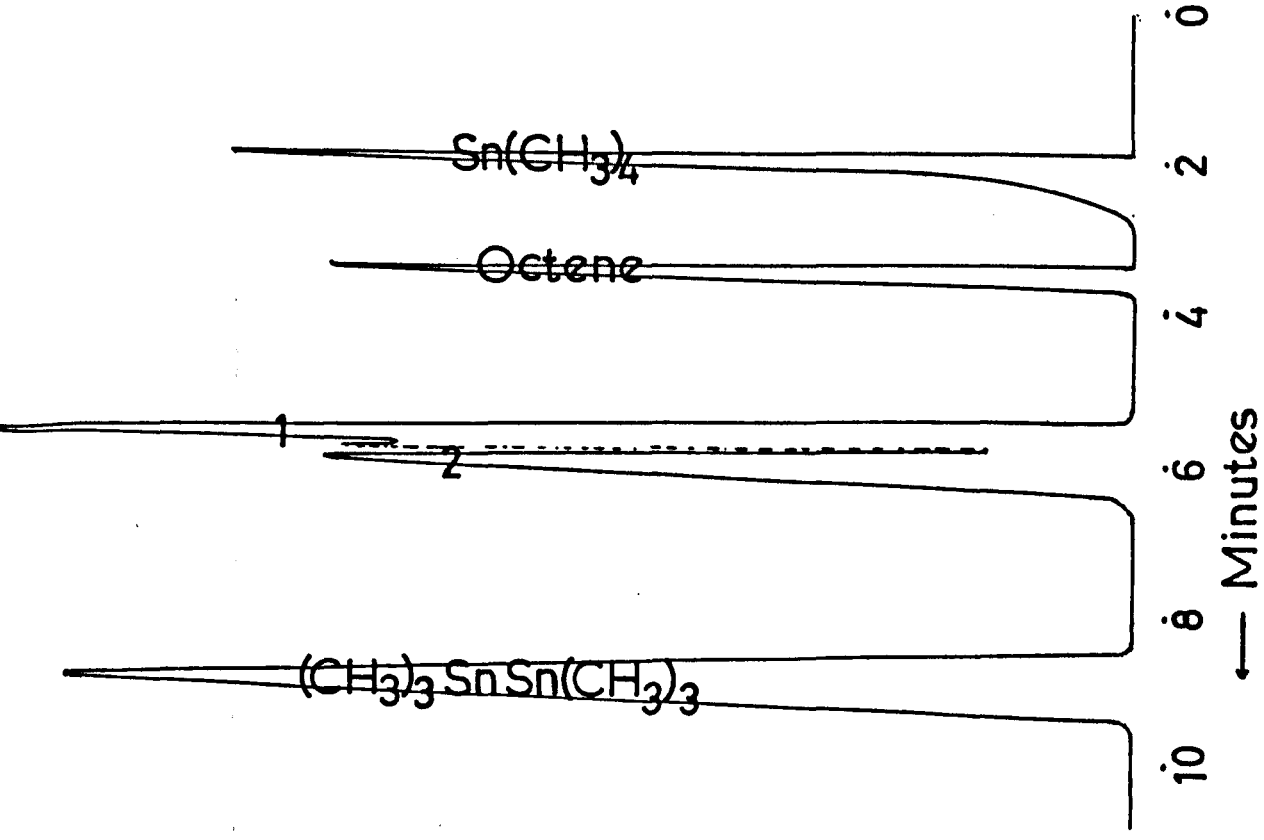

Figure 6.12

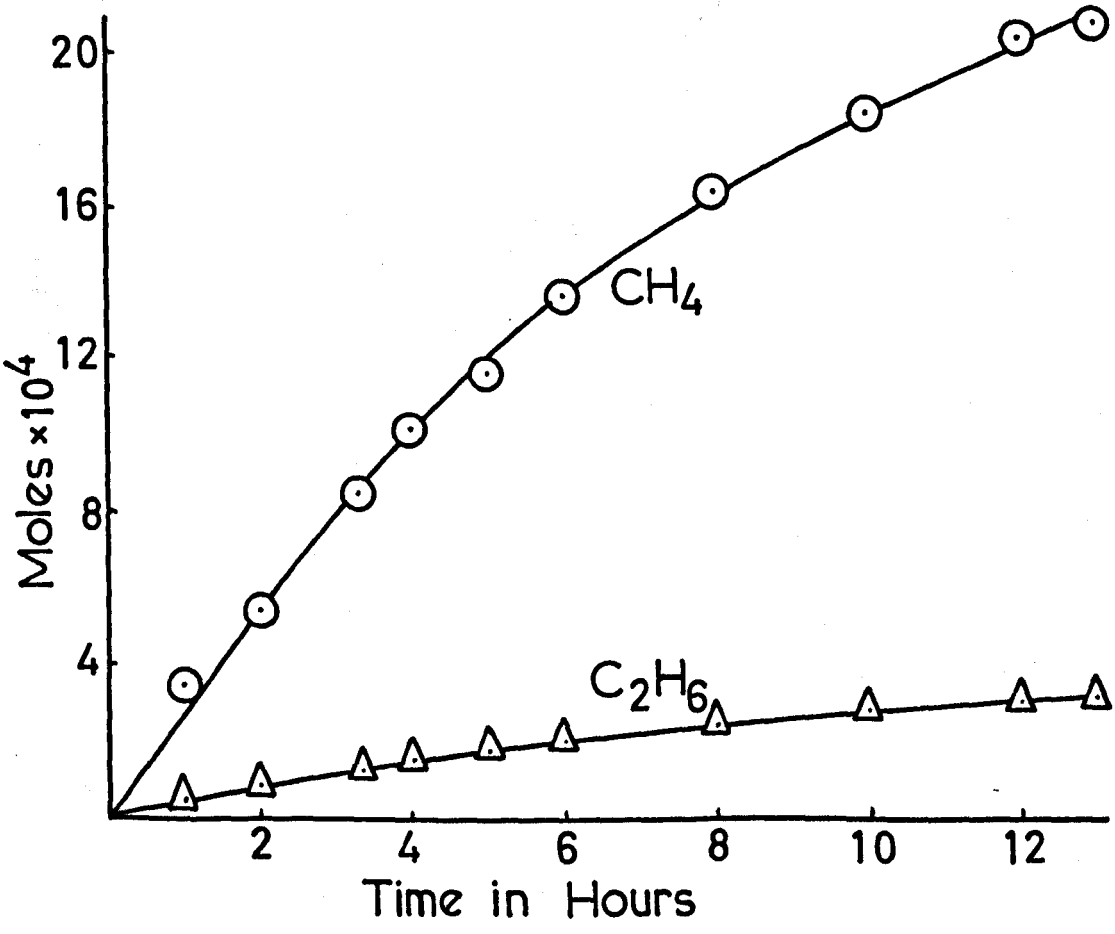

Figure 6.13

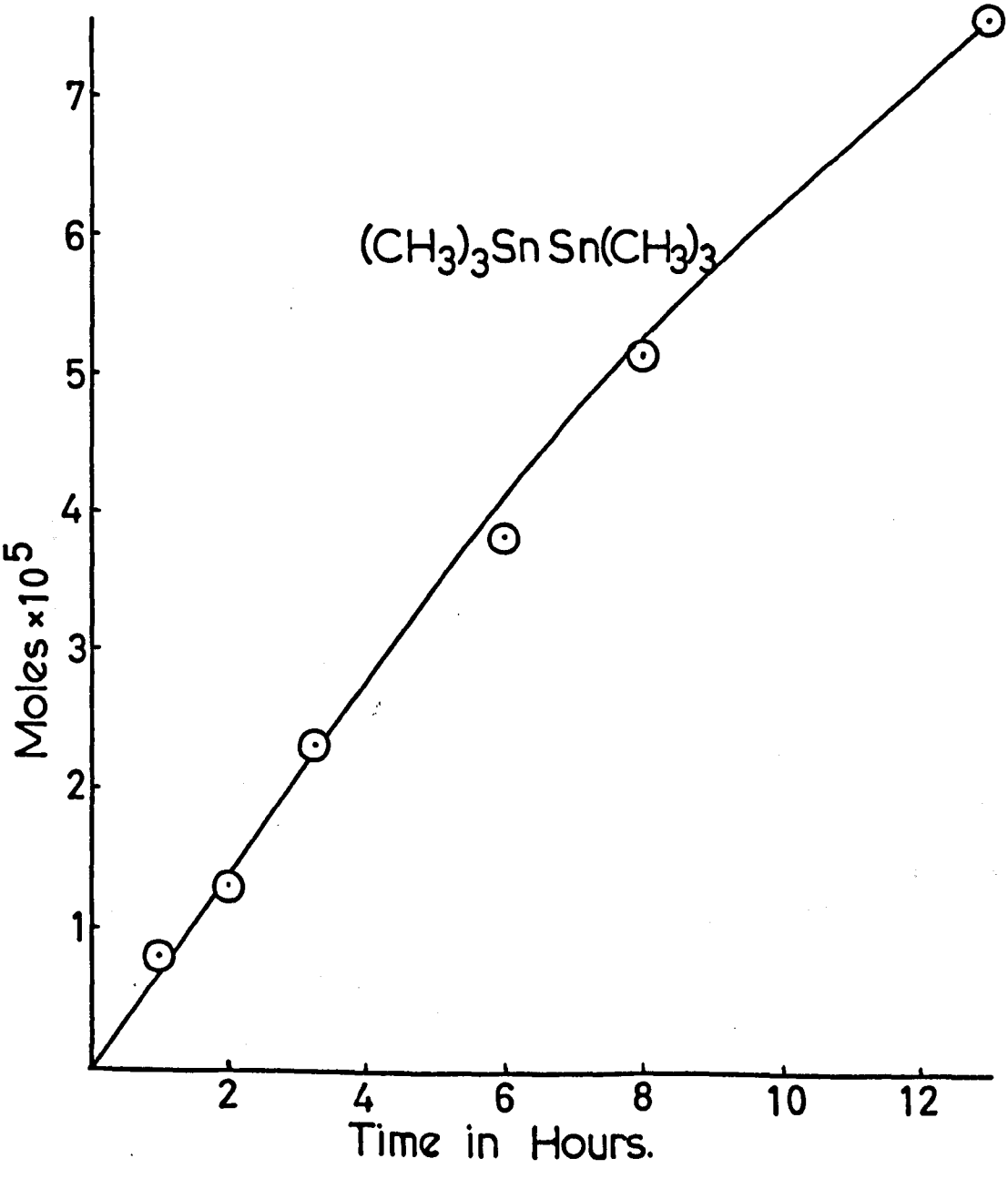
$(CH_3)_3Sn\,Sn(CH_3)_3$
Moles $\times 10^5$
1
2
3
4
5
6
7
2
4
6
8
10
12
Time in Hours.

Figure 6.14

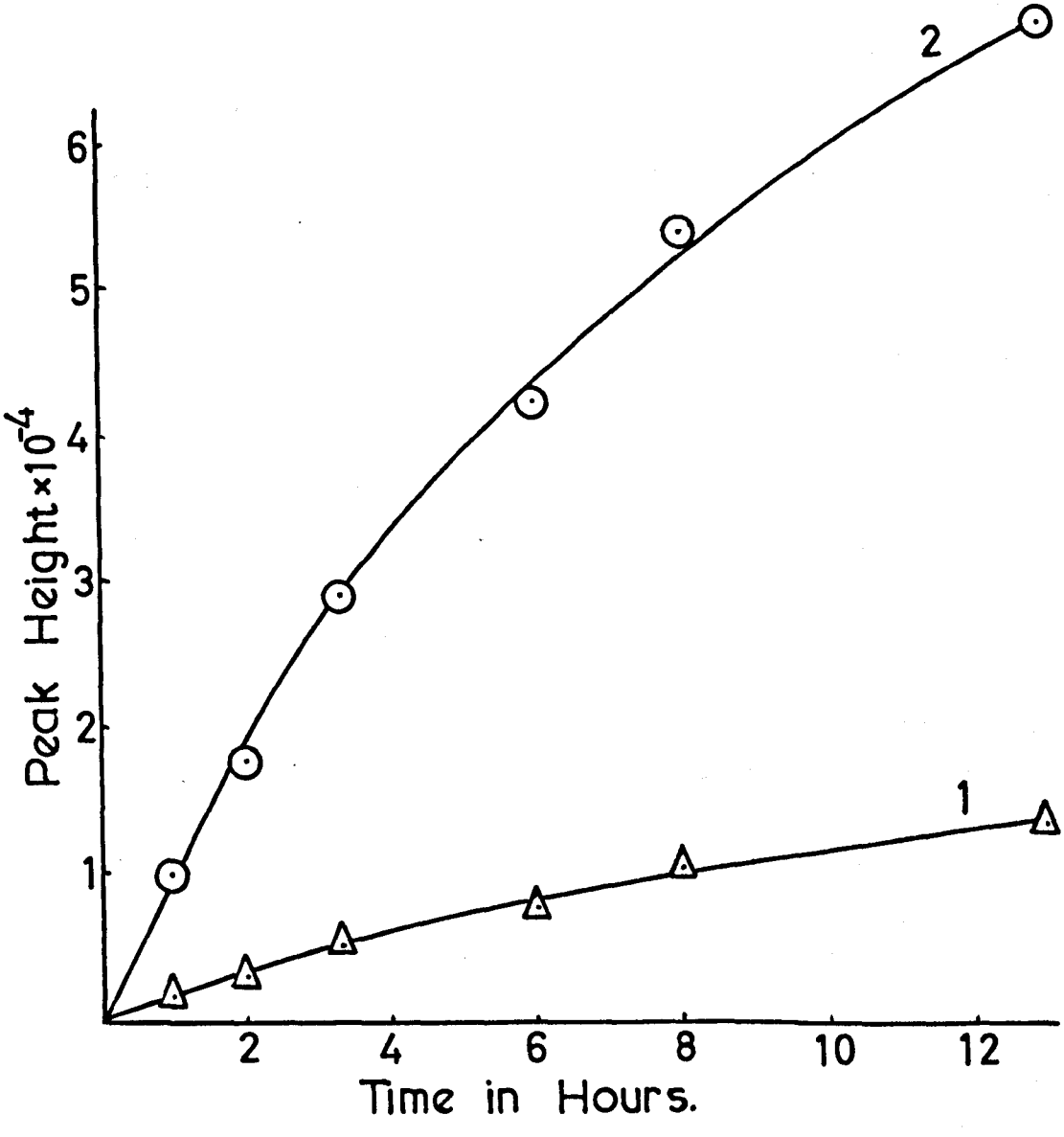

6.4 2-Methyl Pentane

Experimentally the conditions were slightly different than as before. 5 mls of tetramethyl stannane were added to 20 mls of 2-methyl pentane. The gaseous products were methane and ethane and the solution contained five product peaks, one of which was hexamethyl distannane. The remaining four peaks were not identified but had longer retention times than hexamethyl distannane. The yields and peak heights versus time are given in Table 6.5. The various retention times are shown in Figure 6.15.

TABLE 6.5

Irradiation Conditions:	20 mls 2-methyl pentane
	5 mls tetramethyl stannane
	Temperature 15°C
	Irradiation time 0 - 12 hrs
Analytical Conditions:	Detector: flame ionisation
	Column: Ap-L and poropak
	Temperature: 130°C and 50°C
	Nitrogen: 20 p.s.i.

TABLE 6.5

Time	CH_4	C_2H_6	$Me_3SnSnMe_3$	Peak 1	Peak 2	Peak 3	Peak 4
15mins	1.140×10^{-4}	1.998×10^{-5}					
30 "	2.089×10^{-4}	3.836×10^{-5}					
45 "	2.849×10^{-4}	4.996×10^{-5}					
75 "	3.988×10^{-4}	6.993×10^{-5}					
90 "	4.747×10^{-4}	8.326×10^{-5}					
105 "	5.318×10^{-4}	9.326×10^{-5}					
2 hrs	5.698×10^{-4}	9.991×10^{-5}	1.434×10^{-5}	2.25×10^{2}	2.3×10^{2}	1.2×10^{2}	0.4×10^{2}
3 "	7.597×10^{-4}	13.32×10^{-5}					
4 "	9.495×10^{-4}	16.65×10^{-5}	2.483×10^{-5}	3.2×10^{2}	3.75×10^{2}	1.7×10^{2}	0.8×10^{2}
5 "	11.40×10^{-4}	19.98×10^{-5}					
6 "	13.10×10^{-4}	22.98×10^{-5}	3.432×10^{-5}	3.3×10^{2}	4.70×10^{2}	1.95×10^{2}	0.9×10^{2}
7 "	14.62×10^{-4}	25.64×10^{-5}					
8 "	15.76×10^{-4}	27.64×10^{-5}	3.995×10^{-5}	3.7×10^{2}	5.75×10^{2}	2.15×10^{2}	1.15×10^{2}
9 "	16.90×10^{-4}	29.64×10^{-5}					
10 "	17.48×10^{-4}	30.64×10^{-5}	4.365×10^{-5}	4.0×10^{2}	5.95×10^{2}	2.25×10^{2}	1.25×10^{2}
12 "			4.646×10^{-5}	4.05×10^{2}	6.40×10^{2}	2.43×10^{2}	1.31×10^{2}
	Moles	Moles	Moles	cms	cms	cms	cms

Figure.6.15

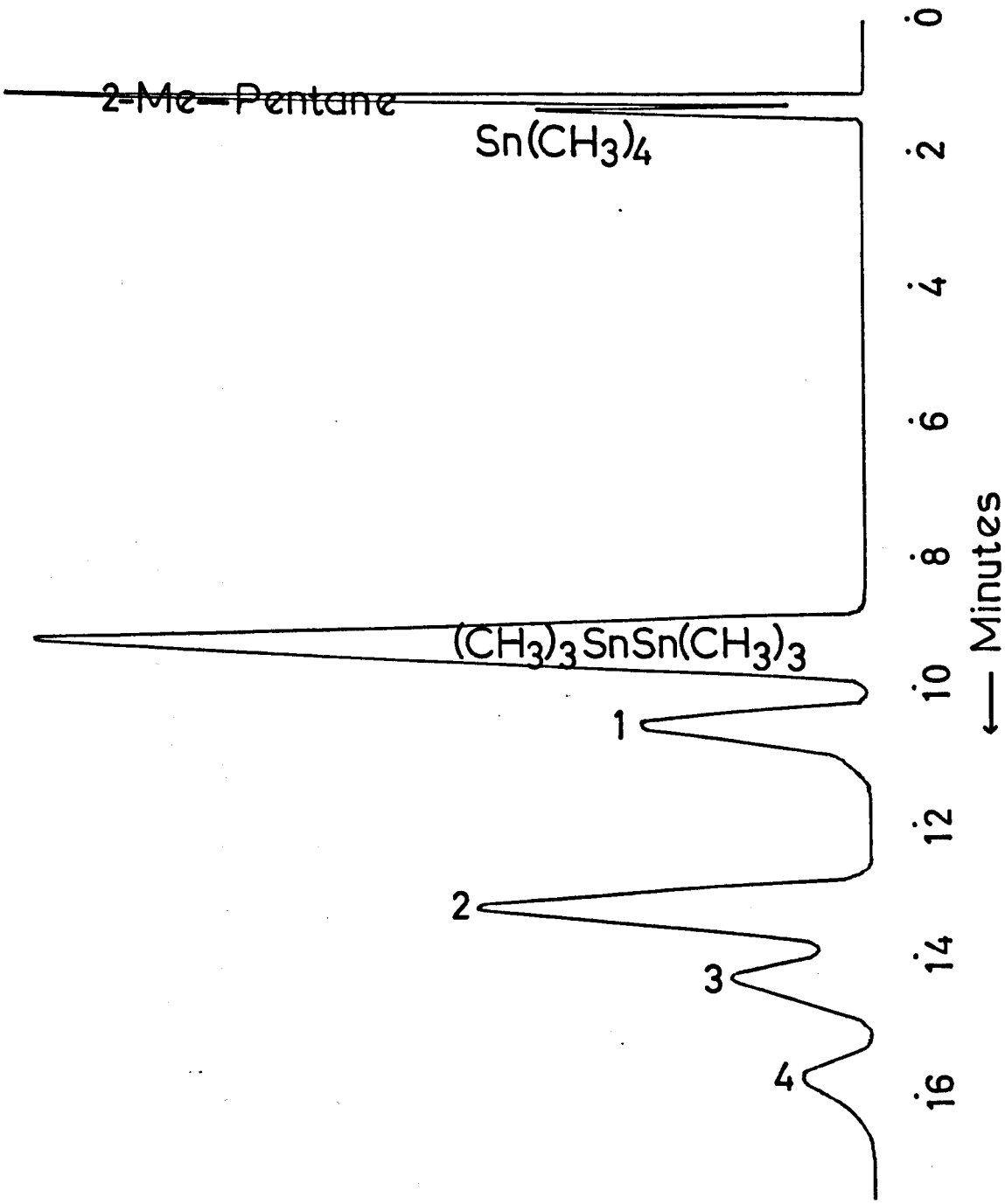
2-Me-Pentane
Sn(CH3)4
(CH3)3SnSn(CH3)3
1
2
3
4
0
2
4
6
8
10
12
14
16
Minutes

Figure 6.16

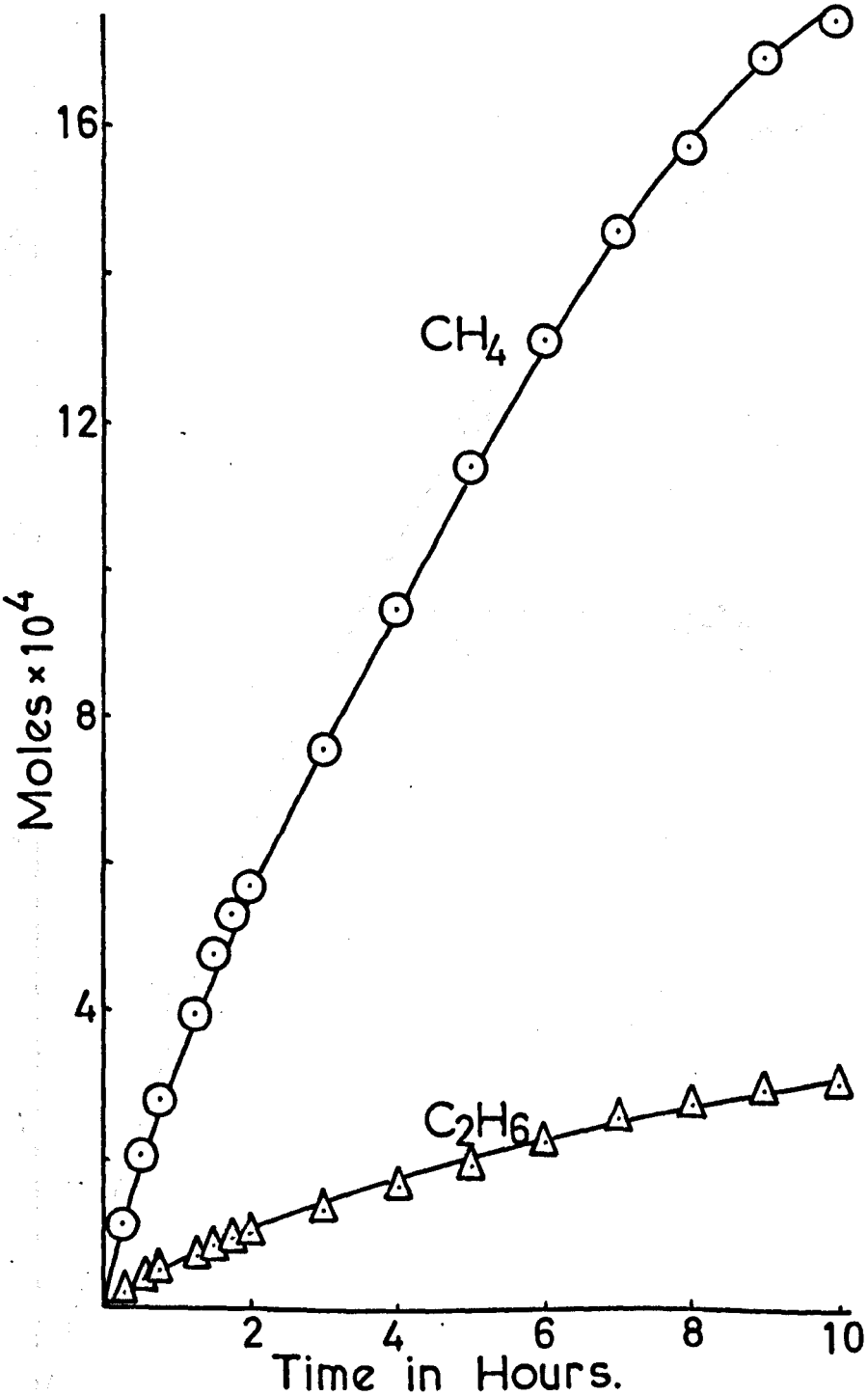

Figure 6.17

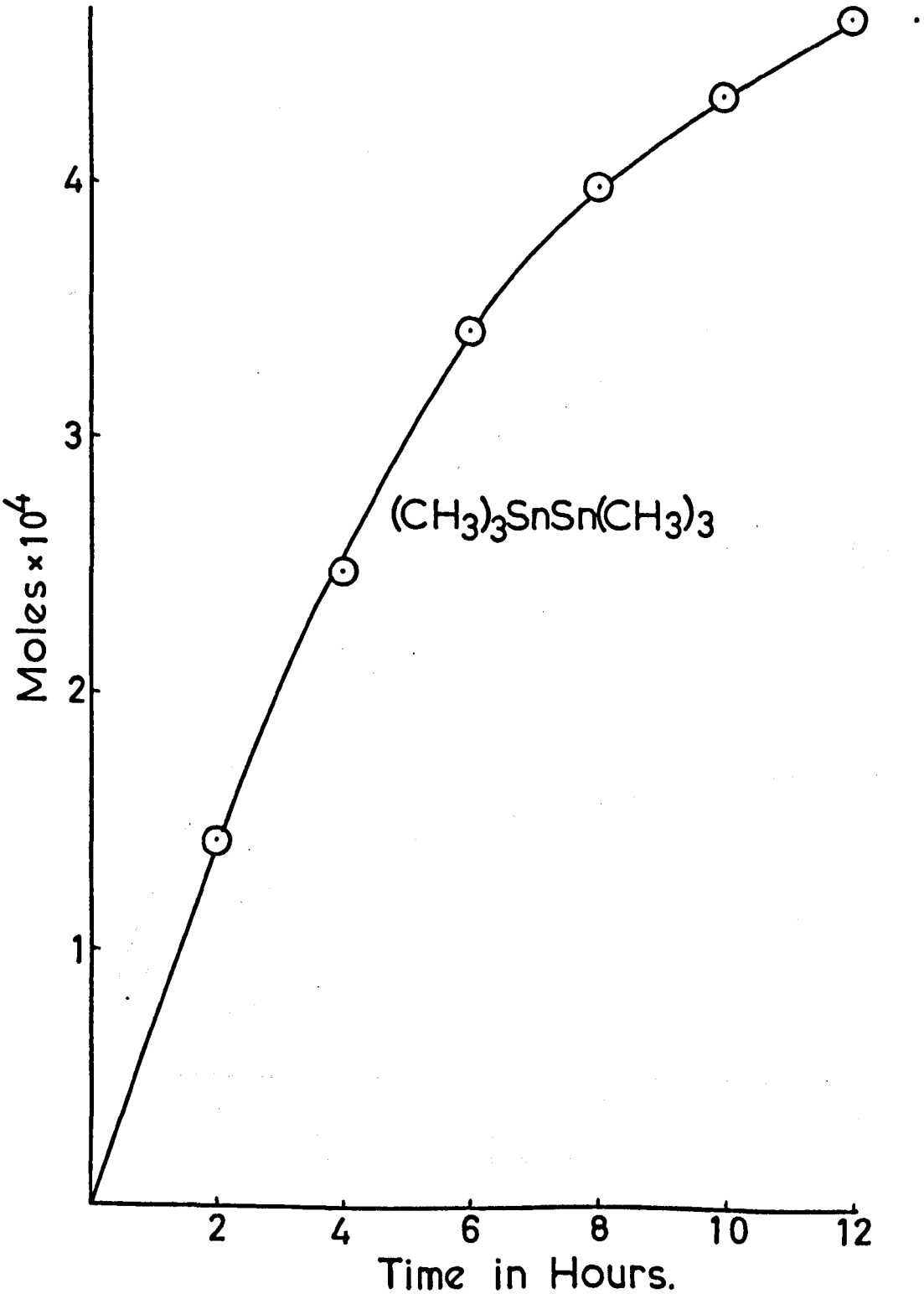

Figure 6.18

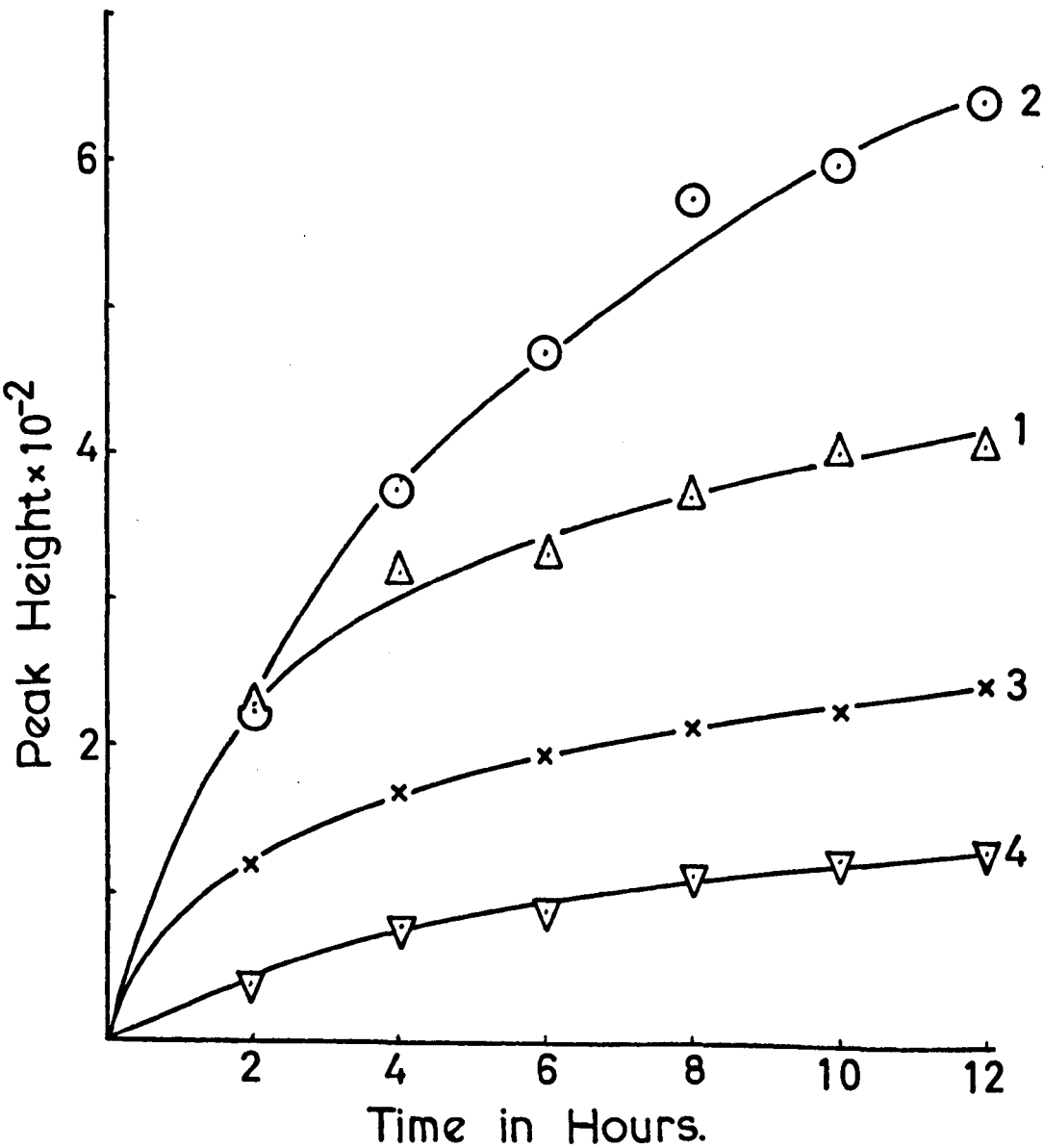

6.5 3-Methyl Pentane

The conditions of this experiment were as in 6.4. However, due to the absorption of 3-methyl pentane in the region of $Sn(CH_3)_4$ the reaction virtually stopped after two hours. The retention times of the products obtained can be seen in Figure 6.19.

6.6 Methanol

The experimental conditions were as in 6.4. Here again the reaction halted after two hours. The retention times of the products in the liquid phase are shown in Figure 6.20.

Figure 6.19

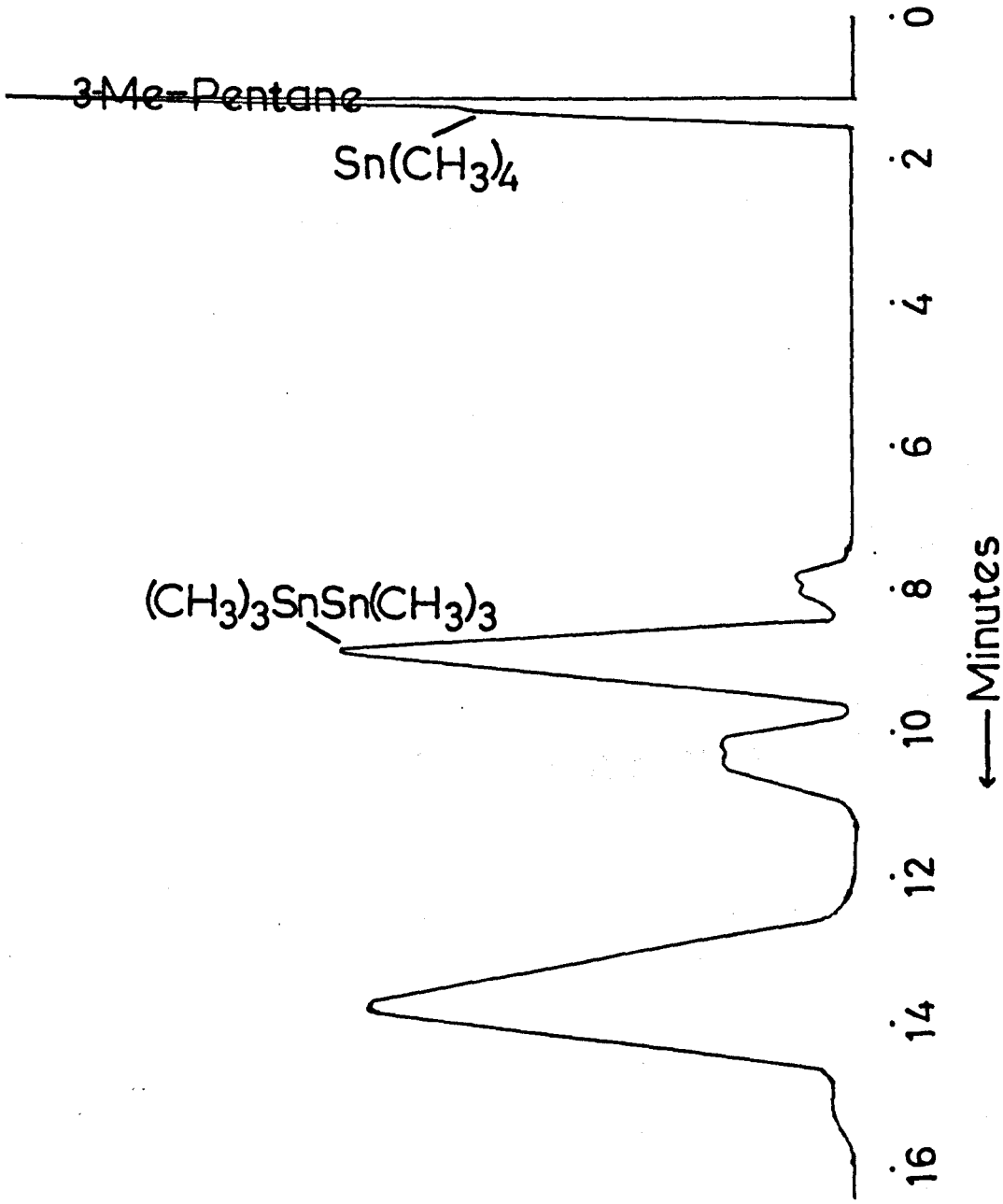

Figure 6.20

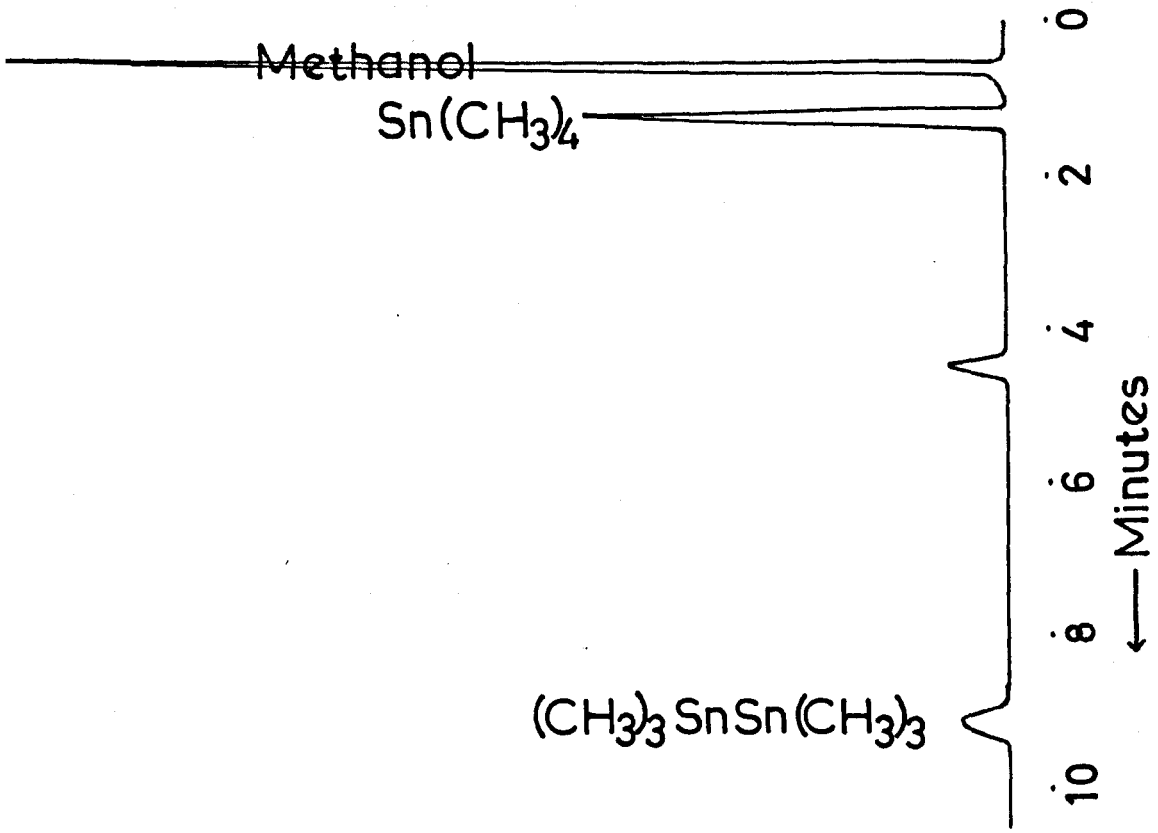

6.7 Tetramethyl Stannane

25mls pure tetramethyl stannane were placed in the reactor and irradiated for a total of 39 hrs. Methane and ethane were evolved as shown in Figure 6.22. Hexamethyl stannane was formed (Figure 6.23) as well as another compound (Figure 6.24). The retention times are shown in Figure 6.21.

TABLE 6.6

Irradiation Conditions: 25 mls tetramethyl stannane
Temperature 15°C
Irradiation time 36 hrs

Analytical Conditions: Detector: flame ionisation
Column: Ap-L and Poropak Q
Temperature: 130°C 50°C
Nitrogen: 20 p.s.i.

Time	CH_4	C_2H_6	$Me_3SnSnMe_3$	Peak
$2\frac{1}{2}$ hrs	3.65×10^{-4}	1.25×10^{-4}	3.03×10^{-5}	0.8×10^{3}
4 hrs	4.82×10^{-4}	1.66×10^{-4}	4.36×10^{-5}	1.03×10^{3}
6 hrs	5.8×10^{-4}	2.15×10^{-4}	5.90×10^{-5}	1.68×10^{3}
12 hrs	9.05×10^{-4}	3.35×10^{-4}	9.20×10^{-5}	2.70×10^{3}
18 hrs	11.75×10^{-4}	4.20×10^{-4}	11.40×10^{-5}	3.33×10^{3}
24 hrs	13.4×10^{-4}	4.70×10^{-4}	12.95×10^{-5}	3.71×10^{3}
30 hrs	14.2×10^{-4}	4.93×10^{-4}	13.90×10^{-5}	3.95×10^{3}
$37\frac{1}{2}$ hrs	14.62×10^{-4}	5.08×10^{-4}	14.52×10^{-5}	4.15×10^{3}
39 hrs	14.62×10^{-4}	5.08×10^{-4}	14.52×10^{-5}	4.15×10^{3}
	Moles	Moles	Moles	cms

Figure 6.21

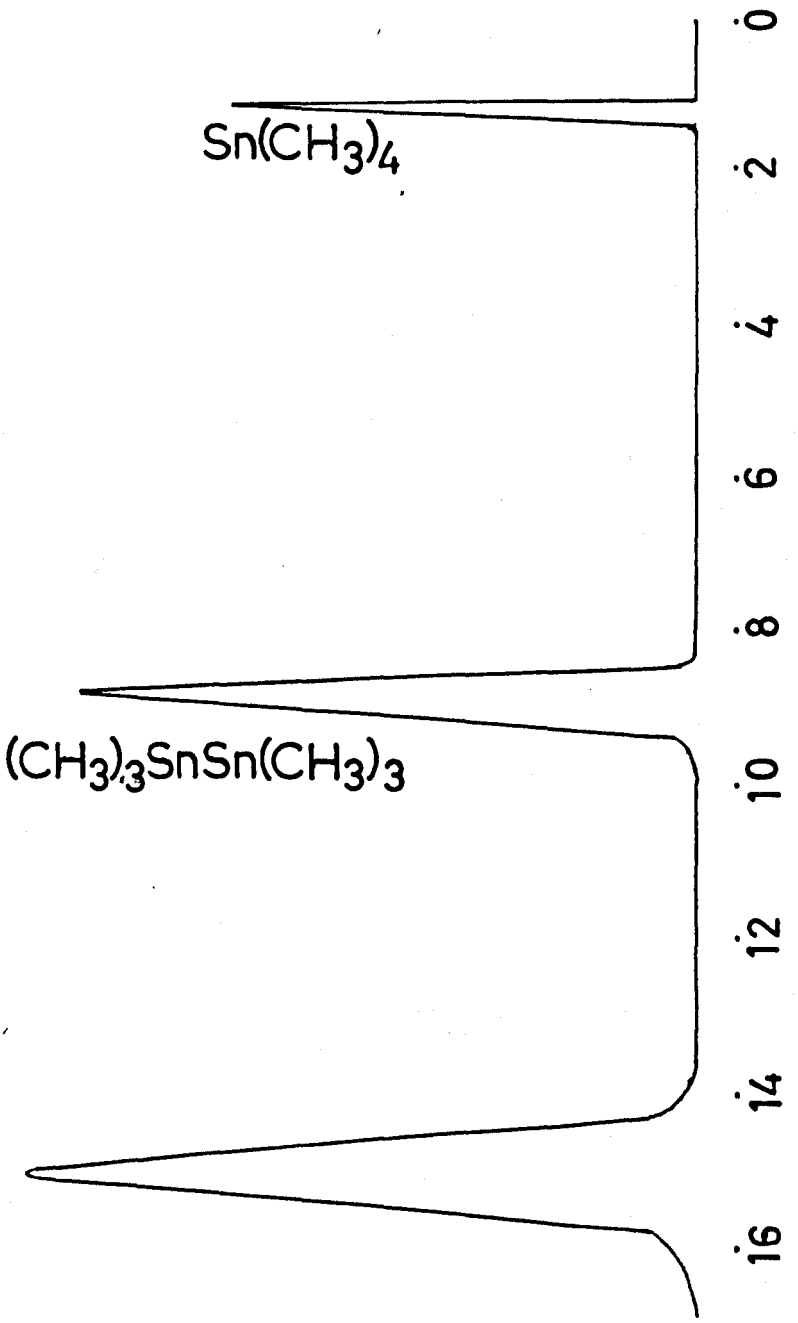

Figure 6.22

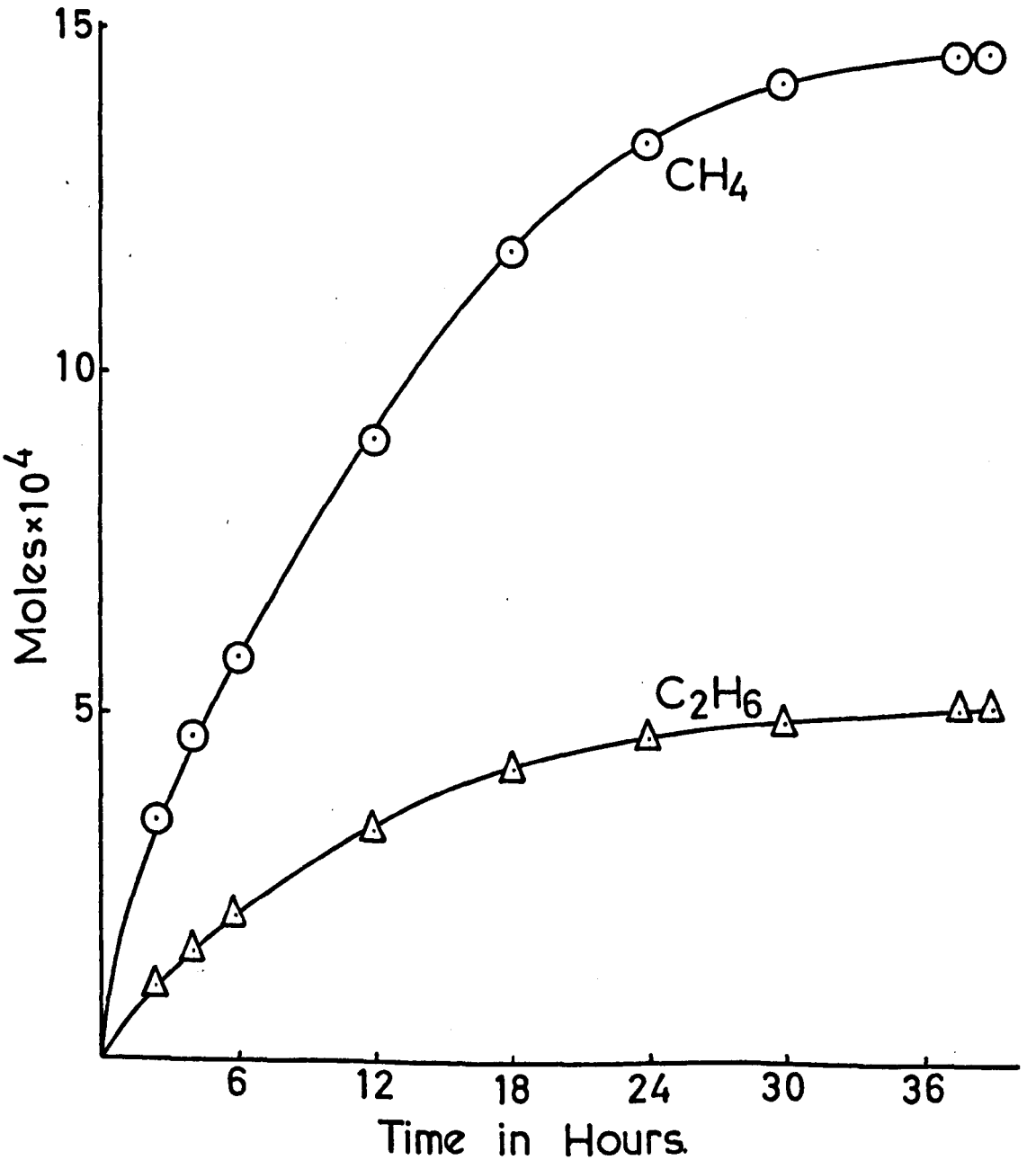

Figure 6.23

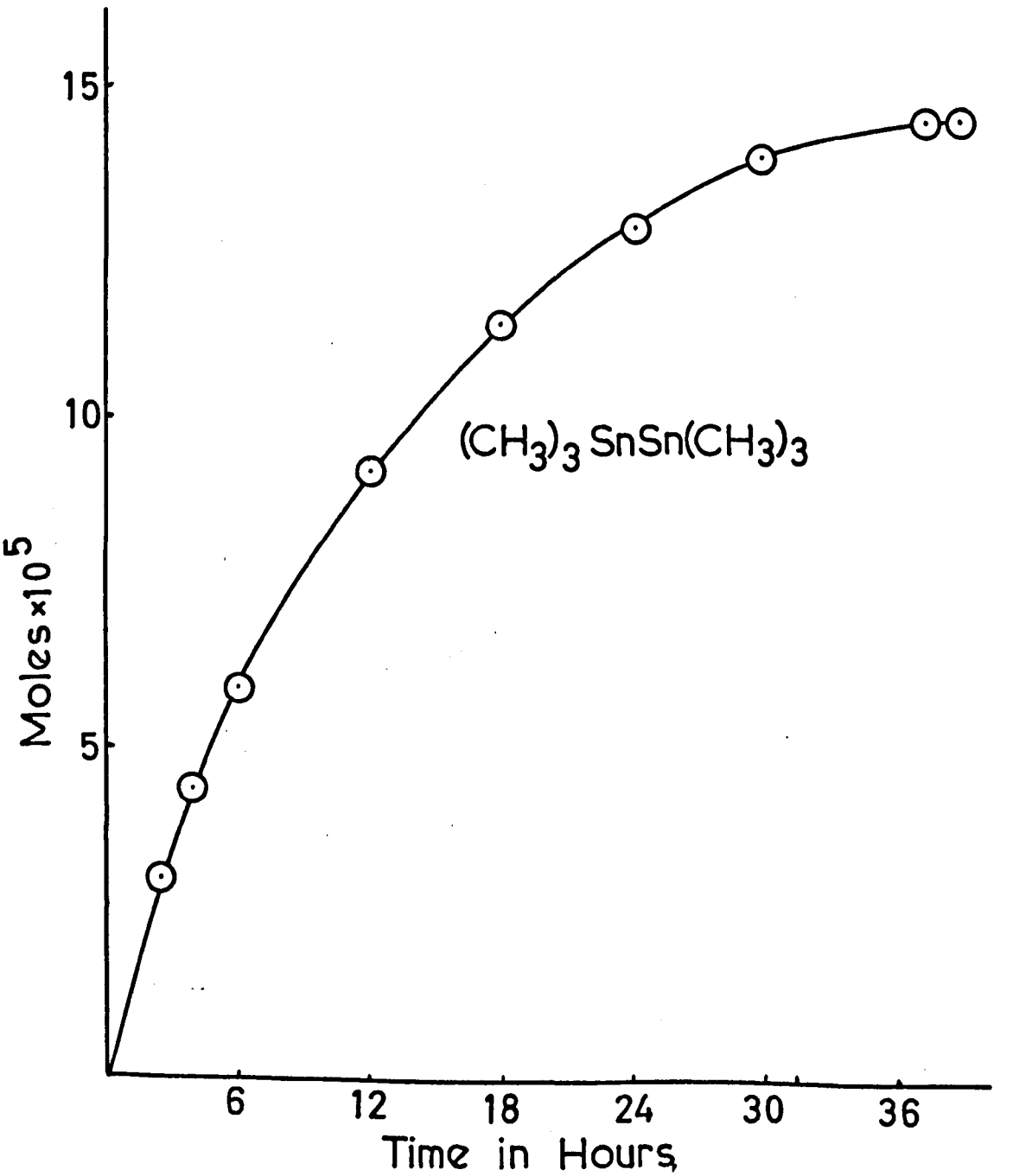

Figure 6.24

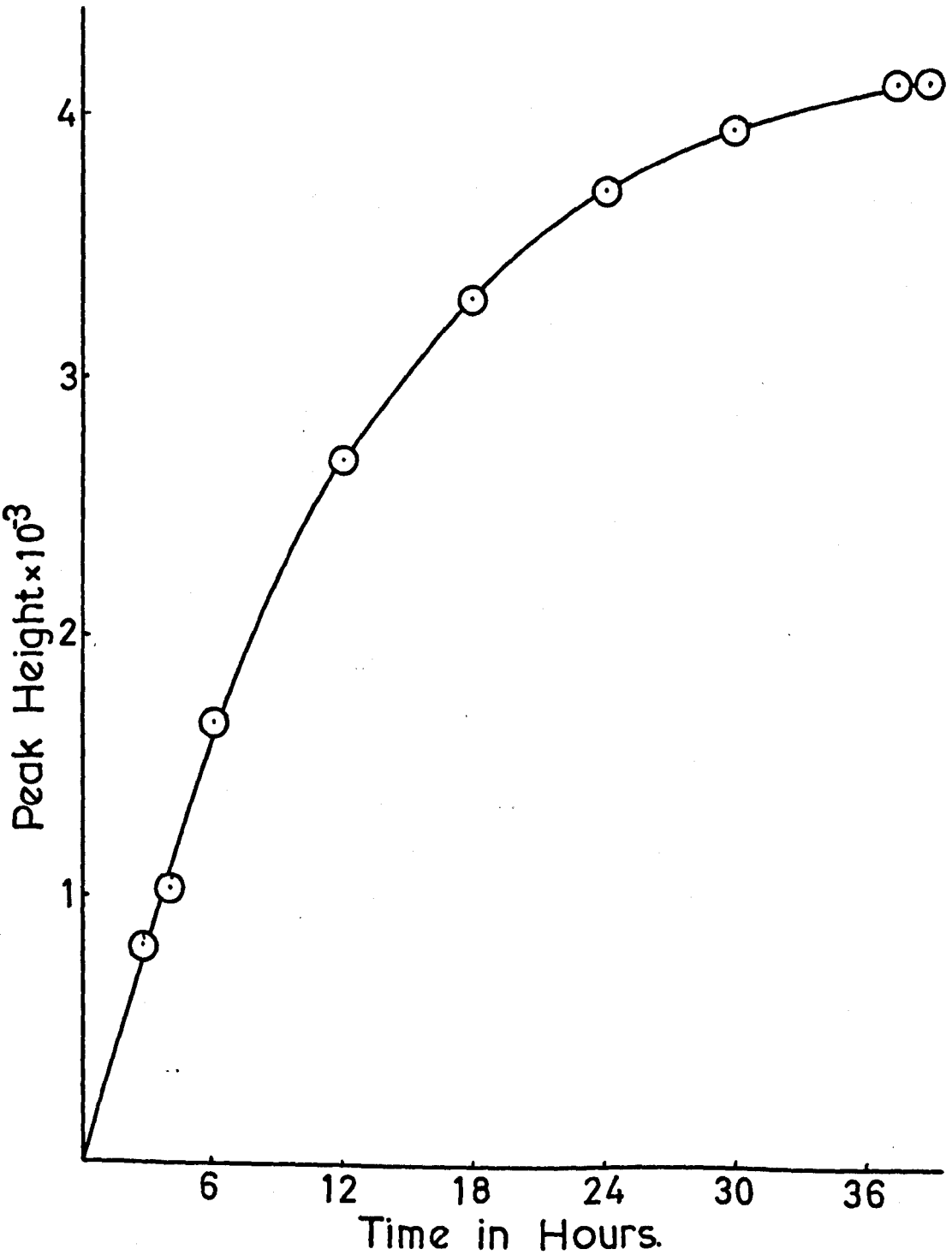

7. DISCUSSION: TETRAMETHYL STANNANE

Before discussing the proposed mechanism and kinetics a summary of the results and the interpretation is useful in explaining the derivation of the radical quantum yield at zero pressure.

7.1 Summary of Results

(1) The rate of formation of methane and ethane, at room temperature, is linear with time up to approximately fifteen minutes and then the rate decreases due to absorption of the exciting light by a film on the cell window. (Figures 3.2 and 3.3).

(2) Added inert gases (nitrogen and carbon dioxide) decreased the rate of formation of both methane and ethane to approximately a half over a very short range of pressure. Increasing the pressure does not affect the rate any further. (Figures 3.15 - 3.18).

(3) Increasing the pressure of tetramethyl stannane, above full absorption of light, increased the rates of formation of methane and ethane linearly, (figures 3.9 and 3.10), the increases do not appear to be related and presumably are derived from separate reactions.

(4) Nitric oxide, a radical scavenger, reduced the methane rate to the same extent as inert gases. The ethane rate was greatly reduced to a rate approximately equivalent to the methane rate. (Figures 3.23 and 3.24).

(5) Both the methane and ethane were linearly dependent on light intensity. (Figures 3.7 and 3.8).

(6) Increase in temperature increased the rates of formation of both methane and ethane. Further products were also observed, namely ethyl trimethyl stannane, trimethyl tin hydride and hexamethyl distannane. (Figures 3.13, 3.14, 3.34 and 3.35).

(7) The amount of tin produced in the reaction cell was not equivalent to the hydrocarbons formed. The cell window had a material remaining on it, after the removal of the tin, which absorbed in the 1849$\mathring{A}$ region and may be polymeric.

7.2 Interpretation

The interpretation of the results is aided by means of the mechanistic diagram below where tetramethyl stannane is represented by A:

Molecular Elimination Products

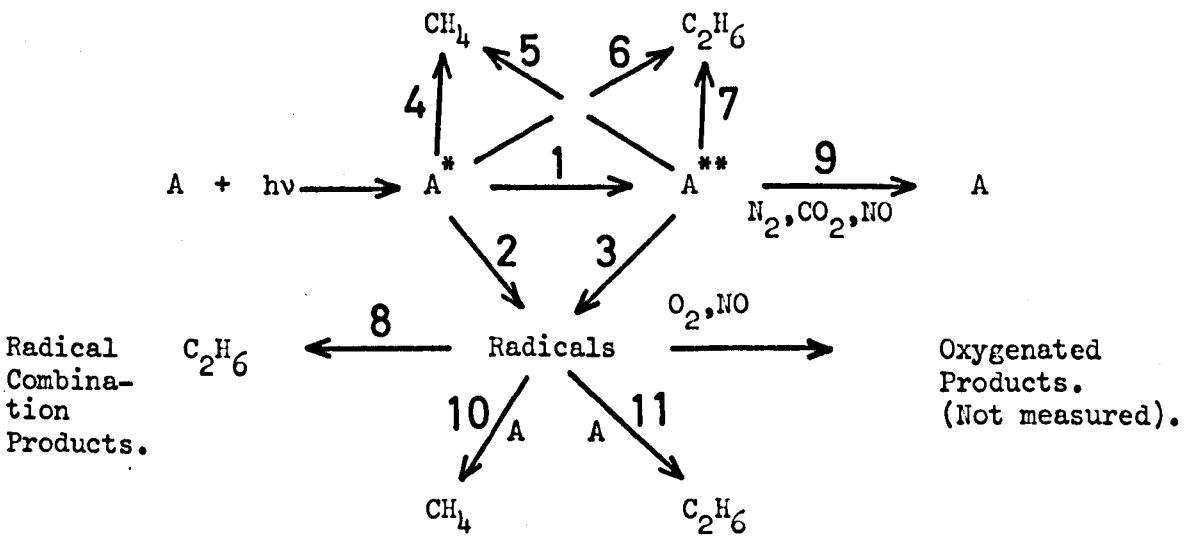

Radical Abstraction Products.

The rate of the individual reactions are subscripted R_1, R_2, R_3 etc.

The most important piece of evidence obtained from the experiments is that given by the addition of inert gases and radical scavengers. Addition of nitric oxide affected the rate of formation of methane to the

same extent as the inert gases. This shows that at room temperature the majority of methane is formed by a molecular elimination reaction. Being mainly molecular the methane rate should be proportional to intensity and this is born out by the intensity experiments. Inert gases affected the methane rate, which is mainly molecular, and the ethane rate, mainly radical combination, to the same extent the rate being reduced by a factor of three. This appears a phenomenon of the excited species in forming both types of products in the same ratio. Since the rates cannot be reduced further the possibility of two excited states arises, one of which can be collisionally deactivated and the other which decomposes before collisions can occur. Increasing the pressure of tetramethyl stannane does not quench the reaction and may be due to

$$A^{*} \text{ or } A^{**} + A \rightarrow A_1^{\neq} + A_2^{\neq} \qquad 7.I$$

the net effect of $A_1^{\neq} + A_2^{\neq}$ being the same as A^{*} or A^{**} in the number of radicals they produce and the amount of molecular elimination that takes place.

Looking at the mechanistic diagram the effects can easily be followed. Absorption of light by A (tetramethyl stannane) produces an electronically excited species A^{*}. The excited species can undergo three possible processes. Firstly, reaction 1 in which A^{*} is converted to the second excited state A^{**}. Secondly, reactions 4 and 6 which give rise to

the molecular elimination products methane and ethane. Thirdly, reaction 2 in which species A^{*} decomposes to give methyl radicals. The excited state A^{**} gives molecular elimination processes by reactions 5 and 7 and forms radicals by reaction 3.

On addition of inert gases the collisional deactivation of A^{**} by reaction 9 becomes predominant and reactions 3, 5 and 7 deminish. However reactions 2, 4 and 6 still occur and so molecular and radically formed products are still formed and at a constant rate. Nitric oxide affects A^{**} similarly to nitrogen and carbon dioxide and so reactions 3, 5 and 7 do not occur. However nitric oxide scavenges radicals forming oxygenated products and so reactions 8, 10 and 12 do not take place. Only reactions 4 and 6 take place forming methane and ethane by molecular elimination from A^{*}.

Increasing the temperature increases the rate constants of reactions 10 and 11, which are both abstraction processes having activation energies, and subsequently their rates. This leads to increases in the rates of formation of both methane and ethane. The increase in both rates of formation on increasing tetramethyl stannane pressure is due to reactions 10 and 11, the concentration of the stannane being fundamental in their rate equations.

7.3 Radical and Molecular Elimination Quantum Yields at Zero Pressure

In calculating the radical quantum yield and the quantum yields of the molecular elimination reactions three basic assumptions have to be considered:

Firstly, the collisional deactivation of species A^{**} occurs to the same extent whether the added gas be nitrogen, carbon dioxide or nitric oxide. In fact this appears to be the case as far as the molecular elimination reactions are concerned.

Secondly, the extrapolation of the linear portions of figures 3.9 and 3.10 to zero pressure of tetramethyl stannane gives a value at the ordinate that eliminates reactions 10 and 12 which depend on the concentration of tetramethyl stannane.

Thirdly, that the ratio of molecular elimination to radical formation is the same for both excited states i.e.

$$\frac{R_4}{R_2} = \frac{R_5}{R_3} = \frac{R_4 + R_5}{R_2 + R_3} \quad \text{and} \quad \frac{R_6}{R_2} = \frac{R_7}{R_3} = \frac{R_6 + R_7}{R_2 + R_3}$$

These equations can be written as follows:

$$\frac{R_4 + R_2}{R_2} = \frac{R_5 + R_3}{R_3} = \frac{R_2 + R_3 + R_4 + R_5}{R_2 + R_3} \qquad 7.II$$

and $$\frac{R_6 + R_2}{R_2} = \frac{R_7 + R_3}{R_3} = \frac{R_2 + R_3 + R_6 + R_7}{R_2 + R_3} \qquad 7.III$$

From the experimental results it is shown that

$$\frac{\text{Methane rate in excess } N_2}{\text{Total Methane Rate}} = \frac{\text{Ethane rate in excess } N_2}{\text{Total Ethane Rate}}$$

i.e. $$\frac{R_4 + R_{10}}{R_4 + R_5 + R'_{10}} = \frac{R_6 + R_8 + R_{11}}{R_6 + R_7 + R'_8 + R'_{11}}$$

here R_{10} is a measure of R_2 and so is $R_8 + R_{11}$

and R'_{10} is a measure of $R_2 + R_3$ and so is $R'_8 + R'_{11}$

thus $$\frac{R_4 + R_2}{R_4 + R_5 + R_2 + R_3} = \frac{R_6 + R_2}{R_2 + R_3 + R_6 + R_7}$$

Dividing 7.II by 7.III and rearranging one obtains this relationship.

As these assumptions are reasonably based then the calculation of the radical quantum yield can be undertaken.

The rate of formation of methane in excess nitrogen is given by $R_4 + R_{10}$. Reaction 10 depends on reaction 2 and thus the rate is given by $R_4 + R_2$. In excess nitric oxide the rate is given by R_2. Therefore

$$\frac{\text{Methane Rate in excess } N_2}{\text{Methane Rate in excess NO } (R_4)} = \frac{R_4 + R_2}{R_4} \qquad 7.IV$$

From this ratio the rate of molecular elimination of methane, R_4, can be calculated and is found to be 0.8×10^{-9} moles/minute. The rate of methane at the ordinate of figure 3.9 is a direct measure of $R_4 + R_5$ and is equal to 2.67×10^{-9} moles/minute and so a value of 1.9 moles/minute is obtained for R_5.

The rate of formation of ethane in excess inert gas is given by the sum $R_6 + R_8 + R_{11}$ and in excess nitric oxide by R_6.

i.e. $$\frac{\text{Ethane rate in excess } N_2}{\text{Ethane rate in excess NO}} = \frac{R_6 + R_8 + R_{11}}{R_6} = 38 \quad 7.V$$

But in excess nitrogen $R_8 + R_{11}$ is a measure of R_2 and so

$$\frac{R_6 + R_2}{R_6} = 38 \qquad 7.VI$$

The rate of ethane formation at 5 mm. $Sn(CH_3)_4$ pressure is given by $R_6 + R_7 + R_8 + R_{11}$, and in this case $R_8 + R_{11}$ can be substituted by $R_2 + R_3$. The rate at the ordinate of figure 3.10 is given by $R_6 + R_7 + R_8$, thus

$$\frac{\text{Ethane Rate at 5 mm. } Sn(CH_3)_4}{\text{Ethane Rate at 0 mm.}} = \frac{R_6 + R_7 + R_2 + R_3}{R_6 + R_7 + R_8} = 1.0 \qquad 7.VII$$

From equation 7.II

$$\frac{R_6 + R_2}{R_6} = \frac{R_6 + R_7 + R_2 + R_3}{R_6 + R_7} \text{ and thus } = 38 \qquad 7.VIII$$

dividing 7.VIII by 7.VII the following equation is obtained

$$\frac{R_6 + R_7 + R_8}{R_6 + R_7} = 38 \qquad 7.IX$$

and at 0 mms. $Sn(CH_3)_4$ the rate is equal to $R_6 + R_7 + R_8$. A value for $R_6 + R_7$, the total molecular elimination of ethane, can be obtained and thus R_8, which is the rate of ethane formation by radical combination and is equal to 10.0×10^{-8} moles/minute. $R_6 + R_7$ is equal to 2.8×10^{-9} moles/minute and R_6, the ethane rate in excess NO, equals 1.0×10^{-9} moles/minute and therefore R_7 equals 1.8×10^{-9} moles/minute.

The rate of formation of methyl radicals at zero pressure is thus equal to twice the value of R_8 and the quantum yield is:

$$\phi \text{ (methyl)} = \frac{10 \times 10^{-8} \times 2 \times 0.61}{3.88 \times 10^{-8}}$$

$$\underline{\phi \text{ (methyl)} = 3.14} \qquad 7.X$$

The molecular elimination reaction giving methane and ethane have

quantum yields below:

$$\phi \text{ (methane)} = \frac{2.67 \times 10^{-9} \times 0.61}{3.88 \times 10^{-8}}$$

$$\underline{\phi \text{ (methane)} = 0.04} \qquad \text{7.XI}$$

$$\phi \text{ (ethane)} = \frac{2.8 \times 10^{-9} \times 0.61}{3.88 \times 10^{-8}}$$

$$\underline{\phi \text{ (ethane)} = 0.04} \qquad \text{7.XII}$$

7.4 Mechanism

The quantum yield of methyl radicals shows that three methyl radicals are formed from the excited states. The thermochemistry data (Section 1.10) shows that insufficient energy is supplied in light of wavelength 1849Å to remove all four groups. There is no evidence to show whether the three methyl groups are removed stepwise or simultaneously and so can only be shown as a complete process. The reactions necessary to explain the experimental phenomena at zero pressure are identical to those shown diagramatically in Section 7.2 and are as follows:

$$Sn(CH_3)_4 + h\nu \xrightarrow{k_0 I} Sn(CH_3)_4^{*} \qquad 7.0$$

$$Sn(CH_3)_4^{*} \xrightarrow{k_1} Sn(CH_3)_4^{**} \qquad 7.1$$

$$Sn(CH_3)_4^{*} \xrightarrow{k_2} 3CH_3 + SnCH_3 \qquad 7.2$$

$$Sn(CH_3)_4^{**} \xrightarrow{k_3} 3CH_3 + SnCH_3 \qquad 7.3$$

$$Sn(CH_3)_4^{*} \xrightarrow{k_4} CH_4 + ... \qquad 7.4$$

$$Sn(CH_3)_4^{**} \xrightarrow{k_5} CH_4 + ... \qquad 7.5$$

$$Sn(CH_3)_4^{*} \xrightarrow{k_6} C_2H_6 + ... \qquad 7.6$$

$$Sn(CH_3)_4^{**} \xrightarrow{k_7} C_2H_6 + ... \qquad 7.7$$

$$CH_3 + CH_3 \xrightarrow{k_8} C_2H_6 \qquad 7.8$$

The fate of the $SnCH_3$ species formed in 7.2 and 7.3 is unknown but it is possible that it may be incorporated in a polymer. At zero pressure there is the possibility of a methyl radical reacting with $SnCH_3$ to form ethane and tin and this would explain non-stoichiometric analysis of tin. It is possible that the molecular portions of methane and ethane are formed in the same molecular elimination from either excited species, however no evidence for this was obtained and therefore they must be separated.

On addition of inert gas, nitrogen, carbon dioxide or nitric oxide, the second excited state is collisionally deactivated;

$$Sn(CH_3)_4^{**} + M \xrightarrow{k_9} Sn(CH_3)_4 + M \qquad 7.9$$

Increasing the pressure of tetramethyl stannane causes further secondary reactions producing methane by hydrogen abstraction and ethane by methyl group abstraction by methyl radicals. The increases in methane and ethane appear to be independent of one another, the ethane rate increasing approximately eight times faster than the methane rate. Consequently they are accorded separate reactions:

$$CH_3 + Sn(CH_3)_4 \xrightarrow{k_{10}} CH_4 + CH_2Sn(CH_3)_3 \qquad 7.10$$

$$CH_3 + Sn(CH_3)_4 \xrightarrow{k_{11}} C_2H_6 + {}^{\bullet}Sn(CH_3)_3 \qquad 7.11$$

The trimethyl stannyl radical and the trimethyl stannyl methylene radical being presumably included in the polymeric material as no combination products were observed at room temperature.

Increasing the temperature increases the rates of reactions 7.10 and 7.11 and radical combination products are observed as well as another abstraction reaction.

$$\cdot Sn(CH_3)_3 + \cdot Sn(CH_3)_3 \xrightarrow{k_{12}} (CH_3)_3SnSn(CH_3)_3 \qquad 7.12$$

$$\cdot Sn(CH_3)_3 + Sn(CH_3)_4 \xrightarrow{k_{13}} HSn(CH_3)_3 + CH_2Sn(CH_3)_3 \qquad 7.13$$

$$CH_3 + CH_2Sn(CH_3)_3 \xrightarrow{k_{14}} C_2H_5Sn(CH_3)_3 \qquad 7.14$$

7.5 Kinetics

Overall the rate of formation of methane is given by:

$$\frac{d[CH_4]}{dt} = k_4[Sn(CH_3)_4^*] + k_5[Sn(CH_3)_4^{**}] + k_{10}[CH_3][Sn(CH_3)_4]. \qquad 7.XIII$$

and the rate of ethane formation is given by:

$$\frac{d[C_2H_6]}{dt} = k_6[Sn(CH_3)_4^*] + k_7[Sn(CH_3)_4^{**}] + k_8[CH_3]^2 + k_{11}[CH_3][Sn(CH_3)_4]. \qquad 7.XIV$$

In order to give rate equations in which no radical or excited state concentrations are included values must be obtained for them by use of the Steady State treatment.

The rate of change of the concentration of the first excited species is given by:

$$\frac{d[Sn(CH_3)_4^*]}{dt} = k_0 I - k_1[Sn(CH_3)_4^*] - k_2[Sn(CH_3)_4^*] - k_4[Sn(CH_3)_4^*] - k_6[Sn(CH_3)_4^*]. \qquad 7.XV$$

No inclusion of deactivation by collision is necessary. Using the Steady State treatment, the rate of change is equal to zero, therefore

$$\left[Sn(CH_3)_4^*\right] = \frac{k_0 I}{k_1 + k_2 + k_4 + k_6} \qquad 7.XVI$$

A similar treatment of the concentration of the second excited state gives

$$\left[Sn(CH_3)_4^{**}\right] = \frac{k_0 k_1 I}{(k_1+k_2+k_4+k_6)(k_3+k_5+k_7+k_9[M])} \qquad 7.XVII$$

The methyl radical concentration is given by the quadratic equation

$$2k_8[CH_3]^2 + [CH_3][Sn(CH_3)_4](k_{10} + k_{11}) - \frac{3k_0 I}{(k_1+k_2+k_4+k_6)} \cdot \left[k_2 + \frac{k_1 k_3}{(k_3+k_5+k_7+k_9[M])} \right] = 0 \qquad 7.XVIII$$

$k_{10} + k_{11} \sim 10^3 \rightarrow 10^5$ $\quad k_8 k_0 k_2/k_1 \sim 10^{20}$

Using the normal equation for solution of quadratics, it can be seen that the 4ac term is much greater than the b^2 term and so the methyl radical concentration is given by:

$$[CH_3] = \left[\frac{3k_0 I}{2k_8(k_1+k_2+k_4+k_6)} \left[k_2 + \frac{k_1 k_3}{(k_3+k_5+k_7+k_9[M])} \right] \right]^{\frac{1}{2}} \qquad 7.XIX$$

Substituting the values obtained for $[Sn(CH_3)_4^*]$, $[Sn(CH_3)_4^{**}]$ and $[CH_3]$ in equation 7.XIII the following is obtained:

$$\frac{d[CH_4]}{dt} = \frac{k_0k_4I}{(k_1+k_2+k_4+k_6)} + \frac{k_0k_1k_5I}{(k_1+k_2+k_4+k_6)(k_3+k_5+k_7+k_9[M])} + k_{10}[Sn(CH_3)_4]\left[\frac{3k_0I}{2k_8(k_1+k_2+k_4+k_6)}\left[k_2 + \frac{k_1k_3}{(k_3+k_5+k_7+k_9[M])}\right]\right]^{\frac{1}{2}} \quad 7.XX$$

At room temperature the methane rate is proportional to I since k_{10} is very small. On increasing the temperature k_{10} increases and the rate becomes dependent on a value of intensity between I and $I^{\frac{1}{2}}$. This can be seen in Figure 7.1. On addition of inert gas $k_9[M]$ increases and k_3, k_5 and k_7 tend to zero. So the equation 7.XX becomes:

$$\frac{d[CH_4]}{dt} = \frac{k_0k_4I}{(k_1+k_2+k_4+k_6)} + k_{10}[Sn(CH_3)_4]\left[\frac{3k_0k_2I}{2k_8(k_1+k_2+k_4+k_6)}\right]^{\frac{1}{2}} \quad 7.XXI$$

Substituting of the values of $[Sn(CH_3)_4^*]$, $[Sn(CH_3)_4^{**}]$ and $[CH_3]$ in equation 7.XIV gives:

Figure 7.1

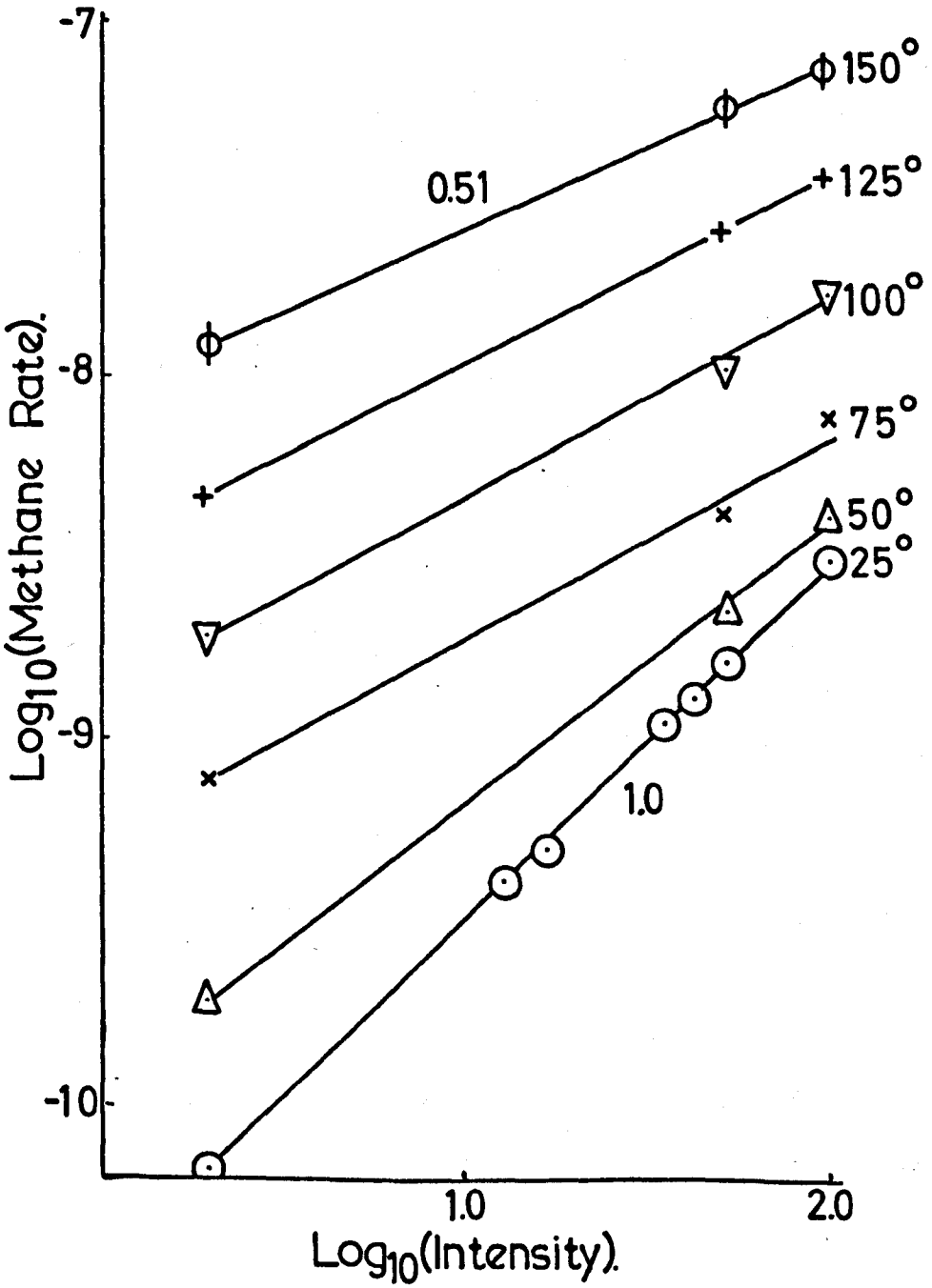
-7
-8
-9
-10
Log10(Methane Rate).
150°
125°
100°
75°
50°
25°
0.51
1.0
1.0
2.0
Log10(Intensity).

$$\frac{d[C_2H_6]}{dt} = \frac{k_0 I}{(k_1+k_2+k_4+k_6)}\left[k_6 + \frac{3k_2}{2} + \frac{k_1k_7 + \frac{3k_1k_2}{2}}{(k_3+k_5+k_7+k_9[M]}\right]$$

$$+ k_{11}[Sn(CH_3)_4]\left[\frac{3k_0 I}{2k_8(k_1+k_2+k_4+k_6)}\left[k_2 + \frac{k_1k_3}{(k_3+k_5+k_7+k_9[M])}\right]\right]^{\frac{1}{2}}$$

7.XXII

The same dependence on intensity applies in the ethane rate, on increasing the temperature increases k_{11} and the rate becomes dependent on a value of intensity between I and $I^{\frac{1}{2}}$, see Figure 7.2. On addition of inert gas k_9 M increases and k_3, k_5 and k_7 tend to zero and the rate equation becomes:

$$\frac{d[C_2H_6]}{dt} = \frac{k_0 I(\frac{3k_2}{2} + k_6)}{(k_1+k_2+k_4+k_6)} + k_{11}[Sn(CH_3)_4]\left[\frac{3k_0k_2 I}{2k_8(k_1+k_2+k_4+k_6)}\right]^{\frac{1}{2}}$$

7.XXIII

The practical result that is obtained on addition of inert gas is that

$$\frac{\text{Methane Rate in excess } N_2}{\text{Total Methane Rate}} = \frac{\text{Ethane Rate in excess } N_2}{\text{Total Ethane Rate}}$$

Figure 7.2

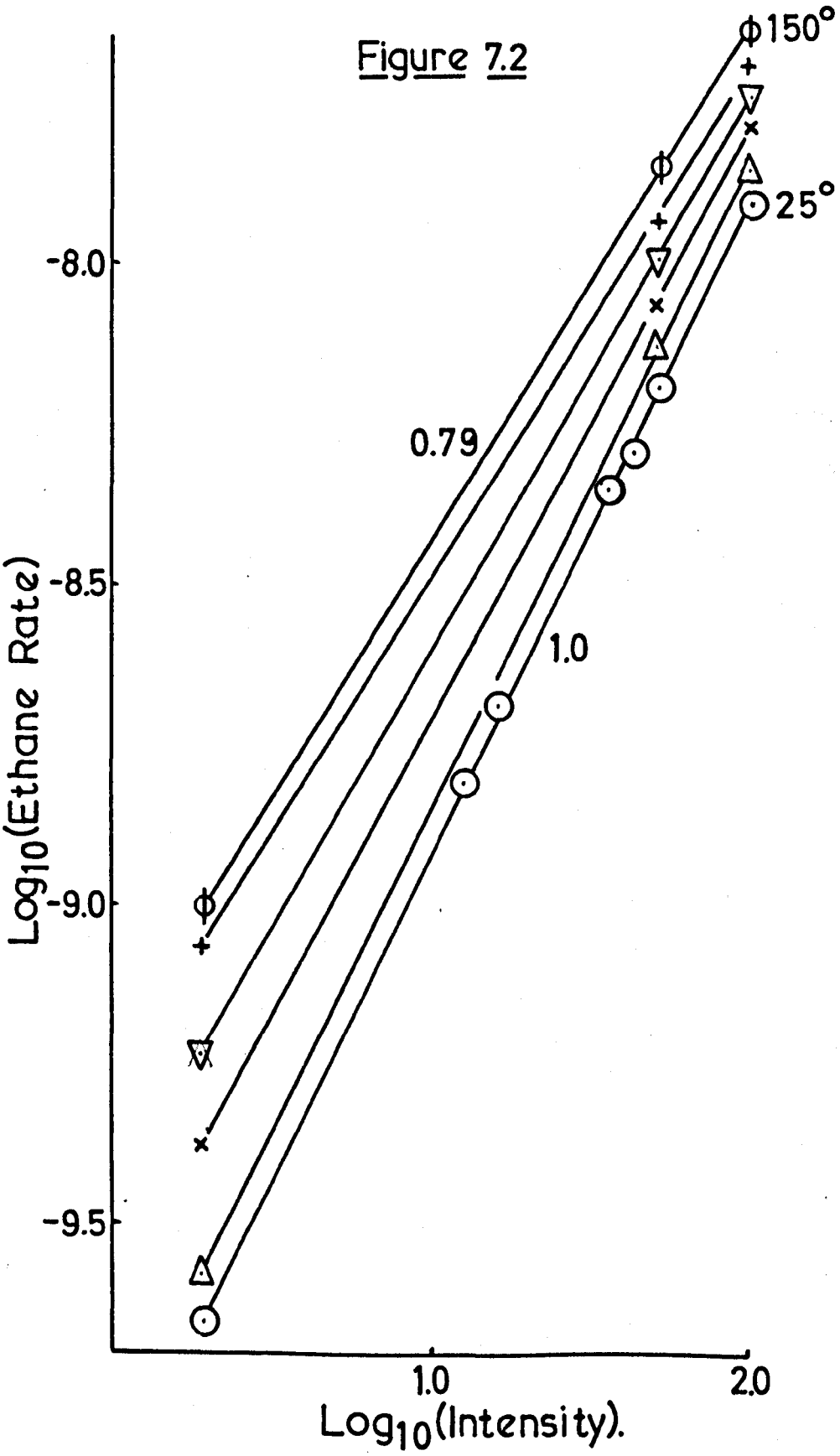
150°
25°
0.79
1.0
-8.0
-8.5
-9.0
-9.5
1.0
2.0
Log10(Ethane Rate)
Log10(Intensity).

From the kinetics this is

$$\frac{7.XXI}{7.XX} \text{ should equal } \frac{7.XXIII}{7.XXII}$$

Neglecting in the methane rate the radical abstraction formation i.e. reaction 7.10, as very small at room temperature and in the ethane rate reaction 7.11 as small as room temperature then the ratios reduce to

$$\frac{k_5}{k_4} \text{ should equal } \frac{k_3}{k_2} \quad \text{which rearranged}$$

gives

$$\frac{k_5}{k_3} \text{ should equal } \frac{k_4}{k_2}$$

This is one of the fundamental principles in Section 7.3 that was shown to be so. That is to say that molecular to radical elimination was the same from both excited species.

7.6 Activation Energies

In equation 7.XIII the rate of methane formation is due to two molecular elimination reactions and a hydrogen abstraction reaction. The effect of temperature on the rate should be entirely due to reaction 7.10:

$$\text{i.e.} \qquad CH_3 + Sn(CH_3)_4 \xrightarrow{k_{10}} CH_4 + CH_3Sn(CH_3)_3 \qquad 7.10$$

This is related to reaction 7.8 by the equation

$$k_{10} = \frac{1}{\left[Sn(CH_3)_4\right]} \cdot \text{Methane Rate} \times \frac{k_8^{\frac{1}{2}}}{\left[k_8\left[CH_3\right]^2\right]^{\frac{1}{2}}}$$

A value of the methyl radical concentration, 6×10^{-10} moles/litre, is obtained from the ethane rate at zero pressure due to radical combination, i.e. $k_8\left[CH_3\right]^2$. The value of k_8 used was that obtained by Gomer and Kistiakovsky[48] from the photolysis of $Hg(CH_3)_2$ using the rotating sector technique and $k_8\left[CH_3\right]^2$ versus temperature can be calculated. The value of $\left[CH_3\right]$ and methane rate versus temperature substituted in equation 7.XIII then gives values of k_{10} versus temperature, see figure 7.3 and table 7.1. Similar values for k_{11} can be obtained from equation 7.XIV, see table 7.1 and figure 7.4. Arrhenius plots, figures 7.5 and 7.6, of the rate constants derive activation energies and pre-exponential factors which give the general equation for k_{10} and k_{11} as

$$k_{10} = 5.6 \times 10^{9} e^{\frac{-10,020}{RT}} \qquad 7.XXIV$$

and

$$k_{11} = 3.9 \times 10^{7} e^{\frac{-5,949}{RT}} \qquad 7.XXV$$

from least squares calculations, see Section 2.9.

TABLE 7.1

Temperature	Rate Constant k_{10}		
	I = 100%	I = 52.4%	I = 1.98%
25°C	424.7	290.1	71.08
50°C	1.137×10^3	708.2	678.6
75°C	4.275×10^3	2.331×10^3	3.182×10^3
100°C	8.820×10^3	7.215×10^3	7.96×10^3
125°C	2.162×10^4	1.968×10^4	1.882×10^4
150°C	5.411×10^4	4.035×10^4	4.576×10^4
	Rate Constant k_{11}		
25°C	-	-	-
50°C	2.153×10^3	1.585×10^3	-
75°C	9.568×10^3	7.688×10^3	4.627×10^3
100°C	2.024×10^4	1.300×10^4	9.165×10^3
125°C	2.200×10^4	2.07×10^4	1.655×10^4
150°C	2.973×10^4	3.344×10^4	1.917×10^4

Figures in litres/mole/sec.

Figure 7.3

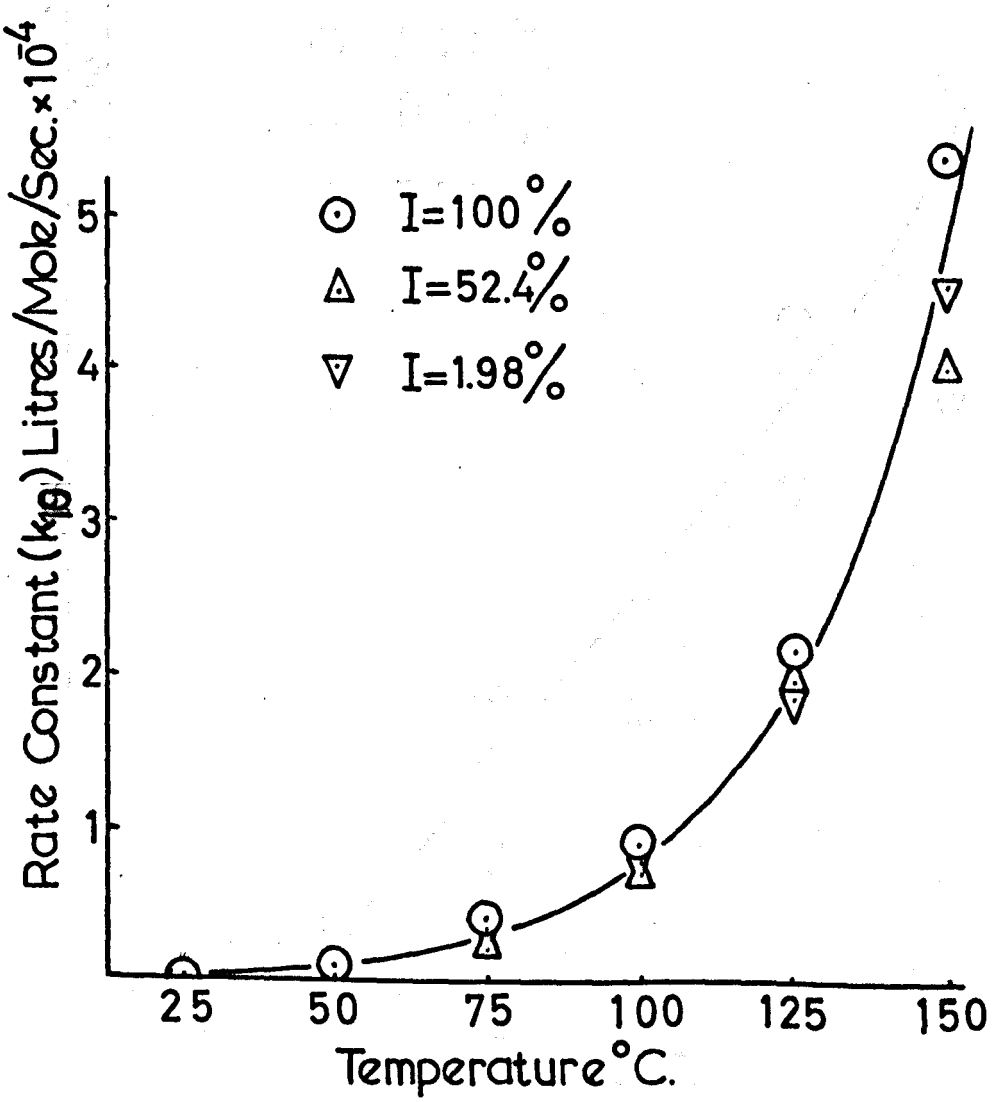
Rate Constant (k_{obs}) Litres/Mole/Sec.×10⁻⁴
1
2
3
4
5
I=100%
I=52.4%
I=1.98%
25
50
75
100
125
150
Temperature °C.

Figure 7.4

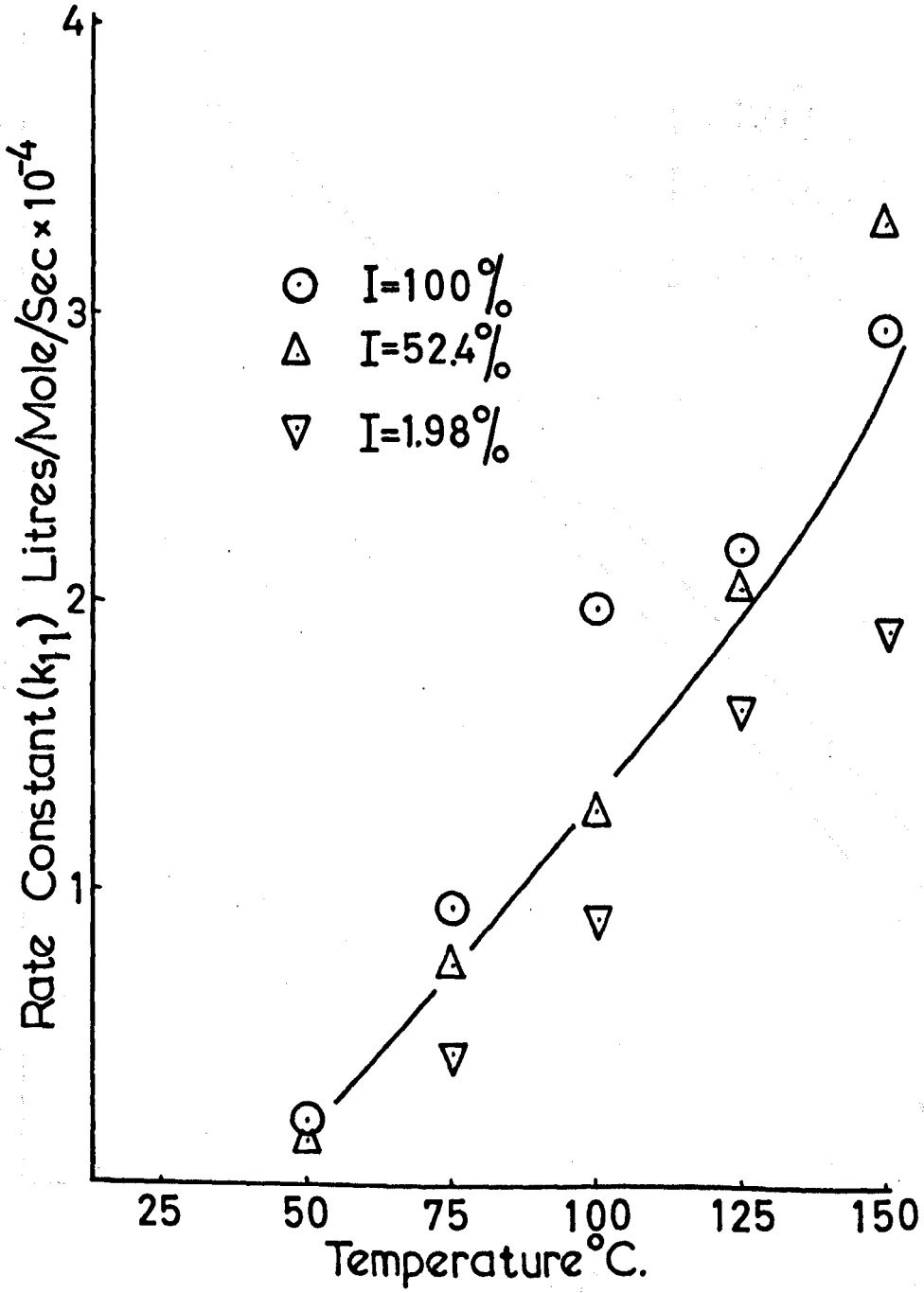
Rate Constant (k_{11}) Litres/Mole/Sec × 10^{-4}
4
3
2
1
I=100%
I=52.4%
I=1.98%
25
50
75
100
125
150
Temperature °C.

Figure 7.5

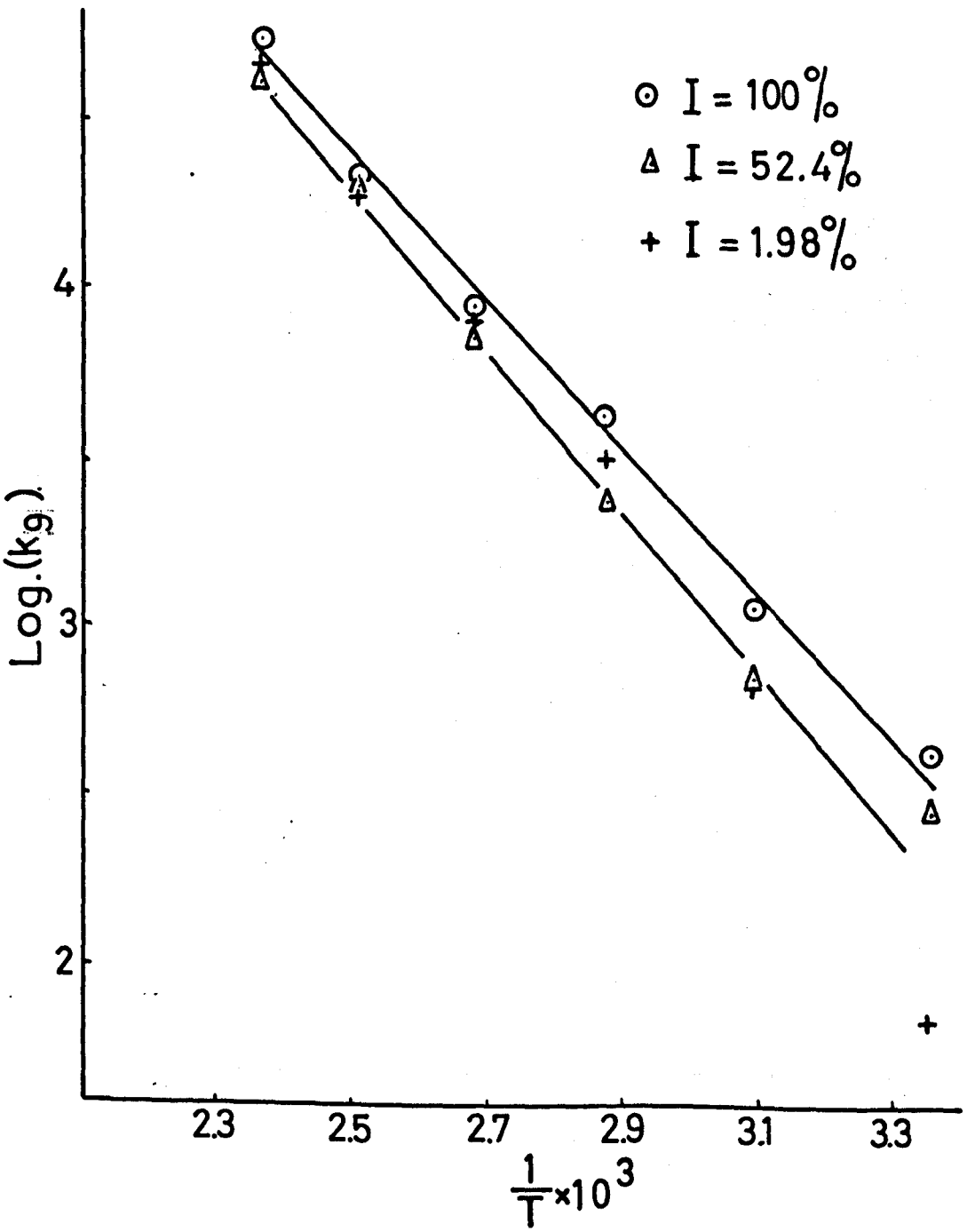

Figure 7.6

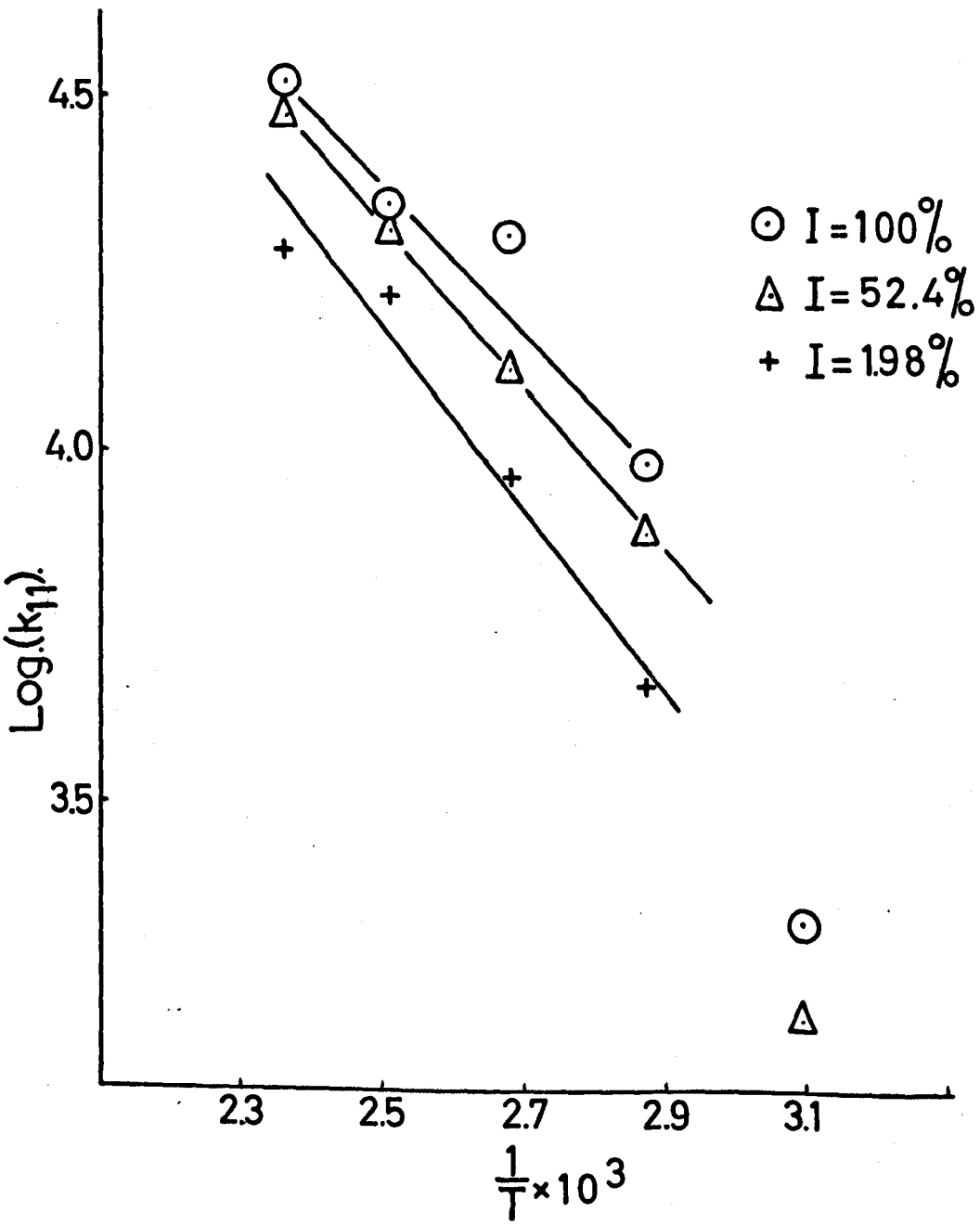

Figure 7.7

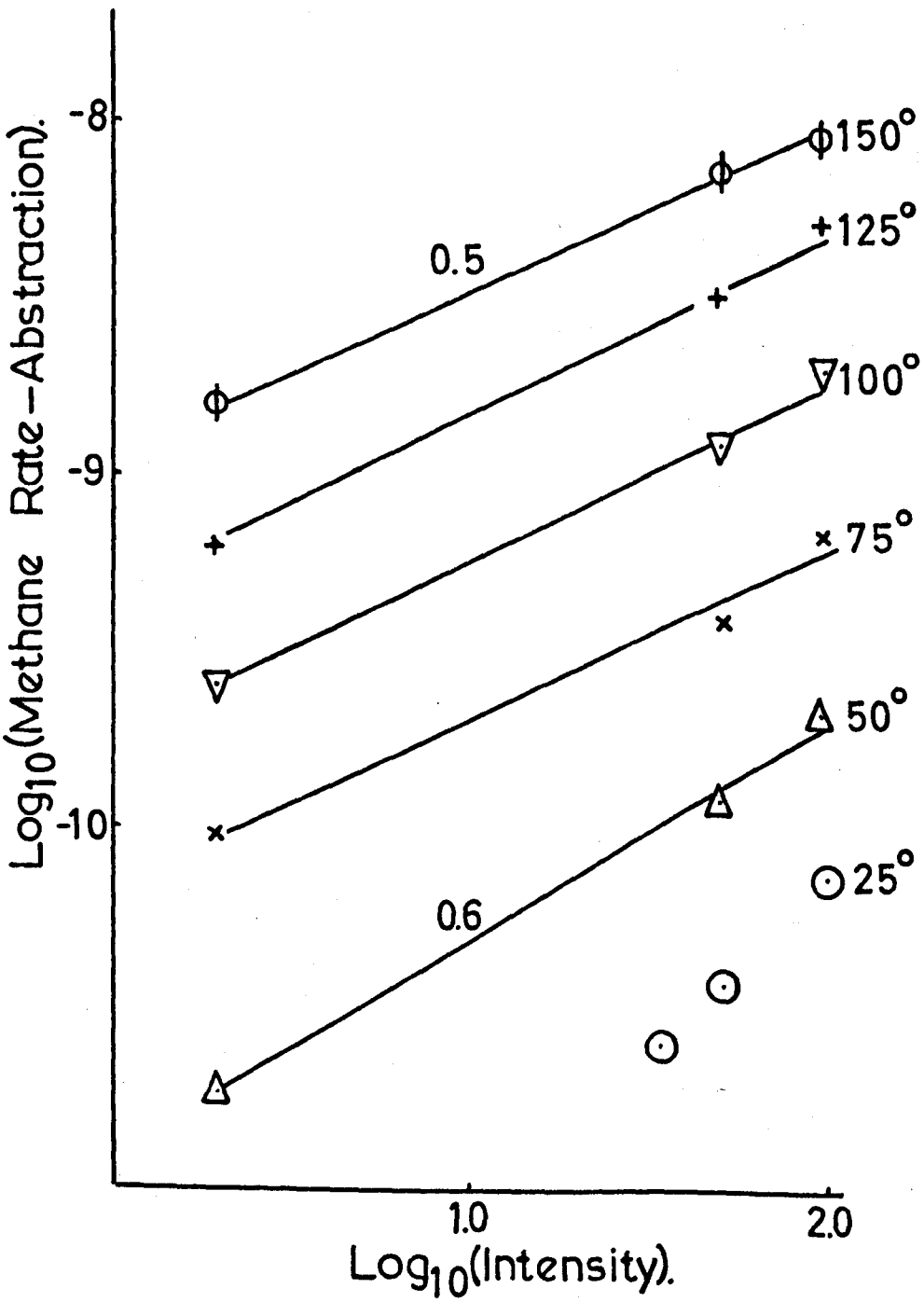
-8
-9
-10
Log10(Methane Rate-Abstraction).
150°
125°
100°
75°
50°
25°
0.5
0.6
1.0
2.0
Log10(Intensity).

Figure 7.8

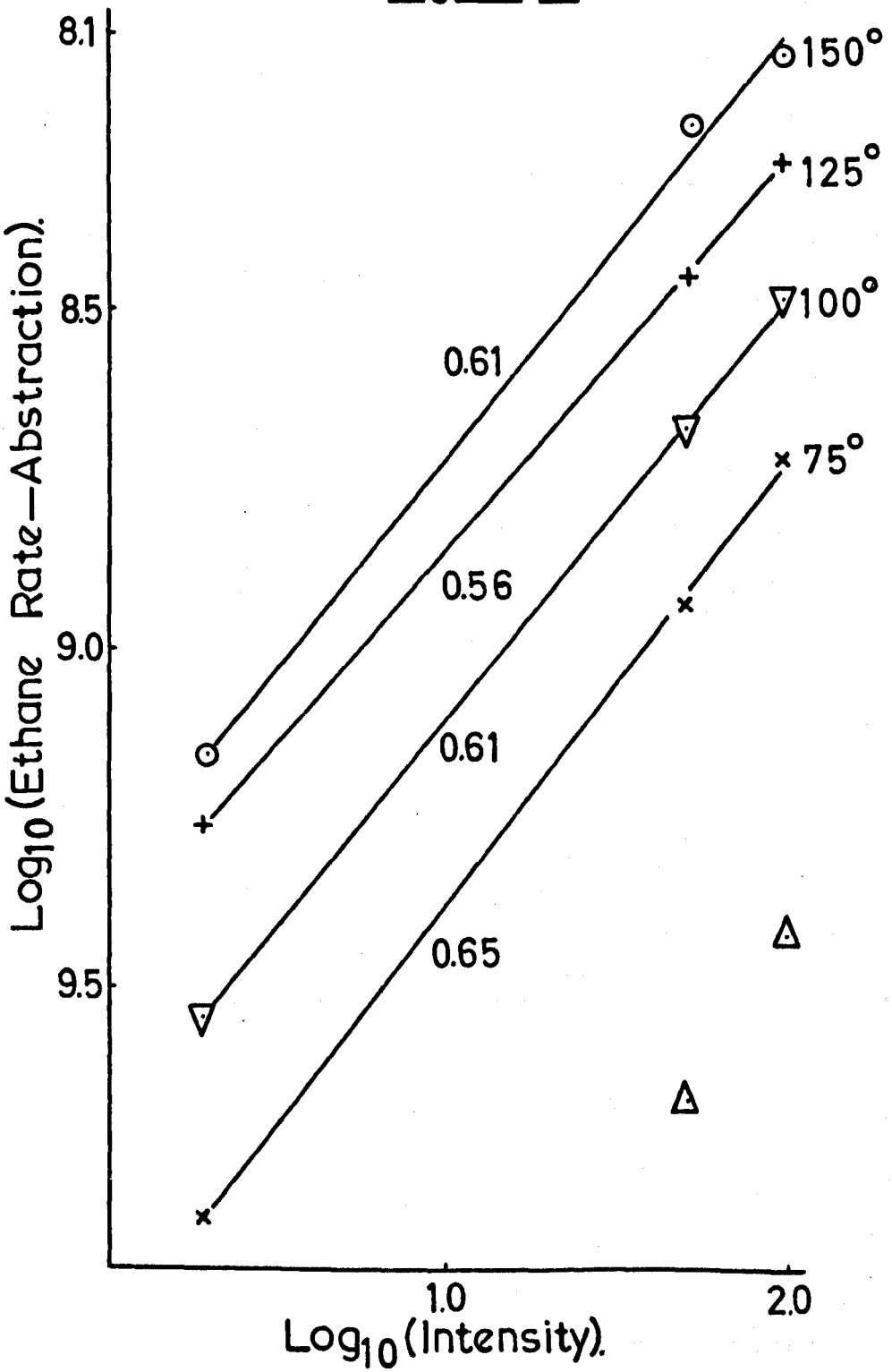
8.1
8.5
9.0
9.5
Log10 (Ethane Rate—Abstraction).
150°
125°
100°
75°
0.61
0.56
0.61
0.65
1.0
2.0
Log10 (Intensity).

Plots of $\log_{10}k$ versus $\log_{10}I$ for both rate constants should yield straight lines with slopes equal to 0.5, see figures 7.7 and 7.8. As can be seen this is not far wrong for both rate constants the errors at low temperature being quite high due to the rates of each reaction being only a small percentage of the total rates of formation of methane and ethane.

Excited State Intermediates

The quenching that takes place by nitrogen, carbon dioxide and nitric oxide on the methane rate, the majority of which is molecularly formed, can be used to estimate the lifetime of the second excited state, the first excited state decomposing too rapidly to be affected by inert gases.

$$Sn(CH_3)_4 \xrightarrow{k_0 I} Sn(CH_3)_4^{*} \qquad 7.0$$

$$Sn(CH_3)_4^{*} \xrightarrow{k_1} Sn(CH_3)_4^{**} \qquad 7.1$$

$$M + Sn(CH_3)_4^{**} \xrightarrow{k_9} M + Sn(CH_3)_4 \qquad 7.9$$

$$Sn(CH_3)_4^{**} \xrightarrow{k_5} CH_4 + \ldots\ldots \qquad 7.5$$

Considering for one moment the above four reactions taking

place then the rate of formation of methane is given by

$$\text{Rate} = \frac{k_5 \times k_0 I}{k_5 + k_9[M]} \qquad 7.XXVI$$

The rate in equation 7.XXVI is the methane rate due to reaction 7.5. In other words the rate of reaction 7.4 is subtracted from the total rate as it is not collisionally deactivated. If the reciprocal of the rate is taken then

$$\frac{1}{\text{Rate}} = \frac{1}{k_0 I} + \frac{k_9[M]}{k_0 I\, k_5} \qquad 7.XXVII$$

A plot of the reciprocal of the rate against the pressure of nitrogen, carbon dioxide or nitric oxide, a Stern-Volmer plot, should give a straight line and dividing the intercept of the ordinate by the slope

i.e. $\frac{k_5}{k_9}$

the ratio of k_5 to k_9 is obtained. It is possible to calculate a value for k_9 and obtain a value for the rate constant k_5. The reciprocal of this rate constant then gives the lifetime of the second excited state. Figure 7.9 illustrates the Stern-Volmer plot and the values obtained are

Figure 7.9

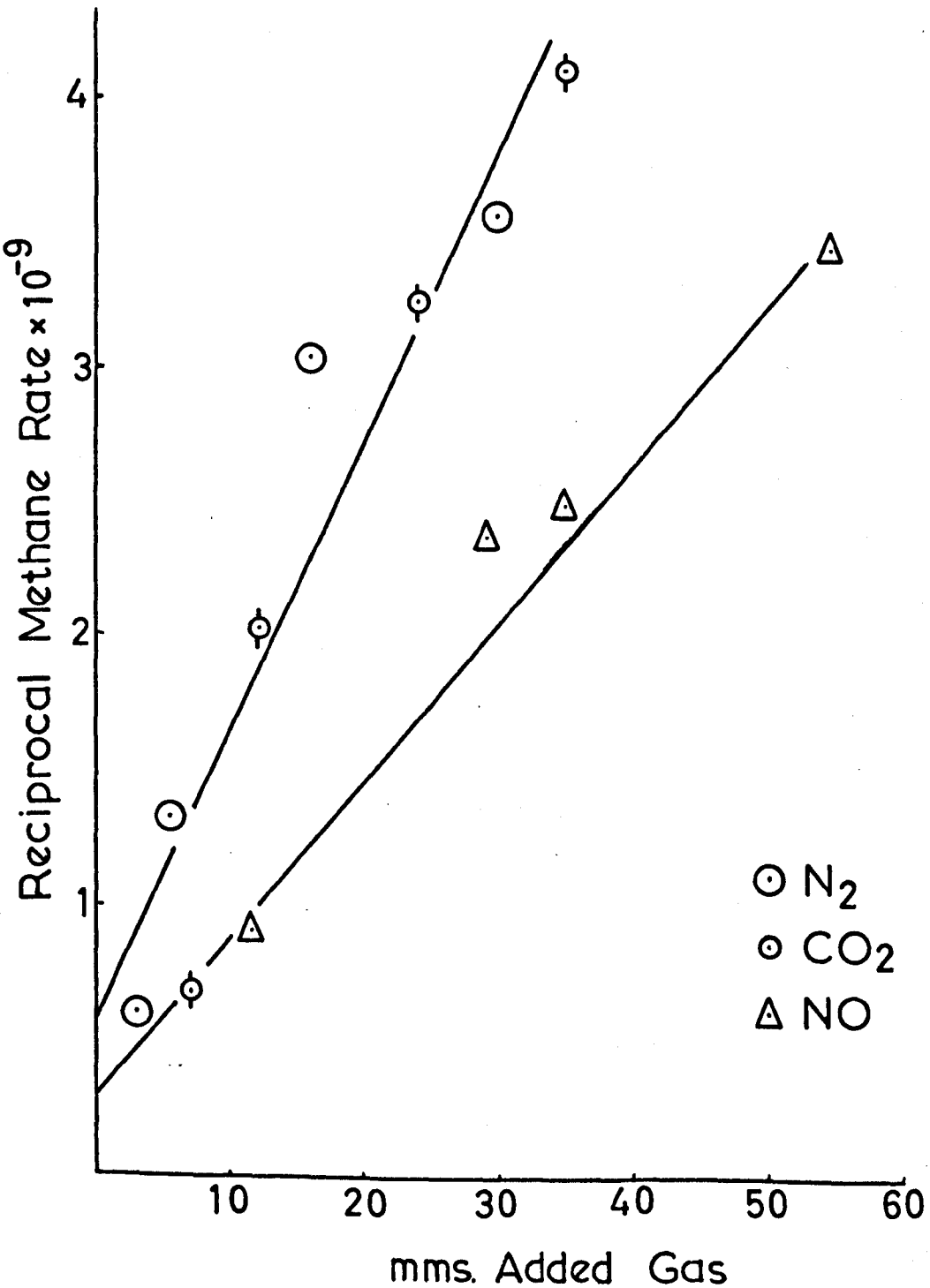
Reciprocal Methane Rate × 10^{-9}
4
3
2
1
10
20
30
40
50
60
mms. Added Gas
N_2
CO_2
NO

a) Nitrogen, CO_2, $\frac{k_5}{k_9} = 3.34 \times 10^{-4}$ moles/litre 7.XXVIII

b) Nitric oxide, $\frac{k_5}{k_9} = 3.15 \times 10^{-4}$ moles/litre 7.XXIX

A value for k_9 has to be estimated and it is in this estimation that the condition of every collision should cause deactivation has to apply. A value of the mean volocity ($\bar{c}$) of the molecules is obtained from

$\bar{c} = \left[\frac{8kT}{\pi m}\right]^{\frac{1}{2}}$ where m is the reduced mass and the number of collisions experience by each molecule is given by $\sqrt{2}\pi\sigma^2\bar{c}n$. Under unit conditions this becomes:

$$= 4\sigma^2 n \left[\frac{\pi kT}{m}\right]^{\frac{1}{2}}$$

$$= 4 \times 16 \times 10^{-6} \times \frac{6.023 \times 10^{23}}{22.4 \times 10^3} \left[\frac{3.1416 \times 1.38 \times 10^{-16} \times 298 \times 6.023 \times 10^{23}}{24.23}\right]^{\frac{1}{2}}$$

$$= 9.755 \times 10^9 \text{ collisions/molecule/sec.}$$

The total number of collisions/cc/sec. is given by:

$$Z = \frac{9.755 \times 10^9}{2} \times \frac{6.023 \times 10^{23}}{22.4 \times 10^3} \qquad 7.XXX$$

the factor 2 being introduced so that each collision is not counted twice.

The concentration c in moles/litre is related to the concentration n in molecules/cc. by

$$c = \frac{10^3 n}{N_o} \qquad 7.XXXI$$

The rate of reaction $^{dc}/_{dt}$ in moles/litre/sec is therefore related to the rate of collisions/cc/sec by

$$\frac{dc}{dt} = \frac{10^3}{N_o} Z \qquad 7.XXVI$$

The second order rate constant is defined by

$$k_9 = \frac{dc/dt}{c^2} = \frac{N_o Z}{10^3 x (n)^2}$$

$$= \frac{9.755 \times 10^9}{2} \times \frac{6.023 \times 10^{23}}{22.4 \times 10^3} \times \frac{6.023 \times 10^{23}}{10^3} \times \frac{(22.4 \times 10^3)^2}{(6.023 \times 10^{23})^2}$$

$$= \frac{9.755 \times 10^9}{2} \times 22.4 \text{ litres}^2/\text{mole}^2/\text{sec.}$$

$$k_9 = \underline{1.093 \times 10^{11} \text{ litres}^2/\text{mole}^2/\text{sec.}} \qquad 7.XXVII$$

The values for k_5 are then

a) Nitrogen, CO_2 = 3.65×10^{7} $sec.^{-1}$ 7.XXVIII

b) Nitric oxide = $3.44 \times 10^{+7} sec.^{-1}$ 7.XXVIII

The lifetime of the second excited state is the reciprocal of k_5 and is thus

a) $\underline{2.74 \times 10^{-8} \text{ secs.}}$ 7.XXIX

b) $\underline{2.91 \times 10^{-8} \text{ secs.}}$ 7.XXIX

Since no spectral data is available the results of the lifetime of the second excited state cannot be compared with other experimental results. However from the value obtained for the lifetime it is possible that the second excited state may be a triplet state or a vibrationally excited ground state. In other words absorption by tetramethyl stannane produces a singlet state which can undergo three processes. First a molecular elimination of methane and ethane, second a fragmentation into three methyl radicals and $SnCH_3$, and lastly transfer by radiationless transition to a triplet state or a vibrationally excited state of the ground electronic state. Once the triplet state or vibrationally excited ground state is formed this has three possible modes of action. First fragmentation into three methyl radicals and $SnCH_3$, secondly molecular elimination of methane and ethane, and thirdly collisional deactivation of the state by an inert gas. This mechanism in which a possible vibrationally excited ground state is formed can be compared with the

experiments of Srinivasan[94] on the photolysis of 1,3,5 cycloheptatriens and Parmenter[95] in the photolysis of glyoxal and they suggested that certain products arise from highly vibrationally excited ground-state species. In these cases the decomposition of these species is almost completely quenched at moderate gas pressures. Parmenter reported that the ratio of rate constants for dissociation of vibrationally excited ground state glyoxal

$$(CHO)_2^{\neq} \rightarrow H_2 + CO$$

to that for the vibrational relaxation

$$(CHO)_2^{\neq} + (CHO)_2 \rightarrow 2(CHO)_2$$

was equal to 12.5 mm; thus at only 100 mm pressure about nine-tenths of the vibrationally excited glyoxal molecules are deactivated before decomposition can occur. This ratio compares with 5.2 - 5.7 mm for the ratio of rate constants of dissociation of the triplet state or vibrationally excited ground state tetramethyl stannane to give molecular methane

$$Sn(CH_3)_4^{**} \xrightarrow{k_5} CH_4 + \ldots\ldots \qquad 7.5$$

to that for the collisional deactivation

$$Sn(CH_3)_4^{**} + M \xrightarrow{k_9} Sn(CH_3)_4 + M \qquad 7.9$$

8. DISCUSSION: ETHYL TRIMETHYL STANNANE

As in Section 7 a summary of the results obtained in Section 4 gives an introduction to the calculation of radical quantum yields and molecular elimination reaction quantum yields.

8.1 Summary

(1) Increasing the pressure of ethyl trimethyl stannane, above the pressure at which full absorption of exciting light occurs, leads to a linear increase in the rates of formations of all the products. See Figures 4.1 to 4.4.

(2) The rates of formation of the products were approximately linear with time up to 15-20 minutes after which the rates decreased due to formation of a film on the window. See Figures 4.5 to 4.8.

(3) All the rates were approximately linear with intensity at room temperature. See Figures 4.9 to 4.13.

(4) Addition of inert gases, nitrogen and argon, reduced all the rates to approximately the same extent and to a constant value showing again the presence of two excited states. In the case of ethyl trimethyl stannane the reduction in the rates was greater on addition of inert gas than in the case of tetramethyl stannane. See Figures 4.14 to 4.22.

(5) Added radical scavengers, oxygen and nitric oxide, showed the propane and butane were wholly formed by radical processes. Methane,

ethane and ethylene rates all showed that fractions of each were formed by molecular elimination processes. See Figures 4.23 to 4.28.

(6) Increasing the temperature increased the rate of methane and ethylene. The ethane rate reached a maximum and then dropped. The propane and butane rates both dropped. See Figures 4.29 to 4.33.

(7) Long irradiation periods at 125°C failed to show any radical combination products containing metal-metal bonds. However, a small amount of tetramethyl stannane was formed.

(8) Long irradiation periods at room temperature showed that a yellow polymeric material was formed on the window. No metallic tin was observed. Hydrocarbon analysis gives the total Sn in polymer equal to 5.07×10^{-5} moles. Analysis of polymer gives 4.67×10^{-5} moles-Sn.

8.2 Interpretation

Again the explanation of the effects described above and the calculation of radical and molecular elimination reaction quantum yields is aided by the mechanistic diagram below in which ethyl tetramethyl stannane is represented by A.

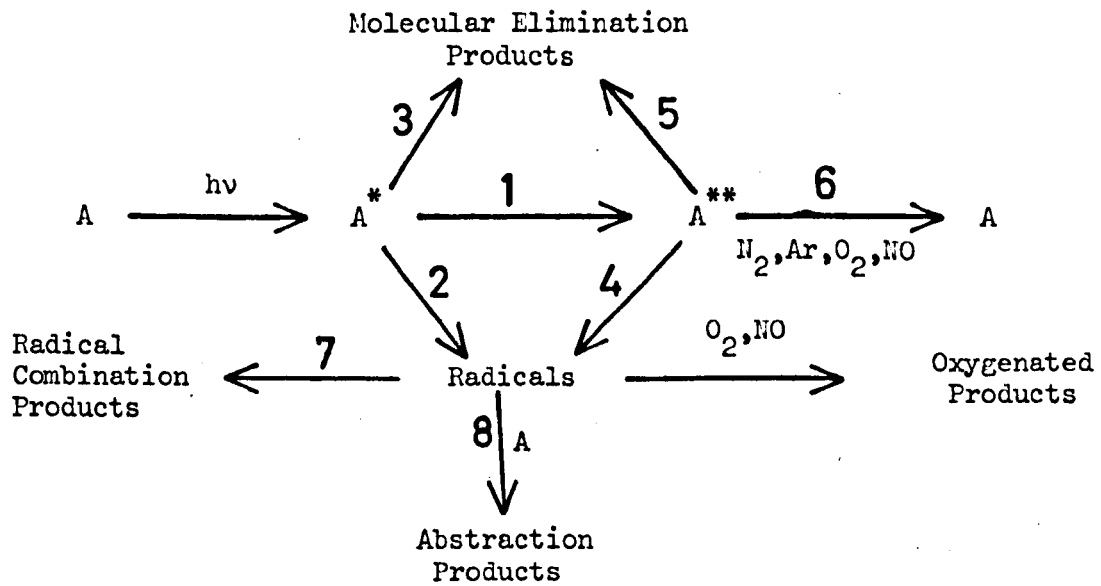

Rates of reactions subscripted R_1, R_2, R_3 etc.

Total Rate of Product = $R_3 + R_5 + R_7 + R_8$

$(R_7 + R_8)$ is a measure of $(R_2 + R_4)$

$\therefore$ Total Rate = $R_2 + R_3 + R_4 + R_5$

Rate in excess Nitrogen = $R_3 + R_7 + R_8$

where $R_7 + R_8$ is a measure of $R_2 . R_4 = R_5 = 0$

$\therefore$ Rate in excess N_2 = $R_2 + R_3$

Rate in excess Oxygen = R_3

Rate at the Intercept, zero pressure = $R_3 + R_5 + R_7$

Calculations carried out in moles/litre/sec. The rates in Section 4 are divided by 7.62 which changes moles/min. to moles/litre/sec.

All the products that are formed can be shown to follow approximately this basic scheme. The same assumptions which were made for tetramethyl stannane are again taken to hold for ethyl trimethyl stannane.

The formation of methane, ethane and ethylene can be discussed together since a fraction of each is formed by molecular elimination. Absorption of light by A forms the first excited species A^* which has three possible modes of reaction:

Firstly, conversion to the second excited state A^{**},

secondly, decomposition to give radicals, reaction 2, from which radical combination or disproportionation products can be formed, reaction 7, and radical abstraction reactions can occur, reaction 8,

and thirdly, molecular elimination reactions giving products directly, reaction 3.

The second excited state A^{**} can also undergo three processes:

Firstly, decomposition to give radicals, reaction 4, which can form combination, disproportionation or abstraction reaction products, reactions 7 and 8,

secondly, molecular elimination to form products directly via reaction 5,

and thirdly, collisional deactivation by nitrogen, argon, oxygen

and nitric oxide to give A.

In the cases of propane and butane no molecular elimination reactions occur so that only radical reactions form these products.

On addition of any of the gases collisional deactivation of A^{**} occurs and so reaction 4 and 5 do not take place. Addition of oxygen or nitric oxide, which are both radical scavengers, causes oxygenated products to be formed and reactions 7 and 8 do not take place. Only reaction 3 is observed.

Increasing the pressure of ethyl trimethyl stannane does not appear to quench the reaction and may be due to

$$A^{*} \text{ or } A^{**} + A \rightarrow A_1^{\neq} + A_2^{\neq}$$

where the transfer of energy occurs but the ultimate number of radicals formed from decomposition of $A_1^{\neq} + A_2^{\neq}$ is the same as that from A^{*} or A^{**}.

8.3 Radical and Molecular Elimination Quantum Yields at Zero Pressure

As in Section 7.3 three assumptions were made:

Firstly, that collisional deactivation of A^{**} occurs to the same extent, in a large excess gas, no matter whether an inert gas or a radical scavenger.

Secondly, that extrapolation of the linear portion of the plots of the rates of formation versus pressure of ethyl trimethyl stannane (Figures 4.1 to 4.4) eliminates any radical abstraction reactions.

Thirdly, that the ratio of molecular elimination to radical elimination is the same for both excited states. This was the case for tetramethyl stannane but cannot be demonstrated in this case since no product is wholly molecular.

Considering ethane formation then the rate of ethane is given by $R_2 + R_3 + R_4 + R_5$. The rate of ethane formation in excess nitrogen is $R_3 + R_2$ therefore

$$\frac{\text{Ethane Rate in excess } N_2}{\text{Ethane Total Rate}} = \frac{R_3 + R_2}{R_2+R_3+R_4+R_5} = 0.12 \qquad 8.I$$

The ethane rate at the ordinate intercept of the ethyl trimethyl stannane pressure variation plot is given by $R_3 + R_5 + R_7$ and in excess oxygen by R_3.

$$\frac{\text{Ethane rate in Oxygen}}{\text{Ethane rate in Nitrogen}} = \frac{R_3}{R_2 + R_3} \text{ which equals } \frac{R_5}{R_5 + R_4}$$

which equals $$\frac{R_3 + R_5}{R_2+R_3+R_4+R_5} = 0.10 \qquad 8.II$$

also $$\frac{\text{Ethane rate at Intercept}}{\text{Ethane total rate}} = \frac{R_3 + R_5 + R_7}{R_2 + R_3 + R_4 + R_5} = 0.89 \qquad 8.III$$

Thus dividing 8.III by 8.I one obtains

$$\frac{R_3 + R_5 + R_7}{R_3 + R_2} = 7.4 \qquad 8.IV$$

Since R_3 is known (rate of formation in excess O_2 = 0.51 x 10^{-10} moles/litre/sec.) then a value for R_2 can be found from the ethane rate in N_2, and also a value for $(R_5 + R_7)$ from equation 8.IV. Dividing 8.II by 8.I one obtains

$$\frac{R_3 + R_5}{R_3 + R_2} = 0.83 \qquad 8.V$$

and so from this equation a value for R_5 and thus R_7 can be obtained from equation 8.IV.

The total molecular elimination of ethane is given by $R_3 + R_5$ which is 4.2 x 10^{-10} moles/litre/sec.

The intercept rate (i.e. rate at 0 mms. $C_2H_5Sn(CH_3)_3$) is equal to 3.72×10^{-9} moles/litre/sec. and subtraction of the total molecular elimination rate leaves R_7, the rate of formation of ethane by radical combination and disproportionation, which equals 3.30×10^{-9} moles/litre/sec. Ethane can be formed by two reactions of radical origin at zero pressure and they are

Combination:	CH_3	+	CH_3	$\xrightarrow{k_1}$	C_2H_6	8.1
Disproportionation:	C_2H_5	+	C_2H_5	$\xrightarrow{k_2}$	$C_2H_6 + C_2H_4$	8.2

and so $$k_1\left[CH_3\right]^2 + k_2\left[C_2H_5\right]^2 = 3.30 \times 10^{-9} \text{ moles/litre/sec.} \qquad 8.IV$$

and the molecular elimination processes can be written

$$C_2H_5Sn(CH_3)_3^{*} \xrightarrow{k_3} C_2H_6 \ldots\ldots \qquad 8.3$$

$$C_2H_5Sn(CH_3)_3^{**} \xrightarrow{k_4} C_2H_6 \ldots\ldots \qquad 8.4$$

Consequently

$$k_3\left[C_2H_5Sn(CH_3)_3^{*}\right] = 0.51 \times 10^{-10} \text{ moles/litre/sec.} \qquad 8.VII$$

$$k_4\left[C_2H_5Sn(CH_3)_3^{**}\right] = 3.79 \times 10^{-10} \text{ moles/litre/sec.} \qquad 8.VIII$$

Considering the formation of ethylene and using the same notation as in the mechanistic diagram in Section 8.2 we obtain

$$\frac{R_2 + R_3}{R_2+R_3+R_4+R_5} = 0.12 \qquad 8.IX$$

$$\frac{R_3}{R_2 + R_3} = \frac{R_3 + R_5}{R_2+R_3+R_4+R_5} = 0.69 \qquad 8.X$$

$$\frac{R_3 + R_5 + R_7}{R_2 + R_3 + R_4 + R_5} = 0.89 \qquad 8.XI$$

Dividing 8.XI by 8.X obtains

$$\frac{R_3 + R_5 + R_7}{R_3 + R_5} = 1.28 \qquad 8.XII$$

and dividing 8.XI by 8.IX

$$\frac{R_3 + R_5 + R_7}{R_2 + R_3} = 7.4 \qquad 8.XIII$$

and dividing 8.X by 8.IX

$$\frac{R_3 + R_5}{R_2 + R_3} = 5.75 \qquad 8.XIV$$

R_3, the rate of ethane in excess oxygen is equal to 2.36×10^{-10} moles/litre/sec. From 8.X a value for $R_2 + R_3$ can be obtained and substituting this value in 8.XIV a value for $R_3 + R_5$ the total molecular

elimination rate is found to be 2.19×10^{-9} moles/litre/sec. The intercept rate ($R_3 + R_5 + R_7$) is equal to 2.80×10^{-9} moles/litre/sec. and so R_7, the rate of ethylene formation which can only be formed by radical disproportionation at zero pressure, is found equal to 6.14×10^{-10} moles/litre/sec. There are two possible reactions which can form ethylene from the radicals formed and they are

$$C_2H_5 + C_2H_5 \xrightarrow{k_2} C_2H_4 + C_2H_6 \qquad 8.2$$

$$CH_3 + C_2H_5 \xrightarrow{k_5} C_2H_4 + CH_4 \qquad 8.5$$

Therefore

$$k_2\left[C_2H_5\right]^2 + k_5\left[CH_3\right]\left[C_2H_5\right] = 6.14 \times 10^{-10} \text{ moles/litre/sec.} \qquad 8.XV$$

The molecular elimination reactions are

$$C_2H_5Sn(CH_3)_3^{*} \xrightarrow{k_6} C_2H_4 + \ldots\ldots \qquad 8.6$$

$$C_2H_5Sn(CH_3)_3^{**} \xrightarrow{k_7} C_2H_4 + \ldots\ldots \qquad 8.7$$

and thus

$$k_6\left[C_2H_5Sn(CH_3)_3^{*}\right] = 2.36 \times 10^{-10} \text{ moles/litre/sec.} \qquad 8.XVI$$

$$k_7\left[C_2H_5Sn(CH_3)_3^{**}\right] = 1.95 \times 10^{-9} \text{ moles/litre/sec.} \qquad 8.XVII$$

Methane formation can be treated by the same method and the same notation as in Section 8.2 so the values obtained for the equations are as follows:

$$\frac{R_2 + R_3}{R_2+R_3+R_4+R_5} = 0.12 \quad \frac{4.33 \times 10^{-10}}{3.52 \times 10^{-9}} \qquad 8.XVIII$$

$$\frac{R_3}{R_2 + R_3} = \frac{R_3 + R_5}{R_2+R_3+R_4+R_5} = 0.63 \qquad 8.XIX$$

$$\frac{R_3 + R_5 + R_7}{R_2 + R_3 + R_4 + R_5} = 0.95 \qquad 8.XX$$

Dividing 8.XX by 8.XVIII and 8.XIX b- 8.XVIII the following equations are obtained.

$$\frac{R_3 + R_5 + R_7}{R_2 + R_3} = 7.9 \qquad \frac{R_3 + R_5}{R_2 + R_3} = 5.25 \qquad 8.XXI$$

The value of R_3, the methane rate in excess nitrogen is 0.35×10^{-10} moles/litre/sec. The value for the total molecular elimination rate ($R_3 + R_5$) is 2.90×10^{-10} moles/litre/sec. and the rate of radical formation (R_7) is 1.48×10^{-10} moles/litre/sec.

There is only one reaction that can produce methane at zero pressure and that is

$$CH_3 + C_2H_5 \xrightarrow{k_5} CH_4 + C_2H_4 \qquad 8.5$$

thus

Disproportionation: $k_5[CH_3][C_2H_5] = 1.48 \times 10^{-10}$ moles/litre/sec. 8.XXII

The molecular elimination reactions are as follows.

$$C_2H_5Sn(CH_3)_3^{*} \xrightarrow{k_8} CH_4 \ldots\ldots \qquad 8.8$$

and

$$C_2H_5Sn(CH_3)_3^{**} \xrightarrow{k_9} CH_4 \ldots\ldots \qquad 8.9$$

and so the rate equations are

$$k_8[C_2H_5Sn(CH_3)_3^{*}] = 0.35 \times 10^{-10} \text{ moles/litre/sec.} \qquad 8.XXIII$$

and

$$k_9[C_2H_5Sn(CH_3)_3^{**}] = 2.55 \times 10^{-10} \text{ moles/litre/sec.} \qquad 8.XXIV$$

The value for $k_5[CH_3][C_2H_5]$ obtained above can now be substituted into 8.XV to obtain

Disproportionation: $k_2[C_2H_5]^2 = 4.66 \times 10^{-10}$ moles/litre/sec. 8.XXV

which if substituted in equation 8.VI gives

Combination: $k_1[CH_3]^2 = 2.82 \times 10^{-9}$ moles/litre/sec. 8.XXVI

In the case of propane there is no molecular elimination reaction

which gives propane and so the intercept at the ordinate of the rate of propane versus pressure of $C_2H_5Sn(CH_3)_3$ (Figure 4.3) must be due entirely to

$$CH_3 + C_2H_5 \xrightarrow{k_{10}} C_3H_8 \qquad 8.10$$

and so

Combination: $k_{10}[CH_3][C_2H_5] = 8.92 \times 10^{-9}$ moles/litre/sec. 8.XXVII

Similarly no fraction of butane is formed molecularly and the value at the intercept of Figure 4.4 must be due to

$$C_2H_5 + C_2H_5 \xrightarrow{k_{11}} C_4H_{10} \qquad 8.11$$

and so

Combination: $k_{11}[C_2H_5]^2 = 2.76 \times 10^{-9}$ moles/litre/sec. 8.XXVIII

From the rates of all the individual reactions it is now possible to calculate the quantum yields of methyl and ethyl radicals formation at zero pressure.

Rate of Reaction	No. of Methyl Radicals	No. of Ethyl Radicals
$k_1[CH_3]^2 = 2.82 \times 10^{-9}$ moles/litre/sec.	5.64×10^{-9}	
$k_2[C_2H_5]^2 = 4.66 \times 10^{-10}$ "	-	0.93×10^{-9}
$k_5[CH_3][C_2H_5] = 1.48 \times 10^{-10}$ "	0.15×10^{-9}	0.15×10^{-9}
$k_{10}[CH_3][C_2H_5] = 8.92 \times 10^{-9}$ "	8.92×10^{-9}	8.92×10^{-9}
$k_{11}[C_2H_5]^2 = 2.76 \times 10^{-9}$ "	-	5.52×10^{-9}
	14.71×10^{-9}	15.52×10^{-9}

Therefore the quantum yield of methyl radicals is

$$\phi \text{ (methyl)} = \frac{14.71 \times 10^{-9} \times 0.61}{5.09 \times 10^{-9}}$$

$$\phi \text{ (methyl)} = 1.76 \qquad \text{8.XXVII}$$

and the quantum yield of ethyl radicals is given by

$$\phi \text{ (ethyl)} = \frac{15.52 \times 10^{-9} \times 0.61}{5.09 \times 10^{-9}}$$

$$\phi \text{ (ethyl)} = 1.86 \qquad \text{8.XXVIII}$$

The quantum yields of the molecular elimination processes are as follows:

$$\text{Ethane (molecular)} = \frac{0.43 \times 10^{-9} \times 0.61}{5.09 \times 10^{-9}}$$

$$\phi \text{ (Ethane-molecular)} = 0.05 \qquad \text{8.XXIX}$$

$$\text{Ethylene (molecular)} = \frac{2.19 \times 10^{-9} \times 0.61}{5.09 \times 10^{-9}}$$

$$\underline{\phi \text{ (Ethylene-molecular)} = 0.26} \qquad 8.XXX$$

$$\text{Methane (molecular)} = \frac{0.29 \times 10^{-9} \times 0.61}{5.09 \times 10^{-9}}$$

$$\underline{\phi \text{ (Methane-molecular)} = 0.03} \qquad 8.XXXI$$

The ratios of disproportionation to combination are well documented for methyl-ethyl and ethyl-ethyl reactions. In the first case the value obtained is 0.016 and the value quoted by Terry and Futrell[93] is 0.036. In the case of ethyl radicals 0.17 is the value obtained and Terry and Futrell[93] quote 0.12. It can be seen that the ratios are of the same order.

8.4 Mechanism

The thermochemical data (Section 1.10) and the radical quantum yield of tetramethyl stannane show that from either excited state only three hydrocarbon radicals are produced. However the results of the experiments on ethyl trimethyl stannane show that, at zero pressure, the total radical quantum yield is 3.6 and an approximate methyl to ethyl radical ratio of 1:1. There are two possible explanations for the large ethyl radical quantum yield.

Firstly, if one assumes that the radical breakdown of both excited species is the same as that in the tetramethyl stannane case i.e.

$$C_2H_5Sn(CH_3)_3^{*} \text{ or } C_2H_5Sn(CH_3)_3^{**} \rightarrow C_2H_5^{\bullet} + 2CH_3^{\bullet} + SnCH_3 \qquad 8.12$$

the probability of one of the three radicals removed being an ethyl radical is quite large. The mass spectral evidence (Figure 3.39) shows that the ethyl group is more susceptable to removal than the methyl from the parent molecule and there is no evidence for ethylene elimination giving a metastable ion $HSn(CH_3)_3^{+}$ which loses a hydrogen atom to give $Sn(CH_3)_3^{+}$. Other hydride ions are quite stable.[73,74] This is also supported by the formation of tetramethyl stannane detected after long irradiation periods at room temperature and at 125°C. This evidence leads to the conclusion that the activated species will give three radicals one of which will be an ethyl radical. Increase of the ethyl

yield can arise from radical abstraction reactions of the type

$$CH_3 + C_2H_5Sn(CH_3)_3 \rightarrow C_3H_8 + Sn(CH_3)_3 \qquad 8.13$$

$$C_2H_5 + C_2H_5Sn(CH_3)_3 \rightarrow C_4H_{10} + Sn(CH_3)_3 \qquad 8.14$$

The first reaction could be the cause of the propane increase with pressure and the second is undoubtedly the cause of the butane increased yield with pressure of ethyl trimethyl stannane. It would be expected, however, that the calculations carried out in Section 8.3 would eliminate these abstraction reactions, also the disproportionation to combination ratios are of reasonable accuracy, compared to rotating sector measurements, to uphold their legitimacy. However, there may be abstraction reactions taking place at lower pressures than that at which the experiments carried out and extrapolation would not take into account these reactions.

Secondly, an expansion of the reaction proposed to account for non-deactivation due to pressure of ethyl triethyl stannane may lead to an increase in ethyl radical yield.

$$C_2H_5Sn(CH_3)_3^* + C_2H_5Sn(CH_3)_3 \rightarrow C_2H_5Sn(CH_3)_3^{\neq 1} + C_2H_5Sn(CH_3)_3^{\neq 2} \qquad 8.15$$

The energy contained in the electronically excited species is sufficient to remove only three radicals. However if this energy is divided between two molecules, in the form of say vibrational energy, it is possible that it may be sufficient to remove three to four radicals from two molecules

(radical yield 3.6). That is to say that the energy is sufficient to remove only three radicals from one molecule but the energy required to remove the first two radicals may be less than that required to remove the third. When divided between two molecules four radicals could be removed. From the mass spectral evidence the likelihood is that the ethyl group would be one of the possible two radicals or in fact the first if only one eliminated, from each vibrationally excited molecule. This possibility could occur at all the pressures at which the experiments were carried and would therefore not be accounted for in the calculations. It is easy to see how the ethyl radical yield would gain from this reaction and the calculations show that the ethyl radical yield is slightly greater than the methyl radical yield although this excess is within the maximum expected error.

Although the rate of formation of the vibrationally excited state appears to depend on the concentration of the ground state ethyl trimethyl stannane, a more important factor is the life-time of the electronically excited state. At 10 mm. pressure the number of collisions experienced by one molecule is of the order of 10^9 sec.$^{-1}$. If reaction 8.15 occurs at every collision experienced by the electronically excited species and the life-time of the excited species is longer than the period between collisions then the products of the vibrationally active state will be independent of ethyl trimethyl stannane pressure. However, if the life-time is of the same order or shorter than the time between collisions then the formation of radicals from the vibrationally excited

state will be dependent on ethyl trimethyl stannane pressure. In the first case where dependence on pressure occurs this would have been taken into account in the calculations but in the second case no measurement of the exchange of energy or increase in radical yield due to the reaction would be eliminated by extrapolation to zero pressure. This appears to be the only possible explanation as to the radical quantum yields. Therefore this leads to the following two mechanisms at zero pressure:

Mechanism 1.

$C_2H_5Sn(CH_3)_3 + h\nu$	$\xrightarrow{k_0 I}$	$C_2H_5Sn(CH_3)_3^*$	8.16
$C_2H_5Sn(CH_3)_3^*$	$\rightarrow$	$C_2H_5Sn(CH_3)_3^{**}$	8.17
$C_2H_5Sn(CH_3)_3^*$	$\rightarrow$	$C_2H_5 + 2CH_3 + SnCH_3$	8.18
$C_2H_5Sn(CH_3)_3^{**}$	$\rightarrow$	$C_2H_5 + 2CH_3 + SnCH_3$	8.19
$CH_3 + CH_3$	$\rightarrow$	C_2H_6	8.1
$C_2H_5 + C_2H_5$	$\rightarrow$	$C_2H_6 + C_2H_4$	8.2
$C_2H_5Sn(CH_3)_3^*$	$\rightarrow$	$C_2H_6 + ...$	8.3
$C_2H_5Sn(CH_3)_3^{**}$	$\rightarrow$	$C_2H_6 + ...$	8.4
$CH_3 + C_2H_5$	$\rightarrow$	$CH_4 + C_2H_4$	8.5
$C_2H_5Sn(CH_3)_3^*$	$\rightarrow$	$C_2H_4 + ...$	8.6
$C_2H_5Sn(CH_3)_3^{**}$	$\rightarrow$	$C_2H_4 + ...$	8.7
$C_2H_5Sn(CH_3)_3^*$	$\rightarrow$	$CH_4 + ...$	8.8
$C_2H_5Sn(CH_3)_3^{**}$	$\rightarrow$	$CH_4 + ...$	8.9

$CH_3 + C_2H_5 \rightarrow C_3H_8$ 8.10

$C_2H_5 + C_2H_5 \rightarrow C_4H_{10}$ 8.11

$CH_3 + C_2H_5Sn(CH_3)_3 \rightarrow CH_4 + ...$ 8.20

$CH_3 + C_2H_5Sn(CH_3)_3 \rightarrow CH_4 + C_2H_4 + ...$ 8.21

$C_2H_5 + C_2H_5Sn(CH_3)_3 \rightarrow C_2H_6 + C_2H_4 + ...$ 8.22

$CH_3 + C_2H_5Sn(CH_3)_3 \rightarrow C_2H_6 + C_2H_5Sn(CH_3)^{\bullet}_2$ 8.23

$C_2H_5 + C_2H_5Sn(CH_3)_3 \rightarrow C_2H_6 + ...$ 8.24

$CH_3 + C_2H_5Sn(CH_3)_3 \rightarrow C_3H_8{}^{\bullet}Sn(CH_3)_3$ 8.25

$C_2H_5 + C_2H_5Sn(CH_3)_3 \rightarrow C_3H_8 + C_2H_5\dot{S}n(CH_3)_2$ 8.26

$C_2H_5 + C_2H_5Sn(CH_3)_3 \rightarrow C_4H_{10} + {}^{\bullet}Sn(CH_3)_3$ 8.27

Reactions 8.20 to 27 would lead to increases in product formation. The main reactions leading to a false increase in ethyl radical formation would be 8.20, 8.21, 8.25 and 8.27.

Increase in temperature would favour hydrogen abstraction reactions and is indicated by a large increase in methane yield with temperature. The yields at 150°C show a tendency to even out the radical yields to a ratio of two methyls to one ethyl.

The second mechanism is as follows:

Mechanism 2.

$C_2H_5Sn(CH_3)_3 + h\nu \xrightarrow{k_0 I} C_2H_5Sn(CH_3)^{*}_3$ 8.28

$C_2H_5Sn(CH_3)^{*}_3 \rightarrow C_2H_5 + 2CH_3 + SnCH_3$ 8.29

$C_2H_5Sn(CH_3)^{*}_3 + C_2H_5Sn(CH_3)_3 \rightarrow 2C_2H_5Sn(CH_3)^{\neq}_3$ 8.30

$C_2H_5Sn(CH_3)_3^{\neq}$	→	$C_2H_5 + CH_3 + :Sn(CH_3)_2$	8.31
$C_2H_5Sn(CH_3)_3^{\neq}$	→	$C_2H_5 + Sn(CH_3)_3$	8.32
$CH_3 + CH_3$	→	C_2H_6	8.1
$C_2H_5 + C_2H_5$	→	$C_2H_6 + C_2H_4$	8.2
$C_2H_5Sn(CH_3)_3^{*}$	→	$C_2H_6 + ...$	8.3
$C_2H_5Sn(CH_3)_3^{\neq}$	→	$C_2H_6 + ...$	8.4
$CH_3 + C_2H_5$	→	C_3H_8	8.5
$C_2H_5Sn(CH_3)_3^{*}$	→	$C_2H_4 + ...$	8.6
$C_2H_5Sn(CH_3)_3^{\neq}$	→	$C_2H_4 + ...$	8.7
$C_2H_5Sn(CH_3)_3^{*}$	→	$CH_4 + ...$	8.8
$C_2H_5Sn(CH_3)_3^{\neq}$	→	$CH_4 + ...$	8.9
$CH_3 + C_2H_5$	→	C_3H_8	8.10
$C_2H_5 + C_2H_5$	→	C_4H_{10}	8.11

This would lead to a more substantial alkyl content in the solid product on the cell window. The fact that a yellow transparent polymeric material is observed rather than a dark-grey opaque in the photolysis of tetramethyl stannane suggests the possibility of more alkyl content.[69]

Increase in yields with pressure of ethyl trimethyl stannane can be explained by reactions 8.20 to 8.27. On addition of inert gases the reaction

$$C_2H_5Sn(CH_3)_3^{\neq} + M \rightarrow C_2H_5Sn(CH_3)_3 + M \qquad 8.33$$

will cause reduction in rates of formation.

8.5 Life-time of the Second Excited State of $C_2H_5Sn(CH_3)_3$

The reciprocal of the rates of formation of ethylene, ethane and propane from the second excited state (total rate - rate with excess inert gas) were plotted against added inert gas pressure giving Stern-Volmer plots shown in Figure 8.1. The rate constant for collisional deactivation used in the calculation was that calculated in Section 7.7. The ratio of the rate constant of decomposition to that of collisional deactivation from the three plots are in the range $1.16 - 1.34 \times 10^{-3}$ moles/litre. This gives the range for the rate constant of decomposition as $1.27 - 1.46 \times 10^{8}$ sec.$^{-1}$. So the life-time of the second excited state, which may be a triplet state or a vibrationally excited ground state is $6.85 - 7.87 \times 10^{-9}$ secs. The first excited state decomposes too rapidly to be collisionally deactivated and is presumably the singlet state.

The value of the ratio of rate constants $1.16 - 1.34 \times 10^{-3}$ moles/litre when converted to millimetres gives 19.7 - 22.8 mm. This compares with 12.5 mms. obtained by Parmenter for the same ratio for the glyoxal photolysis.

Figure 8.1

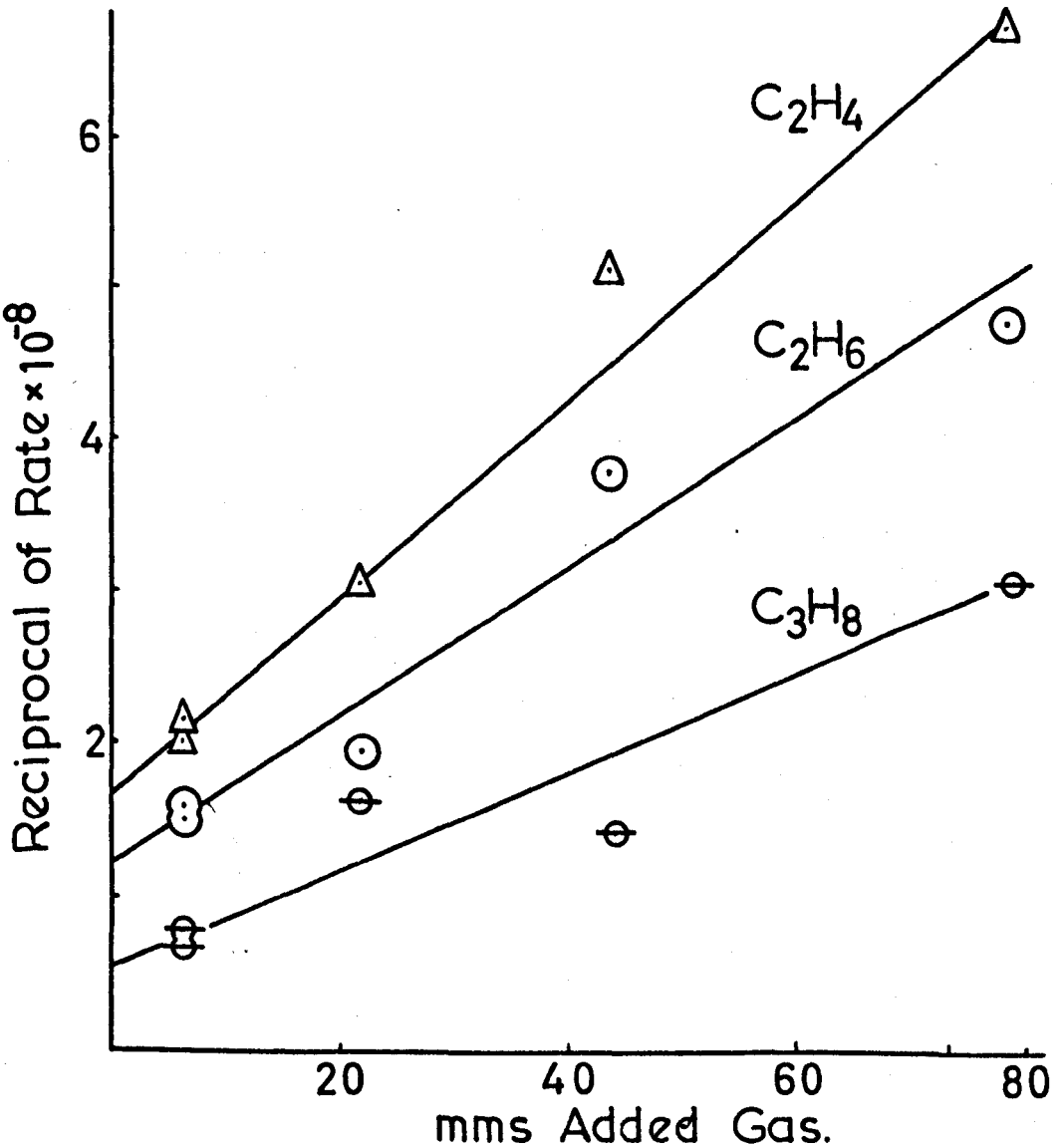
C_2H_4
C_2H_6
C_3H_8
6
4
2
Reciprocal of Rate $\times 10^{-8}$
20
40
60
80
mms Added Gas.

9. DISCUSSION: n-PROPYL TRIMETHYL STANNANE

As in Sections 7 and 8 a summary of the results obtained in Section 5 gives an introduction to the discussion.

9.1 Summary

(1) Increasing the pressure of n-propyl trimethyl stannane, above the pressure required for full absorption of exciting light, leads to a linear increase in the rates of formation of all the products. See Figures 5.1 to 5.4.

(2) Addition of inert gas reduces all the rates to approximately the same extent and to a constant value. This suggests the pressure of two excited states. See Figures 5.5 to 5.8.

(3) Addition of oxygen, a radical scavenger, reduces the rates of methane, ethylene, ethane and propylene to a greater extent than nitrogen. The butane rate was reduced as well to a greater extent, but still had a small yield showing a molecular elimination process. See Figures 5.8 to 5.12.

9.2 Discussion

Since the analysis of n-hexane proved difficult due to impurities in the n-propyl trimethyl hexane it is not possible to calculate any complete sets of rates of formation by molecular elimination reactions or radical reactions although several can be. From the set of results obtained in Section 5 it is clear that similar reactions of the excited species are occurring. Referring to the mechanistic diagram below it is possible to calculate certain rates of the products which were analysed.

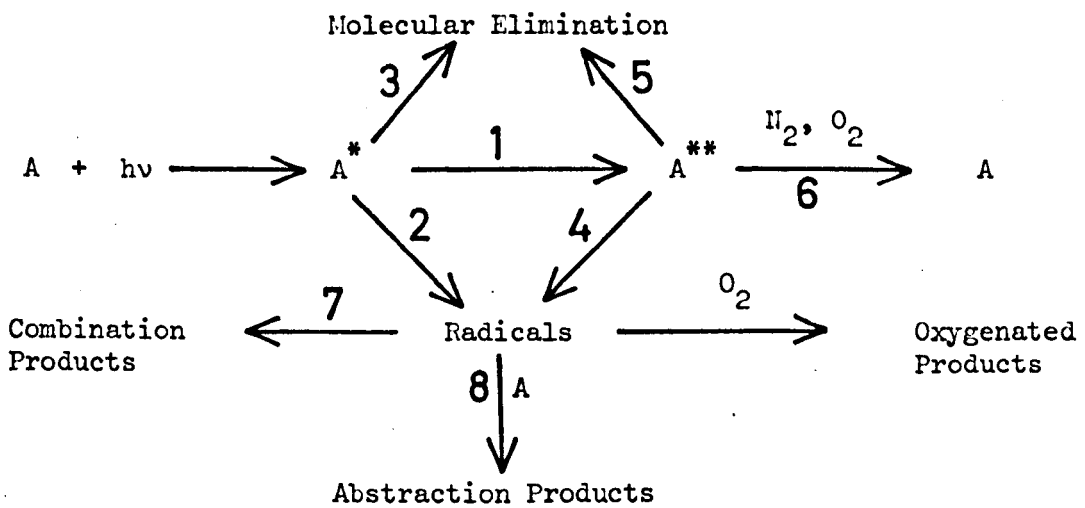

Total Rate of Product = $R_3 + R_5 + R_7 + R_8$ where $R_7 + R_8$ equal $R_2 + R_4$ so that the total rate = $R_2 + R_3 + R_4 + R_5$

Rate in excess Nitrogen = $R_3 + R_7 + R_8$ where $R_7 + R_8$ is dependent on R_2 thus Rate in excess Nitrogen = $R_2 + R_3$

Rate in excess Oxygen = R_3

Rate at the Intercept = $R_3 + R_5 + R_7$

The formation of methane, ethylene, ethane and propylene can be discussed together. Absorption of light by A forms the first excited state which has three possible modes of reaction:

Firstly, conversion to the second excited state A^{**}.

Secondly, decomposition to give radicals by reaction 2, from which radical combination and disproportionation products can be formed by reaction 7, and abstraction products by reaction 8.

Thirdly, molecular elimination products by reaction 3.

The second excited state A^{**} can also undergo three processes:

Firstly, decomposition to give radicals, reaction 4.

Secondly, molecular elimination, reaction 5, and

thirdly, collision deactivation by nitrogen and oxygen, by reaction 6, which if in large excess then reaction 6 is the sole reaction of A^{**}. Increase in oxygen pressure also

eliminated by reacting with the radicals to form oxygenated products.

Calcualtion of radical yields and molecular elimination reaction yields is not possible until sufficient experiments, with other added gases, have been carried out.

9.3 Life-time of Second Excited State of n-Propyl Trimethyl Stannane

The reciprocal of the rates of formation of butane, propylene and ethylene from the second excited state were plotted against inert gas pressure giving typical Stern-Volmer plots shown in Figure 9.1. The ratio of the rate constant of decomposition to that of collisional deactivation from the three plots is in the range 1.15 - 1.20 x 10^{-3} moles/litre. The value for the rate constant of deactivation obtained in Section 7.7 is 1.093 x 10^{11} litres^2/mole^2/sec. and this gives a value for the range of the rate constant of decomposition as 1.26 - 1.31 x 10^8 sec.$^{-1}$. Therefore the life-time of the second excited state, which is the reciprocal of the decomposition rate constant is

$$7.63 - 7.84 \times 10^{-9} \text{ sec.}$$

Figure 9.1

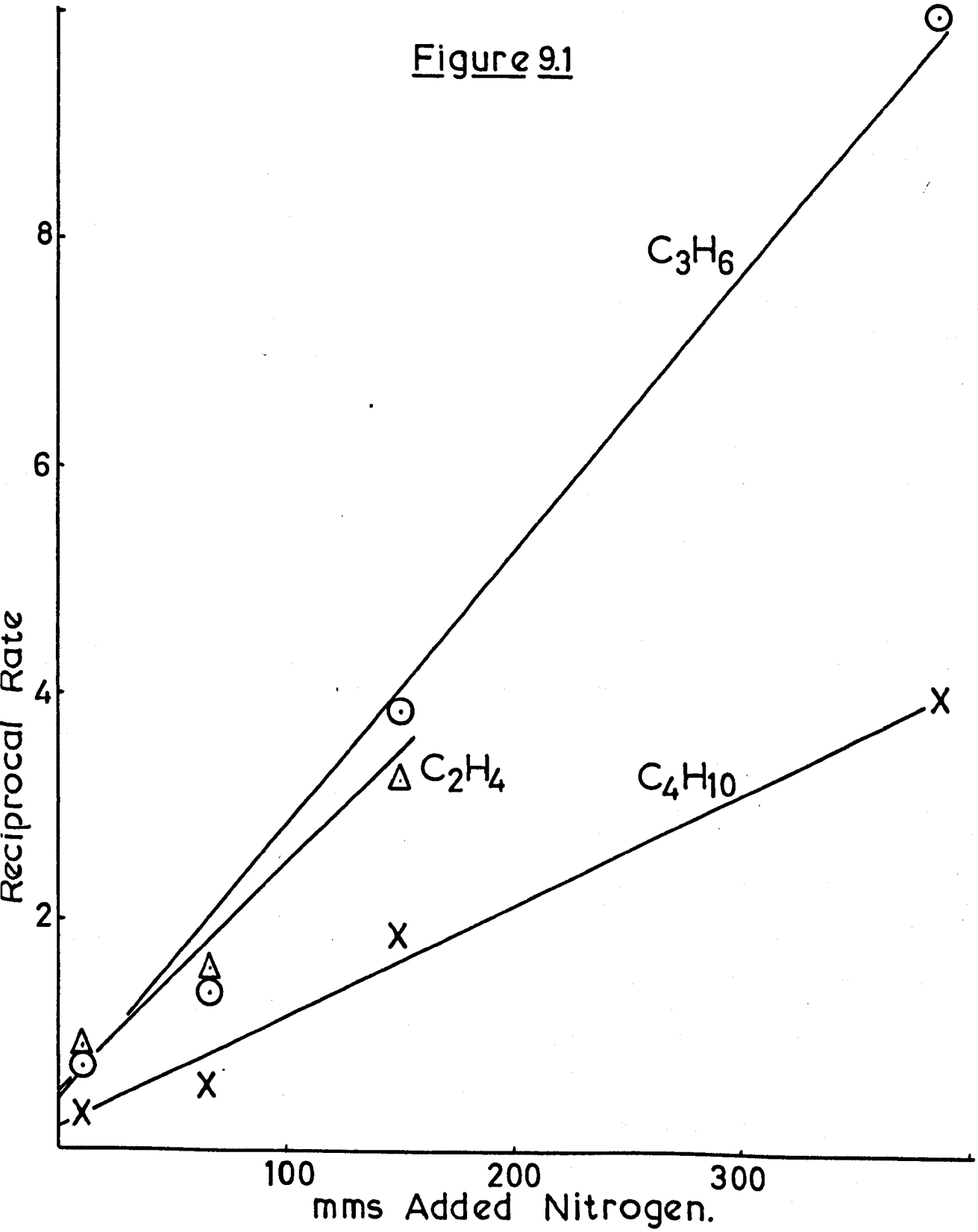
8
6
4
2
Reciprocal Rate
C_3H_6
C_2H_4
C_4H_{10}
100
200
300
mms Added Nitrogen.

10. DISCUSSION: LIQUID PHASE PHOTOLYSIS OF TETRAMETHYL STANNANE

10.1 In Cyclohexane

The initial rate of formation of methane (Figure 6.3) indicates the possibility of a chain mechanism occurring. The formation of a yellow solid, which on exposure to air became white, is presumably a polymer which contains Sn-Sn bond.[69] (The mass spectrum of white solid - Figure 6.6). In the liquid phase the possibility of complete loss of all four methyl groups is not possible and since the quantum yield could not be measured the yield of methyl radicals may not be obtained.

The methyl radicals formed have three possible modes of action:

Firstly, recombination with the tin alkyl residue.

Secondly, abstraction of hydrogen or a methyl group to give methane and ethane and

thirdly, combination to form ethane. Hexamethyl distannane is formed by combination of trimethyl stannyl radicals. Since methyl cyclohexane is a product, it appears that the cyclohexyl radical is formed and probably from hydrogen abstraction. The first unknown peak (Figures 6.1 - 6.2) may be $C_6H_{11}Sn(CH_3)_3$ but this is not confirmed. The second unknown peak with a greater retention time than hexamethyl distannane is not bicyclohexyl and may be a compound of the type $CH_3\left[Sn(CH_3)_2\right]_nSn(CH_3)_3$ where n = 2. However this peak does not appear again in the remainder of the solvents and so is probably a derivative

of cyclohexane. There is also a small peak, not shown in Figures 6.1 and 6.2, which has a retention time of approximately $14\frac{1}{2}$ minutes (Figure 6.1) which does appear in other experiments. Since it is the only other product in the photolysis of pure tetramethyl stannane it is probably $(CH_3)_3Sn\text{-}CH_2\text{-}Sn(CH_3)_3$.

10.2 In Iso-Pentane

A much faster rate of formation of methane and ethane (Figure 6.7) was observed during the photolysis in iso-pentane. This is presumably due to the presence of a tertiary hydrogen which will be abstracted much easier than secondary or primary hydrogen atoms. The products which are not identified, peaks 1 and 2 (Figure 6.10), may be combination products of the pentyl radicals $(CH_3)_2C^{\bullet}CH_2CH_3$ and $(CH_3)_2CH.\dot{C}HCH_3$. The third product has a retention time the same as the proposed $(CH_3)_3SnCH_2Sn(CH_3)_3$. The yellow solid material was again formed.

10.3 In 1-Octene

The initial rates of formation of methane and ethane (Figure 6.12) were approximately the same as for cyclohexane even though the solvent molecule contains a double bond. This should weaken the hydrogen bond β to the double bond but apparently the affect is not noticeable. Again hexamethyl distannane is produced (Figure 6.13) along with the yellow solid material. Two unknown peaks were observed which had very close retention times (Figure 6.11). It is possible that they are isomeric decanes formed from addition of methyl radicals to 1-octene and the radical formed by abstraction of the hydrogen atom β to the double bond.

10.4 In 2-Methyl Pentane

In 2-methyl pentane the initial rates of formation of methane and ethane (Figure 6.16) were not as fast as in the case of isopentane even though a tertiary hydrogen is present. This may be due to difference in light absorption. The unidentified products (Figure 6.15) have long retention times. Product 3 has the same retention time as the proposed $(CH_3)_3SnCH_2Sn(CH_3)_3$. Again hexamethyl distannane and the yellow solid were formed.

10.5 In 3-Methyl Pentane

Although the rate of photolysis was extremely slow, due to absorption of light by the solvent, the products formed could be observed by gas chromatography, Figure 6.19. Two doublet peaks were observed and may be isomeric. Also hexamethyl distannane and the proposed $(CH_3)_3SnCH_2Sn(CH_3)_3$ were formed. Although the solution became yellow no solid was formed.

10.6 In Methanol

The rate of reaction was even slower in methanol and besides methane, ethane and hexamethyl distannane only one further product was formed (Figure 6.20). This may be a methoxy alkyl stannane.

10.7 Tetramethyl Stannane

Although the rates of formation of methane and ethane (Figure 6.22) were slower than had been obtained in the previous experiments the rate of formation of hexamethyl distannane remained the same (Figure 6.23). Only one further product was observed and is proposed to be $(CH_3)_3SnCH_2Sn(CH_3)_3$. However, the ratio of ethane to methane was greater than previously obtained and this may be due to the case of abstraction of a methyl group from tetramethyl stannane.

10.8 Suggested Mechanism

A mechanism that may be proposed to account for some of the reactions that occurred in the photolysis:

$$Sn(CH_3)_4 + h\nu \rightarrow Sn(CH_3)_4^*$$

$$Sn(CH_3)_4^* \rightarrow 3CH_3 + {:}\dot{S}nCH_3$$

$$\text{or} \quad 2CH_3 + :Sn(CH_3)_2$$

$$CH_3 + RH \rightarrow CH_4 + R^\bullet$$

$$CH_3 + R^\bullet \rightarrow RCH_3$$

$$CH_3 + Sn(CH_3)_4 \rightarrow C_2H_6 + Sn(CH_3)_3$$

$$CH_3 + Sn(CH_3)_4 \rightarrow CH_4 + CH_2Sn(CH_3)_3$$

$$2Sn(CH_3)_3 \rightarrow (CH_3)_3SnSn(CH_3)_3$$

$$CH_2Sn(CH_3)_3 + Sn(CH_3)_3 \rightarrow (CH_3)_3SnCH_2Sn(CH_3)_3$$

$$2R^\bullet \rightarrow R\text{-}R$$

$$CH_3 + CH_3 \rightarrow C_2H_6$$

$$R^\bullet + {}^\bullet Sn(CH_3)_3 \rightarrow RSn(CH_3)_3$$

Without evidence of further products and quantum yields little can be obtained from the experiments carried out although further experiments may lead to interesting products.

Analysis of the white solid material obtained on exposure to air of the yellow solid formed in the photolysis was unsatisfactory.

(1)	%C	12.80	%H 2.80	%Sn	32.50	$SnC_4H_{10}O_{12}$
(2)		10.14	2.39		65.0	$Sn_2C_3H_9O_5$
(3)		9.58	2.30		65.0	$Sn_2C_3H_8O_5$

No exact formula can be obtained and the mass spectrum is inconclusive. The work by Razuvaev[69] showed that the polymeric coloured product of irradiation of tetraethyl stannane contained Sn-Sn bonds. The study of the products of the interaction between the polymeric compounds and benzoyl peroxide proves their branched structure.

11. GENERAL SUMMARY ON THE PHOTOLYSIS OF ALKYL-SUBSTITUTED STANNANES

The thermochemistry of alkyl substituted stannanes showed that complete removal of four alkyl substituents was not possible and this was confirmed by the radical quantum yields at zero pressure. Molecular eliminations of olefins from substituents containing more than one carbon atom supported mass spectral evidence. Normal radical combinations and interactions occurred and disproportionation to combination ratios were of the same order as have been obtained in rotating sector experiments. Abstraction reactions of complete alkyl groups by radicals appear to be of general acceptance along with hydrogen abstraction.

Increasing the temperature at which the photolysis is carried out favours hydrogen abstraction reactions and in general leads to an increase in total yields. Above 150°C thermal reactions tend to compete with photolytic processes. Activation energies of hydrogen abstraction reactions compare favourably with similar processes of hydrocarbon analogues.

The effects of inert gases on the photolytic reaction of alkyl-substituted stannanes suggests the presence of two excited intermediates. The life-time of the second being of the order of 10^{-8} seconds. Whether this second excited species is a triplet or a vibrationally excited molecule is undecided. However supression of reactions from this second species is virtually complete with addition of 100 mm. of inert gas.

As far as previous photochemical research on metal alkyls is concerned the reactions of the intermediate radicals are comparable. However the decomposition of the tetraalkyl stannane, to give three hydrocarbon radicals and a metal alkyl radical, is unique in that monoalkyl, dialkyl and trialkyl metal compounds as well as tetraalkyl lead compounds decompose completely to give the corresponding metal and four alkyl radicals. It is probable that the photolysis of substituted germanes and silanes with light of wavelength 1849 Å will show even less tendency to complete elimination from the central heavy atom as is indicated by their thermochemistry.

REFERENCES

1. H.S. Taylor, Trans. Faraday Soc., 21, 560 (1925)
2. F. Paneth and W. Hofeditz, Ber., 62B, 1335 (1929)
3. R.K. Asundi, C.M. Bhasker Rao and R. Samuel, Proc. Ind. Acad. Science 1A, 542 (1935)
4. H.W. Thompson and J.W. Linnett, Proc. Roy. Soc. London, A150, 603, (1935)
5. H.W. Thompson and J.W. Linnett, Proc. Roy. Soc. London, A156, 108, (1936)
6. H.W. Thompson and J.W. Linnett, Trans. Farad. Soc., 33, 501 (1937)
7. H.W. Thompson and J.W. Linnett, Trans. Farad. Soc., 33, 874 (1937)
8. A.N. Terenin and N.A. Prilezhaeva, J. Chem. Phys. 2, 441 (1934)
9. A.B.F. Duncan and J.W. Murray, J. Chem. Phys., 2, 636 (1934)
10. Popala Pai, Proc. Roy. Soc. London A149, 35, (1935)
11. V.A. Petuchoff, V.F. Miranoff, and P.P. Schorigin, Izvestiza akademii nauk S.S.S.R. Seriza chemstsetskaya, No. 12, 2202, (1964)
12. Photochemistry, J.G. Calvert and J.N. Pitts, Jnr., Wiley and Sons Inc. N.Y., P.246.
13. There is a tendency to consider triplet molecules as diradicals. This is not correct. Paramagnetism is symptomatic of, but does not in itself confer all the properties we associate with diradical behaviour. The ultimate diradical possesses the following properties:
    a) Paramagnetism
    b) The charge densities of the two odd electrons are spatially separate.

    Whilst triplets possess a) they do not always have b) and when they do the singlet state has also.

    S.P. McGlynn, F.J. Smith, G. Silento, Photochem. & Photobiol. 3, 269 (1964)

14. R.S. Mulliken, J. Chem. Phys., 7, 14, (1939)

15. R.S. Mulliken and C.A. Ricke, Rept. Progress in Phys. 8, 231, (1941)

16. M. Kasha, Discussions Farad. Soc., 9, 14, (1950)

17. Beer, Ann. Phys. Chem. 163 (Dritte Reihe 86) 78, (1852)

18. A.C.G. Mitchell, M.W. Zemansky, Resonance Radiation and Excited Atoms, Camb. Press. 1961, p.96

19. Photochemistry, J.G. Calvert and J.N. Pitts, Jnr., Wiley & Sons Inc., N.Y.

20. P. Kebarle, J. Phys. Chem. 67, 351, (1963)

21. J.N. Simons, R.G. McNamee and C.D. Hurd, J. Phys. Chem., 36, 939, (1932)

22. F.O. Rice and K.F. Herzfeld, J. Amer. Chem. Soc., 56, 284 (1934)

23. L.M. Yeddanapalli and C.C. Schubert, J. Chem. Phys., 141, (1946)

24. H.S. Taylor and J.P. Cunningham, J. Chem. Phys., 6, 357, (1938)

25. Chas. E. Waring and W.S. Horton, J. Amer. Chem. Soc., 67, 450 (1945)

26. T.V. Sathyamurphy, S. Swaminathan and Lourdi M. Yeddanapalli, J. Ind. Chem. Soc., 27, 509, (1950)

27. P.A. Pratt and J.H. Parnell, Trans. Faraday Soc., 60, 319 (1964)

28. D.E. Hoare, Ting-Man Li and A.D. Walsh, Private Communications

29. K. Hoeppner, Proc. Tihany Symp. Radiat. Chem. 2nd. Tihany Hung. 33-6 (1966)

30. R. Barker, Trans. Faraday Soc., 63, 2640-50 (1967)

31. A. Smits and A.H.W. Asen, Z. Electrochem. 16, 264 (1910)

32. G.H. Cheesman and H.J. Emeleus, J. Chem. Soc., 2847 (1932)

33. W.A. Noyes and H. Romeyn, J. Amer. Chem. Soc., 54, 4143 (1932)

34. N.L. Simmons and A.O. Beckman, J. Amer. Chem. Soc., 58, 454 (1936)

35. H.J. Emeleus and K. Stewart, Trans. Faraday Soc. 32, 1577 (1936)

36. H. Nicki and G.J. Mains, J. Phys. Chem. 68, 304 (1964)

37. A.P. Garrat and H.W. Thompson, J. Chem. Phys. 524 (1934)

38. H.W. Thompson and A.P. Garrat, J. Chem. Phys. 1817 (1934)

39. A.B. Callear, Proc. Roy. Soc. A 265, 71-87 (1961)

40. R.O. Adams and E.E. Donaldson, J. Chem. Phys. 42(3), 770 (1965)

41. A.N. Terenin, Acta Physicochimica (U.R.S.S.) 1, 762 (1935)

42. A.N. Terenin and N. Prilezhaeva, Trans. Faraday Soc., 31, 1483, (1935)

43. P.A. Leighton and R.A. Mortensen, J. Amer. Chem. Soc., 58, 448 (1936)

44. H.S. Taylor and C. Rosenblum, J. Chem. Phys. 6, 119 (1938)

45. J.W. Moore and H.S. Taylor, J. Chem. Phys., 8, 396 (1940)

46. R. Gomer and W. Albert Noyes Jnr. J. Amer. Chem. Soc., 71, 3390 (1949)

47. K.J. Ivin and E.W.R. Steacie, Proc. Roy. Soc. London A208, 25 (1951)

48. R. Gomer and G.B. Kistiakowsky, J. Chem. Phys., 19, 85 (1951)

49. L.M. Dorfman and R. Gomer, Chem. Rev. 46, 499 (1950)

50. A.E. Trotman-Dickenson and E.W.R. Steacie, J. Amer. Chem. Soc., 72, 2310 (1950)

51. H.G. Plust, U.S. Patent, 2,898,278, Aug. 4th 1951

52. R.D. Anderson and H.A. Taylor, J. Phys. Chem. 56, 498 (1952)

53. D.M. Miller and E.W.R. Steacie, J. Chem. Phys., 19, 73 (1951)

54. J.S.A. Forsyth, Trans. Faraday Soc., 37, 312 (1941)

55. A.E. Trotman-Dickenson, J.R. Birchard and E.W.R. Steacie, J. Chem. Phys. 19, 163 (1951)

56. A.E. Trotman-Dickenson and E.W.R. Steacie, J. Chem. Phys. 19, 329 (1951)

57. R.E. Rebbert and E.W.R. Steacie, Can. J. Chem., 31, 631 (1953)

58. J.C. Polanyi, Ph.D. Thesis, Manchester 1952.

59. J.N. Bradley, H.W. Melville, F.R.S. and J.C. Robb, Proc. Roy. Soc. London A236, 318, (1956)

60. J.C. Clouston and C.L. Cook, Trans. Faraday Soc., 54, 1001 (1958)

61. R.E. Rebbert and P. Ausloos, J. Amer. Chem. Soc., 85, 3086 (1963)

62. L.C. Fischer and G.L. Mains, J. Phys. Chem. 9, 2522, (1964)

63. A.G. Sherwood and H.E. Gunning, J. Phys. Chem. 7, 2323, (1965)

64. D.H. Derbyshire and E.W.R. Steacie, Can. J. Chem. 32, 457, (1954)

65. G.A. Razuevaev et al. Problemy Meckhanizina Org. Reaktani Akad. Nauk Ukr. S.S.R. Otdel Fiz-Mati Khim Nauk 78-87 (1953) review of all his work.

66. G.A. Razuevaev et al. Zh. Obshch. Khim 32, 2154 (1962)

67. G.A. Razuevaev et al. Zh. Vses. Khim. Obshch. Im. D.I. Mendeleeva 7, 325 (1962) review of all 1960-61 work.

68. G.A. Razuevaev et al. Tetrahedron, 19, 341 (1963)

69. G.A. Razuevaev et al. Tetrahedron, 18, 667 (1962)

70. W. Strohmeier, Angew. Chem. 75, 453 (1963)

71. All values of heats of formation of liquid and gaseous metal alkyls and carbonyls were obtained from "Advances in Organometallic Chemistry", Vol. 2 in the section by H.A. Skinner "The strength of metal-to-carbon bonds" p. 49-110.

72. V.H. Dibeler, J. Res. Nat. Bureau Standards, 49, 235 (1952)

73. D.B. Chambers, F. Glocking, J.R.C. Light and M. Weston, Chem. Comm. 281, (1966)

74. J.L. Occalowitz, Tetrahedron Letters, 5291 (1966)

75. H.J. Rommel, Private Communications

76. H.D. Beckey, W. Groth, H. Okabe, H.J. Rommel, Z. Naturforschg. 19a, 1511 (1964)

77. W.A. Noyes, J. Chem. Phys., 5, 807 (1937)

78. M. Zelikoff, L.M. Sschenbrand, J. Chem. Phys., 22, 1685 (1954)

79. N.R. Greiner, J. Chem. Phys., 47, 4374 (1967)

80. Peter Borrell, P. Cashmore and A.E. Platt, J. Chem. Soc. A, 3063 (1968)

81. G.B. Kistiakowsky and E.K. Roberts, J. Chem. Phys. 21, 1637 (1953)

82. K.U. Ingold and F.P. Lossing, J. Chem. Phys., 21, 1135 (1953)

83. A. Shepp, J. Chem. Phys., 24, 939 (1956)

84. R.E. March and J.C. Polanyi, Proc. Roy. Soc., A273, 360 (1963)

85. P. Ausloos and E.W.R. Steacie, Canad. J. Chem., 33, 1062 (1955)

86. J. Grotewold and J.A. Kerr, J. Chem. Soc. (London) 4337 (1963)

87. C.A. Heller, J. Chem. Phys., 28, 1255 (1958)

88. A. Shepp and K.O. Kutschke, J. Chem. Phys. 26, 1020 (1957)

89. C.I. Awramenko and R.W. Kolesnikova, Izvest. Akad Nauk S.S.S.R. Otd. Chim. 806 (1960)

90. J.A. Kerr and A.F. Trotman-Dickenson, J. Chem. Soc. (London) 1611, (1960)

91. J.A. Kerr, Chem. Rev. Vol. 66 No. 5, 494.

92. B.G. Gowenlock, Private Communications

93. J.O. Terry and J.H. Futrell, Canad. J. Chem. 45, 2327, (1967)

94. R. Srinivasan, J. Am. Chem. Soc., 84, 3982 (1962)

95. C.S. Parmenter, J. Chem. Phys., 41, 658 (1964)